

PILING: Peptide-based Ionic liquids towards heaLING of complicated skin infections

Ana Gomes

Programa Doutoral em Química Sustentável,
Departamento de Química e Bioquímica
2021

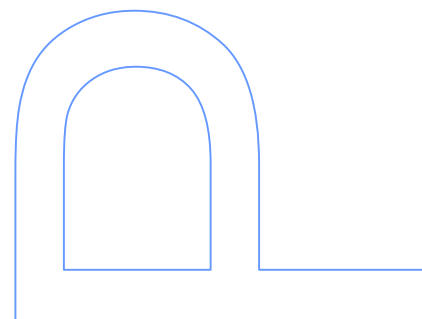
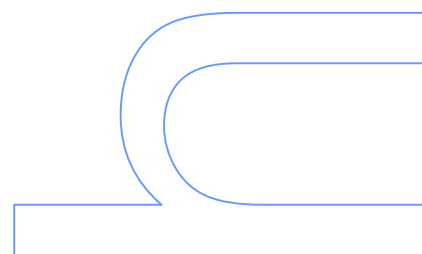
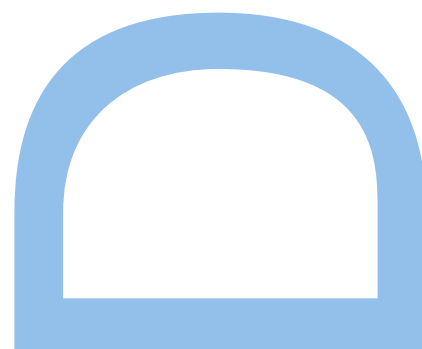
Orientadora

Paula Alexandra de Carvalho Gomes,
Professora Associada, Faculdade Ciências da Universidade do Porto

Coorientadores

Cátia Andreia Silva Teixeira,
Investigadora Auxiliar, Faculdade Ciências Universidade do Porto

Ricardo João Vieira Ferraz,
Professor Coordenador, Escola Superior de Saúde -Instituto Politécnico
do Porto



Acknowledgements

Quero em primeiro lugar agradecer aos meus queridos orientadores. Ao decidir embarcar nesta aventura, de fazer um doutoramento, um dos fatores que mais pesou na minha decisão foi com quem iria trabalhar. Não faria o doutoramento de outra forma, acho fundamental conhecer com quem vamos trabalhar num projeto tão longo. Eu sabia o que me esperava, ao trabalhar convosco, e não me desiludi. Vocês foram incansáveis. Sabia que poderia contar com o vosso apoio incondicional e liberdade para explorar o mundo dos péptidos e outras novas áreas que não conhecia. Foi tão bom, OBRIGADA!

Professora Paula, obrigada por toda a paciência, compreensão, carinho e apoio. SEMPRE, mas SEMPRE que precisei esteve disposta a ajudar e pronta a ouvir-me. Obrigada por todas as correções, pelas reuniões de grupo e acima de tudo pela paciência com o meu perfeccionismo. São muitos anos a crescer e aprender consigo, a Professora será sempre uma REFERÊNCIA para mim!

Cátia, agradeço também todo o apoio e ombro amigo. Por compreenderes muitas vezes o meu cansaço, os desabafos e por me dizeres “eu sei como é, sei e como te sentes!”. Ouvir isso foi sempre muito libertador e fez-me sentir compreendida. Obrigada pela tua presença constante no laboratório, foste quem eu mais massacrei com perguntas (inclusive as mais parvinhas!), com quem eu partilhei medos, desabafos... obrigada por me ouvires. APRENDI MUITO CONTIGO. Obrigada por estares lá, ao meu lado, na bancada.

Ricardo, agradeço por toda a boa disposição e pelo ponto de vista sempre positivo que tantas vezes me deixou animada e mais tranquila. Obrigada, também por me dares a oportunidade de saber o que é dar uma aula e por poder falar sobre o meu trabalho com os teus alunos na ESS. Foi sem dúvida uma excelente oportunidade onde aprendi imenso, com eles e contigo. NÃO ESQUECEREI!

As meninas do Lab. 2.28, Mélanie, Teresa, Ritinha e Natália que mais de perto me acompanharam, obrigada por toda a boa disposição e acima de tudo pelo espírito de equipa. Sim, ainda é possível verificar isso num local de trabalho e eu tive essa sorte. Sempre dispostas a ajudar. E o melhor? Além do trabalho e empenho havia também muita alegria, música, vídeos... tudo isto sempre acompanhado com uma excelente relação entre todos. Vocês são incríveis! Obrigada!

Luisinha, obrigada pela paciência para quase todos os dias de manhã, principalmente nesta fase final, ouvires os meus lamentos e ansiedades. Obrigada, também pelos momentos de parvoíces que tanto nos faziam rir e pelas ajudas que também deste para o meu trabalho. “tu sabes! ;)”

Não poderia deixar também de agradecer a duas pessoas com quem colaborei, durante um maior período de tempo, que foram a Iva Fernandes e a Lucinda Bessa. Obrigada por não desistirem de mim e do projeto, pela quantidade insana de ensaios, que me permitiram ter tantos resultados. Não posso deixar de fazer um agradecimento especial à Iva pela resiliência nos ensaios do colagénio, foi difícil, mas conseguimos. Vocês foram incansáveis!

Por fim, queria mesmo mostrar o quão grata estou por ter tido a sorte de me cruzar com pessoas tão maravilhosas, que em conjugação do enorme apoio que tenho em casa, me permitiu, ainda que com percalços porque nada é perfeito, conseguir uma boa harmonia casa-trabalho e assim levar esta aventura a um bom porto.

Termino esta aventura com uma mulher mais enriquecida (pessoal e cientificamente), mudada e feliz. Obrigada com todo o meu coração.

Abstract

The treatment of skin infections inclusively of their most severe cases, namely, complicated skin and soft tissue infections (cSSTI), is compromised by the lack of effective antibiotics. The development of antimicrobial resistance to the last available antibiotic options is one of the most serious health threats worldwide. Antimicrobial peptides (AMP) have emerged as an appealing alternative to the classic antibiotics, mainly due to their low propensity to induce bacterial resistance, and high wide spectrum activity even at low concentrations. Also, the treatment of cSSTI is a slow progressing one, due the difficult healing process that is delayed not only by the bacterial infection but also by the frequent occurrence of other co-morbidities. One of the steps in the healing process is collagen production, which could be enhanced not only by adequate AMP, many of which can also display wound healing properties, but also by collagenesis-boosting peptides (CBP), like matrikines, which are widely employed in the cosmetics industry for skin care (anti-ageing products).

In connection with the above, the global aim of this Doctoral Thesis was the development of new molecular constructs based on peptides and ionic liquids able to both provide antibacterial action and fast healing, thus with potential interest to tackle skin infections, including cSSTI. As such, it was intended to take advantage both of bioactive peptides and of ionic liquids known to act as dermal permeation enhancers and to possess intrinsic antibacterial activity.

At the initial stage, the possibility to build molecular constructs able to display both a strong antibacterial action and collagenesis-boosting properties was investigated. To this end, two peptides were selected, namely, one AMP (3.1) known to possess wide spectrum antibacterial activity, and one CBP (pentapeptide-4, or PP4) used in the cosmetics industry, which were linked to each other in different ways. The chimeric peptides thus produced were tested *in vitro* against antibiotic susceptible strains and multidrug resistant (MDR) clinical isolates. The best performing chimera, named 3.1-PP4, was selective against the Gram-negative species tested. Moreover, this peptide also displayed anti-biofilm properties on a MDR clinical isolate of *Klebsiella pneumoniae*, both through inhibition of biofilm installation, and disaggregation of preformed biofilms. Furthermore, the 3.1-PP4 chimera peptide displayed a collagenesis-inducing effect comparable to that of the reference cosmeceutical peptide Matrixyl, which is the *N*-palmitoylated derivative of the parent CBP, PP4.

The next step was an investigation on whether *N*-terminal modification of peptide 3.1-PP4 might enhance its resistance to enzymatic conversion, as this is a well-known downside of many peptide-based therapeutics. For the reasons explained above, and because ionic liquids are gaining relevance for several pharmaceutical applications, a methyl imidazolium-based ionic liquid was covalently linked to the *N*-terminus of peptide 3.1-PP4 through a copper(I)-catalyzed alkyne-azide cycloaddition (CuAAC), which is one of the most popular “click” reactions. The resulting construct, named Melm-3.1-PP4, was shown to retain the antibacterial and antibiofilm activity of the parent chimeric peptide, while being significantly more stable than the latter towards tyrosinase-mediated modification.

The selectivity of both 3.1-PP4 and Melm-3.1-PP4 against Gram-negative bacteria makes them quite relevant leads to face the scarcity of alternatives to antibiotics currently in use against those specific pathogens. Still, considering the main goal of the Doctoral Project and the fact that cSSTI are predominantly associated to methicillin-resistant *Staphylococcus aureus* (MRSA), a Gram-positive MDR bacterium, it was decided to recover one of the chimeric peptides initially developed, namely, PP4-3.1. This peptide, an isomer of 3.1-PP4 where only the sequence in which the AMP and CBP building blocks are linked to each other is changed, had already shown activity against both Gram-positive and Gram-negative pathogens. Therefore, it was further explored, together with its *N*-methylimidazolium derivative, Melm-PP4-3.1, for its antimicrobial (antibacterial and antifungal) and anti-biofilm activity. Of this couple of constructs, the fully peptidic one, PP4-3.1, stood out by showing the strongest (i) antibacterial activity against both planktonic and biofilm forms of Gram-negative and Gram-positive bacteria, (ii) antifungal activity, and (iii) improved activity against *S. aureus* in simulated wound fluid.

Having all the promising results above in hand and considering the intrinsic antibacterial activity of many imidazolium-based ionic liquids, new constructs were designed whereby the AMP building block (peptide 3.1) linked to the CBP (peptide PP4) was replaced by an imidazolium-based ionic liquid. The goal in this approach was to retain the dual antimicrobial and collagenesis-boosting action, while substantially cutting down the size of the full peptide sequence, enabling a more cost-effective synthesis process. The new ionic liquid-peptide conjugates, IL-PP4 or IL-KKTKS, were produced via “click” chemistry (CuAAC) as previously done for the Melm-3.1-PP4 and the Melm-PP4-3.1 constructs. The new IL-PP4 conjugates showed potent activity against both antibiotic susceptible strains and MDR clinical isolates of either Gram-negative or Gram-

positive pathogens. Moreover, the new conjugates displayed antifungal activity and retained the collagenesis-inducing behavior of the parent peptide PP4, being comparable to the reference cosmeceutical Matrixyl. Anticipating the behavior of the peptides in a real wound context, the activity of the best permeating IL-KTTKS peptides against *S. aureus* in simulated wound fluid was also assessed and remained unchanged.

In face of exciting findings with IL-PP4 conjugates, one final investigation was made to determine whether this approach of *N*-terminal “clicking” an antimicrobial ionic liquid to a non-antimicrobial CBP could add antimicrobial activity to other cosmeceutical peptides. Hence, as a preliminary proof-of-concept on the value of this approach, the same chemical modification was applied to a couple of well-known cosmeceutical tripeptides, KVK and GHK. The resulting constructs were confirmed to display potent antibacterial activity against antibiotic susceptible strains and MDR clinical isolates.

Altogether, results obtained offer a new window of opportunity towards future development of strategies to effectively fight cSSTI in the fast-approaching post-antibiotic era. The peptide/ionic liquid-based constructs herein disclosed, combining antimicrobial, antibiofilm and collagenesis-inducing effects, emerge as valuable leads to such end.

Keywords

antibiofilm, antifungal, antimicrobial peptides, collagen, cosmeceutical peptides, ESKAPE, imidazolium, ionic liquid, Matrixyl, multidrug-resistant bacteria, skin and soft tissue infection, wound-healing

Resumo

O tratamento de infeções cutâneas, especialmente em casos mais graves de infeções de pele e tecidos moles (IPTM), pode ser comprometido pela falta de antibióticos eficazes. O crescente aumento de estirpes de agentes patogénicos que são resistentes aos antibióticos atualmente em uso clínico é uma das maiores ameaças em saúde pública. Neste contexto, os péptidos antimicrobianos têm vindo a ganhar proeminência como uma possível alternativa aos antibióticos clássicos, principalmente devido quer à sua baixa propensão para induzir a seleção de estirpes microbianas resistentes, quer pelo seu largo espectro e elevada potência de ação mesmo a baixas concentrações. O tratamento das IPTM é um processo geralmente lento, devido à dificuldade de cicatrização, que é retardada não só pela própria infeção, mas também por outras patologias eventualmente presentes. Um dos passos no processo de cicatrização é a produção de colagénio, que pode ser estimulada por alguns péptidos antimicrobianos que também apresentam propriedades de cicatrização. Existem, também, os chamados péptidos indutores de produção de colagénio, como as matriquinas, largamente utilizados em produtos dermocosméticos com ação anti-idade.

Tendo em conta o acima exposto, o objetivo global desta tese de doutoramento foi o desenvolvimento de novas moléculas baseadas em péptidos e líquidos iónicos capazes de apresentar, simultaneamente, ação antimicrobiana e ação indutora de colagénese. Portanto, visou-se criar novas moléculas com potencial interesse em futuras abordagens inovadoras ao tratamento de infeções cutâneas, em especial de IPTM. Assim, pretendeu-se tirar partido da bioatividade não só de péptidos, mas também de líquidos iónicos reconhecidos como potenciadores de permeação dérmica e como possuidores de atividade antimicrobiana intrínseca.

Numa fase inicial do projeto, foi investigada a possibilidade de criar novas moléculas peptídicas que exibissem potente ação antibacteriana e capacidade de induzir a produção de colagénio. Para tal, foram selecionados dois péptidos parentais, nomeadamente, um péptido antimicrobiano (3.1) com potente ação de largo espectro e um péptido indutor de produção de colagénio (pentapéptido-4, PP4) utilizado na indústria cosmética, os quais se conjugaram de diferentes formas. Os péptidos quiméricos produzidos foram testados *in vitro* contra bactérias sensíveis a antibióticos e contra isolados clínicos multirresistentes. O péptido que exibiu a melhor performance, denominado 3.1-PP4, apresentou uma ação potente e seletiva contra as espécies Gram-negativas testadas. Além disso, o mesmo péptido mostrou atividade anti-biofilme

em isolado clínico multirresistente de *Klebsiella pneumoniae*, quer por inibição da formação de biofilme, quer por desagregação de biofilmes pré-estabelecidos. O péptido 3.1-PP4 mostrou, ainda, uma capacidade de indução de colagénese comparável à observada para o conhecido agente dermocosmético Matrixyl, que corresponde ao derivado *N*-palmitoilado do péptido parental PP4.

O passo seguinte consistiu em investigar se seria possível introduzir uma modificação *N*-terminal no péptido 3.1-PP4 que aumentasse a sua resistência à ação de enzimas, que se sabe ser uma das maiores desvantagens dos péptidos terapêuticos. Atendendo à crescente relevância dos líquidos iónicos para aplicações farmacêuticas, optou-se por ligar um líquido iónico de imidazólio ao extremo *N*-terminal do péptido 3.1-PP4, através de uma cicloadição azida-alcino catalisada por cobre(I), uma das reações “click” mais conhecidas. O novo conjugado, chamado Melm-3.1-PP4, mostrou reter a atividade antibacteriana e antibiofilme do péptido quimérico de origem, apresentando-se significativamente mais resistente do que este último à ação da enzima tirosinase.

A seletividade dos dois péptidos 3.1-PP4 e Melm-3.1-PP4 contra bactérias Gram-negativas é de grande relevância, face à escassez de alternativas para os antibióticos correntemente em uso contra este tipo de bactérias. No entanto, tendo em conta o objetivo principal deste projeto de doutoramento e o facto de as IPTM serem predominantemente causadas por *Staphylococcus aureus* resistente à metilina, uma bactéria Gram-positiva, optou-se por resgatar um outro péptido quimérico inicialmente desenvolvido, PP4-3.1, que mostrara ser ativo contra bactérias Gram-positivas e Gram-negativas. Este péptido é um isómero do péptido 3.1-PP4, onde apenas está alterada a ordem pela qual se ligam entre si os péptidos parentais, 3.1 e PP4. Assim, foram produzidos e avaliados *in vitro*, quer o péptido PP4-3.1, quer o seu derivado *N*-modificado com um líquido iónico derivado de imidazólio, Melm-PP4-3.1. Destas duas moléculas, destacou-se o péptido PP4-3.1, que exibiu (i) potente atividade antibacteriana forte contra espécies bacterianas quer na forma planctónica, quer em biofilme, tanto Gram-positivas quanto Gram-negativas, (ii) atividade antifúngica, e (iii) atividade melhorada contra *S. aureus* em fluido de ferida simulado.

Tendo em mãos os resultados promissores acima descritos, e considerando a atividade antimicrobiana intrínseca de vários líquidos iónicos, foram concebidos novos conjugados em que se substituiu o segmento peptídico antimicrobiano (3.1) por um líquido iónico do tipo imidazólio. Esta nova abordagem teve por finalidade reduzir significativamente o tamanho da porção peptídica, consequentemente reduzindo custos

de produção, mas procurando reter a ação dual, ou seja, antimicrobiana e indutora de colagénese. Os novos conjugados líquido iónico-péptido, genericamente designados como IL-PP4 ou IL-KTTKS, foram sintetizados de forma semelhante à anteriormente utilizada para produzir os conjugados Melm-3.1-PP4 e Melm-PP4-3.1. Os conjugados IL-PP4 exibiram potente atividade contra bactérias quer suscetíveis a antibióticos, quer multirresistentes, tanto Gram-positivas quanto Gram-negativas. Além disso, os conjugados apresentaram atividade antifúngica e conservaram uma capacidade de indução de produção de colagénio semelhante à do péptido de referência Matrixyl. Para melhor prever o comportamento dos conjugados num contexto real de uma lesão cutânea, os péptidos com melhor performance foram testados *in vitro* contra *S. aureus* em fluido de ferida simulado, constatando-se que a sua atividade foi preservada.

Face aos resultados obtidos com os novos conjugados IL-KTTKS, prosseguiu-se para uma investigação final, com vista a determinar se a estratégia de conjugar, via reação “click”, um líquido iónico ao extremo *N*-terminal de outros péptidos cosméticos sem ação antimicrobiana, poderia conferir atividade antimicrobiana aos mesmos. Assim, em forma de prova de conceito preliminar desta estratégia, a mesma modificação foi realizada em péptidos muito conhecidos e utilizados na indústria cosmética, KVK e GHK. Confirmou-se que os conjugados resultantes exibem atividade antibacteriana contra espécies suscetíveis a antibióticos e em isolados clínicos multirresistentes.

Em suma, todos os resultados obtidos, apresentados nesta Tese, abrem uma nova janela de oportunidade para o desenvolvimento de novas estratégias para combater de forma eficaz as infeções e pele e tecidos moles, para fazer face à “era pós-antibiótico” que se avizinha. Os conjugados à base de péptidos/líquidos iónicos, aqui explorados, ao combinarem atividade antimicrobiana, ação antibiofilme e capacidade de indução de colagénese, surgem como potenciais protótipos para o futuro desenvolvimento de abordagens inovadoras ao tratamento de infeções cutâneas.

Palavras-chave

antibiofilme; antifúngico; bactérias multirresistentes; cicatrização; colagénio; ESKAPE; imidazole; infeções de pele e tecidos moles; líquidos iónicos, Matrixyl; péptidos antimicrobianos; péptidos cosméticos.

Table of Contents

| | |
|--|------|
| Acknowledgements..... | I |
| Abstract | III |
| Resumo | VII |
| Table of Contents | XI |
| Abbreviations..... | XIII |
| Doctoral Thesis Overview | XVII |
| Chapter 1. Introduction | 1 |
| Chapter 2. Results and Discussion | 83 |
| 2.1. Development of a dual-action chimeric peptide | 85 |
| 2.2. Chimeric peptide stability enhancement via conjugation to an IL | 111 |
| 2.3. Simple structural changes to widen the antimicrobial action range | 127 |
| 2.4. Conjugation to IL to confer antimicrobial action on to pentapeptide-4 | 147 |
| 2.5. Conjugation of cosmeceutical tripeptides to IL..... | 173 |
| Chapter 3. Conclusion and future perspectives..... | 185 |
| Annexes..... | 189 |

Abbreviations

A

| | |
|-------|-----------------------------------|
| AA | Amino Acid |
| AAA | Amino Acid Analysis |
| ACN | Acetonitrile |
| AgNPs | Silver-Based NPs |
| AMP | Antimicrobial Peptide |
| APIs | Active Pharmaceutical Ingredients |
| ATCC | American Type Culture Collection |

B

| | |
|-----|----------------------|
| BSA | Bovine Serum Albumin |
|-----|----------------------|

C

| | |
|---------------------|--|
| C ₁₄ -Im | 1-tetradecylimidazole |
| C ₁₆ -Im | 1-hexadecylimidazole |
| CBP | Collagen-Boosting Peptide |
| CFU | Colony-Forming Units |
| CLSI | Clinical and Laboratory Standards Institute |
| CLSM | Confocal Laser Scanning Microscopy |
| CPEs | Chemical Permeation Enhancers |
| cSSTI | Complicated Skin and Soft Tissue Infections |
| CuAAC | Copper(I)-Catalyzed Azide Alkyne Cycloaddition |

D

| | |
|---------------------|---|
| DCM | Dichloromethane |
| DFU | Diabetic Foot Ulcers |
| DIEA | <i>N</i> -ethyl- <i>N,N</i> -diisopropylamine |
| DMEM | Dulbecco's Modified Eagle Medium |
| DMF | Dimethylformamide |
| DMSO | Dimethylsulfoxide |
| DMSO-d ₆ | Hexadeuterated Dimethylsulfoxide |
| DTD | Dermal and Transdermal Delivery |

E

| | |
|-----------|--|
| ECM | Extracellular Matrix |
| EDTA | Ethylenediaminetetraacetic Acid |
| ELISA | Enzyme-Linked Immunosorbent Assays |
| eq | Molar Equivalent |
| ESI-IT MS | Electrospray Ionization – Ion Trap Mass Spectrometry |
| EUCAST | European Committee on Antimicrobial Susceptibility Testing |

F

| | |
|------|----------------------------|
| FBS | Fetal Bovine Serum |
| Fmoc | 9-fluorenylmethoxycarbonyl |
| FNAs | Framework Nucleic Acids |

H

| | |
|-------|---|
| HaCaT | Human Epidermal Keratinocytes |
| HAI | Hospital-Acquired Infections |
| hBDs | Human β -Defensins |
| HBSS | Hank's Balanced Salt Solution |
| HBTU | <i>O</i> -(benzotriazol-1-yl)- <i>N,N,N',N'</i> tetramethyluronium hexafluorophosphate |
| HCTU | <i>O</i> -(6-chlorobenzotriazol-1-yl)- <i>N,N,N',N'</i> -tetramethyluronium hexafluorophosphate |
| HDF | Human Dermal Fibroblasts |
| HDPs | Host Defense Peptides |
| hEPCs | Human Endothelial Progenitor Cells |
| HFF-1 | Human Foreskin Fibroblasts |
| HPLC | High Performance Liquid Chromatography |

I

| | |
|----|--------------|
| IL | Ionic Liquid |
|----|--------------|

M

| | |
|------|--------------------------------------|
| MBC | Minimum Bactericidal Concentration |
| MDR | Multidrug-Resistant |
| Melm | 1-Methylimidazole |
| MHB | Mueller-Hinton Broth |
| MHB2 | Cation-Adjusted Mueller-Hinton Broth |

| | |
|--------|--|
| MIC | Minimum Inhibitory Concentration |
| MMPs | Matrix Metalloproteinases |
| MNs | Microneedles |
| MRSA | Methicillin-Resistant <i>Staphylococcus Aureus</i> |
| MTT | 3-(4,5-dimethylthiazol-2-yl)-2,5-diphenyltetrazolium bromide |
| MW | Molecular Weights |
| NCs | Nanocarriers |
| NEs | Nanoemulsions |
| NLCs | Nanostructured Lipid Carriers |
| NMM | <i>N</i> -Methylmorpholine |
| NMR | Nuclear Magnetic Resonance |
| NPs | Nanoparticles |
| NSAIDs | Non-Steroidal Anti-Inflammatory Drugs |

O

| | |
|------|-------------------------|
| OD | Optical Density |
| OMVs | Outer Membrane Vesicles |

P

| | |
|-----------------------|---|
| PBS | Phosphate Buffered Saline |
| Pr-C ₁₄ Im | 1-Tetradecyl-3-(prop-2-enyl)imidazolium Bromide |
| Pr-C ₁₆ Im | 1-Hexadecyl-3-(prop-2-enyl)imidazolium Bromide |
| Pr-Melm | 1-Methyl-3-(prop-2-enyl)imidazolium Bromide |

R

| | |
|---------|--|
| r.t. | Room Temperature |
| RP-HPLC | Reverse-Phase High Performance Liquid Chromatography |

S

| | |
|------|---------------------------------|
| SAP | Self-Assembling Peptides |
| SC | Stratum Corneum |
| SD | Standard Deviation |
| SI | Selectivity Index |
| SLNs | Solid Lipid Nanoparticles |
| SPPS | Solid Peptide Phase Synthesis |
| SSTI | Skin and Soft Tissue Infections |

SWF Simulated Wound Fluid

T

TFA Trifluoroacetic Acid

TIS Triisopropylsilane

TMS Tetramethylsilane

Trp Tryptophan

TSA Tryptic Soy Agar

TSB Tryptic Soy Broth

Tyr Tyrosine

U

UTI Urinary Tract Infections

VNs Vesicular Nanocarriers

W

WHO World Health Organization

WHP Wound-Healing Peptides

Doctoral Thesis Overview

Scope and Aim

Infections that involve deeper skin structures, named complicated skin and soft tissue infections (cSSTI), are amongst the most severe type of cutaneous disorders, where microbial invasion affects subcutaneous tissue and can even reach the muscle. Severely infected burns, surgical site infections, skin ulcers of different origin, and major abscesses are examples of cSSTI, whose treatment is slow, painful, and often impaired by installation of biofilms, often populated by antibiotic-resistant microbial pathogens. The cSSTI standard-of-care involves essentially, surgical drainage, antibiotic therapy, and physiological supportive care. [1] As such, people affected with cSSTI are often hospitalized for treatment, resulting in long hospital stays, and in the worst scenario in hospital readmissions, which altogether represents a high burden in healthcare. [2]

The cSSTI have a typically polymicrobial nature, where methicillin-resistant *Staphylococcus aureus* (MRSA) is the most common pathogen. However, due to the development of community-associated bacterial resistance, severe skin infections have also a strong relation with other nosocomial bacterial species of the so-called ESKAPE (*Enterococcus faecium*, *Staphylococcus aureus*, *Klebsiella pneumoniae*, *Acinetobacter baumannii*, *Pseudomonas aeruginosa*, and *Enterobacter species*) group, especially in cSSTI cases associated to recurrent hospitalization and surgical interventions. This obviously turns the treatment of cSSTI even more challenging, given the current lack of efficient antibiotics to fight multi-drug resistant (MDR) bacteria. [3] In this regard, the international guidelines recommended an initial treatment of cSSTI with an empiric antibiotic active against MRSA strains prevalent in the country, but there are very few options in the market able to meet this need. One recent example is delafloxacin, a novel fluoroquinolone that stands out as a new alternative to the conventional antibiotics of the same family, by being active against both Gram-positive and Gram-negative bacteria.[4] Still, new potent and wide-spectrum antimicrobial agents remain an urgent need to face the tremendous challenges of the incoming “post-antibiotic era”.

Besides use of antibiotics, treatment of cSSTI often involves an initial debridement step, which is painful but frequently necessary for the most severe cases. Debridement is aimed at removing the bacterial biofilm and necrotic tissue from the infected wound, providing an appropriate wound bed for a fast wound closure. However, the debridement itself is not enough to fully eliminate fast-reforming biofilms or to protect the wound bed from new microbial invasions. Thus, patient’s adhesion to debridement

is often low, contributing to a further aggravation of the cSSTI. Therefore, several approaches alternative to debridement have been developed in the past years, many of which based in nanotechnology, encompassing, e.g., nanoparticles for antibiotic delivery directly inside microbial biofilms, or antibiotic-loaded hydrogels able to disrupt and remove biofilms from, e.g., an infected burn.[5] Relevantly, a 2017 consensus guideline for identification and treatment of biofilms in chronic wounds pointed out a “window gap of action”, corresponding to application of a topical antiseptic immediately after debridement [6] as a great opportunity to fully eliminate traces of wound biofilms, hence impeding their quick restoration. This could promote fast recovery from cSSTI and consequently favor an early discharge from the hospital.

Topical antiseptics can act directly on wound biofilms, which is a clear advantage over systemic antibiotics that cannot eradicate them.[6] On the other hand, topically applied medicines, despite having to be optimized to display a suitable dermatokinetics, can elude important pharmacokinetic and pharmacodynamics hurdles associated to other administration routes, such as, e.g., premature metabolic inactivation or adverse systemic side effects, respectively. For these reasons, topical antiseptics offer a fertile ground for antimicrobial peptides to thrive. Antimicrobial peptides (AMP) have been intensively investigated as surrogates of classical antibiotics, since they exhibit low propensity to induce resistance and are highly active against bacteria, fungi, and viruses. Additionally, their bioavailability is usually much higher when administered topically, as compared to the oral or intravenous routes. This allows to keep active concentrations for longer periods at the application site, with consequent reduction of both systemic toxicity and protease-mediated degradation.[7, 8] As such, AMP have been gaining notoriety as relevant players in the topical treatment of cSSTI. This is reinforced by the fact that many AMP have also wound healing properties, hence contributing to fast and correct wound closure. This wound healing ability offers the double benefit of, on the one hand, reducing the time available for reinstallation of persistent biofilms on the open wound and, on the other hand, avoiding permanent scarring by promoting proper skin rebuilding. This ability is not universal amongst AMP, and – if present – may be due to stimulation of one or more distinct steps of the skin rebuilding process, such as, e.g., induction of collagen synthesis. Interestingly, many peptides are known to possess this collagenesis-stimulating action which have been either used as ingredients in skin care cosmetics or advanced as wound healing peptides (WHP). Unfortunately, many of the best known WHP, such as, e.g., the matrikines, are devoid of antimicrobial action.

In view of the above, this doctoral project was built on the working hypothesis that ***“through a sensible choice of peptide building blocks, it is possible to produce***

peptide/ionic liquid-based constructs with potent antimicrobial and antibiofilm activity, together with the ability of stimulating collagen production; hence being valuable leads for future development of topical formulations to tackle cSSTI.”

In other words, this thesis was aimed at developing new peptide/ionic liquid-based constructs able to (i) display potent antimicrobial activity, including against MDR bacteria belonging to the ESKAPE group, (ii) avoid installation of, and/or disrupt pre-installed, bacterial biofilms, (iii) possess collagenesis-inducing properties, and (iv) present suitable properties (e.g. stability, solubility, and permeability) for potential topical applications.

Scientific questions

Considering its working hypothesis, this doctoral project was planned to sequentially address the following scientific questions:

1. By linking an AMP to a WHP, can we produce a dual-action peptide chimera that is able to retain or even enhance the biological properties of the two parent peptides?
2. Can resistance to enzymatic modification of the peptide chimera be increased, with no loss in activity, via *N*-terminal modification with an ionic liquid (IL)?
3. How relevant will be the order through which both AMP and WHP building blocks are linked to each other in the chimera, regarding its biological properties?
4. Can we preserve the dual-action of the peptide chimera by replacing its AMP building block with an imidazolium-based IL possessing intrinsic antimicrobial activity?
5. If the answer to question 4 is positive, can the same approach be successfully applied to other WHP?

Experimental approach and structure of the thesis

The scientific questions above were addressed through a series of experimental studies making use of diverse chemical and microbiological tools, namely, solid-phase peptide synthesis and solution phase organic synthesis, including click chemistry approaches, and *in vitro* assays on selected peptide-based constructs, encompassing: (ii) activity against relevant bacterial species (including MDR clinical isolates, and in simulated wound fluid); (iii) anti-biofilm action on selected MDR clinical isolates; (iv) activity against *Candida spp.* fungi; (v) toxicity to the HFF-1 and HaCat human cell lines; (vi) stability to tyrosinase-mediated modification; and (vi) collagenesis-inducing properties.

The work carried out, as well as the results and conclusions thereof, are reported in this Thesis, which is structured as a coherent collection of scientific articles, as follows:

Chapter 1 – INTRODUCTION

The introductory chapter offers the scientific background on two relevant topics for this work that are (i) wound healing peptides for treatment of skin infections and (ii) ionic liquids as dermal permeation enhancers for a wide diversity of bioactive molecules and macromolecules. The resulting two review articles constitute this chapter and report: review article 1) the importance of the wound-healing peptides in the context of a cSSTI, particularly for DFU, (published in *Molecules*) and review article 2) a brief overview of what has been done in the field of transdermal drug delivery with an important emphasis to the role of ionic liquids (submitted to *International Journal of Molecular Sciences*).

Chapter 2 – RESULTS AND DISCUSSION

2.1 – Development of a dual-action chimeric peptide

This section describes the synthesis and *in vitro* assessment of a series of chimeric peptides resulting from conjugation of the antimicrobial peptide 3.1, earlier described to possess broad-spectrum antimicrobial activity, to the wound healing peptide PP4 (pentapeptide-4), with widely recognized collagenesis-boosting properties. The best performing construct, 3.1-PP4, which showed selectivity against both antibiotic-

susceptible and multidrug resistant Gram-negative bacteria, was further investigated, revealing both antibiofilm properties and ability to induce collagenesis. This study was published as an original research article in *Frontiers in Microbiology*.

2.2 – Chimeric peptide stability enhancement via conjugation to an IL

This section reports the synthesis and concise study of an *N*-terminally modified derivative of peptide 3.1-PP4, produced by attaching a methyl imidazolium ionic liquid to the peptide's *N* terminus through click chemistry. The resulting construct, MeIm-3.1-PP4, was found to retain the antibacterial and antibiofilm activity of the parent chimeric peptide, 3.1-PP4, while having a significantly improved stability against tyrosinase-mediated modification. This study was published as an original research paper in *International Journal of Molecular Sciences*.

2.3 – Simple structural changes to widen the antimicrobial action range

In this section, the relevance of changing the order through which the two parent peptides are linked to each other is highlighted. Thus, while peptide 3.1-PP4 had shown superior antibacterial activity against Gram-negative bacteria, its isomer PP4-3.1 and its *N*-terminally modified derivative, MeIm-PP4-3.1, herein addressed, were found highly active against both Gram-negative and Gram-positive bacteria. In particular, the fully peptidic construct, PP4-3.1, stood out as the most promising, exhibiting antimicrobial and antibiofilm activity. This study was submitted as an original research paper to *Pharmaceutics* and is currently under revision.

2.4 – Conjugation to IL to confer antimicrobial action onto pentapeptide-4

This section addresses how the intrinsic antimicrobial activity of imidazolium ionic liquids can be exploited to confer antimicrobial action to a cosmeceutical peptide devoid of it. As such, ionic liquids were covalently linked, through click chemistry, to the *N*-terminus of pentapeptide-4, i.e., PP4. The new ionic liquid-peptide conjugates (IL-PP4) displayed antibacterial activity against Gram-negative and Gram-positive bacteria. Moreover, the best constructs have also shown ability to retain or enhance the collagen inducing behavior of the parent peptide PP4, being comparable to the reference cosmeceutical Matrixyl. This study has been recently submitted as an original research paper to *International Journal of Antimicrobial Agents*.

2.5 – Conjugation of cosmeceutical tripeptides to IL

In this section, the pursuit of a preliminary proof of concept regarding the value of “clicking” an imidazolium-based ionic liquid to a collagenesis-boosting peptide as a general tool to produce dual-action constructs is addressed. To this end, the same chemical approach leading to the aforementioned IL-PP4 conjugates was applied to a couple of tripeptides used in the cosmeceutics industry, GHK and KVK, which do not possess antimicrobial activity on their own. Relevantly, it was possible to demonstrate that IL-GHK and IL-KVK conjugates have potent antibacterial activity against antibiotic-susceptible and multidrug resistant clinical isolates of both Gram-positive and Gram-negative bacteria. Both the antibiofilm and the collagenesis-boosting properties of these conjugates will be timely tested.

Chapter 3 – CONCLUSION AND FUTURE PERSPECTIVES

This closing chapter presents the main conclusions that could be drawn from the work undertaken, and the perspectives on how it should be advanced in the near future.

Annexes

Compilation of all relevant supplementary data to support Chapter 2.

References cited in this section

- [1] Leong HN, Kurup A, Tan MY, Kwa ALH, Liau KH, Wilcox MH. Management of complicated skin and soft tissue infections with a special focus on the role of newer antibiotics. *Infect Drug Resist.* **2018**;11:1959-74.
- [2] Eckmann C, Lawson W, Nathwani D, Solem CT, Stephens JM, Macahilig C, et al. Antibiotic treatment patterns across Europe in patients with complicated skin and soft-tissue infections due to meticillin-resistant *Staphylococcus aureus*: a plea for implementation of early switch and early discharge criteria. *Int. J. Antimicrob. Agents.* **2014**;44:56-64.
- [3] Vale de Macedo GHR, Costa GDE, Oliveira ER, Damasceno GV, Mendonça JSP, Silva LDS, et al. Interplay between ESKAPE Pathogens and Immunity in Skin Infections: An Overview of the Major Determinants of Virulence and Antibiotic Resistance. *Pathogens* (Basel, Switzerland). **2021**;10.
- [4] Bassetti M, Righi E, Pecori D, Tillotson G. Delafloxacin: an improved fluoroquinolone developed through advanced molecular engineering. *Future Microbiol.* **2018**;13:1081-94.
- [5] Dhar Y, Han Y. Current developments in biofilm treatments: Wound and implant infections. *Engineered Regeneration.* **2020**;1:64-75.
- [6] Schultz G, Bjarnsholt T, James GA, Leaper DJ, McBain AJ, Malone M, et al. Consensus guidelines for the identification and treatment of biofilms in chronic nonhealing wounds. *Wound Repair Regen.* **2017**;25:744-57.
- [7] Moretta A, Scieuzo C, Petrone AM, Salvia R, Manniello MD, Franco A, et al. Antimicrobial Peptides: A New Hope in Biomedical and Pharmaceutical Fields. *Front Cell Infect Microbiol.* **2021**;11.
- [8] Williamson DA, Carter GP, Howden BP. Current and Emerging Topical Antibacterials and Antiseptics: Agents, Action, and Resistance Patterns. *Clin Microbiol Rev.* **2017**;30:827-60.

Chapter 1. Introduction

Review article 1

Wound-Healing Peptides for Treatment of Chronic Diabetic Foot Ulcers and Other Infected Skin Injuries

Ana Gomes, Cátia Teixeira, Ricardo Ferraz, Cristina Prudêncio and Paula Gomes

Molecules **2017**, *22*, 1743

doi: 10.3390/molecules22101743

Abstract

As the incidence of diabetes continues to increase in the western world, the prevalence of chronic wounds related to this condition continues to be a major focus of wound care research. Additionally, over 50% of chronic wounds exhibit signs and symptoms that are consistent with localized bacterial biofilms underlying severe infections that contribute to tissue destruction, delayed wound-healing and other serious complications. Most current biomedical approaches for advanced wound care aim at providing antimicrobial protection to the open wound together with a matrix scaffold (often collagen-based) to boost reestablishment of the skin tissue. Therefore, the present review is focused on the efforts that have been made over the past years to find peptides possessing wound-healing properties, towards the development of new and effective wound care treatments for diabetic foot ulcers and other skin and soft tissue infections.

Keywords: antimicrobial; chronic infection; diabetes; peptides; ulcers; wound-healing; skin and soft tissue infections (SSTI)

1. Introduction

In 2015, 8.8% of the adult population worldwide is estimated to have diabetes. This figure is projected to rise to 10.4% by the year 2040, which underpins an alarming public health problem that needs urgent control [1]. Diabetes is a chronic disease that stems from pancreas dysfunction, impairing normal production of insulin which leads to high, and also fluctuating, blood glucose levels. This, in turn, leads to an imbalance in the homeostatic regulation of the body, causing serious health problems such as blindness, kidney failure, heart disease, venous insufficiency and peripheral neuropathy [1]. A combination of these latter two conditions with improper footwear leads to loss of sensitivity in the feet of diabetic patients, which facilitates installment of chronically-infected lesions, the so-called diabetic foot ulcers (DFU), ultimately leading to limb amputations [1,2]. According to a 2012 report from the European Wound Management Agency, about 2% of the population in developed countries suffers from non-healing injuries like DFU, and it is estimated that 25–50% of hospital beds are occupied by patients with such an acute wound. DFU are the most common reason for hospitalization of people with diabetes, and about one in every six people with diabetes develops at least one foot ulcer during their lifetime. Moreover, 40–70% of all lower extremity amputations are related to diabetes, of which 85% are preceded by DFU [3]. In addition, the quite recent “EpiCast report: Diabetic Foot Ulcers-Epidemiology Forecast to 2025”—based on data from seven countries, namely US, France, Germany, Italy, Spain, UK and Japan—points to over 1 million cases in 2015 and an estimated increase rate of 4.03% per year, which will expectedly lead to approximately 1.5 million cases by 2025 [4].

Management of DFU should always start with prevention, through policies for foot inspection and use of custom therapeutic footwear to prevent ulceration, as DFU are tremendously difficult to heal once installed [3,5]. The wound-healing process comprises complex biological mechanisms triggered by the injury, involving four key steps: (i) hemostasis; (ii) inflammation; (iii) proliferation and (iv) tissue remodeling (Figure 1). In each of these processes, several cellular and biophysical events occur, such as monocyte differentiation to macrophage, neutrophil infiltration and lymphocyte infiltration, in the inflammation stage; or increased angiogenesis and re-epithelialization by fibroblast migration, during the proliferation phase. These events may be impaired by different factors, which can be divided into local and systemic ones. As a local factor, we can take the example of wound oxygenation, which influences healing. In what concerns systemic factors, we can take the example of a diabetic patient and respective individual characteristics: age, nutrition or other diseases (e.g., fibrosis, uremia), which may give

rise to problems that impair healing, such as hypoxia, dysfunction in fibroblasts and epidermal cells, or incorrect angiogenesis, among others [6].

Management of DFU requires good knowledge of their complexity for a correct classification of stage and severity; for instance, it is important to distinguish sloughy and necrotic tissues (severe infection) from granulation and epithelializing ones (healing wound). Treatment of severe DFU usually requires initial debridement to remove sloughy and necrotic tissue, followed by the use of scaffolds to support skin rebuilding, along with efficient antimicrobial protection through a combination of several topical agents [7,8]. Collagen-based wound dressings have been used as healing scaffolds in both skin burns and DFU with overall promising results [9]. Those are based on animal collagens (bovine, porcine, equine), acting as biocompatible wound/environment barriers, rather than replacing or promoting formation of endogenous (human) collagen. While efficient production of either recombinant human collagen or “perfect” collagen-like peptides remains an unmet goal [10], an alternative sensible option may be the design of formulations comprising collagen-boosting instead of collagen-like components. Actually, collagen-boosting peptides, e.g., Matrikines® like KTTKS, are already used in cosmetics to promote extracellular matrix (ECM) production, rebuilding structure and restoring all functions of healthy skin [11,12]. Moreover, many antimicrobial peptides (AMP) can also act as wound-healing peptides (WHP), thus displaying the dual antimicrobial and tissue-regenerating properties highly desired in novel topical formulations for treatment of DFU [13,14].

Today, the therapeutic value of AMP against infectious pathogens, including antibiotic-resistant strains, is well recognized [15,16], and topical formulations of AMP have reached either the market, like polymyxins or gramicidins, or clinical trials, such as Pexiganan (Locilex®), Lytixar, OP-145 or Novexatin, for cutaneous, ocular and otorhinolaryngological infections [17,18]. Understandably, the literature is quite rich in both original reports and comprehensive reviews on AMP of either natural or synthetic origin, addressing all relevant aspects in the topic, from discovery or design to spectrum of activity, mechanisms of action, patents, and clinical applications [15–22]. In contrast, literature focusing on the wound-healing properties exhibited by some peptides is still emergent. As such, and considering the undeniable timeliness of the topic, this review is

focused on peptides whose wound-healing effects may find application in the topical treatment of DFU and other skin and soft tissue infections (SSTI).

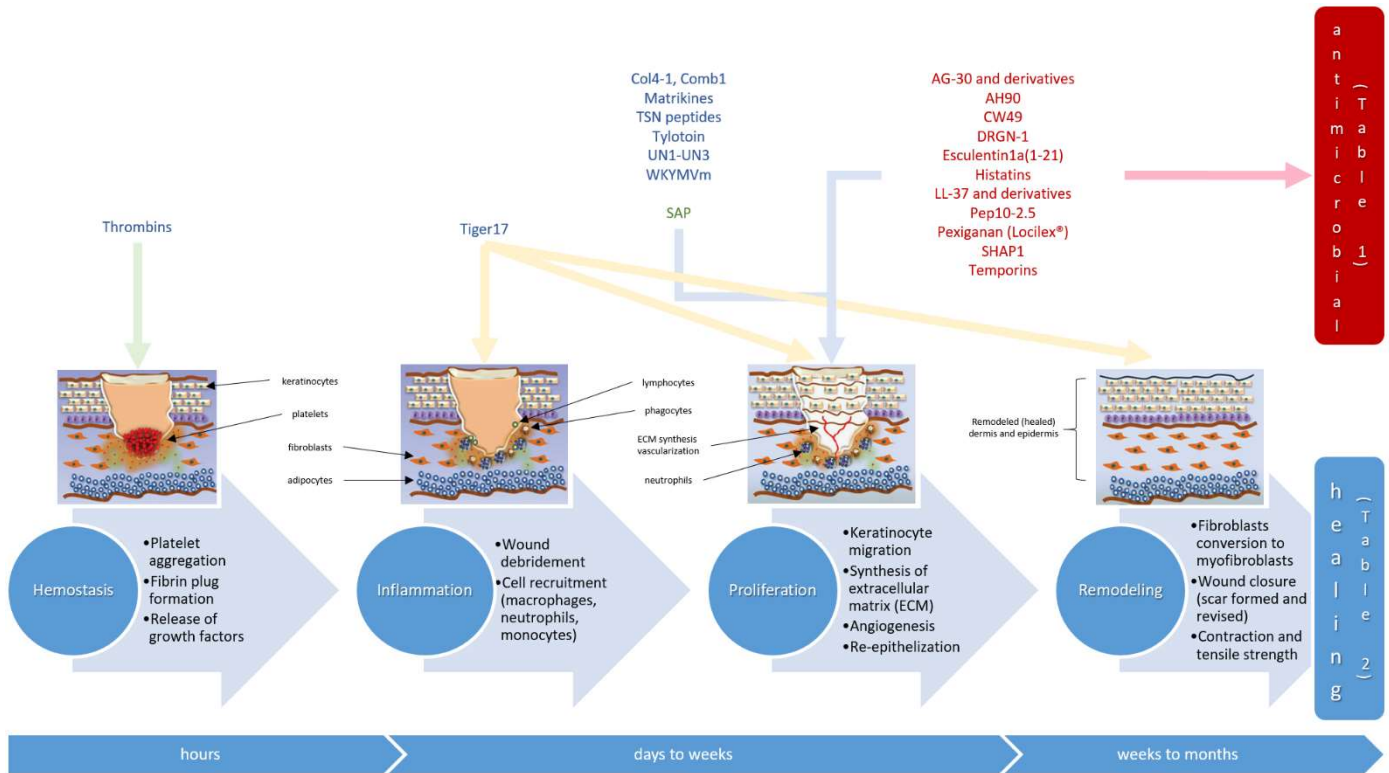


Figure 1. Schematic overview of major stages of wound-healing. Most wound-healing peptides were found to act on one or more biochemical pathways of the proliferation stage, although a few have been reported to act either on earlier stages (e.g., thrombin-related peptides) or on multiple stages (e.g., Tiger17)—see text. Examples of wound-healing antimicrobial peptides (Table 1) in dark red, and of wound-healing non-antimicrobial peptides (Table 2) in dark blue; SAP: self-assembling peptides (green).

2. Wound-Healing Antimicrobial Peptides

Commonly, non-healing wounds are simultaneously colonized by different bacteria; bacterial species most frequently isolated from such wounds typically include *Staphylococcus aureus* (93.5%), *Enterococcus faecalis* (71.1%) and *Pseudomonas aeruginosa* (52.2%), among others [23]. In healthy individuals, the innate immune system produces gene-encoded AMP that control proliferation of pathogenic microorganisms on skin, while triggering a signaling cascade in response to injuries [24]. However, due to their typical venous insufficiency and other diabetes-related conditions, diabetic patients are not immunocompetent, which favors formation of bacterial biofilms that are highly refractive to current antibiotics [25]. Topical application of AMP on the infected injury may overcome this barrier, as AMP have shown the ability to: (i) prevent infection due to their

antimicrobial activity; (ii) reduce the pro-inflammatory response; (iii) promote cell migration and proliferation [14]. As such, many known AMP have been reported to also display wound-healing properties; some of which are addressed in this section and compiled in Table 1.

Table 1. Examples of peptides with dual antimicrobial and wound-healing properties. Peptide sequences are displayed using the one-letter amino acid code, as per the IUPAC-IUBMB Joint Commission on Biochemical Nomenclature rules.

| Peptide Name | Peptide Sequence | Reference |
|---------------------------------------|---|-----------|
| AG30 | MLSLIFLHRLKSMRKRLDRKLRLWHRKNYP | [26] |
| AG30/5C | MLKLIFLHRLKRMKRLKRKLRLWHRKRYK | |
| AH90 | ATAWDFGPHGLLPIRPIRIRPLCG | [27] |
| CW49 | APFRMGICTTN | [28] |
| Cys-KR12 | KRIVKRIKKWLR | [29] |
| Esculentin-1a(1-21) | GIFSKLAGKKIKNLLISGLKG | [30] |
| hBD-1 | DHYNCVSSGGQCLYSACPIFTKIQGTTCYRGKAKCCK (Disulfide bridges: 5-34, 12-27, 17-35) | [31,32] |
| hBD-2 | GIGDPVTCLKSGAICHVPVFCPRRYKQIGTCGLPGTKCCKKP (Disulfide bridges: 8-37, 15-30, 20-38) | |
| hBD-3 | GIINTLQKYCRVRGGRCVAVLSCLPKKEEQIGKCSTRGRKCCR RKK (Disulfide bridges: 11-40, 18-33, 23-41) | |
| hBD-4 | ELDRICGYGTARCRKKCRSQEYRIGRCPNTYACCLRK (Disulfide bridges: 6-33; 13-27; 17-34) | |
| Histatin-1 | <u>D</u> SEKRRHHGYRRKFHEKHSHSHREFPFYGDYGSNYLYDN1 | [33] |
| Histatin-2 | RKFHEKHSHSHREFPFYGDYGSNYLYDN | |
| Histatin-3 | DSHAKRRHHGYKRFHEKHSHSHRGYRSNYLYDN | |
| IDR-1018 | VRLIVAVRIWRR | [34] |
| LL-37 | LLGDFFRKSKEKIGKEFKRIVQRIKDFLRNLPRTES | [35] |
| MSI-78 (pexiganan)² | GIGKFLKKAKKFGKAFVKILKK | [36] |
| Pep19-2.5 | GCKKYRRFRWKFKGKFWFWG | [37] |
| PLL-37 | PLLGDFFRKSKEKIGKEFKRIVQRIKDFLRNLPRTES | [38] |
| SHAP1 | APKAMKLLKLLKLQKGGI | [39] |
| SR-0007 | MLKLIFLHRLKRMKRLKRK | [40] |
| SR-0379 | MLKLIFLHRLKRMKRLkRK ¹ | |
| Temporin A | FLPLIGRVLSGIL | [41] |
| Temporin B | LLPIVGNLLKSLI | |

¹ Lowercase letters indicate D-amino acid residues; Peptide highlighted in bold was entered into clinical trials for its assessment in the treatment of diabetic foot ulcers; S: phosphoserine.

2.1. Human-Based Defence Peptides

Human genetically-encoded AMP that are expressed on skin, among other tissues, as part of the body's immune response to injury include the well-known human β -defensins (hBDs) [31], cathelicidin LL-37 [35] and dermcidins [42]. One of the endogenous AMP that gained more attention in the context of DFU healing was human cathelicidin LL-37. In 2008, Carretero et al. reported that *in vivo* adenoviral transfer of LL-37 AMP to excisional wounds in diabetic-ob/ob mice (mutant obese mice used as animal models of type II diabetes), improved re-epithelialization and granulation tissue formation [43]. This was later confirmed by Ramos et al., who tested both LL-37 and PLL-37 (LL-37 derivative with an N-terminal proline) *in vitro* and *in vivo* skin lesions with impaired wound-healing, as they found both peptides to promote re-epithelialization and angiogenesis [38]. Shortly after, in 2012, LL-37 was compared to another AMP, the innate defense regulator peptide 1018 (IDR-1018) [34]. The study revealed that IDR-1018 was less toxic than LL-37 *in vitro*, and demonstrated significantly accelerated wound-healing in *S. aureus*-infected porcine and non-diabetic murine wounds. However, the study showed that IDR-1018 neither accelerated healing nor differed significantly from LL-37 with regards to bacterial colonization of DFU in diabetic mice. Moreover, diabetes seemed to have a negative impact on mice immune responses, eventually blocking signaling pathways where innate defense regulators like LL-37 and IDR-1018 are involved [34].

Also in 2012, Rivas-Santiago et al. used primary cell cultures from DFU to study the expression and role of human endogenous AMP, including LL-37 and β -defensins hBD-1, hBD-2, hBD-3 and hBD-4, in wound-healing [32]. These authors found that although β -defensins are expressed in DFU, their production seems to be not high enough to contain infection and promote proper wound-healing. The study also showed that when compared with healthy skin, DFU biopsies presented low or null levels of LL-37, which might contribute to DFU pathogenesis. Moreover, topically-applied exogenous LL-37, i.e., peptide added to the wound site, was degraded by proteases presented in the wound [32]. These observations were later confirmed by McCrudden et al., who found that topically-administered LL-37 was unstable in the microenvironment of DFU, probably by the action of both host and bacterial proteinases that cleaved LL-37 into smaller peptides [44]. The authors thus suggested that to overcome the degradation process, LL-37 analogues should be developed to include some simple structural modifications, e.g., the replacement of α - by β -amino acids [44]. While investigating how to increase concentration of endogenous LL-37 at wound sites, Gonzalez-Curiel et al.

found that the addition of 1,25-dihydroxyvitamin D3 and L-isoleucine to the wound increased production of hBD-2 and LL-37 during the regeneration process in primary cultures of cells from DFU sites [45]. All these promising findings on the wound-healing potential of LL-37 have culminated with this peptide entering clinical trials for venous leg ulcer treatment in 2014; results thereof suggested that LL-37 is safe and has a significant dose-response activity, although in no case could total wound closure be observed, which was attributed to the short trial period [46]. More recently, Song et al. immobilized an LL-37 derivative, Cys-KR12, onto electrospun silk fibroin (SF) nanofiber membranes [29]. Cys-KR12 includes residues 18–29 of the LL-37 sequence, and was chosen due to its antimicrobial and anti-biofilm action against four different bacterial strains (*S. aureus*, *S. epidermidis*, *E. coli* and *P. aeruginosa*). The peptide-modified membranes were found to promote proliferation of keratinocytes, fibroblasts and monocytes, all important players in the wound-healing process [29]. Taken together, results gathered thus far on the potential of LL-37 towards the healing of DFU and other SSTI are quite promising, regarding the use of LL-37 both for adequate formulation as a topical antimicrobial agent and for the coating of biomedical materials amenable to being applied as wound dressings.

At the same time as LL-37 was gaining more attention in the context of DFU healing, Nishikawa and co-workers developed an antimicrobial helical peptide—AG-30 (Table 1)—with angiogenic properties potentially similar to those of LL-37 [47]. However, since peptides are typically unstable in vivo, they engaged in the synthesis of AG30-related peptides as leads for clinical applications [26]. In this context, and in order to stabilize the AG-30 helical structure, the design strategy consisted of replacing several neutral residues (specifically proline, asparagine and serine) with cationic or hydrophobic amino acids [26]. As a result, AG30/5C (Table 1), where five residues of the original sequence AG30 were replaced by cationic amino acids, displayed improved antimicrobial and angiogenic activities when tested in vivo in a diabetic mouse wound-healing model with methicillin-resistant *S. aureus* (MRSA) infection [26]. By further evaluating the metabolic stability of AG30/5C, Tomioka et al. found that SR-0007 (Table 1), a 20-residue metabolite, stimulated cell proliferation at levels similar to those of the parent peptide [40]. However, as SR-0007 was rapidly degraded by human serum at 37 °C, a native L-lysine residue was replaced by its D enantiomer, yielding an analogue (SR-0379, Table 1) with significantly improved stability [40]. This peptide displayed antimicrobial activity against several distinct bacteria, including drug-resistant strains, and significantly accelerated wound-healing on a full-thickness wound model with a skin

flap in a streptozotocin-induced diabetic rat model, holding great promise in the treatment of MRSA-positive diabetic ulcers [40].

Motivated by the fact that wounds in the oral cavity heal much faster than skin lesions, Oudhoff and co-workers engaged in a study to assess the factors in human saliva that contribute to its wound-healing properties [33]. By testing saliva and saliva protein fractions in an *in vitro* model for wound closure using an epithelial cell line, these researchers identified histatin-1 (Hst1), histatin-2 (Hst2) and histatin-3 (Hst3) (Table 1), rather than epidermal growth factor as primarily thought, as the major wound-healing factors in human saliva [33]. This finding was quite surprising because salivary histatins had, up to then, only been implicated in the antifungal saliva weaponry. Still, Oudhoff et al. found that the two activities—cell-stimulating and antimicrobial—are very distinct in their mode of action as the latter is independent of the chirality of the peptide and occurs via disruption of the phospholipid membrane of the target cell [33]. On the contrary, the stimulating activity on host cells involves a stereospecific interaction with a putative membrane receptor [33]. To ascertain whether histatins have potential applicability as general wound-healing agents, Oudhoff et al. further tested those peptides in a tissue-engineered epidermal skin that closely resembled native healthy skin [48]; the study showed that histatins enhance re-epithelialization by stimulating cell spreading and migration, but do not increase cell proliferation [48]. Additionally, by comparing the wound-healing activities of Hst1 fragments that differ by 2-residue-stepwise truncation in the N- or C-terminus, or both, they found that the region comprising residues 20 to 32 (SHREFPFYGDYGS) is critical for peptide biological activity [48]. Interestingly, they have also shown that constraining the conformation of Hst1 by cyclization resulted in a 1000-fold increase of its wound-healing activity in the *in vitro* wound-scratch assay [48]. These results have clearly established synthetic histatins as potential candidates for novel topical medicines to treat skin lesions, namely chronic ones. However, peptide-based therapeutics for wound-healing stimulation are sensitive to several proteases present in the chronic wound bed. Therefore, Boink et al. tested the *in vitro* stability of some histatin variants (Hst1, Hst2, cyclic Hst1 and minimal active domain of Hst1) in diluted chronic wound extracts, in order to determine if those peptides would remain stable in chronic ulcers long enough to exert their migration-stimulating activity [49]. The results showed a breakdown of ca. 50% for Hst1 and Hst2, and of ca. 20% for the minimal active domain of Hst1 and cyclic Hst1, in 8 h. As such, Boink et al. suggested that further investigations on the potential of the latter two Hst1 derivatives as topical therapeutics for SSTI should be undertaken [49].

2.2. Amphibian-Based Defence Peptides

Pexiganan, also known as MSI-78, is another AMP whose therapeutic potential against DFU has been widely recognized; it is a 22-residue linear cationic AMP analogue to magainins, which are natural AMP isolated from the skin of the African clawed frog *Xenopus laevis* [50]. By the turn of the century, 1% pexiganan acetate cream was proposed for topical treatment of mild to moderate DFU, as an alternative to the classical ofloxacin-based oral antibiotherapy [36]. Indeed, in the course of earlier clinical trials where patients were treated either with pexiganan cream or with active oral antibiotics, and compared with the placebo group, pexiganan's performance proved it to be a possible alternative to oral antibiotics [51]. These findings triggered several research works focused on pexiganan and related peptides [52–54], and motivated the patenting of a 0.8% pexiganan acetate cream (Locilex®, earlier known as Cytalex) in several countries, by the pharmaceutical company Dipexium Pharmaceuticals, Inc. (Houston, TX, USA) in 2016 [55,56]. However, Locilex® failed approval by the competent international organizations, on the grounds that its efficacy was not proven superior to that of classic oral antibiotics in any of the clinical trials undertaken to date, which include a recent Phase 3 clinical trial promoted by Dipexium, now merged with PLx Pharma, Inc. (Houston, TX, USA) [57]. Remarkably, AMP such as magainins and related peptides, like pexiganan, are not the only wound-healing peptides found, or inspired, in secretions from the skin of amphibians including frogs, toads and salamanders [58,59]. In fact, many known AMP are of amphibian origin, and most of them have revealed wound-healing properties, possibly contributing to the fast wound re-epithelialization typical in many species of the *Amphibia* class: e.g., the process takes less than 10 h in salamanders, while needing two to three days in mammalians. In agreement with this assumption, Liu et al. were able to isolate a new short (11 residues) AMP from the skin of *Odorrana grahami* frogs, CW49 (Table 1), which was found to promote angiogenesis while preventing excessive anti-inflammatory response when tested in DFU [14,28]. Interestingly, the same authors isolated another wound-healing AMP, peptide AH90 (Table 1), from the skin of the same frog species, and found it to have wound-healing activity, although this was not tested in DFU [27].

In addition to the above, there is a large collection of AMP of diverse origin whose healing ability has been demonstrated on SSTI other than DFU. Regardless of having been tested in DFU or not, any wound-healing AMP encloses the potential to become a useful topical agent against this particular type of SSTI. In this connection, one such recent example is the work performed by Di Grazia and co-workers, who have reported

that temporins A and B (Table 1), two short AMP isolated from the skin of the European red frog *Rana temporaria*, promote in vitro wound-healing in a monolayer of immortalized human keratinocytes (HaCaT cells) [41]. Moreover, they have also found that both temporins, although to different extents, can reduce the number of *S. aureus* bacteria inside HaCaT keratinocytes in a dose-dependent manner. Temporin B, the most active of both peptides, kills ca. 80% of the bacterial cells at its highest non-cytotoxic dosage (16 μM) within 2 h [41]. These results suggested that temporins are attractive candidates for the generation of new therapeutics to treat *S. aureus*-related SSTI. The same researchers further reported that esculentin-1a(1-21) (Table 1), a derivative of AMP esculentin-1a isolated from the skin of the frog *Rana esculenta*, significantly stimulates migration of HaCaT cells over a wide range of peptide concentrations (0.025–4 μM), being notably more efficient than LL-37 [30]. This observation, allied with the established antimicrobial activity for the same esculentin-1a derivative, namely its high anti-*Pseudomonas* activity, makes this AMP a promising wound-healing promoter, especially against chronic, often *Pseudomonas*-infected, skin ulcers [30].

2.3. Synthetic Peptides

Synthetic AMP, designed for improved structural stability and high antimicrobial activity under physiological conditions, have been found to also present wound-healing activity [37,39]. One example was reported in 2014 by Kim et al., who demonstrated that SHAP1 (Table 1), a synthetic AMP with potent antimicrobial activity against fungi and bacteria in the presence of 200 mM NaCl, also produces wound closure both in vitro and in vivo [39]. Indeed, SHAP1 displayed stronger in vitro wound-healing activity than LL-37 by inducing HaCaT cell migration, which was reported to occur via transactivation of the epidermal growth factor receptor [39]. One important finding was that topical application of SHAP1 accelerated closure and healing of full-thickness excisional wounds in mice at the same low concentration (1 μM) that was used in in vitro assays [39], indicating that SHAP1 stands as a highly promising topical agent for treatment of SSTI.

In 2016, Pfalzgraff et al. also assessed the potential of Pep19-2.5 (Table 1), a synthetic anti-lipopolysaccharide peptide presenting antimicrobial activity for Gram-negative and Gram-positive bacteria, for therapeutic applications in bacterial skin infections [37]. The results showed that Pep19-2.5 displays low in vitro cytotoxicity in primary human keratinocytes and fibroblasts. Furthermore, it reduces the immune and inflammatory responses in skin cells stimulated with potent bacterial pathogenicity

factors, with concurrent potent stimulation of keratinocyte migration; this suggests that Pep19-2.5 might be a promising option for the treatment of acute and chronic wounds most commonly infected with *S. aureus* and *P. aeruginosa* [37].

An interesting and very recent example of a highly promising synthetic wound-healing AMP is that of DRGN-1, developed by Chung et al. who sought inspiration in a histone H1-derived peptide from the Komodo dragon (*Varanus komodoensis*) [60]. DRGN-1 was found to display potent antimicrobial and anti-biofilm activity, and to permeabilise bacterial membranes, while being equally able to promote significant tissue regeneration ability in vitro; according to the authors, based on data from scratch wound closure assays, the wound-healing ability of DRGN-1 is due to promotion of migration of HEKa keratinocytes and activation of the EGFRSTAT1/3 pathway. The potential of DRGN-1 as a wound-healing agent was further confirmed in vivo, as the peptide was able to significantly enhance wound-healing in both uninfected and mixed biofilm (*P. aeruginosa* and *S. aureus*)-infected murine wounds [60].

3. Tissue Regeneration Peptides

As seen in the previous section, some AMP are considered promising agents for wound care because, in addition to their intrinsic antimicrobial activity, they can influence different mechanisms of the wound-healing orchestration such as inflammation, epithelialization, tissue granulation and remodeling. Still, although some wound-healing peptides do not display antimicrobial properties, some of them have great therapeutic potential towards healing chronically-infected wounds, like DFU and other SSTI. Recent examples of such peptides are summarized in Table 2 and next reviewed.

Table 2. Examples of non-antimicrobial peptides presenting wound-healing activity. Peptide sequences are displayed using the one-letter amino acid code, as per the IUPAC-IUBMB Joint Commission on Biochemical Nomenclature rules.

| Peptide Name | Peptide Sequence | Reference |
|---------------|-------------------------------------|-----------|
| Ac-PGP | <i>N</i> -acetylated-PGP | [61] |
| BioGHK | Biotinylated-GHK | [62] |
| Col4-1 | MFRKPIPSTVKA | [63] |
| Comb1 | DINECEIGAPAGEETEVTVEGLEPG | |
| E1 | GETGPAGPAGPIGPVARGPAGPQGPRGDKGETGEQ | [64] |
| Tiger17 | WCKPKPKPRCH | [65] |
| TP-508 | AGYKPDEGKRGDACEGDSGGPFV | [66] |
| TSN1 | NFQGVQNRVFGTP | |
| TSN2 | MENAELDVPIQSVFTR | |
| TSN3 | NTDNIYPESSC | |
| TSN4 | PYLGYYVK | |
| TSN5 | MQTVAQLFKTVSSLSLST | |
| TSN6 | HSPDIQLQKGLTFEPIQIK | |
| TSN7 | STITQPYKTLNNARSP | |
| TSN8 | RPGPSPEGTGQSYNY | |
| TSN9 | MENAELDPPYLGYYVK | |
| TSN10 | TGQSYNQYSQRPYLGYYVFK | [67] |
| TSN11 | LYGQTPLETL | |
| TSN12 | ELADSPAIEG | |
| TSN13 | LYGQTPLETLELADSPAIEG | |
| TSN14 | VSGNTVEYALPTLE | |
| TSN15 | LDSPTAPTQSTALTWRP | |
| TSN16 | LDGSAPGPLYTGSAIDF | |
| TSN17 | GSEGVRSRSG | |
| TSN18 | QPQPLPSPGVGGKN | |
| Tylotoin | KCVRQNNKRVCK | [59] |
| UN1 | ELLESYIDGR | |
| UN2 | TATSEYQTFNPR | [68] |
| UN3 | ELLESYIDGRPTATSEYQTFNPR | |
| WKYMVm | WKYMVm ¹ | [69] |

¹ Lowercase letters indicate D-amino acid residues; Peptide highlighted in bold was entered into clinical trials for its assessment in the treatment of diabetic foot ulcers.

3.1. Human-Based Peptides

One class of non-antimicrobial peptides that promote tissue repair is that of thrombins. Thrombins and related peptides are known for their important role in blood clotting, whereby they promote cleavage of soluble fibrinogen into fibrins. TP-508 (Table 2) is a peptide fragment of the receptor-binding domain of native human thrombin, whose saline solutions, also known as Chrysalin®, have been tested for DFU healing. In the course of phase I and phase II clinical trials, Chrysalin® showed 45–72% of complete healing compared with the placebo group, without relevant local wound reactions or observable adverse effects [66].

In 2011, Demidova-Rice et al. reported that several bioactive peptides, liberated from capillary endothelial cells degradation by *Clostridium histolyticum* collagenase, facilitate endothelial responses to injury and angiogenesis [63]. Two peptides in

particular, Col4-1 and Comb1 (Table 2), when used at 10–100 nM, were found to increase rates of microvascular endothelial cell proliferation by up to 47% and in vitro angiogenesis by 200% when compared with serum-stimulated controls [63]. These researchers later assessed whether these peptides could improve wound-healing in vivo, and found that Comb1, when applied into impaired cranial dermal wounds created in cyclophosphamide-treated mice, could stimulate the rate of wound closure [68]. Moreover, they identified three novel peptides derived from human platelet-rich plasma, UN1-UN3 (Table 2), which stimulate epithelial migration as well as angiogenesis in vitro [68]. Yet, UN3 was shown as the most potent stimulator of cellular responses, by causing a 250% increase in angiogenic response, a 50% increase in endothelial proliferation and a tripling of epithelial cell migration in response to injury [68]. Additionally, results of in vivo experiments where UN3 and Comb1 were added together to impaired cranial wounds in cyclophosphamide-treated mice showed an increase of the number of blood vessels present in the wound beds. Interestingly, combining the peptides before addition to the cells in vitro did not produce any synergistic effects [68]. Motivated by these promising findings, the same authors further investigated whether Comb1 and UN3 could stimulate healing in a diabetic porcine model highly reminiscent of human healing impairments in type-I and -II diabetes [70]. This study revealed that both peptides significantly improve angiogenesis and re-epithelialization in diabetic porcine wounds when compared to saline-treated controls. Although the authors found that both peptides stimulate wound closure through upregulation of cytokines and multiple reparative growth factors, their precise mechanism of action remains unclear [70]. At the same time, this same research group postulated that Santyl®, a FDA approved debridement agent containing *Clostridial* collagenases and other non-specific proteases, could also provide healing through the production of bioactive peptides able to stimulate tissue and cellular responses to injury [67]. Indeed, they were able to identify several bioactive peptides (TSN1-8, TSN11-12, TSN14-17; Table 2) when doses of Santyl® collagenase, comparable to those used clinically, were applied to human dermally-derived capillary ECM [67]. Interestingly, there is little overlap between these peptides, arising from Santyl® collagenase, and the endothelial peptides (Comb1 and UN3) produced by purified *Clostridial* collagenase. The authors next found that the individual peptides released from Santyl®-digested ECM, as well as the combinatorial peptides (TSN9-10, TSN13 and TSN18; Table 2) induced wound-healing in vitro, highlighting TSN6 and TSN18 as those having the greatest stimulatory activity over all cell types and parameters assayed [67]. When they further applied these peptides to healing-impaired cyclophosphamide-treated mice, they observed that 0.1 mg/mL TSN18 stimulated a

>100% increase of epithelial responses, while 1.0 mg/mL TSN18 produced a 60% increase in epithelialization when compared to controls [67]. Overall, these results indicate TSN18 as an exciting new opportunity for creating advanced wound-healing therapies. In parallel to the aforementioned studies, the therapeutic effect of WKYMMVm (Table 2)—a short synthetic agonist of formyl peptide receptor 2 known to promote angiogenesis—on DFU was investigated by Kwon and co-workers [69]. As such, this peptide was tested in cutaneous wounds of streptozotocin-induced diabetic rats, where it was found to accelerate angiogenesis, granulation tissue formation, re-epithelialization and wound closure, suggesting its potential usefulness to treat chronic cutaneous wounds [69].

Findings like the above motivated other approaches to non-antimicrobial wound-healing peptides that sought inspiration on platelet-rich plasma and ECM proteins. This gave rise to new classes of wound-healing peptides, such as the so-called matrikines, matricryptins, and laminin analogues, among others. Matrikines, i.e., ECM-inspired peptides, have been described to promote collagen formation in fibroblasts, leading to skin repair, but their therapeutic potential has also been surveyed for cancer, inflammation and neurodegenerative disorders, as well as for cosmetic applications [12,71]. A typical matrikine is tripeptide GHK (Figure 2), well known for its ability to form copper(II) complexes, anti-inflammatory and wound-healing properties, as well as for its capacity to improve skin density and firmness [62]. In 2005, Arul et al. reported that a biotinylated GHK derivative (BioGHK, Figure 2) incorporated in a collagen matrix showed better wound-healing in vivo than the collagen matrix alone [72].

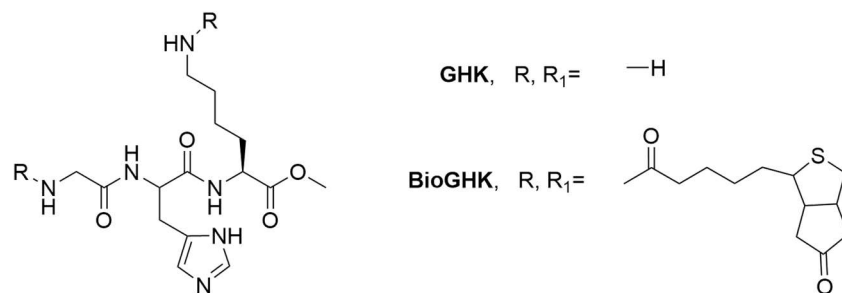


Figure 2. Structure of the matrikine tripeptide GHK and its biotinylated derivative BioGHK [62,72].

Later on, the same group tested the same system in skin wounds of diabetic rats, and were able to observe an increase in collagen biosynthesis, along with activation and growth of fibroblasts [73]. This result is rather encouraging regarding the potential of matrikines for topical treatment of DFU and other SSTI. A very recent example of the tremendous potential of matrikines regards the work from Banerjee and co-workers, who have investigated the wound-healing ability of E1 (Table 2), a cryptic peptide derived from bovine Achilles tendon collagen [64]. The results showed that topical administration of E1 at a concentration of 60 μM greatly increased wound closure throughout the duration of the experiment, while >90% tissue restoration was observed on the 12th day, when compared to 55% restoration for the control group [64]. Similarly, Kwon and co-workers have explored the effects of Ac-PGP (Table 2), a peptide derived from degradation of collagen, on cutaneous wound-healing and neovascularization in human endothelial progenitor cells (hEPCs) [61]: following enhanced proliferation, migration and tube-forming activity of hEPCs upon in vitro treatment with Ac-PGP, in vivo assays further demonstrated that topical application of this peptide accelerates wound closure by 11 to 23% with promotion of neovascularization, in comparison with the control group [61]. These results suggested that Ac-PGP should be pursued as a potential therapeutic product for treatment of chronic and acute wounds.

3.2. Amphibian-Based Peptides

As mentioned in the previous section, several AMP of diverse origin, namely those isolated from amphibians, have demonstrated healing properties on different wound types in addition to their intrinsic antimicrobial activity. Interestingly, some peptides derived from such AMP were found to lose their antimicrobial ability, while retaining strong wound-healing activity. One such example is that of tylotoin (Table 2), a short peptide derived from the C-terminus of a cathelicidin extracted from the skin of the *Tylotriton verrucosus* salamander [59]. Mu et al. found that, although tylotoin did not show any antimicrobial activity, it significantly improved in vitro proliferation and migration of vascular endothelial cells, fibroblasts and keratinocytes [59]. In vivo assays further demonstrated the wound-healing ability of tylotoin as its topical application markedly enhanced wound-healing in a mouse model of full-thickness skin wounding. The same work further revealed that tylotoin also promotes the release of transforming growth factor β 1 and interleukin 6, which are essential in the wound-healing process, thus suggesting tylotoin as a valuable template for development of novel wound-healing agents [59]. Similarly, Tang and co-workers have reported Tiger17 (Table 2), a cyclic peptide derived from the AMP tigerinin isolated from skin secretions of the *Fejervarya*

cancrivora frog, as a non-AMP with excellent skin wound-healing ability [65]. These authors found that topical application of Tiger17 greatly diminished wound closure time in a full-thickness skin wound mouse model, and that the peptide was involved in three stages of wound-healing: (i) the inflammatory stage, by recruiting macrophages to the wound site; (ii) re-epithelialization and granulation tissue formation, by promoting proliferation and migration of both keratinocytes and fibroblasts; and (iii) the tissue remodeling phase, by activating mitogen-activated protein kinases signaling pathways and by stimulating the release of interleukin 6 and transforming growth factor β 1 in murine macrophages [65]. Altogether, these results clearly indicate Tiger17 as a promising wound-healing lead.

3.3. Self-Assembling Peptides

One other quite promising class of peptides for wound-healing, given their ability to promote tissue regeneration, is that of self-assembling peptides (SAP). Peptide amphiphiles (hybrid compounds that comprise both an alkyl and a peptide tail) are examples of important SAP-based scaffolds for tissue engineering [74]. By virtue of their properties, SAP and other peptides able to promote tissue regeneration can assume an important role in wound-healing, being potentially useful for topical treatment of DFU and other SSTI. In 2006, Ranjagam et al. developed peptide amphiphile PA (Figure 3) [75], based on the consensus sequence XBBBXXBX (X = hydrophobic amino acid; B = basic amino acid) earlier designed for heparin-binding [69], since heparin plays an important role in nanostructure nucleation into macromolecules able to efficiently activate, and bind to, angiogenic growth factors.

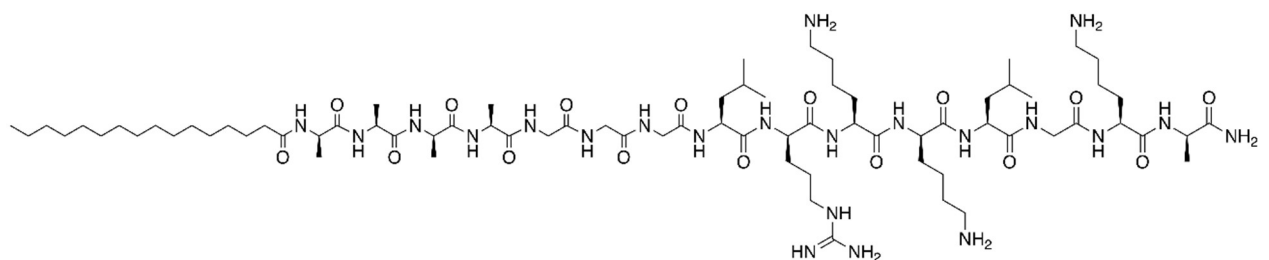


Figure 3. Structure of the peptide amphiphile PA, developed by Ranjagam and co-workers [75].

The authors observed that aqueous mixtures of PA, heparin, vascular endothelial, and fibroblast 2 growth factors, were able to promote extensive blood vessel formation in vivo. Moreover, they found a peptide sequence that self-assembled into nanofibers upon interaction with heparin [75]. Later, Mammadov et al. developed a heparin-mimetic PA (hmPA, Figure 4), designed to display the angiogenesis-promoting properties of heparin, without the need to add this glucosaminoglycan, or exogenous growth factors; their working hypothesis was confirmed, as hmPA was able, by itself, to promote angiogenesis and tissue regeneration [76].

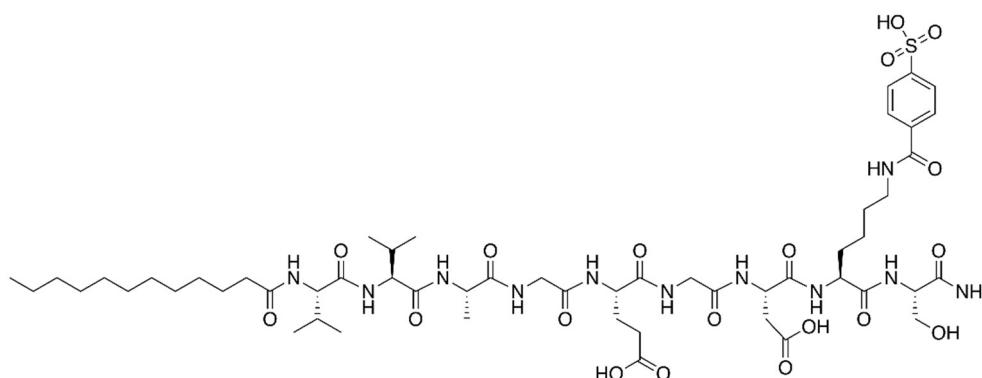


Figure 4. Structure of the heparin-mimetic peptide amphiphile developed by Mammadov and co-workers [76].

These findings motivated Senturk et al. to test the ability of hmPA-based gels to heal diabetic wounds, in streptozotocin-induced diabetic mice; results confirmed the bioactive gels to have a key role in both inflammation and proliferation phases of wound-healing, by promoting angiogenesis, re-epithelialization and inflammatory response [77].

Several wound dressings are available in the clinics for superficial treatment of mild to severe wounds, starting from simple gauze up to highly complex materials which include films, hydrogels, foams, hydrofibers and engineered skin substitutes [78]. Current biomedical approaches for advanced wound care aim at providing scaffolds to support skin rebuilding, along with efficient antimicrobial protection, given that over 50% of chronic SSTI are associated with bacterial biofilms underlying severe infections that contribute to tissue destruction, delayed wound-healing, and other complications [8]. Under certain conditions, SAP self-assemble to produce supramolecular structures; hence, several groups have looked into their use as appropriate scaffolds for the production of wound dressings. This is a broad and fascinating topic that has been reviewed in great detail by others, and is therefore outside the scope of the present review [79,80]. Still, some recent examples of peptide-based wound dressings will be addressed next.

4. Peptide-Based Wound Dressings

Collagen-based wound dressings have been used as healing scaffolds in both skin burns and DFU with overall promising outcomes, as collagen plays an important role in tissue regeneration, stabilizing the vascular and cellular components in the wound [9,81]. Collagen applied in saline-moistened gauze has been tested in DFU, with encouraging results [82]. Recently, Choudhary et al. reported the wound-healing activity of collagen-based dressings as compared to conventional (dry) dressings; the study included 60 diabetic patients, most of them with traumatic foot injuries followed by installation of a diabetic ulcer, with those being treated with the collagen-based dressing showing more pronounced regression of infection and appearance of granulation tissue [83]. Still, collagen alone cannot provide antimicrobial protection, which motivated research initiatives where collagen was mixed with other biocompatible biopolymers, such as chitosan, whose intrinsic antimicrobial and wound-healing properties are very well known [84]. Other polysaccharides (e.g., dextrin and alginate) and AMP have also been considered as relevant components to build new generation wound dressings able to simultaneously provide (i) scaffold for skin rebuilding; (ii) tissue-regeneration; and (iii) antimicrobial action [85,86]. In this context, Xiao et al. recently prepared a chitosan-collagen hydrogel grafted with peptide QHREDGS, an angiopoietin-1 derivative that promotes migration of human primary keratinocytes and activates kinase B Akt, thus being potentially useful against DFU. The peptide-tethered hydrogel was proven to (i) protect keratinocytes against hydrogen peroxide stress in a dose-dependent manner; (ii) promote migration of keratinocytes from both healthy and diabetic people; (iii) accelerate and enhance wound closure; and (iv) promote angiogenesis, as the total number of blood vessels was greater in the peptide-hydrogel treated wounds, although no difference was observed in vessel density or size inside the wound [87].

Cellulose and derivatives embedding wound-healing peptides have also been tested on DFU. One recent example concerns the use of peptide ACT1 (RQPKIWFPNRRKPWKKRPRPDDLEI), a mimetic of the C-terminus of connexin43, a protein identified as potentially useful for treatment of DFU. ACT1 was embedded in a hydroxyethyl-cellulose hydrogel, and this formulation was topically applied on DFU [88]. As the results demonstrated the peptide-embedded gel to expedite re-epithelization while being non-toxic [88], a randomized phase III clinical trial was initiated in July 2015 to determine whether this gel (Granexin) is safe and effective in the treatment of diabetic foot ulcers [89].

Whole cells have also been regarded as potentially useful “biomaterials” for topical delivery of wound-healing peptides. Very recently, Seo et al. tested a combination of peptide exendin-4 (HGEGTFTSDLSKQMEEEAVRLFIEWLKNGGPSSGAPPPS), a glucagon-like peptide-1 receptor agonist, with adipose tissue-derived stem cells, for healing DFU on db/db mice, which are animal models of diabetic dyslipidemia. This combination performed significantly better than local injection of only the stem cells, but it remains to be determined whether the effect of the combination is synergistic or additive [90].

5. Conclusions

Wound-healing is a complex multi-stage process towards the rebuilding of skin. In many diverse pathologies, such as diabetes mellitus, normal wound-healing is impaired, which may lead to severe complications, from ulcers to chronic skin infections. As such, advanced biomedical approaches for effective wound care aim at providing antimicrobial protection to the open wound together with promotion of fast and correct healing, so that a fully functional healthy skin can be swiftly restored. Today, the therapeutic value of AMP against infectious pathogens, including parasites, is well recognized, and several topical formulations containing AMP are currently in clinical use. In parallel, a plethora of wound-healing peptides and peptide-grafted dressings has been unveiled in the past few years, holding great promise for novel strategies for treatment of chronically infected wounds. The development of peptide-based materials for topical application in DFU and other SSTI is still in its infancy, and its future seems quite promising and exciting: based on findings made thus far, future joint efforts of peptide scientists and healthcare professionals working in this area will likely produce innovative solutions to this health issue, increasingly prevalent worldwide.

Acknowledgments: The authors thank Fundação para a Ciência e Tecnologia (FCT, Portugal) for funding research unit LAQV-REQUIMTE (ref. UID/QUI/50006/2013), and for Ph.D. grant PD/BD/135073/2017 to AG. Thanks are also due to “Comissão de Coordenação e Desenvolvimento Regional do Norte (CCDR-N)/NORTE2020/Portugal 2020” for funding through project DESignBIOtechHealth (ref. Norte-01-0145-FEDER-000024).

Author Contributions: A.G. and C.T. carried out the bibliographic research, primary selection of literature reports that fitted the scope of the review paper, and organized and wrote the manuscript in consultation with P.G. R.F. and C.P. provided critical feedback

and helped shape the manuscript, whose final version was thoroughly and critically reviewed by P.G.

References

1. International Diabetes Federation. *IDF Diabetes Atlas*, 7th ed.; IDF: Brussels, Belgium, **2015**.
2. Uckay, I.; Gariani, K.; Pataky, Z.; Lipsky, B.A. Diabetic foot infections: State-of-the-art. *Diabetes Obes. Metab.* **2014**, *16*, 305–316.
3. Alexiadou, K.; Doupis, J. Management of diabetic foot ulcers. *Diabetes Ther.* **2012**, *3*,
4. Epicast Report: Diabetic Foot Ulcers-Epidemiology Forecast to 2025. Available online: https://www.researchandmarkets.com/research/l9r7nt/epicast_report (accessed on 28 July 2017).
5. Hingorani, A.; LaMuraglia, G.M.; Henke, P.; Meissner, M.H.; Loretz, L.; Zinszer, K.M.; Driver, V.R.; Frykberg, R.; Carman, T.L.; Marston, W.; et al. The management of diabetic foot: A clinical practice guideline by the society for vascular surgery in collaboration with the american podiatric medical association and the society for vascular medicine. *J. Vasc. Surg.* **2016**, *63*, 3S–21S.
6. Guo, S.; Dipietro, L.A. Factors affecting wound healing. *J. Dent. Res.* **2010**, *89*, 219–229.
7. Kavitha, K.V.; Tiwari, S.; Purandare, V.B.; Khedkar, S.; Bhosale, S.S.; Unnikrishnan, A.G. Choice of wound care in diabetic foot ulcer: A practical approach. *World J. Diabetes* **2014**, *5*, 546–556.
8. Murphy, P.S.; Evans, G.R. Advances in wound healing: A review of current wound healing products. *Plast. Surg. Int.* **2012**, *2012*, 190436.
9. Holmes, C.; Wrobel, J.S.; Maceachern, M.P.; Boles, B.R. Collagen-based wound dressings for the treatment of diabetes-related foot ulcers: A systematic review. *Diabetes Metab. Syndr. Obes.* **2013**, *6*, 17–29.
10. He, L.; Theato, P. Collagen and collagen mimetic peptide conjugates in polymer science. *Eur. Polym. J.* **2013**, *49*, 2986–2997.

11. Abu Samah, N.H.; Heard, C.M. Topically applied kttks: A review. *Int. J. Cosmet. Sci.* **2011**, *33*, 483–490.
12. Ricard-Blum, S.; Salza, R. Matricryptins and matrikines: Biologically active fragments of the extracellular matrix. *Exp. Dermatol.* **2014**, *23*, 457–463.
13. Hancock, R.E.; Haney, E.F.; Gill, E.E. The immunology of host defence peptides: Beyond antimicrobial activity. *Nat. Rev. Immunol.* **2016**, *16*, 321–334.
14. Mangoni, M.L.; McDermott, A.M.; Zasloff, M. Antimicrobial peptides and wound healing: Biological and therapeutic considerations. *Exp. Dermatol.* **2016**, *25*, 167–173.
15. Mahlapuu, M.; Hakansson, J.; Ringstad, L.; Bjorn, C. Antimicrobial peptides: An emerging category of therapeutic agents. *Front. Cell. Infect. Microbiol.* **2016**, *6*, 194.
16. Mai, S.; Mauger, M.T.; Niu, L.N.; Barnes, J.B.; Kao, S.; Bergeron, B.E.; Ling, J.Q.; Tay, F.R. Potential applications of antimicrobial peptides and their mimics in combating caries and pulpal infections. *Acta Biomater.* **2017**, *49*, 16.
17. Fox, J.L. Antimicrobial peptides stage a comeback. *Nat. Biotechnol.* **2013**, *31*, 379.
18. Fosgerau, K.; Hoffmann, T. Peptide therapeutics: Current status and future directions. *Drug Discov. Today* **2015**, *20*, 122–128.
19. Kang, H.K.; Kim, C.; Seo, C.H.; Park, Y. The therapeutic applications of antimicrobial peptides (AMPs): A patent review. *J. Microbiol.* **2017**, *55*, 1.
20. Fuente-Nuñez, C.; Silva, O.N.; Lu, T.K.; Franco, O.L. Antimicrobial peptides: role in human disease and potential as immunotherapies. *Pharmacol. Ther.* **2017**, *178*, 132.
21. Mishra, B.; Reiling, S.; Zarena, D.; Wang, G. Host defense antimicrobial peptides as antibiotics: Design and application strategies. *Curr. Opin. Chem. Biol.* **2017**, *38*, 87.
22. Travkova, O.; Moehwald, H.; Berezinski, G. The interaction of antimicrobial peptides with membranes. *Adv. Colloid Interface Sci.* **2017**, *247*, 521.
23. Suleman, L. Extracellular bacterial proteases in chronic wounds: A potential therapeutic target? *Adv. Wound Care New Rochelle* **2016**, *5*, 455–463.
24. Barton, G.M. A calculated response: Control of inflammation by the innate immune system. *J. Clin. Investig.* **2008**, *118*, 413–420.

25. Zhao, G.; Usui, M.L.; Lippman, S.I.; James, G.A.; Stewart, P.S.; Fleckman, P.; Olerud, J.E. Biofilms and inflammation in chronic wounds. *Adv. Wound Care* **2013**, *2*, 389–399.
26. Nakagami, H.; Nishikawa, T.; Tamura, N.; Maeda, A.; Hibino, H.; Mochizuki, M.; Shimosato, T.; Moriya, T.; Morishita, R.; Tamai, K.; et al. Modification of a novel angiogenic peptide, ag30, for the development of novel therapeutic agents. *J. Cell. Mol. Med.* **2012**, *16*, 1629–1639.
27. Liu, H.; Mu, L.; Tang, J.; Shen, C.; Gao, C.; Rong, M.; Zhang, Z.; Liu, J.; Wu, X.; Yu, H.; et al. A potential wound healing-promoting peptide from frog skin. *Int. J. Biochem. Cell Biol.* **2014**, *49*, 32–41.
28. Liu, H.; Duan, Z.; Tang, J.; Lv, Q.; Rong, M.; Lai, R. A short peptide from frog skin accelerates diabetic wound healing. *FEBS J.* **2014**, *281*, 4633–4643.
29. Song, D.W.; Kim, S.H.; Kim, H.H.; Lee, K.H.; Ki, C.S.; Park, Y.H. Multi-biofunction of antimicrobial peptide-immobilized silk fibroin nanofiber membrane: Implications for wound healing. *Acta Biomater.* **2016**, *39*, 146–155.
30. Di Grazia, A.; Cappiello, F.; Imanishi, A.; Mastrofrancesco, A.; Picardo, M.; Paus, R.; Mangoni, M.L. The frog skin-derived antimicrobial peptide esculentin-1a(1-21) NH₂ promotes the migration of human hacaT keratinocytes in an egf receptor-dependent manner: A novel promoter of human skin wound healing? *PLoS ONE* **2015**, *10*, e0128663.
31. Dhople, V.; Krukemeyer, A.; Ramamoorthy, A. The human beta-defensin-3, an antibacterial peptide with multiple biological functions. *Biochim. Biophys. Acta* **2006**, *1758*, 1499–1512.
32. Rivas-Santiago, B.; Trujillo, V.; Montoya, A.; Gonzalez-Curiel, I.; Castaneda-Delgado, J.; Cardenas, A.; Rincon, K.; Hernandez, M.L.; Hernandez-Pando, R. Expression of antimicrobial peptides in diabetic foot ulcer. *J. Dermatol. Sci.* **2012**, *65*, 19–26.
33. Oudhoff, M.J.; Bolscher, J.G.; Nazmi, K.; Kalay, H.; van't Hof, W.; Amerongen, A.V.; Veerman, E.C. Histatins are the major wound-closure stimulating factors in human saliva as identified in a cell culture assay. *FASEB J.* **2008**, *22*, 3805–3812.

34. Steinstraesser, L.; Hirsch, T.; Schulte, M.; Kueckelhaus, M.; Jacobsen, F.; Mersch, E.A.; Stricker, I.; Afacan, N.; Jenssen, H.; Hancock, R.E.; et al. Innate defense regulator peptide 1018 in wound healing and wound infection. *PLoS ONE* **2012**, *7*, e39373.
35. Duplantier, A.J.; van Hoek, M.L. The human cathelicidin antimicrobial peptide II-37 as a potential treatment for polymicrobial infected wounds. *Front. Immunol.* **2013**, *4*, 143.
36. Lamb, H.M.; Wiseman, L.R. Pexiganan acetate. *Drugs* **1998**, *56*, 1047–1052.
37. Pfalzgraff, A.; Heinbockel, L.; Su, Q.; Gutschmann, T.; Brandenburg, K.; Weindl, G. Synthetic antimicrobial and Ips-neutralising peptides suppress inflammatory and immune responses in skin cells and promote keratinocyte migration. *Sci. Rep.* **2016**, *6*, 31577.
38. Ramos, R.; Silva, J.P.; Rodrigues, A.C.; Costa, R.; Guardao, L.; Schmitt, F.; Soares, R.; Vilanova, M.; Domingues, L.; Gama, M. Wound healing activity of the human antimicrobial peptide II37. *Peptides* **2011**, *32*, 1469–1476.
39. Kim, D.J.; Lee, Y.W.; Park, M.K.; Shin, J.R.; Lim, K.J.; Cho, J.H.; Kim, S.C. Efficacy of the designer antimicrobial peptide shap1 in wound healing and wound infection. *Amino Acids* **2014**, *46*, 2333–2343.
40. Tomioka, H.; Nakagami, H.; Tenma, A.; Saito, Y.; Kaga, T.; Kanamori, T.; Tamura, N.; Tomono, K.; Kaneda, Y.; Morishita, R. Novel anti-microbial peptide SR-0379 accelerates wound healing via the PI3 kinase/Akt/mTOR pathway. *PLoS ONE* **2014**, *9*, e92597.
41. Di Grazia, A.; Luca, V.; Segev-Zarko, L.A.; Shai, Y.; Mangoni, M.L. Temporins a and b stimulate migration of hacat keratinocytes and kill intracellular Staphylococcus aureus. *Antimicrob. Agents Chemother.* **2014**, *58*, 2520–2527.
42. Yamasaki, K.; Gallo, R.L. Antimicrobial peptides in human skin disease. *Eur. J. Dermatol.* **2008**, *18*, 11–21.
43. Carretero, M.; Escámez, M.J.; García, M.; Duarte, B.; Holguín, A.; Retamosa, L.; Jorcano, J.L.; Ríó, M.d.; Larcher, F. In vitro and in vivo wound healing-promoting activities of human cathelicidin II-37. *J. Investig. Dermatol.* **2008**, *128*, 223–236.
44. McCrudden, M.T.C.; McLean, D.T.F.; Zhou, M.; Shaw, J.; Linden, G.J.; Irwin, C.R.; Lundy, F.T. The host defence peptide II-37 is susceptible to proteolytic degradation by

wound fluid isolated from foot ulcers of diabetic patients. *Int. J. Pept. Res. Ther.* **2014**, *20*, 457–464.

45. Gonzalez-Curiel, I.; Trujillo, V.; Montoya-Rosales, A.; Rincon, K.; Rivas-Calderon, B.; deHaro-Acosta, J.; Marin-Luevano, P.; Lozano-Lopez, D.; Enciso-Moreno, J.A.; Rivas-Santiago, B. 1,25-dihydroxyvitamin D3 induces LL-37 and HBD-2 production in keratinocytes from diabetic foot ulcers promoting wound healing: An in vitro model. *PLoS ONE* **2014**, *9*, e111355.

46. Gronberg, A.; Mahlapuu, M.; Stahle, M.; Whately-Smith, C.; Rollman, O. Treatment with LL-37 is safe and effective in enhancing healing of hard-to-heal venous leg ulcers: A randomized, placebo-controlled clinical trial. *Wound Repair Regen.* **2014**, *22*, 613–621.

47. Nishikawa, T.; Nakagami, H.; Maeda, A.; Morishita, R.; Miyazaki, N.; Ogawa, T.; Tabata, Y.; Kikuchi, Y.; Hayashi, H.; Tatsu, Y.; et al. Development of a novel antimicrobial peptide, ag-30, with angiogenic properties. *J. Cell. Mol. Med.* **2009**, *13*, 535–546.

48. Oudhoff, M.J.; Kroeze, K.L.; Nazmi, K.; van den Keijbus, P.A.; van't Hof, W.; Fernandez-Borja, M.; Hordijk, P.L.; Gibbs, S.; Bolscher, J.G.; Veerman, E.C. Structure-activity analysis of histatin, a potent wound healing peptide from human saliva: Cyclization of histatin potentiates molar activity 1000-fold. *FASEB J.* **2009**, *23*, 3928–3935.

49. Boink, M.A.; Roffel, S.; Nazmi, K.; van Montfrans, C.; Bolscher, J.G.; Gefen, A.; Veerman, E.C.; Gibbs, S. The influence of chronic wound extracts on inflammatory cytokine and histatin stability. *PLoS ONE* **2016**, *11*, e0152613.

50. Zasloff, M. Magainins, a class of antimicrobial peptides from xenopus skin: Isolation, characterization of two active forms, and partial cDNA sequence of a precursor. *Proc. Natl. Acad. Sci. USA* **1987**, *84*, 5449–5453.

51. Lipsky, B.A.; Holroyd, K.J.; Zasloff, M. Topical versus systemic antimicrobial therapy for treating mildly infected diabetic foot ulcers: A randomized, controlled, double-blinded, multicenter trial of pexiganan cream. *Clin. Infect. Dis* **2008**, *47*, 1537–1545.

52. Gottler, L.M.; Ramamoorthy, A. Structure, membrane orientation, mechanism, and function of pexiganan—a highly potent antimicrobial peptide designed from magainin. *Biochim. Biophys. Acta* **2009**, *1788*, 1680–1686.

53. Monteiro, C.; Fernandes, M.; Pinheiro, M.; Maia, S.; Seabra, C.L.; Ferreira-da-Silva, F.; Costa, F.; Reis, S.; Gomes, P.; Martins, M.C. Antimicrobial properties of membrane-active dodecapeptides derived from msi-78. *Biochim. Biophys. Acta* **2015**, 1848, 1139–1146.
54. Monteiro, C.; Pinheiro, M.; Fernandes, M.; Maia, S.; Seabra, C.L.; Ferreira-da-Silva, F.; Reis, S.; Gomes, P.; Martins, M.C. A 17-mer membrane-active msi-78 derivative with improved selectivity toward bacterial cells. *Mol. Pharm.* **2015**, 12, 2904–2911.
55. Newswire, P. Dipexium Pharmaceuticals Announces Issuance of Locilex® Patent by European Union. Available online: <http://www.prnewswire.com/news-releases/dipexium-pharmaceuticals-announces-issuance-of-locilex-patent-by-european-union-300323725.html> (accessed on 28 July 2017).
56. Newswire, P. Dipexium Pharmaceuticals Announces Issuance of Locilex® Patent in Japan. Available online: <http://www.prnewswire.com/news-releases/dipexium-pharmaceuticals-announces-issuance-of-locilex-patent-in-japan-300241111.html> (accessed on 28 July 2017).
57. Newswire, P. Dipexium Announces Top-Line Data from Onestep Phase 3 Trials with Locilex® in Mild Diabetic Foot Infection Did not Meet Primary Clinical Endpoint of Superiority Versus Vehicle Plus Standardized Wound Care. Available online: <http://www.prnewswire.com/news-releases/dipexium-announces-top-line-data-from-onestep-phase-3-trials-with-locilex-in-mild-diabetic-foot-infection-did-not-meet-primary-clinical-endpoint-of-superiority-versus-vehicle-plus-standardized-wound-care-300350302.html> (accessed on 28 July 2017).
58. Ladram, A.; Nicolas, P. Antimicrobial peptides from frog skin: Biodiversity and therapeutic promises. *Front. Biosci.* **2016**, 21, 1341–1371.
59. Mu, L.; Tang, J.; Liu, H.; Shen, C.; Rong, M.; Zhang, Z.; Lai, R. A potential wound-healing-promoting peptide from salamander skin. *FASEB J.* **2014**, 28, 3919–3929.
60. Chung, E.M.C.; Dean, S.N.; Propst, C.N.; Bishop, B.M.; van Hoek, M.L. Komodo dragon-inspired peptide DRGN-1 promotes wound-healing of a mixed-biofilm infected wound. *NPJ Biofilms Microb.* **2017**, 3, 9.
61. Kwon, Y.W.; Heo, S.C.; Lee, T.W.; Park, G.T.; Yoon, J.W.; Jang, I.H.; Kim, S.C.; Ko, H.C.; Ryu, Y.; Kang, H.; et al. N-acetylated proline-glycine-proline accelerates cutaneous

wound healing and neovascularization by human endothelial progenitor cells. *Sci. Rep.* **2017**, *7*, 43057.

62. Pickart, L.; Vasquez-Soltero, J.M.; Margolina, A. GHK peptide as a natural modulator of multiple cellular pathways in skin regeneration. *Biomed. Res. Int.* **2015**, *2015*, 648108.

63. Demidova-Rice, T.N.; Geevarghese, A.; Herman, I.M. Bioactive peptides derived from vascular endothelial cell extracellular matrices promote microvascular morphogenesis and wound healing in vitro. *Wound Repair Regen.* **2011**, *19*, 59–70.

64. Banerjee, P.; Suguna, L.; Shanthi, C. Wound healing activity of a collagen-derived cryptic peptide. *Amino Acids* **2015**, *47*, 317–328.

65. Tang, J.; Liu, H.; Gao, C.; Mu, L.; Yang, S.; Rong, M.; Zhang, Z.; Liu, J.; Ding, Q.; Lai, R. A small peptide with potential ability to promote wound healing. *PLoS ONE* **2014**, *9*, e92082.

66. Fife, C.; Mader, J.T.; Stone, J.; Brill, L.; Satterfield, K.; Norfleet, A.; Zwernemann, A.; Ryaby, J.T.; Carney, D.H. Thrombin peptide chrysalin® stimulates healing of diabetic foot ulcers in a placebo-controlled phase i/ii study. *Wound Repair Regen.* **2007**, *15*, 23–34.

67. Sheets, A.R.; Demidova-Rice, T.N.; Shi, L.; Ronfard, V.; Grover, K.V.; Herman, I.M. Identification and characterization of novel matrix-derived bioactive peptides: A role for collagenase from santyl(r) ointment in post-debridement wound healing? *PLoS ONE* **2016**, *11*, e0159598.

68. Demidova-Rice, T.N.; Wolf, L.; Deckenback, J.; Hamblin, M.R.; Herman, I.M. Human platelet-rich plasma- and extracellular matrix-derived peptides promote impaired cutaneous wound healing in vivo. *PLoS ONE* **2012**, *7*, e32146.

69. Kwon, Y.W.; Heo, S.C.; Jang, I.H.; Jeong, G.O.; Yoon, J.W.; Mun, J.H.; Kim, J.H. Stimulation of cutaneous wound healing by an fpr2-specific peptide agonist wkyvmv. *Wound Repair Regen.* **2015**, *23*, 575–582.

70. Sheets, A.R.; Massey, C.J.; Cronk, S.M.; lafrati, M.D.; Herman, I.M. Matrix- and plasma-derived peptides promote tissue-specific injury responses and wound healing in diabetic swine. *J. Transl. Med.* **2016**, *14*, 197.

71. Maquart, F.X.; Pasco, S.; Ramont, L.; Hornebeck, W.; Monboisse, J.C. An introduction to matrikines: Extracellular matrix-derived peptides which regulate cell activity. Implication in tumor invasion. *Crit. Rev. Oncol. Hematol.* **2004**, *49*, 199–202.
72. Arul, V.; Gopinath, D.; Gomathi, K.; Jayakumar, R. Biotinylated ghk peptide incorporated collagenous matrix: A novel biomaterial for dermal wound healing in rats. *J. Biomed. Mater. Res. B Appl. Biomater.* **2005**, *73*, 383–391.
73. Arul, V.; Kartha, R.; Jayakumar, R. A therapeutic approach for diabetic wound healing using biotinylated ghk incorporated collagen matrices. *Life Sci.* **2007**, *80*, 275–284.
74. Loo, Y.; Goktas, M.; Tekinay, A.B.; Guler, M.O.; Hauser, C.A.; Mitraki, A. Self-assembled proteins and peptides as scaffolds for tissue regeneration. *Adv. Healthc. Mater.* **2015**, *4*, 2557–2586.
75. Rajangam, K.; Behanna, H.A.; Hui, M.J.; Han, X.; Hulvat, J.F.; Lomasney, J.W.; Stupp, S.I. Heparin binding nanostructures to promote growth of blood vessels. *Nano Lett.* **2006**, *6*, 2086–2090.
76. Mammadov, R.; Mammadov, B.; Toksoz, S.; Aydin, B.; Yagci, R.; Tekinay, A.B.; Guler, M.O. Heparin mimetic peptide nanofibers promote angiogenesis. *Biomacromolecules* **2011**, *12*, 3508–3519.
77. Senturk, B.; Mercan, S.; Delibasi, T.; Guler, M.O.; Tekinay, A.B. Angiogenic peptide nanofibers improve wound healing in stz-induced diabetic rats. *ACS Biomater. Sci. Eng.* **2016**, *2*, 1180–1189.
78. Han, G.; Ceilley, R. Chronic wound healing: A review of current management and treatments. *Adv. Ther.* **2017**, *34*, 599–610.
79. Chattopadhyay, S.; Raines, R.T. Review collagen-based biomaterials for wound healing. *Biopolymers* **2014**, *101*, 821–833.
80. Vigneswaran, Y.; Han, H.; De Loera, R.; Wen, Y.; Zhang, X.; Sun, T.; Mora-Solano, C.; Collier, J.H. Peptide biomaterials raising adaptive immune responses in wound healing contexts. *J. Biomed. Mater. Res. Part A* **2016**, *104*, 1853–1862.
81. Cereceres, S.; Touchet, T.; Browning, M.B.; Smith, C.; Rivera, J.; Höök, M.; Whitfield-Cargile, C.; Russell, B.; Cosgriff-Hernandez, E. Chronic wound dressings based on collagen-mimetic proteins. *Adv. Wound Care* **2015**, *4*, 444–456.

82. Collagenase Diabetic Foot Ulcer Study Group. Tallis, A.; Motley, T.A.; Wunderlich, R.P.; Dickerson, J.E., Jr.; Waycaster, C.; Slade, H.B. Clinical and economic assessment of diabetic foot ulcer debridement with collagenase: Results of a randomized controlled study. *Clin. Ther.* **2013**, *35*, 1805–1820.
83. Choudary, D.; Insen, S.G.; Goyal, S.; Chhabra, U.; Singal, G. A comparative study of collagen dressings versus conventional dressings in wound healing in chronic ulcers. *J. Evol. Med. Dent. Sci.* **2017**, *6*, 361–363.
84. Ahmed, S.; Ikram, S. Chitosan based scaffolds and their applications in wound healing. *Achiev. Life Sci.* **2016**, *10*, 27–37.
85. Chen, S.; Zhang, M.; Shao, X.; Wang, X.; Zhang, L.; Xu, P.; Zhong, W.; Zhang, L.; Xing, M.; Zhang, L. A laminin mimetic peptide sikvav-conjugated chitosan hydrogel promoting wound healing by enhancing angiogenesis, re-epithelialization and collagen deposition. *J. Mater. Chem. B* **2015**, *3*, 6798–6804.
86. Silva, J.P.; Dhall, S.; Garcia, M.; Chan, A.; Costa, C.; Gama, M.; Martins-Green, M. Improved burn wound healing by the antimicrobial peptide llkkk18 released from conjugates with dextrin embedded in a carbopol gel. *Acta Biomater.* **2015**, *26*, 249–262.
87. Xiao, Y.; Reis, L.A.; Feric, N.; Knee, E.J.; Gu, J.; Cao, S.; Laschinger, C.; Londono, C.; Antolovich, J.; McGuigan, A.P.; et al. Diabetic wound regeneration using peptide-modified hydrogels to target re-epithelialization. *Proc. Natl. Acad. Sci. USA* **2016**, *113*, E5792–E5801.
88. Grek, C.L.; Prasad, G.M.; Viswanathan, V.; Armstrong, D.G.; Gourdie, R.G.; Ghatnekar, G.S. Topical administration of a connexin43-based peptide augments healing of chronic neuropathic diabetic foot ulcers: A multicenter, randomized trial. *Wound Repair Regen.* **2015**, *23*, 203–212.
89. National Library of Medicine. A Study of Granexin Gel in the Treatment of Diabetic Foot Ulcer (Identifier: Nct02667327). Available online: <https://clinicaltrials.gov/ct2/show/NCT02667327> (accessed on 14 June 2017).
90. Seo, E.; Lim, J.S.; Jun, J.B.; Choi, W.; Hong, I.S.; Jun, H.S. Exendin-4 in combination with adipose-derived stem cells promotes angiogenesis and improves diabetic wound healing. *J. Transl. Med.* **2017**, *15*, 35.

Review article 2

The emerging role of ionic liquid-based approaches for enhanced skin permeation of bioactive molecules: a snapshot of the past couple of years

Ana Gomes, Luísa Aguiar, Ricardo Ferraz, Cátia Teixeira, and Paula Gomes

Submitted at International Journal of Molecular Sciences

Abstract

Topical and transdermal delivery systems are of undeniable significance and ubiquity in healthcare, to facilitate the delivery of active pharmaceutical ingredients, respectively, onto or across the skin to enter the systemic circulation. From ancient ointments and potions to modern micro/nanotechnological devices, a variety of approaches has been explored over the ages to improve the skin permeation of diverse medicines and cosmetics. Amongst the latest investigational dermal permeation enhancers, ionic liquids have been gaining momentum, and the recent years have been prolific in this regard. As such, this review offers an overview of current methods for enhancing percutaneous permeation, highlighting selected reports where ionic liquid-based approaches have been investigated for this purpose. Future perspectives on use of ionic liquids for topical delivery of bioactive peptides are also presented.

Keywords: active pharmaceutical ingredients, cosmetics, ionic liquids, peptides, transdermal delivery, wound-healing, complicated skin and soft tissue infections

1. Introduction

The skin is the largest organ of the human body, protecting it against external aggressions while keeping its thermal regulation and conveying the sense of touch. Being such a formidable barrier, the skin may also be a considerable obstacle for efficient topical absorption and/or transdermal delivery of many active pharmaceutical ingredients (APIs) and cosmetics. Different strategies have been developed and explored over time to promote dermal permeation of different substances, since empirical formulations developed over five thousand years ago in the ancient Egyptian and Babylonian civilizations, to cutting-edge physical, chemical and [bio]nanotechnological approaches that build on current knowledge of skin physiology, composition, and permeation routes (Figure 1) [1-3].

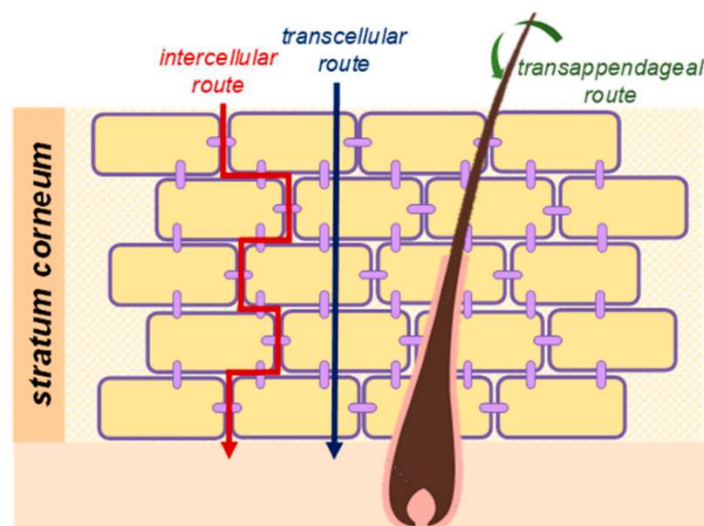


Figure 1. Schematic view of skin permeation pathways: intercellular, transcellular, and transappendageal [4].

The evolution of strategies to promote percutaneous penetration of molecules and macromolecules is schematized in Figure 2 [5]. Current approaches encompass: (i) physical methods like sonophoresis, iontophoresis, thermophoresis, electroporation, laser microporation, thermal ablation, or microneedle patches [6]; (ii) encapsulation in suitable nanocarriers (nanoparticles, liposomes, ethosomes, niosomes, aquasomes, etc.) [7]; (iii) use of engineered controlled-release and/or stimuli-responsive materials (patches, wearable devices, and others) [8]; and (iv) addition of [bio]chemical permeation enhancers (e.g., fatty acids, fatty alcohols, alcohols, glycols, peptides, [bio]surfactants) [9]. Some of these methods can be combined, to further improve the percutaneous permeation efficiency.

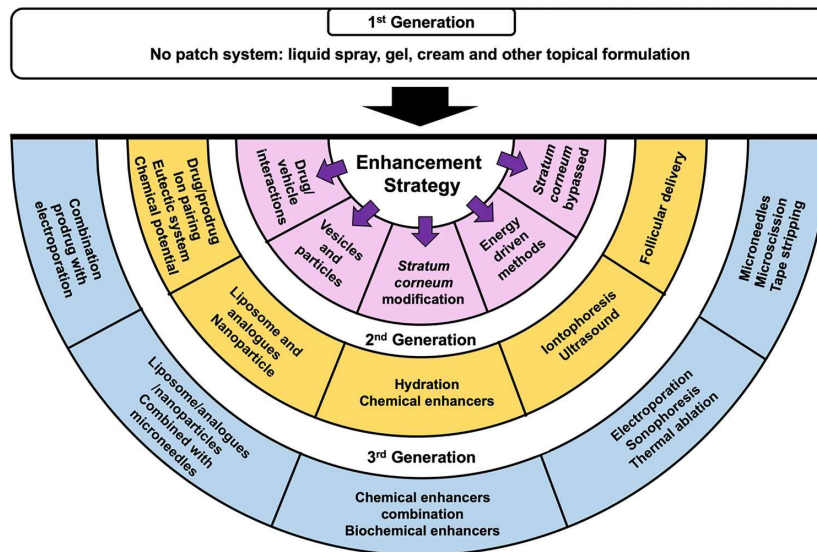
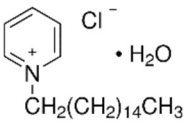
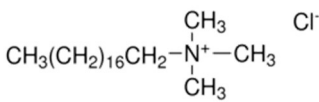
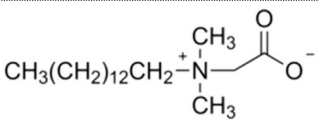
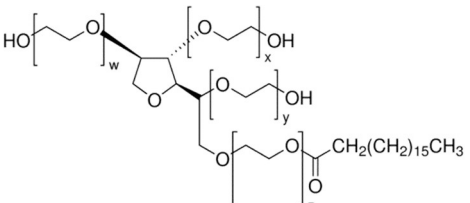


Figure 2. Diagram on the progress in the development of percutaneous absorption enhancement strategies [5].

Chemical permeation enhancers (CPEs) act through interactions with molecules that compose the stratum corneum (SC), the outermost layer of the skin that limits the rate of dermal/transdermal permeation. CPEs include different chemical families, such as alcohols (e.g. isopropyl alcohol), glycols (e.g., propylene glycol), terpenes and terpenoids (e.g., menthol), essential oils (e.g., eucalyptus), sulfoxides (e.g., dimethylsulfoxide), ether alcohols (Transcutol®), and amides (Azone®), among many others [9]. The over 600 CPEs reported to date act *via* different pathways, the most common of which is disturbance of the cell membrane phospholipid bilayers [10]. As such, it comes with no surprise that an important portion of CPEs regard amphiphilic molecules such as fatty acids and respective esters, fatty alcohols, and several other anionic, cationic, zwitterionic, and non-ionic surfactants (Table 1) [9].

Table 1. Examples of amphiphilic chemical permeation enhancers (CPEs).

| Class | Examples | |
|--------------------------|------------------------------------|--|
| | Name | Structure |
| Fatty acids | Lauric acid | $\text{CH}_3(\text{CH}_2)_{10}\text{COOH}$ |
| | Oleic acid | <i>cis</i> - $\text{CH}_3(\text{CH}_2)_7\text{CH}=\text{CH}(\text{CH}_2)_7\text{COOH}$ |
| | Linoleic acid | <i>cis, cis</i> - $\text{CH}_3(\text{CH}_2)_4\text{CH}=\text{CHCH}_2\text{CH}=\text{CH}(\text{CH}_2)_7\text{COOH}$ |
| Fatty esters | Isopropyl myristate | $\text{CH}_3(\text{CH}_2)_{12}\text{COOCH}(\text{CH}_3)_2$ |
| | Isopropyl palmitate | $\text{CH}_3(\text{CH}_2)_{14}\text{COOCH}(\text{CH}_3)_2$ |
| Fatty alcohols | Octanol | $\text{CH}_3(\text{CH}_2)_7\text{OH}$ |
| | Decanol | $\text{CH}_3(\text{CH}_2)_9\text{OH}$ |
| Cationic surfactants | Cetylpyridinium chloride (hydrate) |  |
| | Cetyltrimethylammonium chloride |  |
| Anionic surfactants | Sodium lauryl sulfate | $\text{CH}_3(\text{CH}_2)_{11}\text{OSO}_3\text{-Na}^+$ |
| Zwitterionic surfactants | Lauryl betaine |  |
| Non-ionic surfactants | Polysorbates (Tween® surfactants) |  |

Cetylpyridinium chloride (Table 1) is one of the amphiphilic CPEs most commonly used in cosmetics, where it also acts as a preservative and antiseptic, due to its antimicrobial properties [11]. Cetylpyridinium chloride, by being an ionic pair that combines an organic cation (cetylpyridinium) with an inorganic (could be organic) anion, has the structural type of an ionic liquid. Ionic liquids (ILs) are generally defined as organic salts composed by an organic cation and an organic or inorganic anion that are stable below their melting point. ILs are known by their remarkable physical and chemical properties and by their possible customization, since they can be designed to exert the desired effect by the correct choice of the ions that compose them [12].

The relevance of ILs is currently consolidated in many areas that explore them as (i) greener alternatives to common organic solvents, (ii) task-specific materials, and (iii) polyvalent players in pharmaceutical sciences. In the latter field, a wide range of ILs have been developed, spanning from ILs with intrinsic bioactivity to those having suitable properties for drug formulation and transport [13,14]. In this regard, ILs have been advanced as high value mediators of dermal and transdermal delivery (DTD) of small and large molecules, whose properties can be tailored through a few simple design principles as recently proposed by Mitragotri and co-workers [15].

In view of the above, this review offers a snapshot of latest developments regarding the most common methods for DTD of [bio]pharmaceuticals, highlighting the emerging role of ILs for enhancement of percutaneous absorption of diverse payloads, including proteins and peptides.

2. Overview of current methods for dermal and transdermal drug delivery

2.1. Physical methods

Physical methods to enhance percutaneous permeation can be divided into indirect and direct approaches (Figure 3). In indirect methods, different types of energy are used to promote penetration and diffusion of bioactive solutes through the SC. Thus, electrical energy is applied in electroporation and iontophoresis procedures, acoustic energy is used in sonophoretic methods (e.g., cavitation, ultrasound pressure), and laser or magnetic energies can also be applied in this context.

Electroporation uses high-voltage electrical pulses to generate transient pores in cell membranes through which a wide variety of substances, from small drugs to nucleic acids, can reach the intracellular milieu. Latest examples on skin applications of electroporation techniques include the permeation of low concentration formic and acetic acids for wound disinfection [16,17]. This type of electroporation applications was found to promote differential regrowth of dermal fibroblasts and keratinocytes [18].

Iontophoresis is based on use of mild electrical currents to increase skin permeation, mostly by electromigration of ions within the electric field applied, but also by electroosmosis or, to a minor extent, to enhanced passive diffusion. Understandably, this method is better suited for the permeation of charged molecules, whose transport can be modulated by a number of parameters [19]. Ongoing investigational work on biomedical applications of iontophoresis spans from pre-clinical studies on transdermal

delivery of anti-hypertensive agents [20], to clinical trials on iontophoresis of treprostinil as a potential treatment for diabetic foot ulcers (DFUs) [21].

Sonophoresis has been also thoroughly explored for enhancement of percutaneous absorption, mainly – but not exclusively – through cavitation or ultrasound (US)-based techniques. Both cavitation [22] and US-based [23] sonophoretic methods have been also recently considered for wound healing approaches, with encouraging results including in diabetic mice.[23] Noteworthy, care must be taken in order to avoid that the intensity and duration of US irradiation are high enough to cause burns at the irradiation site [1].

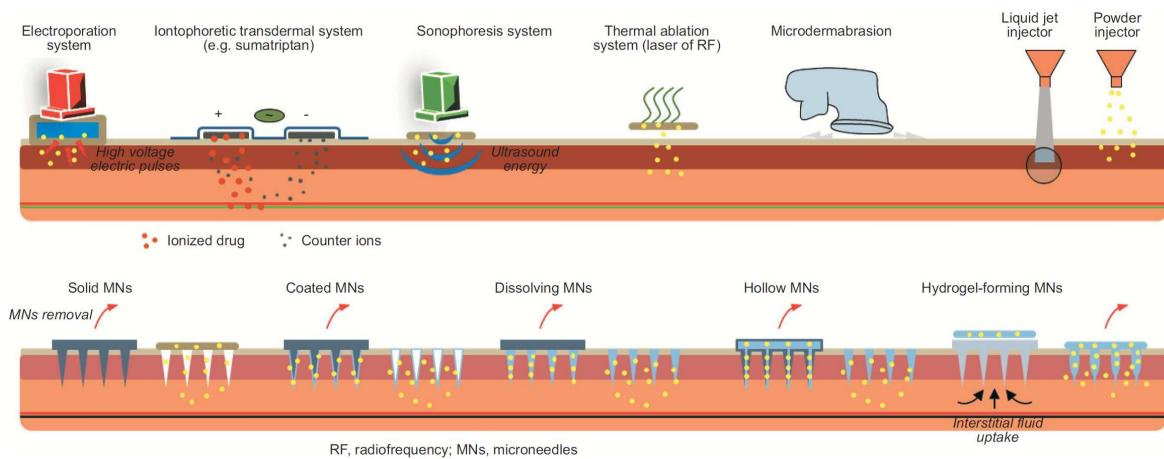


Figure 3. Physical methods for enhancement of percutaneous absorption [1].

In direct methods, though considered little invasive, pores are created in the SC, through which the entry of solutes into the epidermis and eventually the dermis is forced by means of mechanical, thermal, or pressure-based approaches. Currently, the most popular direct methods include (i) the use different types of microneedles (MNs) – solid, coated, hollow, dissolving, or hydrogel-forming – to force percutaneous permeation of bioactive compounds, and (ii) microdermabrasion (mechanics-driven) and thermal ablation (heat-driven). Other physical methods have been used to promote percutaneous permeation, though to a lesser extent; one example is that of jet injectors, whereby solid, liquid, or plasma jets force drug delivery by means of the high pressure exerted when they hit the skin [1].

Microneedles (MNs)-based approaches are amongst the most widely explored physical methods to promote DTD. In recent years, different types of MN arrays have been thoroughly studied as hurtless alternatives to classical injections, being well advanced in the clinics [1,24]. MNs-based technologies are being pushed forward mainly for transdermal delivery of peptides, proteins and antibodies [25], and for cosmetic applications [26]. Still, latest reports highlight the therapeutic potential of MNs to tackle non-healing wounds [27], based on the promising performance of diverse MN arrays such as Manuka honey MNs able to promote healing and exert potent bactericidal action against methicillin-resistant *S. aureus* (MRSA) [28].

[Photo]thermal ablation techniques are also regarded as a promising way to enhance percutaneous permeation of therapeutics. In classical thermal ablation approaches, components of the outermost skin layer are literally vaporized upon ultrafast exposure to an extremely high (>300 °C) temperature, which disrupts the SC barrier, facilitating subsequent absorption of the drug, typically administered through a transdermal patch. [Photo]thermal ablation methods have been also considered for tackling mild to severe skin infections [29], by means of (i) direct ablation of the microbial pathogens [30], (ii) sensitization of bacterial biofilms to standard antibiotics [31], or (iii) accelerating wound healing [32,33]. One recent example advances a laser-activatable nanosystem able to exert a potent action against multidrug resistant (MDR) bacteria often associated to non-healing wounds, by a combined photothermal effect and controlled release of copper(II) ions [34].

The distinct physical methods mentioned above act through different permeation mechanisms and have been employed alone or combined, with each other or with non-physical methods, to enhance the absorption of a wide range of APIs, and also cosmeceuticals, through the skin [1,9,35,36].

2.2. Non-physical methods - nanosized delivery systems

Nanosized [bio]materials and formulations are regarded as the gold standard of non-physical methods for drug delivery, with emphasis on dermal and transdermal applications. Lipid-based or -inspired nanosystems are by far the most common, covering from the classical examples of nanoemulsions and liposomes (Figure 4) to solid lipid nanoparticles and nanostructured lipid carriers.

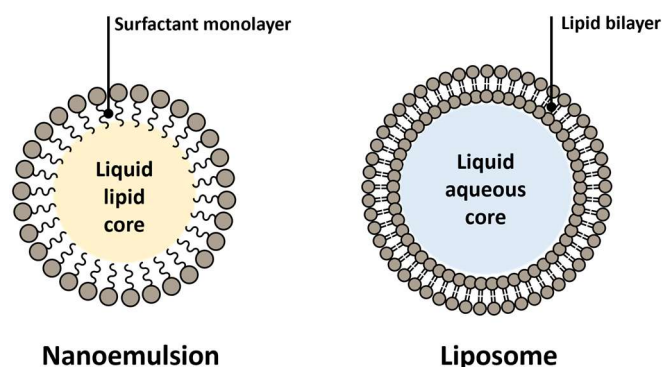


Figure 4. General representation of nanoemulsion and liposome.

Nanoemulsions (NEs) allow the dispersion of drug-containing droplets in very high interfacial areas, and their relevance towards the enhancement of percutaneous absorption of either hydrophilic (water-in-oil NEs) or lipophilic (oil-in-water NEs) substances is well established [37,38]. NEs in use or under investigation today offer diverse compositions and degrees of complexity, based on diverse amphiphiles, from natural lipids to synthetic surfactants, and combinations thereof [37,38]. Use of essential oils in the formulation of NEs has also been addressed. For instance, a clove oil-based NE was developed to combine the anti-inflammatory and antifungal properties of the main oil component, eugenol, with those of the drug cargo, naftifine, used to tackle skin fungal infections [39]. Lately, other types of liposome-inspired vesicles (figure 5), such as ethosomes, transfersomes, niosomes, among other, have been advanced [1,3,40,41]. Lipid-based/inspired nanosystems stem from ancient knowledge on the value of fatty acids and derived hydrolyzable lipids, especially phospholipids, to enhance percutaneous absorption of a variety of substances for both health- and beauty-care. Phospholipid-based emulsions, as well as micellar and liposomal formulations for skin care are all around us, hence it comes with no surprise that lipid-based/inspired nanocarriers have a prominent role in current approaches for DTD of [bio]pharmaceuticals [1,3,40-43]. Still, nanosystems that do not [exclusively] derive from natural lipids have been thoroughly explored for percutaneous permeation of bioactive molecules; organic nanoformulations comprising either natural or synthetic polymers and/or surfactants other than natural lipids can be found in recent literature, covering distinct types of dendrimers, nanoparticles (NPs), nanoemulsions (NEs), micelles, and hydrogels, for diverse purposes. Likewise, inorganic nanosystems, including metallic, non-metallic, and magnetic NPs, among others, have been employed for DTD of [bio]pharmaceuticals [42,44].

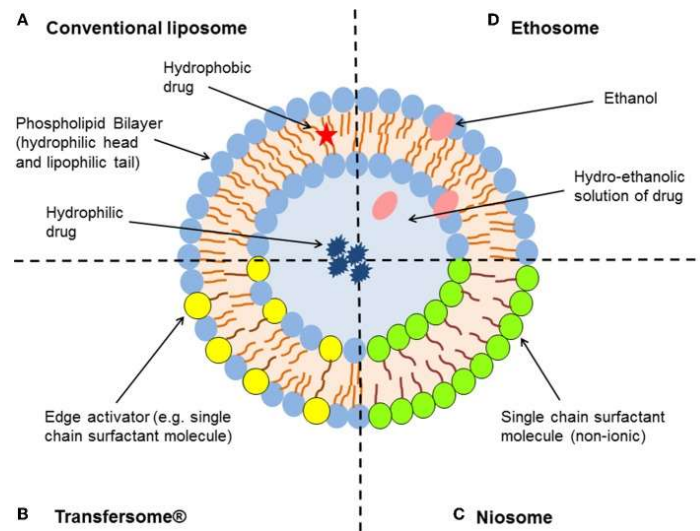


Figure 5. Examples of liposome-inspired vesicles [45].

Vesicular nanocarriers (VNs) currently encompass a myriad of different, mostly spherical, structures that share the common trait of having single or multiple bilayer lamellae separating one or more aqueous or hydroalcoholic inner compartments from the outer medium, and which have been widely used for topical disorders and cosmetics [9,46]. The best known and most commonly employed VNs are liposomes, spherical colloidal bilayer structures formed spontaneously by amphipathic phospholipids in aqueous environments, which were originally reported in 1965 [47]. But a variety of liposome-inspired VNs has evolved since, such as:

- *ethosomes*, soft VNs whose structure is closely related to that of liposomes, the main difference being the presence of ethanol in moderate to high concentrations, which confers the vesicles high malleability and the ability to significantly enhance the percutaneous permeation of highly lipophilic molecules [48];
- *transfersomes*, ultra-flexible VNs composed by either phospholipids or other bilayer-forming amphipathic molecules packed together with edge activators that decrease the vesicle’s interfacial tension; this conveys a very high elasticity enabling a much better permeation through the SC probably *via* the intercellular route [49];
- *niosomes* are VNs usually composed by cholesterol and alkyl or polyglycerol-based non-ionic surfactants that usually offer higher osmotic stability and involve lower production costs as compared to phospholipid-based VNs. Yet, like in

liposomes, the physical stability of niosomes is not adequate for prolonged storage [50,51].

- *other “somes”* are continuously emerging as novel VNs for drug delivery, particularly for topical applications. Among others, these comprise: *invasomes* – terpene-containing ethosome analogues with enhanced penetration into deeper layers of the skin^[105]; *aspasomes* – multilayered VNs formed by combination of ascorbyl palmitate with cholesterol and charged lipids [52]; and other self-assembling hollow nanostructures based on, e.g., solid crystalline cores (*aquasomes*), liquid crystalline phases (*cubosomes*, *hexosomes*), or hollow coagulated nanoparticles (*colloidosomes*) [53], as well as polymer-based vesicles (*polymersomes*) [54].

All these types of artificially produced VNs have been recently explored and optimized to create increasingly efficient formulations for DTD of bioactive molecules and macromolecules. For instance, different hydrogels have been investigated as suitable vehicles for topical delivery of drug-loaded niosomes [55]. In another recent report, an ethosome-based gel showed good performance both *in vitro* and *in vivo* for delivery of thymosin β -4, a protein that is relevant for wound repair [56]. Less common VNs have been lately advanced for diverse purposes, such as unsaturated fatty-acid based nanovesicles (*ufasomes*) for DTD of terbinafine hydrochloride to address *Candida albicans*-associated topical fungal infections [57]. Interestingly, when looking at the forefront of VNs-mediated drug delivery, we can witness the increasing relevance of cell-based VNs such as *exosomes* [58] or *outer membrane vesicles* (OMVs) from Gram-negative bacteria [59], whose major hallmark is their expectedly high biocompatibility and low immunogenicity. Exosomes are extracellular vesicles that integrate proteins and nucleic acids of their secreting cells, and which can affect function and properties of other cells able to internalize them [58]; as such, recent efforts address their engineering for targeted drug delivery [60,61], also for diverse dermatological applications [62-64] and wound healing [65]. Besides exosomes, OMVs are also becoming prominent actors in several biomedical applications, including recent examples where engineered OMVs from transgenic *Escherichia coli* have been used for DTD of biopharmaceuticals, alone [59] or in combination with phototherapy [66].

Nanocarriers (NCs) include many other structures besides bilayered VNs, with diverse properties and applications, including targeted delivery of [bio]pharmaceutics (Figure 7) [67]. NCs are typically colloidal particulate systems having at least one dimension not larger than 100 nm. NCs can be categorized in different ways, i.e., based on morphology (nanorods, nanoshells, nanocages, nanostars, etc.), core material (metallic, ceramic, polymeric, carbon-based, lipid-based, etc.), specific physical and/or chemical properties (magnetic, [semi-]conductivity, thermoconductivity, stiffness, porosity, etc.), among other criteria (e.g., surface charge or functionalization) [68]. It should be outlined that most current nanodelivery approaches rely on hybrid/composite systems often comprising inorganic, biopolymeric and several other natural and/or synthetic organic components, which blurs the frontiers between different types of NCs. While nanosized liposomal and liposome-like VNs addressed in the previous section are also NCs, this section is aimed at pinpointing a few recent cases where NCs with other than bilayered structures have been explored for topical delivery focusing on the treatment of skin and soft tissues infections and wound-healing enhancement.

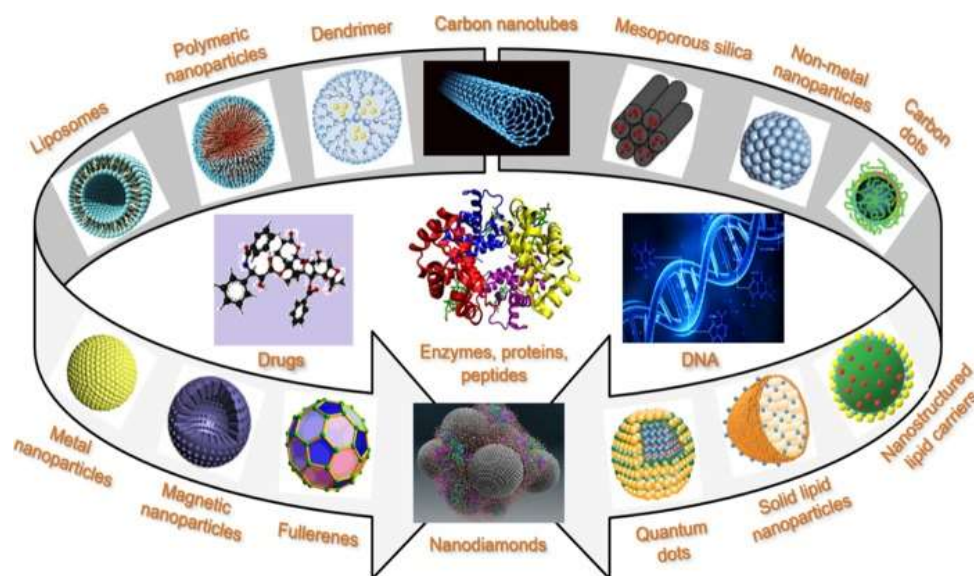


Figure 7. Different types of particulate systems with potential interest as nanocarriers for targeted delivery of drugs and biological macromolecules [67].

Lipid-based NCs, of which solid lipid nanoparticles (SLNs) and nanostructured lipid carriers (NLCs) are the most representative examples (Figure 8), are currently regarded as enhanced alternatives to classical liposomal-based formulations. SLNs emerged as the first-generation of non-liposomal lipid-based nanocarriers, featured by a spherical shape and a payload-containing solid core stabilized by an outer layer lined with surfactants. SLNs offer many advantages over other types of NCs, the main of which are their high biocompatibility and biodegradability, but also high compatibility with a wide range of payloads and cost-effective production, among others. Still, the solid nature of SLNs poses a few limitations, such as low loading capacity and the risks of premature drug release, unexpected gelation, and crystallization upon storage. NLCs emerged to circumvent these hurdles, by offering a nanostructured core containing low-melting point lipids (liquid at room temperature) [69-71].

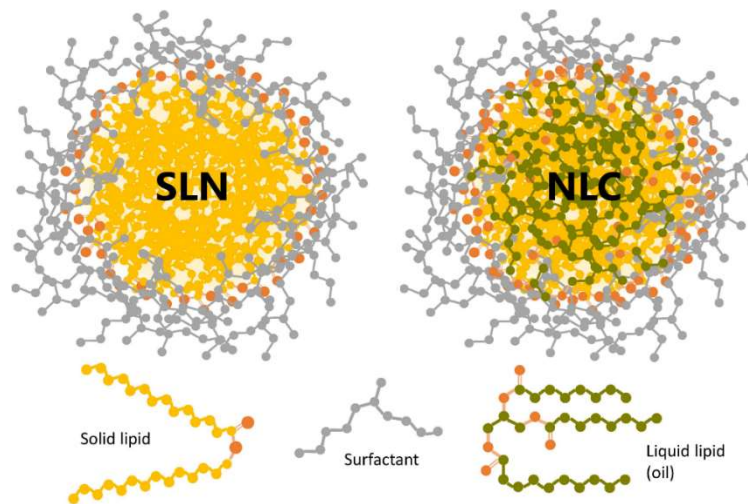


Figure 8. General structures of SLNs and NLCs [71].

The potential of both SLNs and NLCs for drug delivery, including across the formidable obstacles that are the blood-brain barrier and the skin, has been widely addressed [70-72]. Promising results have been lately reported to DTD of anti-inflammatory, antibacterial, antiviral, antifungal, antiacneic, and anticancer agents, among others, as nicely reviewed by Souto *et al.* [72]. Also, SLNs and NLCs have been explored for DTD of cosmetics, with encouraging performances [73]. Importantly, the formulation of SLNs and NLCs for DTD of [bio]pharmaceuticals and cosmeceuticals can be easily tailored according to their specific application and payload [72,73]. SLNs and NLCs are also showing promise to promote skin regeneration [74-76]. Recent

investigations have focused on DTD of essential oils having healing effects due to either a dual anti-inflammatory/collagenesis-inducing action of the oil itself [77], or to a synergic antimicrobial and healing action elicited by combination of the essential oil with specific components in the lipid nanocarrier (e.g., oleic acid) [78]. Very recently, different SLNs and NLCs have been tested along with NEs for DTD of curcumin, a hydrophobic photosensitive phytomolecule whose anti-inflammatory, antimicrobial and healing properties are known for long.[79] This study revealed that all tested NCs were efficient for photoprotection of the phytopharmaceutical, with NLCs offering the best pharmacological performance, provided the matrix fluidity was tuned for optimized skin occlusion and drug release rate [79]. In line with this, multiple benefits of SLNs/NLCs-mediated delivery of natural and synthetic antimicrobials have been advocated in the recent literature [80-82], including for fighting multidrug-resistant (MDR) infections [83,84]. Thus, a new “nanoantibiotic era” is on the rise [85] that will likely have great impact on the management of complicated skin and skin structure infections (cSSTI), given the unique ability of lipid-based NCs to overcome the skin barrier[86]. One illustrative example is “nanoRIF”, a rifampicin-loaded hybrid lipidic/polymeric NC that showed *in vivo* efficacy against *Staphylococcus aureus*-associated infection on skin [87].

Non-lipidic NCs enclose a broad variety of organic and inorganic nanomaterials, a few of which are next highlighted for their recent interest for the enhancement of percutaneous permeation:

- *dendrimers* are hyperbranched arborescent spherical NPs that may be composed by either natural (e.g., amino acid- or peptide-based) or artificial (e.g., ethylene glycol-based) dendrons, whose individual structure and tridimensional arrangement in the final dendrimer have great impact on the physical, chemical, and drug loading/release properties of the whole nanosystem [88]. The biomedical relevance of dendrimers, including for drug delivery, is growing exponentially [89,90], and interest is now falling on topical applications. Latest reports in this regard concern, e.g., use of poly(amidoamine)-, or PAMAM-, based dendrimers for enhanced skin permeation of the chlorhexidine digluconate antiseptic [91], or dermal delivery and follicular targeting of the antiacneic agent adapalene [92].
- *[bio]polymer-based NCs*, encompassing [bio]polymeric NPs, films, gels, nanofibers, among others, have been thoroughly investigated for drug delivery

applications [93], including for topical use [94]. Natural polymers such as chitosan, poly(glycolic acid), poly(lactic acid), hyaluronic acid, and poly(arginine) are amongst the most popular components of polymeric NCs, given their biocompatibility and biodegradability, along with their chemical “flexibility” to enable the production of a wide range of multi-component customized stimuli-responsive nanomaterials [94]. Chitosan-based polymeric NCs have been thoroughly explored for topical applications, given the intrinsic antimicrobial and healing properties of chitosan [95]. One recent example concerns development of a chitosan/carboxymethyl cellulose-based nanogel for transdermal co-delivery of atorvastatin and *Nigella sativa* oil for wound management, taking advantage of the anti-inflammatory, immunomodulatory, antioxidant, and antibacterial properties of both bioactive cargoes; *in vitro* permeation, cytotoxicity, healing, and bactericidal activity assays delivered quite promising results [96]. Many other polymer-based nanomaterials have been explored in recent years for topical applications from, e.g., extracellular matrix-mimicking nanofibrous scaffolds [97] to promote accelerated healing of chronic wounds.

- *inorganic NCs* integrate metal-, metal oxide-, and mesoporous silica-based NPs as the most popular examples, although other nanosystems, such as inorganic polymer-based NCs, carbon-, carbon oxide- or black phosphorus-based nanomaterials, also fit this category [98-101]. Although the majority of inorganic NCs in drug delivery, including DTD, has been addressed to cancer theranostics [102] they have also been explored for antimicrobial therapies [103], where silver-based NPs (AgNPs) occupy a prominent role, given the intrinsic antibacterial properties of silver [104,105]. For instance, AgNPs synthesized from silver nitrate in the aqueous extract of a medicinal plant (*Acanthospermum australe*) used in South America to treat cSSTI, were recently reported to have potent wide spectrum antimicrobial activity [106]. Yet, AgNPs, as well as other inorganic NPs such as zinc oxide-based ones, may pose toxicity issues for dermatological and dermocosmetic use [107]. As such, recent reports on use of AgNPs, or even of other inorganic NCs, for DTD of [bio]pharmaceuticals are relatively scarce. Notwithstanding, graphene oxide-based NCs have been lately highlighted for topical applications [108], either as bioactive agents able to tackle cSSTI *per se* [109,110]. Other carbon-based inorganic NCs have also been explored to tackle skin disorders, with emphasis on wound healing and control of cSSTI, as recently revised elsewhere [111]. Additional examples on use of inorganic NCs for DTD of

[bio]pharmaceuticals mainly address combination with physical methods, in particular with microneedle-based technologies [112-114].

2.3. Chemical permeation enhancers

As already mentioned, chemical permeation enhancers (CPEs) are molecules able to temporarily alter the structure of the SC, thus enhancing the percutaneous permeation of different substances. The performance of a CPE depends on its ability to both efficiently partition from the applied medium into the skin lipid layer and interact with the constituents of this layer, causing momentary but significant perturbations that lead to the desired higher permeability of the SC. While the solution-to-SC partition is influenced by the lipophilicity of the CPEs, the size and structure of the latter dictate the permeation enhancement pathway(s) (Table 2, Figure 9). Thus, some CPEs, like alcohols and polyols, act mainly as solvents that increase the solubility of the drug and its partitioning into the SC, whereas other solvents used as CPEs, as dimethylsulfoxide, are further able to extract lipid molecules from the SC, creating channels that turn the SC more permeable. Other CPEs, like fatty acids or their esters, are able to insert into the bilayer structures of skin lipids, altering their ordered packing and thus increasing permeability [10,115,116]. Relevantly, though CPEs are usually associated to lipophilic or amphiphilic organic compounds (Table 2), water is the safest and most widely employed CPE for dermatological and dermocosmetic applications; water offers the simplest way to deliver hydrophilic compounds across the skin, but is also able to enhance the permeation of lipophilic ones, as it can both interact with the polar head groups in the SC lipid bilayer and disrupt hydrogen bonding (e.g. in proteins) in intra- and intercellular compartments of the skin [116].

While physical and nanotechnological approaches like those addressed in previous sections undeniably lie at the forefront of dermal and transdermal drug delivery research, CPEs remain the simplest and most cost-effective way to permeate different solutes across the skin, and their use is widely disseminated [116]. This explains the strong interest towards a better understanding of their modes of action [10,117] and on development of novel CPEs, searching for greener and more biocompatible alternatives, such as those derived from essential oils [118] or amino acids [4].

Table 2. Examples of different classes of CPEs and their recognized modes of action [116].

| CPE class | Example(s) | Mode(s) of action |
|--------------------------------------|---|--|
| low molecular weight linear alcohols | ethanol hexanol octanol | extraction of intercellular lipids increased solubility/partitioning of the solute into the SC |
| glycols and polyols | propylene glycol polyethylene glycol | increased solubility/partitioning of the solute into the SC |
| esters | octyl salicylate | accumulation in the SC lipid bilayer enhancing solute diffusivity |
| amides | laurocapram (Azone®) | disruption of the ordered packing of the bilayers of skin lipids |
| sulfoxides | dimethylsulfoxide dodecyl methyl sulfoxide | extraction of intercellular lipids increased solubility/partitioning of the solute into the SC interaction with keratin and/or corneocytes, and with the polar head groups of the SC lipid bilayer |
| pyrrolidones | <i>N</i> -methyl-pyrrolidone 2-pyrrolidone | interaction with keratin and/or corneocytes, and with the polar head groups of the SC lipid bilayer |
| terpenes | menthol limonene nerol | disruption of the ordered packing of the bilayers of skin lipids |
| fatty acids | oleic acid | disruption of the ordered packing of the bilayers of skin lipids |
| fatty esters | isopropyl myristate propylene glycol monocaprylate propyleneglycolmonolaurate | extraction of intercellular lipids phase separation disruption of the ordered packing of the bilayers of skin lipids |
| surfactants | sodium lauryl or dodecyl sulfate (anionic) | interaction with keratin and/or corneocytes incorporation into the SC lipid bilayer and induction of lamellar phases |
| | quaternary ammonium salts (cationic) | significant disruption of the ordered packing of the bilayers of skin lipids |
| | cetyl or stearyl alcohol (non ionic) | disruption of the ordered packing of the bilayers of skin lipids |
| ether alcohols | 2-(2-ethoxyethoxy)ethanol (Transcutol®) | insertion between the polar head groups of the skin lipid bilayers, inducing swelling of the SC |

The wide diversity and relevance of CPEs recently motivated Bozdaganyan and co-workers to create an Open Access CPEs database, CPE-DB (<http://intbio.org/cpedb/>), that includes ca. 650 CPEs covering all classes shown in Table 2 and a few more miscellaneous structural types [119].

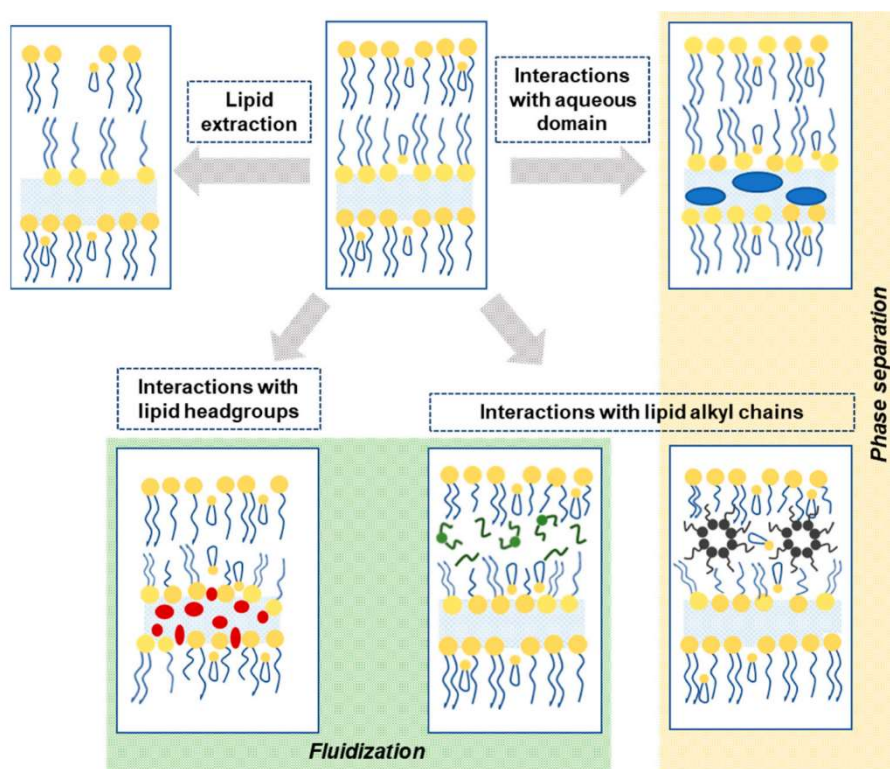


Figure 9. Schematic view of the modes of action of CPEs [4].

Amidst the chemically diverse CPEs known to date, examples can be found that can be categorized as ionic liquids (ILs), where organic cations are paired with organic or inorganic anions [120]. One emblematic IL that is widely employed as a topical antiseptic with high percutaneous permeation is cetylpyridinium chloride (CPC) [11], but others have also shown high potential as CPEs for DTD applications, including ILs based on natural building blocks like choline geranate (CAGE) [15,121] or obtained by pairing the [ionizable] drug itself with a proper counterion as in, e.g., dodecyldimethylammonium ibuprofenate [13]. Undeniably, ILs are rising stars for a broad variety of applications. As recently advocated, “The time is now for ionic liquids” [122]; the next section emphasizes this is also true for DTD of [bio]pharmaceuticals.

3. Ionic liquid-based approaches in dermal and transdermal drug delivery

3.1. A bird's eye view on ionic liquids

ILs are salts formed by organic cations and organic or inorganic anions, which possess unique physical and chemical properties that differentiate them from the other (“conventional”) salts. The most emblematic feature of ILs is their very low melting points (usually, but not necessarily, below 100 °C), due to a lack of ion symmetry and to low charge density, which results in Coulombic interactions in the solid phase that are weaker than those in other salts [14]. Given the huge number of possible cation/anion combinations, reports to date cover an immense panoply of different ILs that can be classified in many different ways, depending on the classification criteria (Figure 10), as thoroughly reviewed elsewhere [123]. In general, three generations of ILs have been recognized, going from the earlier examples of ILs proposed as “greener” surrogates of classical organic solvents to the next generation of ILs whose chemical and physical properties were adjustable to their specific applications (task-specific ILs, or TSILs), and finally to ILs displaying low toxicity, biocompatibility, biodegradability and, in some cases, even bioactivity [120,121,123-125].

ILs are particularly appealing for pharmaceutical applications, given their (i) non-crystalline nature, avoiding fluidity/polymorphism-related liabilities of many drug formulations, and (ii) easy customization and adjustable-properties, through a sensible choice of the ion components [12,124,125]. Hence, ILs properties such as vapor pressure, thermal stability, chemical and electrochemical stability, polarity, solubility, amphipathicity, and even bioactivity, can be finely tuned [14]. For instance, ionizable active pharmaceutical ingredients (APIs) have been paired with selected counterions to deliver ILs, including room-temperature ILs (RTILs), that possess intrinsic bioactivity [13,125,126]. Also, amphipathic ILs have been developed which are miscible in a wide range of solvents and display surface activity (surface-active ILs, or SAILs), representing a new class of surfactants, some of which possessing interesting biological properties, such as antimicrobial action. Relevantly, though emerging from the 2nd generation of ILs for applications as, e.g., emulsifiers, SAILs enclose a tremendous potential for biomedical and pharmaceutical applications [14,126,127].

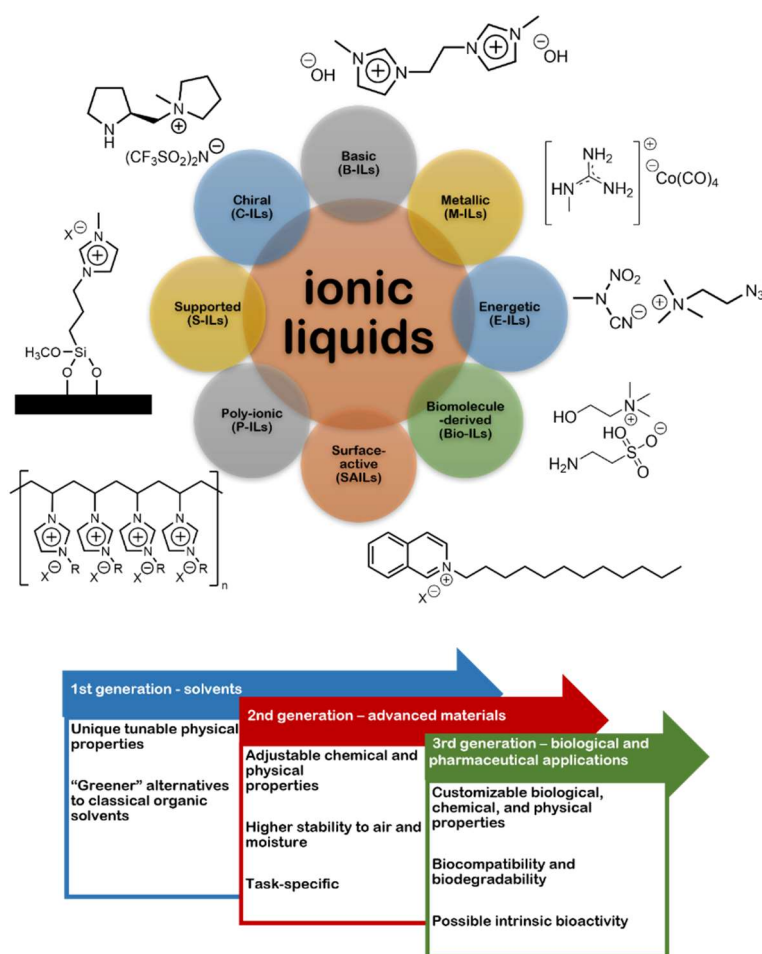


Figure 10. A few examples of different types of ILs, and their three recognized generations.

3.2. Ionic liquids in skin permeation – a closer look at the past couple of years

Over the last decade, the interest on using ILs to promote topical delivery of bioactive molecules and APIs has been steadily growing. For instance, several reports from 2010 to 2018 highlight the promising role of ILs, most of which imidazolium-based, towards enhanced percutaneous permeation of drugs and bioactive compounds as diverse as acyclovir, methotrexate, dantrolene sodium, etodolac, 5-fluoroacyl, salicylic acid, caffeine, dencichine, peptides and proteins. Interestingly, some of these reports address studies on skin permeation of API-ILs, i.e., ILs resulting from combination of an ionizable drug (or API) with an adequate counterion (e.g., lidocaine chloride), or even of two ionizable APIs with opposed polarities (e.g., lidocaine docusate, lidocaine ibuprofenate, or lidocaine/etodolac) [128,129].

The mechanisms through which ILs or API-ILs display enhanced skin permeation are not fully unveiled and are primarily – though not exclusively – dependent on the specific structural and physico-chemical features of the IL. Thus, the CPE action of hydrophilic ILs (e.g. 1-ethyl-3-methylimidazolium-based) has been mostly ascribed to their role as polar enhancers able to (i) increase solubility and partition of hydrophilic drugs, and/or (ii) fluidize the SC by disrupting the tight packing of both proteins and lipids (at the headgroups level – Figure 9). In turn, hydrophobic ILs, many of which are SAILs (e.g., CPC, 1-dodecyl-3-methylimidazolium-based ILs), may exert their skin permeation action by (i) increasing solubility and partition of hydrophobic drugs, (ii) inserting into the SC lipid bilayers, causing a disruption of the ordered packing of the phospholipid bilayers or even phase separation or induction of lamellar phases (Figure 9), and/or (iii) extracting SC lipids [124,128-131]. Interestingly, SC lipid extraction followed by replacement of the extracted lipids with the IL and water has been recently advanced as the mechanism by which CAGE enhances the skin permeation of macromolecules like dextran [132].

ILs alone, and in combination with other percutaneous permeation methods, have been lately explored for DTD of diverse [bio]pharmaceuticals, so a few illustrative examples reported in the past couple of years are next highlighted.

3.2.1. IL-based topical delivery approaches for small bioactive compounds

Non-steroidal anti-inflammatory drugs (NSAIDs), often ibuprofen but also others, are amongst the most common low molecular weight bioactive compounds that have been explored for IL-mediated topical delivery [125,130]. In this connection, Wu *et al.* have recently investigated the role of the counterion in the physico-chemical and biological properties of ibuprofen-derived ILs, with emphasis on transdermal delivery applications [133]. This study, which integrated nine different ibuprofen-based ionic liquids using tetraalkylammonium and tetraalkylphosphonium counterions, confirmed the superior permeation of the ILs across an *in vitro* skin model as compared to the free drug, highlighting the didecyldimethylammonium and tetrahexylammonium counterions as the most beneficial for such effect [133]. Moreover, it was possible to establish a correlation between percutaneous permeation efficiency and (i) ILs' lipophilicity (higher logP and lower water solubility), and (ii) strength of ionic association between the anionic form of the drug and the cationic counterion [133]. In another latest study, Yuan *et al.* established that even minor amounts of choline/amino acid-based ILs, namely, cholinium glycinate and cholinium alaninate, contribute to a significant enhancement of the water solubility and permeation of ibuprofen across a model skin membrane, along with the

advantage of showing low toxicity to mouse embryonic fibroblasts [134]. Cholinium-based ILs have also been the focus of another quite interesting recent approach for enhanced DTD of NSAIDs, by Silvestre and co-workers [135]. These authors synthesized a series of API-ILs derived from ibuprofen, ketoprofen and (*S*)-naproxen, using cholinium as the counterion, (Figure 11a) whose aqueous solubility were about one order of magnitude higher than those of the free NSAIDs. Moreover, incorporation of the API-ILs into bacterial nanocellulose afforded flexible and transparent membranes with adequate properties for use as DTD systems, while offering equal anti-inflammatory potency and a faster drug release as compared to loading of the parent NSAIDs alone [135].

NSAIDs other than the profens (2-aryl-propionic acid derivatives) have also been subject of recent investigations addressing IL-mediated topical delivery. For instance, Carneiro and co-workers have reported the synthesis and characterization of diclofenac imidazolium monohydrate, an API-IL with increased water solubility as compared to the parent API that the authors advocate as promising for transdermal delivery approaches, although its cytotoxicity remains to be evaluated [136]. Current research is also addressing pairing diclofenac with local anesthetics or analgesics to afford dual-action ILs that are next embedded into suitable materials for topical application. For example, Suksaeree and Maneewattanapinyo have recently reported the ion-pair reaction between lidocaine hydrochloride and diclofenac sodium (Figure 11b) to afford a dual-action diclofenac/lidocaine IL that was next incorporated into a polymer matrix suitable for fabrication of transdermal patches [137]. The authors investigated the influence of the polymer matrix composition onto IL loading capacity, controlled drug release rate, and drug crystallization, advancing a few guidelines for future development of similar formulations [137]. The same research group further tested the controlled release of the diclofenac/lidocaine IL from gelatin/poly(vinyl alcohol) transdermal patches, which conveyed high release rates for both APIs and suitable physicochemical and stability features for pharmaceutical applications [138].

Incorporation of lidocaine/NSAIDs-based dual-action ILs into polyvinylidene fluoride/hyaluronic acid-based membranes has also been addressed by Abednejad *et al.*, who found (i) an up to 470-fold enhancement of the water solubility of the ILs as compared to the free APIs, (ii) improved release of the APIs from the IL-loaded membranes, (iii) suitability of the IL-loaded membranes for use as wound-dressings, (iv) enhanced membrane adhesion and viability of membrane-adhered fibroblasts, and (v) anti-inflammatory activity similar to that of the free APIs [139].

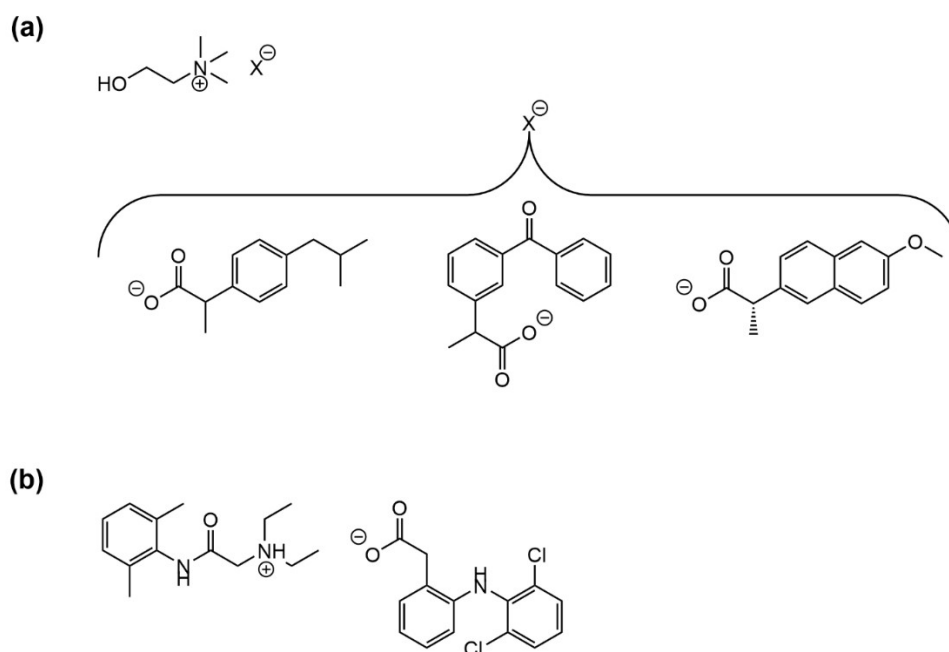


Figure 11. examples of NSAIDs-derived ILs advanced for transdermal delivery: **(a)** ILs produced by pairing the cholinium cation with the anionic forms of (from left to right) ibuprofen, ketoprofen, and (S)-naproxen [135]; **(b)** dual-action IL composed by the cationic form (conjugate acid) of lidocaine and the anionic form (conjugate base) of diclofenac [137].

IL-based strategies have also been lately addressed for enhanced skin permeation of other types of small bioactive compounds, from anticancer or neuroactive drugs to antioxidant or other anti-ageing agents, among others. For instance, amino acid-based ILs have been recently considered for topical treatment of cancer. In this regard, Zheng *et al.* have recently screened 15 methyl amino acid ester hydrochlorides as potential CPEs for model drugs like 5-fluoroacyl, and found that the L-proline and the L-leucine-based ILs were the most promising of the set, owing their percutaneous permeation ability to a combined lipid fluidization and lipid extraction effect [140]. Another amino acid, taurine, has been recently investigated for production of ILs with intrinsic antitumor activity and enhanced percutaneous permeation [141]. To this end, taurine was paired with bioactive alkaloids, namely, L-carnitine and betaine, affording ILs with high thermal stability, biocompatibility and *in vitro* antitumor activity. The taurine-derived ILs were further shown to enhance percutaneous permeation of both insulin and dextran, possibly *via* a lipid extraction mechanism [141].

IL-mediated topical delivery of neuroactive molecules such as the memory-enhancing agents donepezil and nobiletin has been equally investigated in the last couple of years. Wu *et al.* ion-paired donepezil with docusate, ibuprofen, and unsaturated

fatty acids, producing ILs that were thoroughly characterized regarding their structural and physicochemical properties, as well as their *in vitro* antiproliferative action on human neuroblastoma cells, acetylcholinesterase (AChE) inhibitory activity, and ability to permeate through model blood-brain and skin barriers [142]. Additional skin permeation assays were carried out using IL-loaded adhesive transdermal patches, and – taken together – results highlighted a higher skin permeability of donepezil α -linolenate and docosahexaenate as compared to free donepezil, which could be further enhanced by loading the ILs onto the adhesive patches [142]. Moreover, despite having slightly decreased anti-AChE activity, the ILs had similar or lower cytotoxicity than the free drug [142].

IL-promoted DTD of another memory-enhancing molecule, the poorly water-soluble flavonoid nobiletin, has been also tested recently by Hattori *et al.*, using choline and geranic acid (CAGE); this IL established multiple hydrogen bonds with the drug, contributing to a substantial increase of its solubility [143]. Additionally, *in vitro* and *in vivo* assays confirmed the superior performance of CAGE, as compared to other CPEs, in enhancing the percutaneous permeation of nobiletin, whose bioavailability via the transdermal route was found to be 20-fold higher than oral administration of the crystalline form of the drug [143].

ILs have also been lately explored as potential CPEs of anti-ageing molecules, such as α -lipoic acid and other natural antioxidants. Fang and co-workers prepared different ILs by acid-base combination of α -lipoic acid with a series of amines, and the ILs subsequently formulated with a liquid oil mixture to form water-in-oil NEs [144]. Transdermal permeation of the NEs was assayed *in vitro* on whole skin, and on medical tape-stripped epidermal and dermal skin layers, and these assays, together with additional structural and rheological studies, showed that different IL-skin layers affinities accounted for distinct skin permeation and retention ability [144]. Still, globally, the IL-based NEs not only provided enhanced solubility and protection to this somewhat unstable drug, but also showed very good *in vivo* action against photo-induced skin ageing and collagen loss in rats [144].

Caparica *et al.* have equally advanced IL-based emulsions as promising tools for enhanced solubility and percutaneous permeation of natural antioxidants relevant in cosmetics, namely, ferulic acid, caffeic acid, *p*-coumaric acid, and rutin [145]. These authors explored eight different ILs, encompassing amino acids, choline, and imidazole building blocks, and, after setting their highest nontoxic concentrations, based on their *in*

in vitro toxicity to human keratinocytes, determined their concentration-dependent ability to solubilize the antioxidants, and the physicochemical properties of IL-loaded oil-in-water NEs. This showed that incorporation of the ILs in the NEs conveyed a higher drug load in all four cases, holding great promise for future exploration of these formulations, especially those based on imidazolium glycinate, for DTD of natural anti-ageing agents as those covered in the study [145].

Also with a focus on dermal care applications, Chantereau *et al.* reported, in early 2020, bioactive ILs obtained by pairing cholinium cations with anionic forms of B-complex vitamins, namely, nicotinate (vitamin B3), pantothenate (vitamin B5), and pyridoxilate (vitamin B6 co-factor) [146]. These vitamin B-derived ILs (Figure 12) showed significantly enhanced solubility as compared to the free vitamins, and their subsequent loading onto bacterial nanocellulose delivered flexible thermostable and nontoxic membranes with enhanced rehydration capacity as compared to non-IL-loaded bacterial cellulose. Moreover, in buffer, the release of the vitamin B-based ILs was faster and more extensive than that of the free vitamins [146].

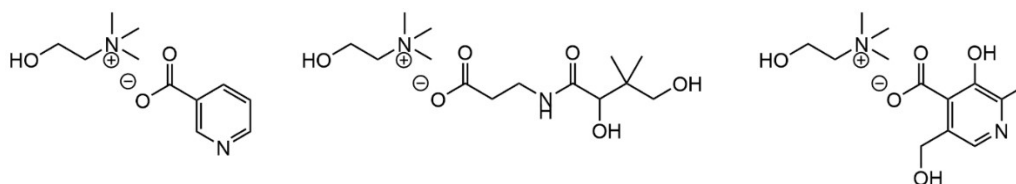


Figure 12. ILs combining the cholinium cation with the anionic forms (conjugate bases) of (from left to right) nicotinic acid (vitamin B3), pantothenic acid (vitamin B5), and pyridoxic acid (vitamin B6 co-factor), reported by Chantereau *et al.* [146].

One of the current greatest health concerns worldwide is that of MDR infections. In line with this, several latest reports address use of IL-based strategies for topical application of diverse anti-infective agents to treat from mild to complicated skin infections of viral, bacterial, or fungal origin. One example concerns acyclovir, whose clinical relevance in the management of herpes virus infections, including herpes labialis, is hampered by its very low water solubility. Hence, Islam *et al.* have recently reported the preparation of “ILs-in-oil” microemulsions (MEs) by combining hydrophilic choline-based ILs (“water”-like) with a mixture of the SAIL choline oleate and sorbitan laurate (“oil” phase), which allowed enhanced permeation of acyclovir through pig skin while showing no significant skin irritation [147]. The same authors have also investigated

ternary systems comprising ethanol, isopropyl myristate, and choline/amino acid-based ILs, also with encouraging results for solubilization and skin permeation of acyclovir [148].

Many ILs have also intrinsic antimicrobial activity, which is putting them under the spotlight for the management of skin infections, including cSSTI. Imidazolium-based ILs have been for long known to possess antimicrobial action [12] although this has been occasionally hampered by their cytotoxicity [149]. Still, imidazolium-based ILs have been used to prepare novel formulations showing encouraging features to be advanced as safe transdermal delivery systems, e.g., IL-in-oil MEs based on 1-ethyl-3-methylimidazolium acetate [150], or intrinsic antibacterial and antibiofilm activity, as is the case of 1-butyl-3-methylimidazolium hexafluorophosphate-incorporated PLGA NPs developed by Takahashi and co-workers [151]. CAGE is another IL well-known for its activity as a CPE that was recently reported to display strong and broad spectrum antibacterial and antibiofilm activity, including against clinical isolates and MDR strains of bacterial species belonging to the so-called ESKAPE group (comprising *Enterococcus faecium*, *Staphylococcus aureus*, *Klebsiella pneumoniae*, *Acinetobacter baumannii*, *Pseudomonas aeruginosa*, and *Enterobacter spp.*) [152]. The antibiofilm action of CAGE was further investigated *in vitro* on biofilms of methicillin-sensitive *S. aureus*, revealing that the neat IL probably acts by contact killing, eradicating even 72 h-grown biofilms in less than a minute [152]. CAGE also shows promise for tackling skin fungal infections, as recently reported by Qi and co-workers [153]. These authors combined different antimicrobial ILs with the antifungal drug ketoconazole, and found CAGE as the most effective in both promoting deep skin penetration of the drug, and displaying a synergistic antifungal action *in vitro* against *Trichophyton interdigitale* [153].

Other IL-based approaches that are emerging in the latest literature are aimed at addressing topical administration of different types of anti-infective agents. For example, Zhang *et al.* have developed ME formulations based on the 1-hydroxyethyl-3-methylimidazolium chloride and lidocaine ibuprofenate ILs that were able to improve the transdermal permeation of the antimalarial drug artemisinin *via* disruption of the regular arrangement of keratin in the SC [154]. In another example, the 3-hexyl-1-vinylimidazolium bromide IL was employed in the production of a polymerized IL (P-IL) next used to fabricate MNs both possessing intrinsic antimicrobial activity and loaded with salicylic acid, for the topical treatment of skin infections associated to *Propionibacterium acnes*. These MNs were able to promote painless and prolonged DTD of salicylic acid, with enhanced anti-acne effects in both *ex vivo* and *in vivo* experiments [155].

Altogether, these examples highlight the tremendous chemical space that is to be explored regarding use of ILs for topical drug delivery, with focus on anti-infective approaches to face the rising menace of MDR pathogens. ILs are opening new avenues for the post-antibiotic era, as recently highlighted by Bento *et al.*, [156] and one of those avenues may pass by IL-based approaches for topical delivery of antimicrobial and wound-healing peptides.

3.2.2. IL-mediated percutaneous permeation of biomacromolecules

One of the general requisites for a molecule to be able to transpose the SC barrier to reach the viable epidermis and, eventually, deeper skin layers, is a maximum molecular weight of 1 kDa, which means that, unaided, [bio]macromolecules are unable to efficiently permeate across the skin [6]. This size limitation, along with solubility and stability issues, explains why many of the physical, nanotechnological, and chemical approaches addressed in section 2 have been widely employed to enhance the percutaneous permeation of biomacromolecules such as nucleic acids, oligonucleotides, proteins, and peptides [6,157,158].

In the connection with the above, ILs are also showing remarkable capabilities as new chemical tools for the DTD of polysaccharides, nucleic acids, proteins, and peptides. The potential of IL-mediated DTD of polysaccharides and proteins has been already hinted in the previous sub-section, when highlighting taurine-based ILs that, besides displaying intrinsic antitumoral activity, were also able to promote transdermal delivery of insulin and dextran [158]. Yet, polysaccharides like dextran, and related structures, seldom are the object of percutaneous permeation enhancement efforts. Still, Wu *et al.* have recently explored the potential of eight different choline-based ILs to mediate the DTD of a glycosaminoglycan, hyaluronic acid (HA), to reduce skin dehydration [159]. The ILs were prepared *via* acid-base neutralization reactions using choline and selected natural acids (malic, sorbic, maleic, succinic, lactic, geranic, citric, and oleic), and cholinium citrate was found as the most capable of promoting penetration into deeper skin layers and, along with cholinium maleate, significantly reducing skin dehydration [159].

Choline-based ILs have been also lately explored for DTD of nucleic acids by Mitragotri and co-workers [160]. These authors prepared six ILs by a 1:2 cation/anion ratio mixing of cholinium bicarbonate, as the cation donor, with geranate, dimethylacrylate, isovalerate, isopropanoate, phosphate, or biphenyl-3-carboxylate

anions, and next tested the ILs either individually or in different combinations, for their ability to promote DTD of a siRNA with therapeutic potential to tackle plaque psoriasis. The mixture combining CAGE and cholinium phenylpropanoate was the most efficient permeation enhancer that further showed high stability [160]. Additional *in vitro* and *in vivo* assays focused on this combination proved it as safe and able to efficiently silence the deviant gene, with observable decrease in psoriasis-related traits, such as thickened epidermis, inflammation, and hyperkeratosis, as compared to control mice [160]. Mitragotri's group further investigated how ILs might contribute to the stabilization of framework nucleic acids (FNAs), whose emerging role as the next generation precision-tailored and safe NCs for gene therapy of skin diseases is hampered by stability and percutaneous permeation limitations [161]. The authors combined the cholinium cation with the conjugate bases of six natural acids, namely, citronellic, glutaric, glycolic, octanoic, hex-2-enoic, and oct-2-enoic acids, *via* salt metathesis, and the six ILs thus obtained were tested *in vitro* and *ex vivo* for their ability to stabilize and permeate FNAs. Cholinium octanoate showed the most encouraging performance, being able both to keep the FNA NCs stable up to one week at room temperature, and to promote their delivery into the deeper layers of porcine skin [161].

Proteins and peptides are, by far, the most widely and deeply studied biomacromolecules, given their multiple pharmaceutical and biomedical applications, stemming from their broad range of structural, physicochemical, and biological properties, associated to a high level of specificity, thus representing the majority of biopharmaceuticals approved for therapeutic use [162]. Yet, most protein and peptides pose many challenges for therapeutic applications, mostly related to their low bioavailability and *in vivo* stability, which underpins intensive research on strategies for efficient protein and peptide delivery specifically aimed at oral and topical administration routes [158,163]. IL-mediated delivery of proteins has been investigated in recent years, with emphasis on insulin, since topical administration of this protein is highly convenient to promote higher comfort and compliance in diabetic patients. Favorable insulin permeation data were recently reported by Mitragotri and co-workers when using CAGE or taurine/carnitine ILs as, respectively, part of a biodegradable polymeric patch for transmucosal delivery [164], or percutaneous permeation enhancer [140]. Balcão and co-workers have also investigated the adequacy of CAGE and choline oleate ILs, prepared in a 1:2 cation/anion ratio, for potential use in transdermal delivery of insulin [165]. The ILs were evaluated regarding cytotoxicity, genotoxicity, oxidative stability, and ability to enhance insulin percutaneous permeation. CAGE presented the best profile, and was

next incorporated in an optimized biopolymer formulation, affording a transdermal patch that efficiently promoted transdermal delivery of human insulin in a pig ear skin *ex vivo* model [165].

Another interesting report by Vieira *et al.* concerns the characterization of fluorinated ILs as potential protein DTD facilitators [166]. In this recent study, 1:1 combination of the perfluorobutanesulfonate anion with 1-ethyl-3-methylimidazolium, 1-ethyl-3-methylpyridinium or cholinium cations (Figure 13) afforded ILs with high surface activity in aqueous media, i.e., SAILs. The self-assembling properties of these fluorinated SAILs were similar either in water or in buffered solutions of lysozyme, selected as the model cargo protein, which could be successfully encapsulated by the SAILs, except in the case of cholinium perfluorobutanesulfonate. Lysozyme release and activity studies showed the SAIL/protein systems to be reasonably stable for storage at 4 °C (no protein release up to 12 h with protein activity kept intact), whereas total protein release is observed after 12 h at 37 °C [166].

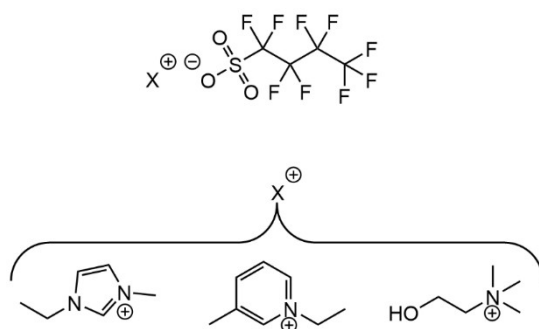


Figure 13. Perfluorobutanesulfonate-based ILs comprising the (from left to right) 1-methyl-3-ethylimidazolium, 1-methyl-3-ethylpyridinium, and cholinium cations, as reported by Vieira *et al.* [166].

Like proteins, bioactive peptides hold great promise for therapeutic applications, with the further advantages of being more cost-effective and less prone to trigger immunoallergenic reactions. Interest is growing on topical delivery approaches for either antigenic peptides of interest for preventive vaccination, or host defense peptides (HDPs) encompassing antimicrobial and/or immunomodulatory effects [167]. Consequently, ILs are under the spotlight of latest research on DTD of therapeutic peptides. For instance, Goto and co-workers developed hydrophobic fatty acid/amino ester-based ILs that were liquid at room temperature (i.e., RTILs) and fully miscible with common CPEs, such as isopropyl myristate (IPM) [168]. Formulations comprising 10% wt of the RTILs in IPM showed lower cytotoxicity than the standard CPE sodium lauryl sulfate and being also

able to better permeate a NSAID (ibuprofen) than the conventional CPE Transcutol®. These formulations (especially the L-proline ethyl ester linoleate-based one), enhanced the percutaneous permeation of an antigenic peptide across porcine skin [168]. The same authors have very recently used similar fatty acid-based ILs to formulate IL-in-oil nanodispersions that were optimized for higher physicochemical stability, as well as increased loading capacity and *in vivo* transdermal delivery of the anticancer nonapeptide leuprolide [169]. The nanodispersions showed no significant toxicity both *in vitro* and *in vivo*, and peptide transdermal delivery could be enhanced by as much as 65-fold compared with the aqueous delivery vehicle [169].

Tahara *et al.* have equally investigated fatty acid/choline-derived ILs as potential facilitators for the solubilization of an antigenic water-soluble peptide in an oil-based percutaneous permeation promoter [170]. The least cytotoxic IL, cholinium oleate, was dispersed with the peptide in the oil phase, and the resulting formulation showed a 28-fold enhancement of peptide transcutaneous permeation as compared to the aqueous vehicle. Moreover, this transdermal delivery formulation did not cause any detectable irritation on skin, and significantly suppressed tumor growth *in vivo* [170].

In regard to transdermal delivery of HDPs, latest efforts have focused on combination of antimicrobial HDPs with ILs possessing intrinsic antimicrobial activity, to afford new formulations whose percutaneous permeation and antimicrobial potency might be mutually enhanced. In this connection, Patel and co-workers mixed an HDP, melittin, with pyrrolidinium-based ILs, and the non-covalent HDP-IL conjugates thus formed displayed superior *in vitro* activity to those of their individual components against both Gram-negative (*E. coli*) and Gram-positive (*S. aureus*) bacteria, while showing no significant cytotoxicity [171]. The same authors further investigated the influence of the alkyl chain length of the pyrrolidinium-based ILs in both their individual antimicrobial potency, and synergistic action upon combination with melittin [172]. This study confirmed the potent synergic action against both *E. coli* and *S. aureus* when the HDP is combined with the ILs, and revealed a correlation between antimicrobial potency, which improved with the increase of the alkyl chain length in the IL [172]. Another example is the work reported by Gomes and co-workers [173]. In this study, coupling an antimicrobial methylimidazolium IL to the *N*-terminus of a collagenesis-inducing peptide with potent antibacterial and antibiofilm properties, delivered a covalent conjugate that retained the parent peptide's activity against multidrug-resistant clinical isolates of Gram-negative bacteria, and antibiofilm action on a resistant clinical isolate of *Klebsiella pneumoniae*, while exhibiting much improved stability towards tyrosinase-mediated

modifications [173]. These above-mentioned works are an overture for the potential held by IL-based strategies as tools to improve the properties of bioactive peptides.

4. Will ionic liquids and peptides become relevant co-players in the future management of skin infections?

The encouraging findings highlighted in the last section, along with latest reports on, e.g., (i) the fabrication of amphiphilic formulations comprising peptides and imidazolium- or betaninium-based ILs as new delivery nanoplatforms [174,175], and (ii) the relevance of developing cationic nanocarriers to overcome negatively-charged tissue barriers like the skin [176], hold great promise for the future management of skin infections, including cSSTI. Current progress in ILs-mediated percutaneous permeation of bioactive compounds, from small anti-inflammatory drugs to host defense peptides, and even lytic bacteriophages [177], together with the intrinsic antimicrobial action of many ILs, underline the capacity of ILs to become important players in innovative approaches to treat skin infections. Likewise, many HDPs combine antimicrobial, immunomodulator and wound-healing properties, with a cationic amphiphilic structure often conveying cell-penetrating and/or self-assembling capacity. Hence, such HDPs will prospectively be useful both as carriers and as bioactive cargoes in transdermal delivery applications.

Effective management of infected wounds should ideally rely on topical formulations able to exert antimicrobial, anti-inflammatory, and healing effects from the outer to the innermost layers of the skin. ILs and HDPs have the potential to jointly contribute to such an achievement.

References

1. Benson, H.A.E.; Grice, J.E.; Mohammed, Y.; Namjoshi, S.; Roberts, M.S. Topical and Transdermal Drug Delivery: From Simple Potions to Smart Technologies. *Curr Drug Deliv* **2019**, *16*, 444-460, doi:10.2174/1567201816666190201143457.
2. Calcutt, J.J.; Roberts, M.S.; Anissimov, Y.G. Modeling drug transport within the viable skin - a review. *Expert Opin. Drug Metab. Toxicol.* **2021**, *17*, 105-119, doi:10.1080/17425255.2020.1832081.
3. Kahraman, E.; Güngör, S.; Özsoy, Y. Potential enhancement and targeting strategies of polymeric and lipid-based nanocarriers in dermal drug delivery. *Ther. Deliv.* **2017**, *8*, 967-985, doi:10.4155/tde-2017-0075.
4. Pereira, R.; Silva, S.G.; Pinheiro, M.; Reis, S.; Vale, M.L. Current Status of Amino Acid-Based Permeation Enhancers in Transdermal Drug Delivery. *Membranes* **2021**, *11*, doi:10.3390/membranes11050343.
5. Ramadon, D.; McCrudden, M.T.C.; Courtenay, A.J.; Donnelly, R.F. Enhancement strategies for transdermal drug delivery systems: current trends and applications. *Drug Deliv. Transl. Res.* **2021**, doi:10.1007/s13346-021-00909-6.
6. Münch, S.; Wohlrab, J.; Neubert, R.H.H. Dermal and transdermal delivery of pharmaceutically relevant macromolecules. *Eur. J. Pharm. Biopharm.* **2017**, *119*, 235-242, doi:<https://doi.org/10.1016/j.ejpb.2017.06.019>.
7. Yu, Y.-Q.; Yang, X.; Wu, X.-F.; Fan, Y.-B. Enhancing Permeation of Drug Molecules Across the Skin via Delivery in Nanocarriers: Novel Strategies for Effective Transdermal Applications. *Front. Bioeng. Biotechnol.* **2021**, *9*, doi:10.3389/fbioe.2021.646554.
8. Municoy, S.; Alvarez Echazu, M.I.; Antezana, P.E.; Galdoporpora, J.M.; Olivetti, C.; Mebert, A.M.; Foglia, M.L.; Tuttolomondo, M.V.; Alvarez, G.S.; Hardy, J.G.; et al. Stimuli-Responsive Materials for Tissue Engineering and Drug Delivery. *Int J Mol Sci* **2020**, *21*, doi:10.3390/ijms21134724.
9. Kim, B.; Cho, H.-E.; Moon, S.H.; Ahn, H.-J.; Bae, S.; Cho, H.-D.; An, S. Transdermal delivery systems in cosmetics. *Biomed. dermatol.* **2020**, *4*, 10, doi:10.1186/s41702-020-0058-7.

10. Gupta, R.; Dwadasi, B.S.; Rai, B.; Mitragotri, S. Effect of Chemical Permeation Enhancers on Skin Permeability: In silico screening using Molecular Dynamics simulations. *Sci. Rep.* **2019**, *9*, 1456, doi:10.1038/s41598-018-37900-0.
11. Hoang, T.P.; Ghori, M.U.; Conway, B.R. Topical Antiseptic Formulations for Skin and Soft Tissue Infections. *Pharmaceutics* **2021**, *13*, doi:10.3390/pharmaceutics13040558.
12. Ferraz, R.; Teixeira, C.; Gomes, P.; Prudêncio, C. CHAPTER 16 Bioactivity of Ionic Liquids. In *Ionic Liquid Devices*; R. Soc. Chem.: 2018; pp. 404-422.
13. Gamboa, A.; Schüßler, N.; Soto-Bustamante, E.; Romero-Hasler, P.; Meinel, L.; Morales, J.O. Delivery of ionizable hydrophilic drugs based on pharmaceutical formulation of ion pairs and ionic liquids. *Eur. J. Pharm. Biopharm.* **2020**, *156*, 203-218, doi:<https://doi.org/10.1016/j.ejpb.2020.09.007>.
14. Silva, A.T.; Teixeira, C.; Marques, E.F.; Prudêncio, C.; Gomes, P.; Ferraz, R. Surfing the Third Wave of Ionic Liquids: A Brief Review on the Role of Surface-Active Ionic Liquids in Drug Development and Delivery. *ChemMedChem* **2021**, *16*, 2604-2611, doi:<https://doi.org/10.1002/cmdc.202100215>.
15. Tanner, E.E.L.; Curreri, A.M.; Balkaran, J.P.R.; Selig-Wober, N.C.; Yang, A.B.; Kendig, C.; Fluhr, M.P.; Kim, N.; Mitragotri, S. Design Principles of Ionic Liquids for Transdermal Drug Delivery. *Adv. Mater.* **2019**, *31*, 1901103, doi:<https://doi.org/10.1002/adma.201901103>.
16. Novickij, V.; Zinkevičienė, A.; Perminaitė, E.; Čėsna, R.; Lastauskienė, E.; Paškevičius, A.; Švedienė, J.; Markovskaja, S.; Novickij, J.; Girkontaitė, I. Non-invasive nanosecond electroporation for biocontrol of surface infections: an in vivo study. *Sci. Rep.* **2018**, *8*, 14516, doi:10.1038/s41598-018-32783-7.
17. Novickij, V.; Lastauskienė, E.; Staigvila, G.; Girkontaitė, I.; Zinkevičienė, A.; Švedienė, J.; Paškevičius, A.; Markovskaja, S.; Novickij, J. Low concentrations of acetic and formic acids enhance the inactivation of *Staphylococcus aureus* and *Pseudomonas aeruginosa* with pulsed electric fields. *BMC Microbiol.* **2019**, *19*, 73, doi:10.1186/s12866-019-1447-1.
18. Das, B.; Shirao, A.; Golberg, A.; Berthiaume, F.; Schloss, R.; Yarmush, M.L. Differential Cell Death and Regrowth of Dermal Fibroblasts and Keratinocytes

- After Application of Pulsed Electric Fields. *Bioelectricity* **2020**, *2*, 175-185, doi:10.1089/bioe.2020.0015.
19. Bakshi, P.; Vora, D.; Hemmady, K.; Banga, A.K. Iontophoretic skin delivery systems: Success and failures. *Int J Pharmaceut* **2020**, *586*, 119584, doi:<https://doi.org/10.1016/j.ijpharm.2020.119584>.
 20. Jiang, C.; Jiang, X.; Wang, X.; Shen, J.; Zhang, M.; Jiang, L.; Ma, R.; Gan, T.; Gong, Y.; Ye, J.; et al. Transdermal iontophoresis delivery system for terazosin hydrochloride: an in vitro and in vivo study. *Drug Deliv.* **2021**, *28*, 454-462, doi:10.1080/10717544.2021.1889719.
 21. Iontophoresis of Treprostinil to Enhance Wound Healing in Diabetic Foot Skin Ulcers. Available online: <https://www.smartpatients.com/trials/NCT03654989> (accessed on 10 October 2021).
 22. Liao, A.-H.; Hung, C.-R.; Chen, H.-K.; Chiang, C.-P. Ultrasound-Mediated EGF-Coated-Microbubble Cavitation in Dressings for Wound-Healing Applications. *Sci. Rep.* **2018**, *8*, 8327, doi:10.1038/s41598-018-26702-z.
 23. Chen, L.; Zheng, Q.; Chen, X.; Wang, J.; Wang, L. Low-frequency ultrasound enhances vascular endothelial growth factor expression, thereby promoting the wound healing in diabetic rats. *Exp Ther Med* **2019**, *18*, 4040-4048, doi:10.3892/etm.2019.8051.
 24. Halder, J.; Gupta, S.; Kumari, R.; Gupta, G.D.; Rai, V.K. Microneedle Array: Applications, Recent Advances, and Clinical Pertinence in Transdermal Drug Delivery. *J. Pharm. Innov.* **2021**, *16*, 558-565, doi:10.1007/s12247-020-09460-2.
 25. Kirkby, M.; Hutton, A.R.J.; Donnelly, R.F. Microneedle Mediated Transdermal Delivery of Protein, Peptide and Antibody Based Therapeutics: Current Status and Future Considerations. *Pharm Res-Dordr* **2020**, *37*, 117, doi:10.1007/s11095-020-02844-6.
 26. Lim, S.H.; Tiew, W.J.; Zhang, J.; Ho, P.C.-L.; Kachouie, N.N.; Kang, L. Geometrical optimisation of a personalised microneedle eye patch for transdermal delivery of anti-wrinkle small peptide. *Biofabrication* **2020**, *12*, 035003, doi:10.1088/1758-5090/ab6d37.

27. Barnum, L.; Samandari, M.; Schmidt, T.A.; Tamayol, A. Microneedle arrays for the treatment of chronic wounds. *Expert Opin Drug Del* **2020**, *17*, 1767-1780, doi:10.1080/17425247.2020.1819787.
28. Frydman, G.H.; Olaleye, D.; Annamalai, D.; Layne, K.; Yang, I.; Kaafarani, H.M.A.; Fox, J.G. Manuka honey microneedles for enhanced wound healing and the prevention and/or treatment of Methicillin-resistant Staphylococcus aureus (MRSA) surgical site infection. *Sci. Rep.* **2020**, *10*, 13229, doi:10.1038/s41598-020-70186-9.
29. Ibelli, T.; Templeton, S.; Levi-Polyachenko, N. Progress on utilizing hyperthermia for mitigating bacterial infections. *Int. J. Hyperth.* **2018**, *34*, 144-156, doi:10.1080/02656736.2017.1369173.
30. Mahmoud, N.N.; Alkilany, A.M.; Khalil, E.A.; Al-Bakri, A.G. Nano-Photothermal ablation effect of Hydrophilic and Hydrophobic Functionalized Gold Nanorods on Staphylococcus aureus and Propionibacterium acnes. *Sci. Rep.* **2018**, *8*, 6881, doi:10.1038/s41598-018-24837-7.
31. Alumutairi, L.; Yu, B.; Filka, M.; Nayfach, J.; Kim, M.-H. Mild magnetic nanoparticle hyperthermia enhances the susceptibility of Staphylococcus aureus biofilm to antibiotics. *Int. J. Hyperth.* **2020**, *37*, 66-75, doi:10.1080/02656736.2019.1707886.
32. Cheng, G.; Li, B. Nanoparticle-based photodynamic therapy: new trends in wound healing applications. *Mater. Today Adv.* **2020**, *6*, 100049, doi:<https://doi.org/10.1016/j.mtadv.2019.100049>.
33. Kokolakis, G.; von Grawert, L.; Ulrich, M.; Lademann, J.; Zuberbier, T.; Hofmann, M.A. Wound Healing Process After Thermomechanical Skin Ablation. *Lasers Surg. Med.* **2020**, *52*, 730-734, doi:<https://doi.org/10.1002/lsm.23213>.
34. Qiao, Y.; Ping, Y.; Zhang, H.; Zhou, B.; Liu, F.; Yu, Y.; Xie, T.; Li, W.; Zhong, D.; Zhang, Y.; et al. Laser-Activatable CuS Nanodots to Treat Multidrug-Resistant Bacteria and Release Copper Ion to Accelerate Healing of Infected Chronic Nonhealing Wounds. *Acs Appl Mater Inter* **2019**, *11*, 3809-3822, doi:10.1021/acsami.8b21766.
35. Park, J.; Lee, H.; Lim, G.-S.; Kim, N.; Kim, D.; Kim, Y.-C. Enhanced Transdermal Drug Delivery by Sonophoresis and Simultaneous Application of Sonophoresis

- and Iontophoresis. *AAPS PharmSciTech* **2019**, *20*, 96, doi:10.1208/s12249-019-1309-z.
36. Parhi, R.; Mandru, A. Enhancement of skin permeability with thermal ablation techniques: concept to commercial products. *Drug Deliv Transl Res* **2021**, *11*, 817-841, doi:10.1007/s13346-020-00823-3.
 37. Rai, V.K.; Mishra, N.; Yadav, K.S.; Yadav, N.P. Nanoemulsion as pharmaceutical carrier for dermal and transdermal drug delivery: Formulation development, stability issues, basic considerations and applications. *J Control Release* **2018**, *270*, 203-225, doi:<https://doi.org/10.1016/j.jconrel.2017.11.049>.
 38. Shaker, D.S.; Ishak, R.A.H.; Ghoneim, A.; Elhuoni, M.A. Nanoemulsion: A Review on Mechanisms for the Transdermal Delivery of Hydrophobic and Hydrophilic Drugs. *Sci. Pharm.* **2019**, *87*, doi:10.3390/scipharm87030017.
 39. Alghaith, A.F.; Alshehri, S.; Alhakamy, N.A.; Hosny, K.M. Development, optimization and characterization of nanoemulsion loaded with clove oil-naftifine antifungal for the management of tinea. *Drug Deliv.* **2021**, *28*, 343-356, doi:10.1080/10717544.2021.1879314.
 40. Zhou, X.; Hao, Y.; Yuan, L.; Pradhan, S.; Shrestha, K.; Pradhan, O.; Liu, H.; Li, W. Nano-formulations for transdermal drug delivery: A review. *Chin. Chem. Lett.* **2018**, *29*, 1713-1724, doi:<https://doi.org/10.1016/j.ccllet.2018.10.037>.
 41. Kassem, A.A.; Abd El-Alim, S.H. Vesicular Nanocarriers: A Potential Platform for Dermal and Transdermal Drug Delivery. In *Nanopharmaceuticals: Principles and Applications Vol. 2*, Yata, V.K., Ranjan, S., Dasgupta, N., Lichtfouse, E., Eds.; Springer International Publishing: Cham, 2021; pp. 155-209.
 42. Jeong, W.Y.; Kwon, M.; Choi, H.E.; Kim, K.S. Recent advances in transdermal drug delivery systems: a review. *Biomater. Res.* **2021**, *25*, 24, doi:10.1186/s40824-021-00226-6.
 43. Patel, D.; Patel, B.; Thakkar, H. Lipid Based Nanocarriers: Promising Drug Delivery System for Topical Application. *Eur J Lipid Sci Technol.* **2021**, *123*, 2000264, doi:<https://doi.org/10.1002/ejlt.202000264>.
 44. Yu, Z.; Meng, X.; Zhang, S.; Chen, Y.; Zhang, Z.; Zhang, Y. Recent Progress in Transdermal Nanocarriers and Their Surface Modifications. *Molecules* **2021**, *26*, doi:10.3390/molecules26113093.

45. Hua, S. Lipid-based nano-delivery systems for skin delivery of drugs and bioactives. *Front Pharmacol* **2015**, *6*, 219-219, doi:10.3389/fphar.2015.00219.
46. Witika, B.A.; Mweetwa, L.L.; Tshiamo, K.O.; Edler, K.; Matafwali, S.K.; Ntemi, P.V.; Chikukwa, M.T.R.; Makoni, P.A. Vesicular drug delivery for the treatment of topical disorders: current and future perspectives. *J. Pharm. Pharmacol.* **2021**, doi:10.1093/jpp/rgab082.
47. Lai, F.; Caddeo, C.; Manca, M.L.; Manconi, M.; Sinico, C.; Fadda, A.M. What's new in the field of phospholipid vesicular nanocarriers for skin drug delivery. *Int J Pharmaceut* **2020**, *583*, 119398, doi:<https://doi.org/10.1016/j.ijpharm.2020.119398>.
48. Paiva-Santos, A.C.; Silva, A.L.; Guerra, C.; Peixoto, D.; Pereira-Silva, M.; Zeinali, M.; Mascarenhas-Melo, F.; Castro, R.; Veiga, F. Ethosomes as Nanocarriers for the Development of Skin Delivery Formulations. *Pharm Res-Dordr* **2021**, *38*, 947-970, doi:10.1007/s11095-021-03053-5.
49. Opatha, S.A.; Titapiwatanakun, V.; Chutoprapat, R. Transfersomes: A Promising Nanoencapsulation Technique for Transdermal Drug Delivery. *Pharmaceutics* **2020**, *12*, doi:10.3390/pharmaceutics12090855.
50. Durga, B.; Veera, L. Recent advances of non-ionic surfactant-based nano-vesicles (niosomes and proniosomes): a brief review of these in enhancing transdermal delivery of drug. *Future J. Pharm. Sci.* **2020**, *6*, 100, doi:10.1186/s43094-020-00117-y.
51. Kauslya, A.; Borawake, P.D.; Shinde, J.V.; Chavan, R. Niosomes: A Novel Carrier Drug Delivery System. *J. drug deliv. ther.* **2021**, *11*, 162-170.
52. Khalil, R.M.; Abdelbary, A.; Arini, S.K.E.; Basha, M.; El-Hashemy, H.A.; Farouk, F. Development of tizanidine loaded aspasomes as transdermal delivery system: ex-vivo and in-vivo evaluation. *J. Liposome Res.* **2021**, *31*, 19-29, doi:10.1080/08982104.2019.1684940.
53. Zoabi, A.; Touitou, E.; Margulis, K. Recent Advances in Nanomaterials for Dermal and Transdermal Applications. *J. Colloid Interface* **2021**, *5*, doi:10.3390/colloids5010018.

54. Miller, A.J.; Pearce, A.K.; Foster, J.C.; O'Reilly, R.K. Probing and Tuning the Permeability of Polymersomes. *ACS Cent. Sci.* **2021**, *7*, 30-38, doi:10.1021/acscentsci.0c01196.
55. Nigro, F.; Cerqueira Pinto, C.d.S.; dos Santos, E.P.; Mansur, C.R.E. Niosome-based hydrogel as a potential drug delivery system for topical and transdermal applications. *Int. J. Polym. Mater.* **2020**, 1-18, doi:10.1080/00914037.2020.1848833.
56. Fu, X.; Shi, Y.; Wang, H.; Zhao, X.; Sun, Q.; Huang, Y.; Qi, T.; Lin, G. Ethosomal Gel for Improving Transdermal Delivery of Thymosin β -4. *Int J Nanomedicine* **2019**, *14*, 9275-9284, doi:10.2147/IJN.S228863.
57. Bhattacharya, S. Preparation and characterizations of glyceryl oleate ufasomes of terbinafine hydrochloride: a novel approach to trigger *Candida albicans* fungal infection. *Future J. Pharm. Sci.* **2021**, *7*, 3, doi:10.1186/s43094-020-00143-w.
58. Zhang, Y.; Liu, Y.; Liu, H.; Tang, W.H. Exosomes: biogenesis, biologic function and clinical potential. *Cell Biosci.* **2019**, *9*, 19, doi:10.1186/s13578-019-0282-2.
59. Gu, T.-W.; Wang, M.-Z.; Niu, J.; Chu, Y.; Guo, K.-R.; Peng, L.-H. Outer membrane vesicles derived from *E. coli* as novel vehicles for transdermal and tumor targeting delivery. *Nanoscale* **2020**, *12*, 18965-18977, doi:10.1039/D0NR03698F.
60. Liang, Y.; Duan, L.; Lu, J.; Xia, J. Engineering exosomes for targeted drug delivery. *Theranostics* **2021**, *11*, 3183-3195, doi:10.7150/thno.52570.
61. Aslan, C.; Kiaie, S.H.; Zolbanin, N.M.; Loffinejad, P.; Ramezani, R.; Kashanchi, F.; Jafari, R. Exosomes for mRNA delivery: a novel biotherapeutic strategy with hurdles and hope. *BMC Biotechnol.* **2021**, *21*, 20, doi:10.1186/s12896-021-00683-w.
62. Riau, A.K.; Ong, H.S.; Yam, G.H.F.; Mehta, J.S. Sustained Delivery System for Stem Cell-Derived Exosomes. *Front. Pharmacol.* **2019**, *10*, doi:10.3389/fphar.2019.01368.
63. Xiong, M.; Zhang, Q.; Hu, W.; Zhao, C.; Lv, W.; Yi, Y.; Wang, Y.; Tang, H.; Wu, M.; Wu, Y. The novel mechanisms and applications of exosomes in dermatology and cutaneous medical aesthetics. *Pharmacol. Res* **2021**, *166*, 105490, doi:<https://doi.org/10.1016/j.phrs.2021.105490>.

64. Cho, B.S.; Lee, J.; Won, Y.; Duncan, D.I.; Jin, R.C.; Lee, J.; Kwon, H.H.; Park, G.-H.; Yang, S.H.; Park, B.C.; et al. Skin Brightening Efficacy of Exosomes Derived from Human Adipose Tissue-Derived Stem/Stromal Cells: A Prospective, Split-Face, Randomized Placebo-Controlled Study. *Cosmetics* **2020**, *7*, doi:10.3390/cosmetics7040090.
65. Hu, P.; Yang, Q.; Wang, Q.; Shi, C.; Wang, D.; Armato, U.; Prà, I.D.; Chiarini, A. Mesenchymal stromal cells-exosomes: a promising cell-free therapeutic tool for wound healing and cutaneous regeneration. *Burns & Trauma* **2019**, *7*, doi:10.1186/s41038-019-0178-8.
66. Peng, L.-H.; Wang, M.-Z.; Chu, Y.; Zhang, L.; Niu, J.; Shao, H.-T.; Yuan, T.-J.; Jiang, Z.-H.; Gao, J.-Q.; Ning, X.-H. Engineering bacterial outer membrane vesicles as transdermal nanopatforms for photo-TRAIL-programmed therapy against melanoma. *Sci. Adv.* **2020**, *6*, eaba2735, doi:10.1126/sciadv.aba2735.
67. Kanwar, R.; Rathee, J.; Salunke, D.B.; Mehta, S.K. Green Nanotechnology-Driven Drug Delivery Assemblies. *ACS Omega* **2019**, *4*, 8804-8815, doi:10.1021/acsomega.9b00304.
68. Khan, I.; Saeed, K.; Khan, I. Nanoparticles: Properties, applications and toxicities. *Arab. J. Chem.* **2019**, *12*, 908-931, doi:<https://doi.org/10.1016/j.arabjc.2017.05.011>.
69. Shirodkar, R.K.; Kumar, L.; Mutalik, S.; Lewis, S. Solid Lipid Nanoparticles and Nanostructured Lipid Carriers: Emerging Lipid Based Drug Delivery Systems. *Pharm. Chem. J.* **2019**, *53*, 440-453, doi:10.1007/s11094-019-02017-9.
70. Dhiman, N.; Awasthi, R.; Sharma, B.; Kharkwal, H.; Kulkarni, G.T. Lipid Nanoparticles as Carriers for Bioactive Delivery. *Front. Chem.* **2021**, *9*, doi:10.3389/fchem.2021.580118.
71. Scioli Montoto, S.; Muraca, G.; Ruiz, M.E. Solid Lipid Nanoparticles for Drug Delivery: Pharmacological and Biopharmaceutical Aspects. *Front. Mol. Biosci.* **2020**, *7*, doi:10.3389/fmolb.2020.587997.
72. Souto, E.B.; Baldim, I.; Oliveira, W.P.; Rao, R.; Yadav, N.; Gama, F.M.; Mahant, S. SLN and NLC for topical, dermal, and transdermal drug delivery. *Expert Opin Drug Del* **2020**, *17*, 357-377, doi:10.1080/17425247.2020.1727883.

73. Khater, D.; Nsairat, H.; Odeh, F.; Saleh, M.; Jaber, A.; Alshaer, W.; Al Bawab, A.; Mubarak, M.S. Design, Preparation, and Characterization of Effective Dermal and Transdermal Lipid Nanoparticles: A Review. *Cosmetics* **2021**, *8*, doi:10.3390/cosmetics8020039.
74. Wang, W.; Lu, K.-j.; Yu, C.-h.; Huang, Q.-l.; Du, Y.-Z. Nano-drug delivery systems in wound treatment and skin regeneration. *J. Nanobiotechnology* **2019**, *17*, 82, doi:10.1186/s12951-019-0514-y.
75. Matei, A.-M.; Caruntu, C.; Tampa, M.; Georgescu, S.R.; Matei, C.; Constantin, M.M.; Constantin, T.V.; Calina, D.; Ciubotaru, D.A.; Badarau, I.A.; et al. Applications of Nanosized-Lipid-Based Drug Delivery Systems in Wound Care. *Appl. Sci.* **2021**, *11*, doi:10.3390/app11114915.
76. Myla Lôbo de, S.; Widson Michael dos, S.; André Luiz Moreira Domingues de, S.; Victor de Albuquerque Wanderley, S.; Fernanda Pontes, N.; Marcos Victor Gregorio de, O.; Pedro José, R.-N. Lipid Nanoparticles as a Skin Wound Healing Drug Delivery System: Discoveries and Advances. *Curr. Pharm. Des.* **2020**, *26*, 4536-4550, doi:<http://dx.doi.org/10.2174/1381612826666200417144530>.
77. Gad, H.A.; Abd El-Rahman, F.A.A.; Hamdy, G.M. Chamomile oil loaded solid lipid nanoparticles: A naturally formulated remedy to enhance the wound healing. *J. Drug Deliv. Sci. Technol* **2019**, *50*, 329-338, doi:<https://doi.org/10.1016/j.jddst.2019.01.008>.
78. Saporito, F.; Sandri, G.; Bonferoni, M.C.; Rossi, S.; Boselli, C.; Icaro Cornaglia, A.; Mannucci, B.; Grisoli, P.; Vigani, B.; Ferrari, F. Essential oil-loaded lipid nanoparticles for wound healing. *Int J Nanomedicine* **2017**, *13*, 175-186, doi:10.2147/IJN.S152529.
79. Liakopoulou, A.; Mourelatou, E.; Hatziantoniou, S. Exploitation of traditional healing properties, using the nanotechnology's advantages: The case of curcumin. *Toxicol. Rep.* **2021**, *8*, 1143-1155, doi:<https://doi.org/10.1016/j.toxrep.2021.05.012>.
80. Thorn, C.R.; Thomas, N.; Boyd, B.J.; Prestidge, C.A. Nano-fats for bugs: the benefits of lipid nanoparticles for antimicrobial therapy. *Drug Deliv. Transl. Res.* **2021**, *11*, 1598-1624, doi:10.1007/s13346-021-00921-w.

81. Pinilla, C.M.; Lopes, N.A.; Brandelli, A. Lipid-Based Nanostructures for the Delivery of Natural Antimicrobials. *Molecules* **2021**, *26*, doi:10.3390/molecules26123587.
82. Araujo, V.H.S.; Delello Di Filippo, L.; Duarte, J.L.; Spósito, L.; Camargo, B.A.F.d.; da Silva, P.B.; Chorilli, M. Exploiting solid lipid nanoparticles and nanostructured lipid carriers for drug delivery against cutaneous fungal infections. *Crit. Rev. Microbiol.* **2021**, *47*, 79-90, doi:10.1080/1040841X.2020.1843399.
83. Arana, L.; Gallego, L.; Alkorta, I. Incorporation of Antibiotics into Solid Lipid Nanoparticles: A Promising Approach to Reduce Antibiotic Resistance Emergence. *Nanomaterials* **2021**, *11*, doi:10.3390/nano11051251.
84. dos Santos Ramos, M.A.; de Toledo, L.G.; Spósito, L.; Marena, G.D.; de Lima, L.C.; Fortunato, G.C.; Araújo, V.H.S.; Bauab, T.M.; Chorilli, M. Nanotechnology-based lipid systems applied to resistant bacterial control: A review of their use in the past two decades. *Int J Pharmaceut* **2021**, *603*, 120706, doi:<https://doi.org/10.1016/j.ijpharm.2021.120706>.
85. Mamun, M.M.; Sorinolu, A.J.; Munir, M.; Vejerano, E.P. Nanoantibiotics: Functions and Properties at the Nanoscale to Combat Antibiotic Resistance. *Front. Chem.* **2021**, *9*, doi:10.3389/fchem.2021.687660.
86. Sguizzato, M.; Esposito, E.; Cortesi, R. Lipid-Based Nanosystems as a Tool to Overcome Skin Barrier. *Int. J. Mol. Sci.* **2021**, *22*, doi:10.3390/ijms22158319.
87. Walduck, A.; Sangwan, P.; Vo, Q.A.; Ratcliffe, J.; White, J.; Muir, B.W.; Tran, N. Treatment of Staphylococcus aureus skin infection in vivo using rifampicin loaded lipid nanoparticles. *RSC Advances* **2020**, *10*, 33608-33619, doi:10.1039/D0RA06120D.
88. Mittal, P.; Saharan, A.; Verma, R.; Altalbawy, F.M.A.; Alfaidi, M.A.; Batiha, G.E.-S.; Akter, W.; Gautam, R.K.; Uddin, M.S.; Rahman, M.S. Dendrimers: A New Race of Pharmaceutical Nanocarriers. *Biomed Res. Int.* **2021**, *2021*, 8844030, doi:10.1155/2021/8844030.
89. Nikzamir, M.; Hanifehpour, Y.; Akbarzadeh, A.; Panahi, Y. Applications of Dendrimers in Nanomedicine and Drug Delivery: A Review. *J. Inorg. Organomet. Polym. Mater.* **2021**, *31*, 2246-2261, doi:10.1007/s10904-021-01925-2.

90. Santos, A.; Veiga, F.; Figueiras, A. Dendrimers as Pharmaceutical Excipients: Synthesis, Properties, Toxicity and Biomedical Applications. *Materials* **2020**, *13*, doi:10.3390/ma13010065.
91. Kirkby, M.; Sabri, A.B.; Scurr, D.J.; Moss, G.P. Dendrimer-mediated permeation enhancement of chlorhexidine digluconate: Determination of in vitro skin permeability and visualisation of dermal distribution. *Eur. J. Pharm. Biopharm.* **2021**, *159*, 77-87, doi:<https://doi.org/10.1016/j.ejpb.2020.12.014>.
92. Gökçe, B.B.; Boran, T.; Emlik Çalık, F.; Özhan, G.; Sanyal, R.; Güngör, S. Dermal delivery and follicular targeting of adapalene using PAMAM dendrimers. *Drug Deliv. Transl. Res.* **2021**, *11*, 626-646, doi:10.1007/s13346-021-00933-6.
93. Sung, Y.K.; Kim, S.W. Recent advances in polymeric drug delivery systems. *Biomater. Res.* **2020**, *24*, 12, doi:10.1186/s40824-020-00190-7.
94. Van Gheluwe, L.; Chourpa, I.; Gaigne, C.; Munnier, E. Polymer-Based Smart Drug Delivery Systems for Skin Application and Demonstration of Stimuli-Responsiveness. *Polymers* **2021**, *13*, doi:10.3390/polym13081285.
95. Praveen, A.; Aqil, M. Transdermal Delivery of Chitosan-Based Systems. In *Functional Chitosan: Drug Delivery and Biomedical Applications*, Jana, S., Jana, S., Eds.; Springer Singapore: Singapore, 2019; pp. 75-106.
96. Bagheri, F.; Darakhshan, S.; Mazloomi, S.; Shiri Varnamkhasti, B.; Tahvilian, R. Dual loading of Nigella sativa oil-atorvastatin in chitosan-carboxymethyl cellulose nanogel as a transdermal delivery system. *Drug Dev Ind Pharm* **2021**, *47*, 569-578, doi:10.1080/03639045.2021.1892742.
97. Sun, L.; Li, J.; Gao, W.; Shi, M.; Tang, F.; Fu, X.; Chen, X. Coaxial nanofibrous scaffolds mimicking the extracellular matrix transition in the wound healing process promoting skin regeneration through enhancing immunomodulation. *J. Mater. Chem. B* **2021**, *9*, 1395-1405, doi:10.1039/D0TB01933J.
98. Paul, W.; Sharma, C.P. 13 - Inorganic nanoparticles for targeted drug delivery. In *Biointegration of Medical Implant Materials (Second Edition)*, Sharma, C.P., Ed.; Woodhead Publishing: 2020; pp. 333-373.
99. Shi, Z.; Zhou, Y.; Fan, T.; Lin, Y.; Zhang, H.; Mei, L. Inorganic nano-carriers based smart drug delivery systems for tumor therapy. *smart mater. res.* **2020**, *1*, 32-47, doi:<https://doi.org/10.1016/j.smaim.2020.05.002>.

100. Zhou, H.; Ge, J.; Miao, Q.; Zhu, R.; Wen, L.; Zeng, J.; Gao, M. Biodegradable Inorganic Nanoparticles for Cancer Theranostics: Insights into the Degradation Behavior. *Bioconjugate Chem.* **2020**, *31*, 315-331, doi:10.1021/acs.bioconjchem.9b00699.
101. Gulin-Sarfraz, T.; Kalantzopoulos, G.N.; Kvalvåg Pettersen, M.; Wold Åsli, A.; Tho, I.; Axelsson, L.; Sarfraz, J. Inorganic Nanocarriers for Encapsulation of Natural Antimicrobial Compounds for Potential Food Packaging Application: A Comparative Study. *Nanomaterials* **2021**, *11*, doi:10.3390/nano11020379.
102. Raviraj, V.; Pham, B.T.T.; Kim, B.J.; Pham, N.T.H.; Kok, L.F.; Painter, N.; Delic, N.C.; Jones, S.K.; Hawkett, B.S.; Lyons, J.G. Non-invasive transdermal delivery of chemotherapeutic molecules in vivo using superparamagnetic iron oxide nanoparticles. *Cancer Nanotechnol.* **2021**, *12*, 6, doi:10.1186/s12645-021-00079-7.
103. Spirescu, V.A.; Chircov, C.; Grumezescu, A.M.; Vasile, B.Ş.; Andronescu, E. Inorganic Nanoparticles and Composite Films for Antimicrobial Therapies. *Int. J. Mol. Sci.* **2021**, *22*, doi:10.3390/ijms22094595.
104. Bruna, T.; Maldonado-Bravo, F.; Jara, P.; Caro, N. Silver Nanoparticles and Their Antibacterial Applications. *Int. J. Mol. Sci.* **2021**, *22*, doi:10.3390/ijms22137202.
105. Dawadi, S.; Katuwal, S.; Gupta, A.; Lamichhane, U.; Thapa, R.; Jaisi, S.; Lamichhane, G.; Bhattarai, D.P.; Parajuli, N. Current Research on Silver Nanoparticles: Synthesis, Characterization, and Applications. *J. Nanomater.* **2021**, *2021*, 6687290, doi:10.1155/2021/6687290.
106. Mussin, J.; Robles-Botero, V.; Casañas-Pimentel, R.; Rojas, F.; Angiolella, L.; San Martín-Martínez, E.; Giusiano, G. Antimicrobial and cytotoxic activity of green synthesis silver nanoparticles targeting skin and soft tissue infectious agents. *Sci. Rep.* **2021**, *11*, 14566, doi:10.1038/s41598-021-94012-y.
107. Gautam, R.; Yang, S.; Maharjan, A.; Jo, J.; Acharya, M.; Heo, Y.; Kim, C. Prediction of Skin Sensitization Potential of Silver and Zinc Oxide Nanoparticles Through the Human Cell Line Activation Test. *Front. Toxicol.* **2021**, *3*, doi:10.3389/ftox.2021.649666.
108. Silva, F.A.L.S.; Costa-Almeida, R.; Timochenco, L.; Amaral, S.I.; Pinto, S.; Gonçalves, I.C.; Fernandes, J.R.; Magalhães, F.D.; Sarmiento, B.; Pinto, A.M.

- Graphene Oxide Topical Administration: Skin Permeability Studies. *Materials* **2021**, *14*, doi:10.3390/ma14112810.
109. Soliman, M.; Sadek, A.A.; Abdelhamid, H.N.; Hussein, K. Graphene oxide-cellulose nanocomposite accelerates skin wound healing. *Vet. Sci. Res. J.* **2021**, *137*, 262-273, doi:<https://doi.org/10.1016/j.rvsc.2021.05.013>.
 110. Mei, D.; Guo, X.; Wang, Y.; Huang, X.; Guo, L.; Zou, P.; Ge, D.; Wang, X.; Lee, W.; Sun, T.; et al. PEGylated Graphene Oxide Carried OH-CATH30 to Accelerate the Healing of Infected Skin Wounds. *Int J Nanomedicine* **2021**, *16*, 4769-4780, doi:10.2147/ijn.s304702.
 111. Pormohammad, A.; Monych, N.K.; Ghosh, S.; Turner, D.L.; Turner, R.J. Nanomaterials in Wound Healing and Infection Control. *Antibiotics* **2021**, *10*, doi:10.3390/antibiotics10050473.
 112. Zhang, X.; Chen, G.; Liu, Y.; Sun, L.; Sun, L.; Zhao, Y. Black Phosphorus-Loaded Separable Microneedles as Responsive Oxygen Delivery Carriers for Wound Healing. *ACS Nano* **2020**, *14*, 5901-5908, doi:10.1021/acsnano.0c01059.
 113. Sully, R.E.; Garelick, H.; Loizidou, E.Z.; Podoleanu, A.G.; Gubala, V. Nanoparticle-infused-biodegradable-microneedles as drug-delivery systems: preparation and characterisation. *Adv. Mater.* **2021**, *2*, 5432-5442, doi:10.1039/D1MA00135C.
 114. Elahpour, N.; Pahlevanzadeh, F.; Kharaziha, M.; Bakhsheshi-Rad, H.R.; Ramakrishna, S.; Berto, F. 3D printed microneedles for transdermal drug delivery: A brief review of two decades. *Int J Pharmaceut* **2021**, *597*, 120301, doi:<https://doi.org/10.1016/j.ijpharm.2021.120301>.
 115. Dragicevic, N.; Atkinson, J.P.; Maibach, H.I. Chemical Penetration Enhancers: Classification and Mode of Action. In *Percutaneous Penetration Enhancers Chemical Methods in Penetration Enhancement: Modification of the Stratum Corneum*, Dragicevic, N., Maibach, H.I., Eds.; Springer Berlin Heidelberg: Berlin, Heidelberg, 2015; pp. 11-27.
 116. Haque, T.; Talukder, M.M.U. Chemical Enhancer: A Simplistic Way to Modulate Barrier Function of the Stratum Corneum. *Adv Pharm Bull* **2018**, *8*, 169-179, doi:10.15171/apb.2018.021.

117. Gupta, R.; Badhe, Y.; Rai, B.; Mitragotri, S. Molecular mechanism of the skin permeation enhancing effect of ethanol: a molecular dynamics study. *RSC Adv.* **2020**, *10*, 12234-12248, doi:10.1039/D0RA01692F.
118. Hasan, A.; Farooqui, H. A Review on Role of Essential Oil as Penetration Enhancer in Transdermal Drug Delivery System. *Sys Rev Pharm* **2021**, *12*, 439-444.
119. Vasyuchenko, E.P.; Orekhov, P.S.; Armeev, G.A.; Bozdaganyan, M.E. CPE-DB: An Open Database of Chemical Penetration Enhancers. *Pharmaceutics* **2021**, *13*, doi:10.3390/pharmaceutics13010066.
120. Welton, T. Ionic liquids: a brief history. *Biophys. Rev.* **2018**, *10*, 691-706, doi:10.1007/s12551-018-0419-2.
121. Rogers, R.D.; Gurau, G. Is “choline and geranate” an ionic liquid or deep eutectic solvent system? *PNAS* **2018**, *115*, E10999, doi:10.1073/pnas.1814976115.
122. Tullo, A.H. The time is now for ionic liquids Available online: <https://cen.acs.org/materials/ionic-liquids/time-ionic-liquids/98/i5> (accessed on 15 September 2021).
123. Lei, Z.; Chen, B.; Koo, Y.M.; MacFarlane, D.R. Introduction: Ionic Liquids. *Chem Rev* **2017**, *117*, 6633-6635, doi:10.1021/acs.chemrev.7b00246.
124. Pedro, S.N.; Freire, C.S.R.; Silvestre, A.J.D.; Freire, M.G. Ionic Liquids in Drug Delivery. *Encyclopedia* **2021**, *1*, doi:10.3390/encyclopedia1020027.
125. Pedro, S.N.; R. Freire, C.S.; Silvestre, A.J.D.; Freire, M.G. The Role of Ionic Liquids in the Pharmaceutical Field: An Overview of Relevant Applications. *Int. J. Mol. Sci.* **2020**, *21*, doi:10.3390/ijms21218298.
126. Silva, A.T.; Lobo, L.; Oliveira, I.S.; Gomes, J.; Teixeira, C.; Nogueira, F.; Marques, E.F.; Ferraz, R.; Gomes, P. Building on Surface-Active Ionic Liquids for the Rescuing of the Antimalarial Drug Chloroquine. *Int. J. Mol. Sci.* **2020**, *21*, doi:10.3390/ijms21155334.
127. Kumar, H.; Kaur, G. Scrutinizing Self-Assembly, Surface Activity and Aggregation Behavior of Mixtures of Imidazolium Based Ionic Liquids and Surfactants: A Comprehensive Review. *Front. Chem.* **2021**, *9*, doi:10.3389/fchem.2021.667941.

128. Ana Rita, D.; João, C.-R.; Cátia, T.; Cristina, P.; Paula, G.; Ricardo, F. Ionic Liquids for Topical Delivery in Cancer. *Curr Med Chem* **2019**, *26*, 7520-7532, doi:<http://dx.doi.org/10.2174/0929867325666181026110227>.
129. Sidat, Z.; Marimuthu, T.; Kumar, P.; du Toit, L.C.; Kondiah, P.P.D.; Choonara, Y.E.; Pillay, V. Ionic Liquids as Potential and Synergistic Permeation Enhancers for Transdermal Drug Delivery. *Pharmaceutics* **2019**, *11*, doi:10.3390/pharmaceutics11020096.
130. Md Moshikur, R.; Chowdhury, M.R.; Moniruzzaman, M.; Goto, M. Biocompatible ionic liquids and their applications in pharmaceutics. *Green Chem.* **2020**, *22*, 8116-8139, doi:10.1039/D0GC02387F.
131. Qi, Q.M.; Duffy, M.; Curreri, A.M.; Balkaran, J.P.R.; Tanner, E.E.L.; Mitragotri, S. Comparison of Ionic Liquids and Chemical Permeation Enhancers for Transdermal Drug Delivery. *Adv. Funct. Mater.* **2020**, *30*, 2004257, doi:<https://doi.org/10.1002/adfm.202004257>.
132. Qi, Q.M.; Mitragotri, S. Mechanistic study of transdermal delivery of macromolecules assisted by ionic liquids. *J Control Release* **2019**, *311-312*, 162-169, doi:<https://doi.org/10.1016/j.jconrel.2019.08.029>.
133. Wu, H.; Deng, Z.; Zhou, B.; Qi, M.; Hong, M.; Ren, G. Improved transdermal permeability of ibuprofen by ionic liquid technology: Correlation between counterion structure and the physicochemical and biological properties. *J. Mol. Liq.* **2019**, *283*, 399-409, doi:<https://doi.org/10.1016/j.molliq.2019.03.046>.
134. Yuan, J.; Wu, J.; Yin, T. Solubility and permeation enhancement of poor soluble drug by cholinium-amino acid based ionic liquids. *J Drug Deliv Sci Technol* **2020**, *60*, 102037, doi:<https://doi.org/10.1016/j.jddst.2020.102037>.
135. Chantereau, G.; Sharma, M.; Abednejad, A.; Neves, B.M.; Sèbe, G.; Coma, V.; Freire, M.G.; Freire, C.S.R.; Silvestre, A.J.D. Design of Nonsteroidal Anti-Inflammatory Drug-Based Ionic Liquids with Improved Water Solubility and Drug Delivery. *ACS Sustain. Chem. Eng.* **2019**, *7*, 14126-14134, doi:10.1021/acssuschemeng.9b02797.
136. da Silva, C.C.P.; Dayo Owoyemi, B.C.; Alvarenga-Jr, B.R.; Alvarez, N.; Ellena, J.; Carneiro, R.L. Synthesis and solid-state characterization of diclofenac

- imidazolium monohydrate: an imidazolium pharmaceutical ionic liquid. *CrystEngComm* **2020**, *22*, 5345-5354, doi:10.1039/D0CE00723D.
137. Suksaeree, J.; Maneewattanapinyo, P. Ionic Liquid Drug-based Polymeric Matrices for Transdermal Delivery of Lidocaine and Diclofenac. *J Polym Environ.* **2020**, *28*, 2771-2779, doi:10.1007/s10924-020-01813-9.
 138. Maneewattanapinyo, P.; Yeasamun, A.; Watthana, F.; Panrat, K.; Pichayakorn, W.; Suksaeree, J. Controlled Release of Lidocaine–Diclofenac Ionic Liquid Drug from Freeze-Thawed Gelatin/Poly(Vinyl Alcohol) Transdermal Patches. *AAPS PharmSciTech* **2019**, *20*, 322, doi:10.1208/s12249-019-1545-2.
 139. Abednejad, A.; Ghaee, A.; Morais, E.S.; Sharma, M.; Neves, B.M.; Freire, M.G.; Nourmohammadi, J.; Mehrizi, A.A. Polyvinylidene fluoride–Hyaluronic acid wound dressing comprised of ionic liquids for controlled drug delivery and dual therapeutic behavior. *Acta Biomater.* **2019**, *100*, 142-157, doi:<https://doi.org/10.1016/j.actbio.2019.10.007>.
 140. Zheng, L.; Zhao, Z.; Yang, Y.; Li, Y.; Wang, C. Novel skin permeation enhancers based on amino acid ester ionic liquid: Design and permeation mechanism. *Int J Pharmaceut* **2020**, *576*, 119031, doi:<https://doi.org/10.1016/j.ijpharm.2020.119031>.
 141. Lu, B.; Yi, M.; Hu, S.; Wu, D.; Zhu, Z.; Wu, C.; Wang, Z.; Li, Y.; Zhang, J. Taurine-Based Ionic Liquids for Transdermal Protein Delivery and Enhanced Anticancer Activity. *ACS Sustain. Chem. Eng.* **2021**, *9*, 5991-6000, doi:10.1021/acssuschemeng.1c01064.
 142. Wu, H.; Fang, F.; Zheng, L.; Ji, W.; Qi, M.; Hong, M.; Ren, G. Ionic liquid form of donepezil: Preparation, characterization and formulation development. *J. Mol. Liq.* **2020**, *300*, 112308, doi:<https://doi.org/10.1016/j.molliq.2019.112308>.
 143. Hattori, T.; Tagawa, H.; Inai, M.; Kan, T.; Kimura, S.-i.; Itai, S.; Mitragotri, S.; Iwao, Y. Transdermal delivery of nobiletin using ionic liquids. *Sci. Rep.* **2019**, *9*, 20191, doi:10.1038/s41598-019-56731-1.
 144. Zhou, Z.; Liu, C.; Wan, X.; Fang, L. Development of a w/o emulsion using ionic liquid strategy for transdermal delivery of anti – aging component α – lipoic acid: Mechanism of different ionic liquids on skin retention and efficacy evaluation. *Eur J Pharm Sci.* **2020**, *141*, 105042, doi:<https://doi.org/10.1016/j.ejps.2019.105042>.

145. Caparica, R.; Júlio, A.; Fernandes, F.; Araújo, M.E.M.; Costa, J.G.; Santos de Almeida, T. Upgrading the Topical Delivery of Poorly Soluble Drugs Using Ionic Liquids as a Versatile Tool. *Int. J. Mol. Sci.* **2021**, *22*, doi:10.3390/ijms22094338.
146. Chantereau, G.; Sharma, M.; Abednejad, A.; Vilela, C.; Costa, E.M.; Veiga, M.; Antunes, F.; Pintado, M.M.; Sèbe, G.; Coma, V.; et al. Bacterial nanocellulose membranes loaded with vitamin B-based ionic liquids for dermal care applications. *J. Mol. Liq.* **2020**, *302*, 112547, doi:<https://doi.org/10.1016/j.molliq.2020.112547>.
147. Islam, M.R.; Chowdhury, M.R.; Wakabayashi, R.; Kamiya, N.; Moniruzzaman, M.; Goto, M. Ionic Liquid-In-Oil Microemulsions Prepared with Biocompatible Choline Carboxylic Acids for Improving the Transdermal Delivery of a Sparingly Soluble Drug. *Pharmaceutics* **2020**, *12*, doi:10.3390/pharmaceutics12040392.
148. Islam, M.R.; Chowdhury, M.R.; Wakabayashi, R.; Tahara, Y.; Kamiya, N.; Moniruzzaman, M.; Goto, M. Choline and amino acid based biocompatible ionic liquid mediated transdermal delivery of the sparingly soluble drug acyclovir. *Int J Pharmaceut* **2020**, *582*, 119335, doi:<https://doi.org/10.1016/j.ijpharm.2020.119335>.
149. Bakshi, K.; Mitra, S.; Sharma, V.K.; Jayadev, M.S.K.; Sakai, V.G.; Mukhopadhyay, R.; Gupta, A.; Ghosh, S.K. Imidazolium-based ionic liquids cause mammalian cell death due to modulated structures and dynamics of cellular membrane. *Biochim Biophys Acta Biomembr* **2020**, *1862*, 183103, doi:<https://doi.org/10.1016/j.bbamem.2019.183103>.
150. Poh, Y.; Ng, S.; Ho, K. Formulation and characterisation of 1-ethyl-3-methylimidazolium acetate-in-oil microemulsions as the potential vehicle for drug delivery across the skin barrier. *J. Mol. Liq.* **2019**, *273*, 339-345, doi:<https://doi.org/10.1016/j.molliq.2018.10.034>.
151. Takahashi, C.; Hattori, Y.; Yagi, S.; Murai, T.; Takai, C.; Ogawa, N.; Tanemura, M.; Fuji, M.; Kawashima, Y.; Yamamoto, H. Optimization of ionic liquid-incorporated PLGA nanoparticles for treatment of biofilm infections. *Mater Sci Eng C* **2019**, *97*, 78-83, doi:<https://doi.org/10.1016/j.msec.2018.11.079>.
152. Greene, J.R.; Merrett, K.L.; Heyert, A.J.; Simmons, L.F.; Migliori, C.M.; Vogt, K.C.; Castro, R.S.; Phillips, P.D.; Baker, J.L.; Lindberg, G.E.; et al. Scope and

- efficacy of the broad-spectrum topical antiseptic choline geranate. *PLOS ONE* **2019**, *14*, e0222211, doi:10.1371/journal.pone.0222211.
153. Wu, X.; Yu, Q.; Wu, J.; Li, T.; Ding, N.; Wu, W.; Lu, Y.; Zhu, Q.; Chen, Z.; Qi, J. Ionic liquids containing ketoconazole improving topical treatment of T. Interdigitale infection by synergistic action. *Int J Pharmaceut* **2020**, *589*, 119842, doi:<https://doi.org/10.1016/j.ijpharm.2020.119842>.
 154. Zhang, Y.; Cao, Y.; Meng, X.; Li, C.; Wang, H.; Zhang, S. Enhancement of transdermal delivery of artemisinin using microemulsion vehicle based on ionic liquid and lidocaine ibuprofen. *Colloids Surf. B* **2020**, *189*, 110886, doi:<https://doi.org/10.1016/j.colsurfb.2020.110886>.
 155. Zhang, T.; Sun, B.; Guo, J.; Wang, M.; Cui, H.; Mao, H.; Wang, B.; Yan, F. Active pharmaceutical ingredient poly(ionic liquid)-based microneedles for the treatment of skin acne infection. *Acta Biomater.* **2020**, *115*, 136-147, doi:<https://doi.org/10.1016/j.actbio.2020.08.023>.
 156. Bento, C.M.; Gomes, M.S.; Silva, T. Looking beyond Typical Treatments for Atypical Mycobacteria. *Antibiotics* **2020**, *9*, doi:10.3390/antibiotics9010018.
 157. Torres-Vanegas, J.D.; Cruz, J.C.; Reyes, L.H. Delivery Systems for Nucleic Acids and Proteins: Barriers, Cell Capture Pathways and Nanocarriers. *Pharmaceutics* **2021**, *13*, doi:10.3390/pharmaceutics13030428.
 158. Long, L.-y.; Zhang, J.; Yang, Z.; Guo, Y.; Hu, X.; Wang, Y. Transdermal delivery of peptide and protein drugs: Strategies, advantages and disadvantages. *J. Drug Deliv. Sci. Technol* **2020**, *60*, 102007, doi:<https://doi.org/10.1016/j.jddst.2020.102007>.
 159. Wu, X.; Zhang, H.; He, S.; Yu, Q.; Lu, Y.; Wu, W.; Ding, N.; Zhu, Q.; Chen, Z.; Ma, Y.; et al. Improving dermal delivery of hyaluronic acid by ionic liquids for attenuating skin dehydration. *Int. J. Biol. Macromol.* **2020**, *150*, 528-535, doi:<https://doi.org/10.1016/j.ijbiomac.2020.02.072>.
 160. Mandal, A.; Kumbhojkar, N.; Reilly, C.; Dharamdasani, V.; Ukidve, A.; Ingber Donald, E.; Mitragotri, S. Treatment of psoriasis with NFKBIZ siRNA using topical ionic liquid formulations. *Sci. Adv.* **2020**, *6*, eabb6049, doi:10.1126/sciadv.abb6049.

161. Tanner, E.E.L.; Wiraja, C.; Curreri, C.A.; Xu, C.; Mitragotri, S. Stabilization and Topical Skin Delivery of Framework Nucleic Acids using Ionic Liquids. *Adv. Ther.* **2020**, *3*, 2000041, doi:<https://doi.org/10.1002/adtp.202000041>.
162. Usmani, S.S.; Bedi, G.; Samuel, J.S.; Singh, S.; Kalra, S.; Kumar, P.; Ahuja, A.A.; Sharma, M.; Gautam, A.; Raghava, G.P.S. THPdb: Database of FDA-approved peptide and protein therapeutics. *PLOS ONE* **2017**, *12*, e0181748, doi:10.1371/journal.pone.0181748.
163. Verma, S.; Goand, U.K.; Husain, A.; Katekar, R.A.; Garg, R.; Gayen, J.R. Challenges of peptide and protein drug delivery by oral route: Current strategies to improve the bioavailability. *Drug Dev. Res.* **2021**, *n/a*, doi:<https://doi.org/10.1002/ddr.21832>.
164. Vaidya, A.; Mitragotri, S. Ionic liquid-mediated delivery of insulin to buccal mucosa. *J Control Release* **2020**, *327*, 26-34, doi:<https://doi.org/10.1016/j.jconrel.2020.07.037>.
165. Jorge, L.R.; Harada, L.K.; Silva, E.C.; Campos, W.F.; Moreli, F.C.; Shimamoto, G.; Pereira, J.F.B.; Oliveira, J.M.; Tubino, M.; Vila, M.M.D.C.; et al. Non-invasive Transdermal Delivery of Human Insulin Using Ionic Liquids: In vitro Studies. *Front. Pharmacol* **2020**, *11*, doi:10.3389/fphar.2020.00243.
166. Vieira, N.S.M.; Castro, P.J.; Marques, D.F.; Araújo, J.M.M.; Pereiro, A.B. Tailor-Made Fluorinated Ionic Liquids for Protein Delivery. *Nanomaterials* **2020**, *10*, doi:10.3390/nano10081594.
167. Costa, F.; Teixeira, C.; Gomes, P.; Martins, M.C.L. Clinical Application of AMPs. In *Antimicrobial Peptides: Basics for Clinical Application*, Matsuzaki, K., Ed.; Springer Singapore: Singapore, 2019; pp. 281-298.
168. Md Moshikur, R.; Chowdhury, M.R.; Fujisawa, H.; Wakabayashi, R.; Moniruzzaman, M.; Goto, M. Design and Characterization of Fatty Acid-Based Amino Acid Ester as a New "Green" Hydrophobic Ionic Liquid for Drug Delivery. *ACS Sustain. Chem. Eng* **2020**, *8*, 13660-13671, doi:10.1021/acssuschemeng.0c03419.
169. Uddin, S.; Islam, M.R.; Chowdhury, M.R.; Wakabayashi, R.; Kamiya, N.; Moniruzzaman, M.; Goto, M. Lipid-Based Ionic-Liquid-Mediated Nanodispersions

- as Biocompatible Carriers for the Enhanced Transdermal Delivery of a Peptide Drug. *ACS Appl. Bio Mater.* **2021**, *4*, 6256-6267, doi:10.1021/acsabm.1c00563.
170. Tahara, Y.; Morita, K.; Wakabayashi, R.; Kamiya, N.; Goto, M. Biocompatible Ionic Liquid Enhances Transdermal Antigen Peptide Delivery and Preventive Vaccination Effect. *Mol. Pharm.* **2020**, *17*, 3845-3856, doi:10.1021/acs.molpharmaceut.0c00598.
171. Saraswat, J.; Wani, F.A.; Dar, K.I.; Rizvi, M.M.A.; Patel, R. Noncovalent Conjugates of Ionic Liquid with Antibacterial Peptide Melittin: An Efficient Combination against Bacterial Cells. *ACS Omega* **2020**, *5*, 6376-6388, doi:10.1021/acsomega.9b03777.
172. Saraswat, J.; Aldahmash, B.; AlOmar, S.Y.; Imtiyaz, K.; Rizvi, M.M.A.; Patel, R. Synergistic antimicrobial activity of N-methyl substituted pyrrolidinium-based ionic liquids and melittin against Gram-positive and Gram-negative bacteria. *Appl. Microbiol. Biotechnol.* **2020**, *104*, 10465-10479, doi:10.1007/s00253-020-10989-y.
173. Gomes, A.; Bessa, L.J.; Correia, P.; Fernandes, I.; Ferraz, R.; Gameiro, P.; Teixeira, C.; Gomes, P. "Clicking" an Ionic Liquid to a Potent Antimicrobial Peptide: On the Route towards Improved Stability. *Int. J. Mol. Sci.* **2020**, *21*, doi:10.3390/ijms21176174.
174. Daso, R.E.; Osborn, L.J.; Thomas, M.F.; Banerjee, I.A. Development of Nanoscale Hybrids from Ionic Liquid–Peptide Amphiphile Assemblies as New Functional Materials. *ACS Omega* **2020**, *5*, 14543-14554, doi:10.1021/acsomega.0c01254.
175. Whalen, M.S.; Daso, R.E.; Thomas, M.F.; Banerjee, I.A. Interactions of betainium and imidazolium-based ionic liquids with peptide amphiphiles and their implications in the formation of nanohybrid composite gels. *J. Sol-Gel Sci. Technol.* **2021**, *97*, 488-504, doi:10.1007/s10971-020-05434-5.
176. Vedadghavami, A.; Zhang, C.; Bajpayee, A.G. Overcoming negatively charged tissue barriers: Drug delivery using cationic peptides and proteins. *Nano Today* **2020**, *34*, 100898, doi:<https://doi.org/10.1016/j.nantod.2020.100898>.
177. Campos, W.F.; Silva, E.C.; Oliveira, T.J.; Oliveira, J.M.; Tubino, M.; Pereira, C.; Vila, M.M.D.C.; Balcão, V.M. Transdermal permeation of bacteriophage particles

by choline oleate: potential for treatment of soft-tissue infections. *Future Microbiol.* **2020**, *15*, 881-896, doi:10.2217/fmb-2019-0290.

Chapter 2. Results and Discussion

2.1. Development of a dual-action chimeric peptide

Turning a Collagenesis-Inducing Peptide Into a Potent Antibacterial and Antibiofilm Agent Against Multidrug-Resistant Gram-Negative Bacteria

Ana Gomes, Lucinda J. Bessa, Iva Fernandes, Ricardo Ferraz, Nuno Mateus, Paula Gameiro, Cátia Teixeira, Paula Gomes

Frontiers in Microbiology **2019**, 10 (1915)

doi:10.3390/fmicb.2019.01915

ABSTRACT

Antimicrobial resistance is becoming one of the most serious health threats worldwide, as it not only hampers effective treatment of infectious diseases using current antibiotics, but also dramatically increases the risks of medical procedures like surgery, transplantation, bone and dental implantation, chemotherapy, or chronic wound management. To date, there are no effective measures to tackle life-threatening nosocomial infections caused by multidrug resistant bacterial species, of which Gram-negative species within the so-called “ESKAPE” pathogens are the most worrisome. Many such bacteria are frequently isolated from severely infected skin lesions such as diabetic foot ulcers. In this connection, we are pursuing new peptide constructs encompassing antimicrobial and collagenesis-inducing motifs, to tackle skin and soft tissue infections by exerting a dual effect: antimicrobial protection and faster healing of the wound. This produced peptide 3.1-PP4 showed MIC values as low as 1.0 and 2.1 μM against *Escherichia coli* and *Pseudomonas aeruginosa*, respectively, and low toxicity to HFF-1 human fibroblasts. Remarkably, the peptide was also potent against multidrug-resistant isolates of *Klebsiella pneumoniae*, *E. coli* and *P. aeruginosa* (MIC values between 0.5 and 4.1 μM), and hampered the formation of/disaggregated *K. pneumoniae* biofilms of resistant clinical isolates. Moreover, this notable hybrid peptide retained the collagenesis-inducing behavior of the reference cosmeceutical peptide C₁₆-PP4 (“Matrixyl”). In conclusion, 3.1-PP4 is a highly promising lead towards development of a topical treatment for severely infected skin injuries.

Keywords: antibiofilm, antimicrobial peptide, collagen, ESKAPE, *Klebsiella pneumoniae*, multidrug-resistant bacteria, wound-healing

INTRODUCTION

According to the World Health Organization (WHO), antimicrobial resistance is currently disseminated worldwide and can affect anyone, regardless of age, health and socio-economic status (WHO, 2014). Amongst drug-resistant infectious pathogens, which include viruses, parasites, fungi and bacteria, the latter are of special concern in healthcare facilities, as the most severe hospital-acquired infections (HAI) are often associated with multidrug-resistant (MDR) bacteria belonging to the so-called “ESKAPE” group: *Enterococcus faecium*, *Staphylococcus aureus*, *Klebsiella pneumoniae*, *Acinetobacter baumannii*, *Pseudomonas aeruginosa*, and *Enterobacter spp.* (WHO, 2014). Antibiotic-resistant HAI are life-threatening and greatly increase the risks of standard medical procedures, from major surgery, organ transplantation, or chemotherapy, to management of complicated skin and soft tissue infections (cSSTI). Actually, cSSTI like diabetic foot ulcers (DFU), venous ulcers, pressure ulcers, frequently culminate in hospitalization, where HAI may exacerbate the severity of the infected wounds (Leong et al., 2018). Also, cSSTI may develop as HAI, associated with, e.g., orthopedic or dental implantation (implant-associated infections, IAI) or use of catheters (catheter-associated infections, CAI) (VanEpps and Younger, 2016). Consequently, efficient options for management of cSSTI are urgently needed, especially because their incidence increases with aging. In fact, cSSTI are a mounting burden to both patients and healthcare due to growth of life expectancy: for instance, according to the European Wound Management Association (EWMA, 2014), about 2% of the population in developed countries suffers from chronic wounds, being estimated that 25–50% of hospital beds are occupied by patients with such non-healing injuries, with average costs adding up to 2–4% of the total European budget for healthcare; in the US, the Center for Disease Control estimates that about 50–70% of the 2 million reported HAI are associated to implants or catheters, with mortality rates ranging from <5% for dental implants to >25% for mechanical heart valves (VanEpps and Younger, 2016).

As efficient options to fight MDR bacteria are being exhausted, preclinical and clinical development of antimicrobial peptides (AMPs) has been experiencing a strong impulse (Aminov, 2010; Gomes et al., 2017; Costa et al., 2019). AMPs have broad-spectrum antibacterial activity, and low propensity to induce resistance, hence latest efforts in this area have been focused on the search for AMPs with potent action, particularly against MDR Gram-negative bacteria (Ballantine et al., 2019; Mant et al., 2019; Wang et al., 2019). Findings thereof are quite encouraging toward devising new options to tackle cSSTI like DFU, as the most prevalent bacterial species isolated from these ulcers

include, besides the Gram-positive *S. aureus*, several Gram-negative species like *P. aeruginosa*, *E. coli*, *K. pneumoniae*, and *Proteus mirabilis* (Ogba et al., 2019). Also, biofilm forming bacteria with a major role in cSSTI, including IAI and CAI, encompass *Staphylococcus epidermidis* (main species associated to IAI and CAI), *S. aureus* (slightly less prevalent than the previous one, but more aggressive), enterococci and Gram-negative bacteria like *E. coli* and *Klebsiella* spp.; in catheter-associated urinary tract infections (UTI), *E. coli* and *Candida* yeasts prevail, whereas Gram-positive pathogens are not so common (VanEpps and Younger, 2016; Li et al., 2019). Still, an efficient treatment of cSSTI should provide not only antibacterial protection, but also promote fast tissue regeneration, which is often deficient in elderly people, especially if bedridden, or affected by diabetes, chronic venous insufficiency, among other conditions (Makrantonaki et al., 2017). Although some AMPs have been reported as having intrinsic skin and soft tissue regenerative properties, in some cases associated with collagenesis-inducing effects (Mangoni et al., 2016; Gomes et al., 2017), most such dual-action AMPs are not potent against Gram-negative bacteria, and/or their activity has not been investigated on MDR clinical isolates and/or bacterial biofilms.

In view of the above, we hypothesized that the conjugation of a collagenesis-inducing, or collagen-boosting peptide (CBP) to an AMP known to be active against both Gram-positive and Gram-negative bacteria might produce dual-action peptide chimeras retaining the properties of their parent CBP and AMP motifs, hence, with potential interest for the management of cSSTI. To this end, the CBP chosen was the matrikine-like peptide KTTKS, also known as “pentapeptide-4” (ahead abbreviated to PP4) whose palmitoylated form (ahead abbreviated to C₁₆-PP4) is widely used as a cosmeceutical known as “Matrixyl” (Jones et al., 2013; Choi et al., 2014; Aldag et al., 2016; Schagen, 2017) and reported to possess tissue regenerative properties (Tsai et al., 2007; Park et al., 2017; Krishnamoorthy et al., 2018). As the AMP motif, we chose a previously de novo designed synthetic peptide, named 3.1, earlier reported as highly active against both Gram-positive and Gram-negative bacteria (Kang et al., 2009). Both CBP and AMP motifs were conjugated in different ways to produce nine distinct chimeric peptides (Table 1). The in vitro activity of these peptide chimeras against relevant bacterial pathogens (both ATCC reference strains and MDR clinical isolates), as well as their toxicity to human fibroblasts (HFF-1), antibiofilm properties, and collagenesis-inducing behavior, were investigated in vitro, and revealed a highly promising peptide lead, 3.1-PP4, as next described.

MATERIALS AND METHODS

Peptide Synthesis

Peptides were assembled by solid peptide phase synthesis (SPPS) on an automated Symphony® X synthesizer from Gyros Protein Technologies (Tucson, AZ, United States). The orthogonal Fmoc/tBu scheme was applied (Benoiton, 2006), using a Rink amide MBHA resin (100–200 mesh, 0.52 mmol/g, NovaBiochem) as solid support, which was pre-conditioned in dimethylformamide (DMF, Sigma-Aldrich, St. Louis, MO, United States) for 10 min. The Fmoc protecting group was then removed by treating the resin twice with a solution of 20% piperidine (Sigma-Aldrich, St. Louis, MO, United States) in DMF for 5 min, thus releasing the resin-bound reactive amine groups. The C-terminal Fmoc-protected amino acid (Fmoc-AA-OH, Bachem) was next coupled to the deprotected resin, which was treated twice for 10 min with a cocktail solution containing 100 mM of the Fmoc-AA-OH, 100 mM of the in situ coupling reagent O-(6-chlorobenzotriazol-1-yl)-N,N,N',N'-tetramethyluronium hexafluorophosphate (HCTU, NovaBiochem) and 200 mM N-methylmorpholine (NMM, Sigma-Aldrich, St. Louis, MO, United States) in DMF.

Table 1 | Synthetic CBP/AMP conjugates produced by SPPS.

| Peptide ^a | Sequence ^b | MW / Da |
|--------------------------|--------------------------------------|---------|
| 3.1 | KKLLKWLLKLL | 1394.9 |
| C ₁₆ -3.1 | Palmitoyl-KKLLKWLLKLL ^c | 1633.3 |
| PP4 | KTTKS | 562.7 |
| C ₁₆ -PP4 | Palmitoyl-KTTKS | 800.6 |
| PP4-3.1 | KTTKSKLLKWLLKLL | 1940.5 |
| C ₁₆ -PP4-3.1 | Palmitoyl-KTTKSKLLKWLLKLL | 2179.0 |
| 3.1-PP4 | KKLLKWLLKLLKTTKS | 1940.5 |
| C ₁₆ -3.1-PP4 | Palmitoyl -KKLLKWLLKLLKTTKS | 2179.0 |
| PP4-βala-3.1 | KTTKS-β-Ala-KKLLKWLLKLL ^d | 2011.6 |

^a All peptides were produced as C-terminal carboxamides; ^b AA residues represented by the single letter code as defined by the IUPAC-IUBMB guidelines on nomenclature and symbolism for amino acids and peptides; ^c palmitoyl corresponds to the hexadecanoyl group, introduced by coupling hexadecanoic (i.e., palmitic) acid to the peptides' N-terminus; ^d β-Ala stands for the non-proteinogenic amino acid β-alanine (3-aminopropanoic acid).

The Fmoc-protecting group was removed as before, to release the amino acid (AA) amine group for subsequent coupling of the next Fmoc-AA-OH. Hence, the peptide chain was grown in the C→N direction through alternating coupling and deprotection cycles, performed as above described, until the full sequence was assembled. For N-palmitoylated peptides (as, e.g., C₁₆-PP4), after deprotection of the N-terminal AA, palmitic acid (Sigma-Aldrich, St. Louis, MO, United States) was coupled by manual synthesis, using an in situ coupling cocktail solution containing 5 molar equivalents (eq) of palmitic acid, 5 eq of *N*-ethyl-*N,N*-diisopropylamine (DIEA, Sigma-Aldrich, St. Louis, MO, United States), and 10 eq of *O*-(Benzotriazol-1-yl)-*N,N,N',N'*-tetramethyluronium hexafluorophosphate (HBTU, NovaBiochem) in DMF. Once fully assembled, the peptides were released from the resins through a 2 h acidolytic cleavage reaction using a cocktail solution containing 95% trifluoroacetic acid (TFA, Sigma-Aldrich, St. Louis, MO, United States), 2.5% triisopropylsilane (TIS, Sigma-Aldrich, St. Louis, MO, United States), and 2.5% of deionized water. The crude peptide thus obtained was purified by a preparative high-performance liquid chromatography (HPLC), on Hitachi- Merck LaPrep Sigma system (VWR) equipped with an LP3104 UV detector and an LP1200 pump, employing a reverse-phase C18 column (250 × 25 mm ID and 5 µm pore size, Merck) and gradient elution using 0.05% TFA in water as solvent A and acetonitrile (ACN, Carlo Erba) as solvent B. The elution method varied according to the specific peptide and all elutions were completed in 60 min, at a 15 mL/min flow-rate. Pure peptide fractions were isolated and pooled, and freeze-dried to produce the peptide as a low-density white solid that was stored at -20°C until further use. Peptide purity was confirmed by analytical HPLC using a Hitachi-Merck LaChrom Elite system equipped with a quaternary pump, a thermostatted automated sampler, and a diode array detector; analyses were performed with a reverse-phase C18 column (150 × 4.6 mm ID and 5 µm pore size, Merck) at a 1 mL/min flow rate using a 1–100% of solvent B (ACN) in solvent A, for 30 min, with detection at 220 nm. Peptide structure was confirmed by electrospray ionization-ion trap mass spectrometry (ESI-IT MS).

Antibacterial Activity

The minimum inhibitory concentration (MIC) of synthetic peptides was determined using the broth microdilution method in cation-adjusted Mueller-Hinton broth (MHB2 – Sigma-Aldrich, St. Louis, MO, United States), according to the recommendations of the Clinical and Laboratory Standards Institute (CLSI, 2012), against four reference strains, namely, *P. aeruginosa* ATCC 27853, *E. coli* ATCC 25922, *S. aureus* ATCC 25923 and *Enterococcus faecalis* ATCC 29212. MIC values of peptide 3.1-PP4 were also

determined against MDR clinical isolates of *P. aeruginosa* (PA002, PA004, Pa3, Pa4), *E. coli* (Ec1, Ec2, EC001, EC002, EC003) and *K. pneumoniae* (KP004, KP007, KP010). The peptides were tested in the concentration range of 1–1024 µg/mL. The minimum bactericidal concentration (MBC) was determined as previously reported (Bessa et al., 2018).

Antibiofilm Activity

The ability of peptide 3.1-PP4 to inhibit the biofilm formation by three *P. aeruginosa* isolates (PA002, PA004, Pa3) and by three *K. pneumoniae* isolates (KP004, KP007 and KP010) was assessed at concentrations equal to the MIC, $\frac{1}{2} \times$ MIC and $\frac{1}{4} \times$ MIC in tryptic soy broth – (TSB – Liofilchem s.r.l., Italy) using the crystal violet assay as reported by Gomes et al. (2014). Two independent experiments were performed in triplicate.

The efficacy of peptide 3.1-PP4 on 24 h preformed biofilms of PA002, PA004, KP004, KP007, and KP010 was also evaluated (Gomes et al., 2014). Briefly, biofilms were grown in TSB from a starting inoculum of 1×10^6 CFU/mL in 96-well microtiter plates. After 24 h of incubation at 37°C, the planktonic cells were gently removed and the wells were rinsed and filled with $20 \times$ MIC of the peptide. The optical density at 600 nm (OD600) was measured at time 0 and after incubation for 24 h at 37°C. The reduction in the biofilm proliferation was calculated in comparison to the respective non-treated biofilms. Two independent experiments were performed in triplicate.

Biofilm Metabolic Activity

Twenty four hours biofilms of PA004, KP004, KP007, and KP010 were formed as described above in 96-well microtiter plates and then treated with $20 \times$ MIC of peptide 3.1-PP4 for further 24 h at 37 C. The respective control biofilms were equally formed but in absence of the peptide (only TSB medium was used). Afterward, the bacterial metabolic activity of biofilms was quantified after adding 3-(4,5-dimethylthiazole-2-yl)-2,5-diphenyl tetrazolium bromide (MTT, 0.5 mg/mL – Sigma- Aldrich, St. Louis, MO, United States) for 3 h at 37°C in the dark. DMSO was used to dissolve the formazan crystals formed and the absorbance at 570 nm was measured. Two independent experiments were performed in four replicates.

Confocal Laser Scanning Microscopy Imaging of Biofilms

For confocal laser scanning microscopy (CLSM) imaging, 24 h biofilms of PA004, KP007, and KP010 were formed in μ -Dish (35 mm, high), ibidi Polymer Coverslips (ibidi GmbH, Planegg-Martinsried, Germany) as previously described by Bessa et al. (2018). Biofilms were non-treated – controls (only medium was used) or treated with 3.1-PP4 at a concentration of $20 \times$ MIC. After 24 h, all biofilms were stained using the LIVE/DEAD™ BacLight™ bacterial viability kit (Molecular Probes, Thermo Fisher Scientific, MA, United States). Biofilms were visualized under a laser scanning confocal system Leica TCS SP5 II (Leica Microsystems, Germany), equipped with an inverted (i) microscope Leica DMI6000-CS, using a HC PL APO CS 63x/1.30 Glycerine 21°C objective and the lasers Diode 405 nm and DPSS561 561 nm, and (ii) the LAS AF software.

Toxicity to Human Fibroblasts

Immortalized human foreskin fibroblasts (HFF-1) were grown as a monolayer from passage number 8–16. For routine maintenance, HFF-1 cells were cultured in Dulbecco's Modified Eagle Medium (DMEM, from Cell Lines Service) supplemented with 15% fetal bovine serum (FBS, from CLS) and 1% antibiotic/antimycotic solution (100 units/mL of penicillin, 100 μ g/mL of streptomycin and 0.25 μ g/mL of amphotericin B, from Sigma-Aldrich, St. Louis, MO, United States) at 37°C in an humidified atmosphere with 5% CO₂. Cells were harvested by trypsinization [0.25% (w/v) trypsin-EDTA4Na, Sigma-Aldrich, St. Louis, MO, United States] twice a week. The cytotoxicity of synthetic peptides to HFF-1 cells was evaluated using the standard MTT assay. Briefly, cells were seeded at a density of 8×10^4 cells/well onto 96-well plate and incubated at 37°C in a 5% CO₂ atmosphere. Cells were allowed to grow for 48 h, and serially diluted peptide solutions (0.78–100 μ M) were added to the wells. Then, cells were incubated for 72 h at 37°C, after which wells were washed once with phosphate buffered saline (PBS, Sigma-Aldrich, St. Louis, MO, United States), followed by addition of a 0.45 mg/mL MTT solution to each well. Crystals were allowed to form for 1.5 h. Reaction was stopped by rejecting the medium and addition of dimethylsulfoxide (DMSO, Sigma-Aldrich, St. Louis, MO, United States). Absorbance was read at 570 nm (Biotek PowerWave XS).

Collagenesis-Inducing Effects

Collagen production was assessed as described by Remoué et al. (2013). Briefly, HFF-1 cells were seeded and incubated as described previously for the cytotoxicity assay. After the 72 h incubation with peptides, cells were washed with PBS and the Sirius Red

dye in picric acid solution (Sigma-Aldrich, St. Louis, MO, United States) was applied to each well. Cells were incubated at 25°C for 1 h under orbital shaking. Dye was then rejected, and cells were washed twice with absolute ethanol (AGA). Once the wells were dry, 1 M aqueous NaOH (Sigma-Aldrich, St. Louis, MO, United States) was added, and absorbance read at 540 nm (Biotek PowerWave XS).

Statistical Analysis

The results regarding the biofilm formation, the treatment of preformed biofilms and the biofilm metabolic activity were expressed as mean values \pm standard deviation. The statistical significance of differences between controls and experimental groups was evaluated using Student's t-test. $P < 0.05$ were considered statistically significant.

RESULTS

Peptide Synthesis

All peptides (Table 1) were successfully obtained in high purity degrees and presenting ESI-MS data in agreement with the expected molecular weights (MW), as shown in the Supplementary Figures S1–S18.

Antibacterial Activity and Cytotoxicity

According to CLSI guidelines for antimicrobial susceptibility testing, MIC values were determined for all peptides against ATCC reference strains of two Gram-positive (*S. aureus* ATCC 25923 and *E. faecalis* ATCC 29212), and two Gram-negative (*P. aeruginosa* ATCC 27853 and *E. coli* ATCC 25922) bacterial species, and are shown in Table 2. At the end of the cytotoxicity assays, the number of viable cells was never below that of initially plated cells. As such, data are represented as peptide concentrations causing 50% growth inhibition (IC_{50}) on HFF-1 cells, rather than as lethal dose values. IC_{50} values thus obtained are also included in Table 2.

As expected, the parent CBP, i.e., the matrikine-like peptide PP4, was inactive ($MIC > 1024 \mu\text{g/mL}$) against all bacterial strains assayed, whereas the parent AMP, peptide 3.1, was highly active against both Gram-positive and Gram-negative bacteria. N-palmitoylation of this AMP led to an increase in cytotoxicity and a significant decrease or even loss of antibacterial activity. Relevantly, the hybrid constructs PP4-3.1 and 3.1-PP4, where the parent CBP and AMP motifs were directly linked together in both possible orientations, displayed potent antibacterial activity, which is retained or even improved

against Gram-negative bacteria, as compared to that of parent peptide 3.1. Also, while PP4-3.1 was considerably more toxic to HFF-1 cells than parent peptide 3.1 (IC₅₀ value of the former is half in comparison to the latter), on the contrary, its reversed analog 3.1-PP4 was less cytotoxic than 3.1. Interestingly, *N*-palmitoylation of any of these conjugates led again to a considerable increase in cytotoxicity and to a decrease in antibacterial activity, whereas insertion of a small flexible linker (β -alanine) between both motifs, as in PP4- β -Ala-3.1 vs. PP4-3.1, did not significantly alter either antibacterial activity or toxicity to HFF-1 cells.

Table 2 | MIC and IC₅₀ values obtained for the synthetic peptides against four ATCC reference bacterial strains and HFF-1 cells, respectively.

| Peptide | MIC in $\mu\text{g/mL}$ (in μM) | | | | IC ₅₀ \pm SEM (μM) ^c on HFF-1 cells |
|--------------------------|---|---------------------------------|-----------------------------|-------------------------------|--|
| | <i>E. coli</i> ATCC 25922 | <i>P. aeruginosa</i> ATCC 27853 | <i>S. aureus</i> ATCC 25923 | <i>E. faecalis</i> ATCC 29212 | |
| 3.1 | 8 (6) | 4 (3) | 4b (3) | 4-8 (3-6) | 50 \pm 3 |
| C ₁₆ -3.1 | 128 (78.4) | 128b (78.4) | >1024 (>627) | 256b (158) | 23.4 \pm 0.7 |
| PP4 | >1024 (>1820) | >1024 (>1820) | >1024 (>1820) | >1024 (>1820) | > 100 |
| C ₁₆ -PP4 | ND ^a | | | | > 100 |
| PP4-3.1 | 4 (2) | 4 (1) | 8 (4) | 16 (8) | 25 \pm 2 |
| C ₁₆ -PP4-3.1 | 32 (15) | 64 (29) | 64b (29) | 64 (29) | 4.98 \pm 0.08 |
| 3.1-PP4 | 2 (1) | 4 (2) | 32 (16) | 64 (33) | 69 \pm 5 |
| C ₁₆ -3.1-PP4 | 64 (29) | 64b (29) | 128b (59) | 64-128 ^b (30-59) | 17.8 \pm 0.5 |
| PP4- β -ala-3.1 | 4 (2) | 4 (2) | 8 (4) | 8 (4) | 24 \pm 2 |

^a Not Determined, peptide was insoluble in the medium MHB2; ^b the MBC was 2 \times the MIC; in all the other cases, the MBC was equal to the MIC; ^c data expressed as mean \pm SEM of two independent experiments (n = 4-8).

Activity of Peptide 3.1-PP4 Against MDR Gram-Negative Isolates

In view of the above results, peptide conjugate 3.1-PP4 was selected for further investigation of its activity against MDR isolates of three Gram-negative bacterial species, namely, *P. aeruginosa* (four isolates), *E. coli* (five isolates), and *K. pneumoniae* (four isolates), whose antimicrobial resistance patterns are provided in the Supplementary Table S1. MDR isolates of *K. pneumoniae* were included in this analysis given (i) the high prevalence of *K. pneumoniae* in HAI (Zheng et al., 2017), (ii) that *K. pneumoniae* isolates used are carbapenem-resistant strains of an *Enterobacteriaceae* species, meaning that they are class 1 priority pathogens for the research and development of new antibiotics according to the WHO (WHO, 2017), and (iii) *K. pneumoniae* bacteria are usually better biofilm producers than the other *Enterobacteriaceae* species used, *E. coli* (Reisner et al., 2006). MIC values obtained are

shown in Table 3, and confirm peptide’s 3.1-PP4 potent action against Gram-negative bacteria, including MDR isolates, with a selectivity index (SI), i.e., ratio of IC₅₀ values for mammalian vs. bacterial cells, ranging from ca. 9–69. In fact, for *P. aeruginosa* and *E. coli*, MIC against MDR isolates were in the same range, or below, of those previously found for ATCC reference strains (Table 2). For *K. pneumoniae*, MIC values ranged between 1 and 4 µM, which is remarkable. Moreover, minimal bactericidal concentrations (MBC) were also determined, and found to match the MIC in all cases, which shows that peptide 3.1-PP4 is bactericidal to all MDR isolates tested.

Table 3 | MIC values for 3.1-PP4 against MDR isolates of Gram-negative bacteria.

| Species | Isolate | MIC in µg/mL (in µM) |
|----------------------|---------|----------------------|
| <i>P. aeruginosa</i> | PA002 | 4 (2) |
| | PA004 | 2 (1) |
| | Pa3 | 2 (1) |
| | Pa4 | 2 (1) |
| | PA002 | 4 (2) |
| <i>E. coli</i> | Ec1 | 4 (2) |
| | Ec2 | 2 (1) |
| | EC001 | 2 (1) |
| | EC002 | 2 (1) |
| | EC003 | 1(0.5) |
| <i>K. pneumoniae</i> | KP010 | 2 (1) |
| | KP007 | 8 (4) |
| | KP004 | 4(2) |

Antibiofilm Activity of Peptide 3.1-PP4

Activity of an antimicrobial agent against planktonic bacteria may not correlate to its action against bacterial biofilms, which are a major cause accounting for the severity and/or chronicity of infections, known as biofilm-associated infections. In fact, the formation of biofilms are described as part of the pathogens’ resistance mechanisms; once established, biofilms represent a stable microbial population that is hidden from the immune system and shielded from antibiotics (Donlan, 2002; Mottola et al., 2016; Omar et al., 2017; Chang, 2018). As such, and since several AMPs have been reported as efficient antibiofilm agents (Yasir et al., 2018; Haney et al., 2019), we have further investigated whether peptide 3.1-PP4 would also display antibiofilm activity. Such activity was assessed in two different stages, (i) in the biofilm formation and (ii) in 24 h mature biofilms. To this end, biofilms of MDR isolates of *P. aeruginosa* and *K. pneumoniae* were used, and results were as described further below. MDR *E. coli* isolates were not good biofilm producers, therefore, they were not used in the antibiofilm activity assays. Indeed,

that was not surprising considering the known significantly distinct ability of different *E. coli* isolates to form biofilms in vitro (Reisner et al., 2006).

Inhibition of Biofilm Formation

Some of the MDR isolates of *P. aeruginosa* and *K. pneumoniae* were randomly selected to form biofilms in the absence (controls) and presence (at MIC, $\frac{1}{2} \times$ MIC and $\frac{1}{4} \times$ MIC) of the peptide 3.1-PP4. In this assay, the test compounds were used at sub-inhibitory concentrations, since if they had been present at the MIC or higher concentrations, bacteria would be killed before starting to produce the biofilms. Hence, by using sub-MIC concentrations, i.e., that are not enough to fully inhibit bacterial growth, it was possible to assess how could the peptide interfere with the normal formation of biofilms. The biofilm biomass formed was next quantitated through the crystal violet assay, and the results are shown in Figure 1. These results are presented as absorbance of crystal violet at 595 nm obtained for each strain in absence (control) and presence of different concentrations (MIC, $\frac{1}{2} \times$ MIC, and $\frac{1}{4} \times$ MIC) of the peptide, as this allows for comparison of the different amounts of biofilm formed by each distinct bacterial strain in the control condition.

One immediate observation at Figure 1 shows that *P. aeruginosa* biofilms have significantly higher biomass than those formed by *K. pneumoniae* isolates, indicating that *P. aeruginosa* isolates are stronger biofilm producers in comparison to those of *K. pneumoniae*. An absorbance under 0.5 anticipates that no biofilm was formed (Stepanovic et al., 2007), therefore, as it was expectable, when peptide 3.1-PP4 was present in a concentration equal to the MIC, no biofilm was actually produced by the isolates, with the exception of isolate PA002. Occasionally for some isolates the MIC is different depending on the medium used (Andrews et al., 2002) and indeed the medium used in the biofilm formation, TSB, is different from that used in the MIC determination assay, MHB2. In the case of isolate PA002, the MIC in TSB is higher than in MHB2, and thus the concentration of peptide assayed as being the MIC is in fact a sub-inhibitory concentration. At sub-inhibitory concentrations, i.e., at $\frac{1}{2}$ and $\frac{1}{4}$ of the MIC, the peptide does not significantly inhibit biofilm formation by any of the three *P. aeruginosa* isolates. However, for *K. pneumoniae* isolates, the peptide is able to reduce the biofilm formed in comparison to the control biofilm.

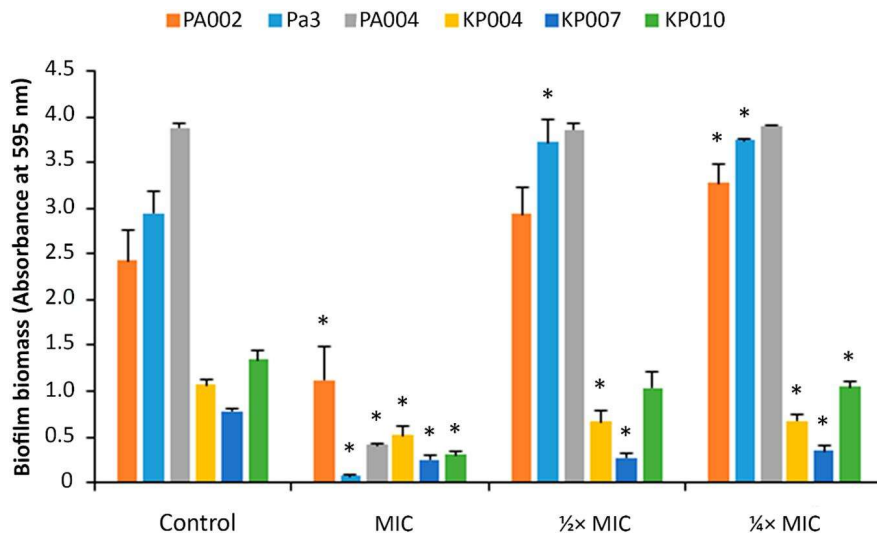


Figure 1. Biofilm biomass quantitation of biofilms formed in the presence of peptide 3.1-PP4. Biofilms of three MDR *P. aeruginosa* (PA002, Pa3, and PA004) and of three MDR *K. pneumoniae* (KP004, KP007, and KP010) were formed in the presence of the peptide at three different concentrations, MIC, $\frac{1}{2} \times$ MIC, and $\frac{1}{4} \times$ MIC. Control biofilms were grown in absence of the peptide. Two independent experiments were performed in triplicate. Error bars represent SD. Statistically significant differences between biofilms formed in presence of the peptide and respective control biofilms ($p < 0.05$) are marked with an asterisk (*).

Effects on Preformed Biofilm

Biofilms of MDR *P. aeruginosa* and *K. pneumoniae* isolates were allowed to form for 24 h, then exposed to the peptide at 20-fold its MIC value to ensure that any antibiofilm effects would be visible, since bacterial biofilms are more difficult to eradicate than their planktonic counterparts, and then allowed to grow for another 24 h. In the case of control biofilms, the second 24 h growth period occurred in the absence of the peptide. Based on the apparent higher efficiency of peptide 3.1-PP4 to inhibit the formation of *K. pneumoniae* than *P. aeruginosa* biofilms, only two MDR isolates of the latter were included in this assay, whereas three MDR *K. pneumoniae* were tested. Optical density of the planktonic phase, as a measure of biofilm proliferation, was reduced in all peptide-treated biofilms, ranging from 3 to 21% reduction on *P. aeruginosa* isolates, and from 34 to 56% reduction on *K. pneumoniae* isolates (Table 4). The influence of the peptide on the metabolic activity of preformed biofilms of one *P. aeruginosa* (PA004) and three *K. pneumoniae* (KP004, KP007, and KP010) isolates was also assessed, through a standard MTT assay. Results, expressed as a percentage of reduction of metabolic activity in peptide-treated vs. untreated biofilms (Table 4), reinforce that peptide 3.1-PP4 significantly affects the viability of MDR *K. pneumoniae* isolates, whose metabolic activity

can be reduced up to nearly 80% in two of them (KP004 and KP010), and to 40% in the other.

Table 4 | Effects of peptide 3.1-PP4, at 20 × MIC, on 24-h preformed MDR bacterial biofilms.

| MDR isolate | OD ₆₀₀ of the planktonic phase in untreated biofilms | OD ₆₀₀ of the planktonic phase in peptide-treated biofilms | % reduction in biofilm proliferation upon treatment ^a | % reduction of metabolic activity in peptide-treated biofilms ^b |
|-------------|---|---|--|--|
| PA002 | 0.65±0.03 | 0.63±0.04 | 2.8 | - |
| PA004 | 0.91±0.03 | 0.71±0.05 | 21 | 8.3 |
| KP004 | 0.63±0.02 | 0.28±0.00 | 56 | 79 |
| KP007 | 0.56±0.01 | 0.37±0.03 | 34 | 40 |
| KP010 | 0.64±0.01 | 0.32±0.02 | 49 | 77 |

^a results are the mean of two independent experiments performed in triplicate; ^b two independent experiments were performed, each in four replicates.

To gain further insight into the peptide’s effects on the bacterial biofilms, a Live/Dead staining assay using CLSM was carried out, where untreated and peptide-treated biofilms delivered the images depicted in Figure 2. For this analysis, we selected strains based on their biofilm formation capability, previously assessed by the crystal violet assay (Figure 1 – control condition); hence, we opted to use one strong biofilm producer (*P. aeruginosa* isolate PA004), one good biofilm producer (*K. pneumoniae* isolate KP010), and one weak biofilm producer (*K. pneumoniae* isolate KP007). Noteworthy, only bacterial cells, not biofilm matrix, are stained when the Live/Dead staining is used, which means that only cells within the biofilm are observed. A qualitative analysis of images obtained show that (i) the ratio of red- to green-stained bacterial cells is consistently higher in peptide-treated compared to their respective untreated biofilms, and (ii) 3.1-PP4 has highest impact on the biofilm of isolate KP010, as significant biofilm disaggregation is observed in this case.

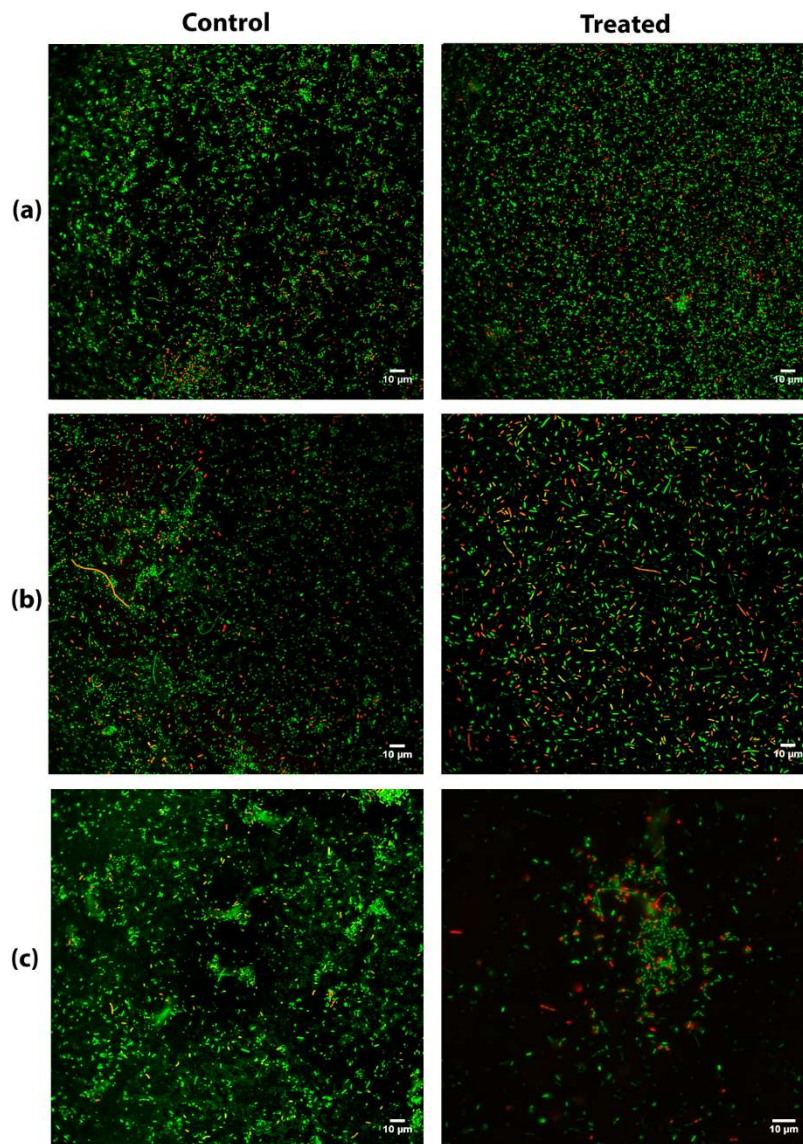


Figure 2. CLSM after Live/Dead staining of *P. aeruginosa* and *K. pneumoniae* biofilms allowed to grow for 24 h and next grown either in absence (control) or presence (treated) of peptide 3.1-PP4 at 20 × MIC; (A) PA004 isolate, (B) KP007 isolate, and (C) KP010 isolate.

Collagenesis-Inducing Effects

The CBP-AMP conjugates herein addressed include a collagenesis-inducing motif, the amino acid sequence KTTKS whose N-palmitoylated derivative is the well-known “Palmitoyl pentapeptide-4” (C₁₆-PP4) that emerged in 2000 under the commercial name Matrixyl as an active ingredient in skin rejuvenating cosmetics. Hence, the most promising synthetic peptide 3.1-PP4 was further tested to establish whether or not it exhibited collagenesis-inducing effects comparable to those of C₁₆-PP4. To this end,

collagen produced by HFF-1 human fibroblasts was determined by the previously validated Picrosirius Red Staining Protocol (Remoué et al., 2013), taking C₁₆-PP4 as reference CBP. Results from this type of assay are better interpreted on a comparative basis, as Picrosirius Red staining may occasionally lead to an overestimation of absolute collagen production (Coentro et al., 2017). Results are presented in Figure 3, and expressed as the ratio between collagen produced and the number of viable cells, as the test peptides had different cytotoxicity against the HFF-1 cell line.

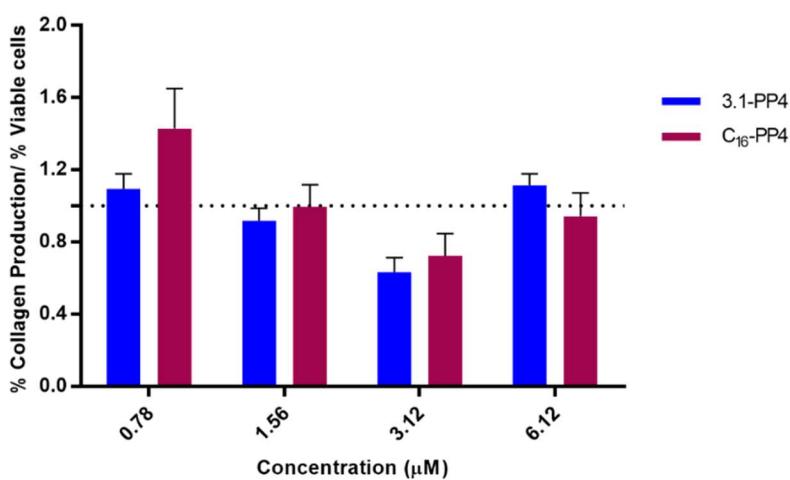


Figure 3. Collagen production by peptide-treated HFF-1 cells, normalized to the number of viable cells for each peptide concentration assayed. No statistically significant differences were observed between the tested peptides at any of the concentrations assayed. The “palmitoyl pentapeptide-4,” C₁₆-PP4, also known as Matrixyl, was taken as the reference CBP.

DISCUSSION

From Fleming’s serendipitous discovery of Penicillin, in 1928, to the end of the 1980’s, many antibiotics have been developed and marketed but, in the last four decades, no truly new antibiotic classes have been disclosed (Fernandes andMartens, 2017; Costa et al., 2019). In the past 4 years, Teixobactin (Ling et al., 2015) and Lungdunin (Zipperer et al., 2016), both cyclic peptides of bacterial origin, were found to have potent action on MDR Gram- positive bacteria. This brought new hope to the management of MDR infections, and refueled the interest on AMP-focused research, which had been cooling down in the first decade of this century. However, Teixobactin, Lungdunin, or synthetic derivatives thereof, are ineffective against Gram-negative bacteria (Ramchuran et al., 2018; Schilling et al., 2019). Hence, seeking for new agents to fight MDR Gram-negative

pathogens remains an urgent need and an active field of research. cSSTI refer to practically all types of severe infections, as soft tissue (SS) includes non-connective tissue like muscles, nerves, and blood vessels, and connective tissue like tendons, ligaments, fascia, nerves, fibrous tissues, fat, and synovial membranes; this leaves out only bone and teeth, the hard tissues in the human body (Skinner, 2006; Stecco et al., 2015). The highly hydrated extracellular matrix (ECM) of SS comprises a gel phase (the so-called ground substance) and a fibrous phase (collagen and elastin), both of which are mainly produced by fibroblast (Sherman et al., 2015). In view of this, we reasoned that peptide antibiotics effective for the management of cSSTI must combine the properties of an AMP with those of a CBP, which we are pursuing through the synthesis and study of AMP/CBP peptide hybrids like those herein reported.

One first observation regarding these new peptide hybrids was the higher cytotoxicity of the palmitoylated constructs as compared to their non-palmitoylated counterparts. Palmitoylated conjugates were included in this study, due to both the reported superiority of C₁₆-PP4 toward PP4 as a collagenesis inducer (Jones et al., 2013; Choi et al., 2014), and literature accounts on the increased bioactivity of AMP upon *N*-acylation with fatty acids (Chicharro et al., 2001; Chu-Kung et al., 2004; Etzerodt et al., 2011; Li et al., 2018). Still, the selectivity of AMP conjugated to fatty acids depends on the size of the latter, with increased toxicity to mammalian cells being often observed for conjugates where fatty acid chains are longer than 14 carbons (Nasompag et al., 2015; Ramachandran et al., 2017), which might explain our results.

The most relevant observation was that all non-palmitoylated peptide conjugates, i.e., PP4-3.1, PP4- β -Ala-3.1, and 3.1-PP4 were markedly active against both Gram-positive and Gram-negative reference bacterial strains, but the latter was the less cytotoxic of the set, being actually safer to human fibroblasts than the reference AMP, peptide 3.1. It was interesting to notice the different behavior of PP4-3.1 as compared to its reversed analog, 3.1-PP4, an observation that comes in line with many reports on the influence of peptide orientation in the antimicrobial properties of peptide-drug conjugates (Aguar et al., 2019), peptide hybrids (Cavalli et al., 2010), and peptide-grafted materials (Li et al., 2015; Barbosa et al., 2019). As such, and despite being slightly less potent against Gram-positive bacteria than the other two, peptide 3.1-PP4 was selected for further investigations on its activity against MDR isolates of Gram-negative pathogens in both planktonic and biofilm forms, on which its notable antibacterial efficiency could be confirmed. In addition, the collagenesis-inducing behavior of 3.1-PP4 was not statistically different from that of the reference CBP, peptide C₁₆-PP4 (Matrixyl). This is an important

observation, as C₁₆-PP4 has widely reported superiority toward PP4 alone as a collagenesis-inducer (Jones et al., 2013; Choi et al., 2014), whereas peptide 3.1 has never been reported to have collagen-boosting effects. Notwithstanding, although fully valid for comparative analyses, the collagenesis-inducing activity assay based on Syrius Red may lead to an overestimation of collagen content due (Coentro et al., 2017), hence ongoing work in our lab is targeting quantitation of total collagen deposition by more accurate methods, e.g., enzyme-linked immunosorbent assays (ELISA) (Hosseininia et al., 2016) or quantitative real-time polymerase chain reaction (RT-q-PCR) analysis of procollagen gene expression (Yamazaki et al., 2005). These analyses will include parent unmodified PP4 and 3.1 peptides, as well as their 1:1 mixtures, for a full profiling of collagenesis-inducing activity.

Taking into account its action on *K. pneumoniae* alone, peptide 3.1-PP4 is a novel antimicrobial peptide lead of undeniable relevance: *K. pneumoniae* is best known for causing pneumonia, typically as bronchopneumonia or bronchitis, with a quite poor prognosis if harboring antibiotic resistance; but the range of clinical diseases caused by this pathogen is much wider, including UTI, cholecystitis, diarrhea, respiratory tract infections, chronic wound infections, osteomyelitis, meningitis, and sepsis. *K. pneumoniae* can also act as an opportunistic pathogen, especially for people having respiratory dysfunctions such as chronic obstructive pulmonary diseases, among other debilitating conditions. MDR *K. pneumoniae* strains are ubiquitous in healthcare settings, where contact with contaminated medical devices put patients at a serious risk, as sepsis is a real menace once the bacteria enter the bloodstream (Li et al., 2014). Considering all the above, a wider and deeper study is underway in order to draw a clearer picture on the dual-action potential of new hybrid peptides derived from 3.1 and PP4, and others inspired on them. Thus, additional sets of peptide hybrids are being synthesized that cover (i) peptide *N*-acylation with fatty acids of different lengths, and (ii) modifications aimed at modulating the peptides physico-chemical properties toward improved bioavailability. Moreover, ongoing additional assays on collagenesis-inducing effects are covering a wider range of peptide concentrations, as well as quantitative determination of total collagen deposition levels, where unmodified parent peptides and their 1:1 mixture are also included. Finally, investigation of the antimicrobial/collagenesis-inducing effects of combinations between AMP/CBP hybrid peptides and conventional antibiotics is being pursued, as such mixtures may reveal important synergistic effects (Bessa et al., 2018; Hollmann et al., 2018; Otvos et al., 2018; Zharkova et al., 2019).

CONCLUSION

The present disclosure of hybrid peptide constructs combining the wide spectrum antimicrobial peptide 3.1 and the collagenesis-inducing peptide PP4 is unprecedented and results herein reported demonstrate the potential that such hybrids enclose for the future development of new potent antibacterial agents that are also collagenesis inducers. This is particularly relevant in the context of cSSTI, especially if associated to MDR Gram-negative bacteria. In this work, by replacing the palmitoyl group of the well-known cosmeceutical peptide C₁₆-PP4 (Matrixyl) with the antimicrobial peptide 3.1, a new peptide was produced with potent action against Gram-negative bacteria, including MDR isolates of *Enterobacteriaceae*, namely *E. coli* and *K. pneumoniae*. These are the two most prevalent species in UTI of the elderly, and also frequently associated to other cSSTI, and to HAI. The potent action of 3.1-PP4 against *K. pneumoniae* was further confirmed on biofilms of different MDR isolates of this pathogen, whose establishment, growth, and metabolic activity were clearly affected in the presence of the peptide. As such, this work represents a new doorway into the ongoing development of new dual antimicrobial and CBPs inspired on 3.1-PP4, which will be challenged against a wider panel of microbial pathogens, and regarding their full profiling as collagenesis inducers. Results thereof will be timely reported.

AUTHOR CONTRIBUTIONS

AG carried out the peptide synthesis, purification and analysis work, as well as antimicrobial activity assays using reference ATCC strains, and prepared the first version of the full manuscript. LB carried out the antimicrobial and antibiofilm assays using multi-drug resistant clinical isolates. IF carried out the collagenesis-inducing activity assays and peptide cytotoxicity screenings. RF participated in the global scientific reasoning. PGa coordinated the microbiology work. NM coordinated the cytotoxicity and collagenesis-inducing assays. CT participated in the rational design of peptides and experiments, and peptide synthesis work. PGo coordinated the overall study, and participated in the rational design of peptides, and manuscript final revision and submission.

FUNDING

This work was financed by FEDER – Fundo Europeu de Desenvolvimento Regional funds through the COMPETE 2020 – Operacional Programme for Competitiveness and Internationalisation (POCI), and by Portuguese funds through FCT – Fundação para a Ciência e a Tecnologia through the Research Grants UID/QUI/50006/2019 and POCI-01-0145- FEDER-031781, Doctoral Grant PD/BD/135073/2017 (AG), and post-doctoral Grant SFRH/BPD/86173/2012 (IF).

REFERENCES

- Aguiar, L., Machado, M., Sanches-Vaz, M., Prudêncio, M., Vale, N., and Gomes, P. (2019). Coupling the cell-penetrating peptides transportan and transportan10 to primaquine enhances its activity against liver-stage malaria parasites. *MedChemComm* 10, 221–226. doi: 10.1039/C8MD00447A
- Aldag, C., Nogueira Teixeira, D., and Leventhal, P. S. (2016). Skin rejuvenation using cosmetic products containing growth factors, cytokines, and matrikines: a review of the literature. *Clin. Cosmet. Investig. Dermatol.* 9, 411–419. doi: 10.2147/CCID.S116158
- Aminov, R. (2010). A brief history of the antibiotic Era: lessons learned and challenges for the future. *Front. Microbiol.* 1:134. doi: 10.3389/fmicb.2010.00134
- Andrews, J., Walker, R., and King, A. (2002). Evaluation of media available for testing the susceptibility of *Pseudomonasaeruginosa* by BSAC methodology. *J. Antimicrob. Chemother.* 50, 479–486. doi: 10.1093/jac/dkf181
- Ballantine, R. D., McCallion, C. E., Nassour, E., Tokajian, S., and Cochrane, S. A. (2019). Tridecaptin-inspired antimicrobial peptides with activity against multidrug-resistant Gram-negative bacteria. *MedChemComm* 10, 484–487. doi: 10.1039/C9MD00031C
- Barbosa, M., Costa, F., Monteiro, C., Duarte, F., Martins, M. C. L., and Gomes, P. (2019). Antimicrobial coatings prepared from Dhvar-5-click-grafted chitosan powders. *Acta Biomater.* 5, 242–256. doi: 10.1016/j.actbio.2018.12.001
- Benoiton, N. L. (2006). *Chemistry of Peptide Synthesis*. Boca Raton, FL: CRC Press.
- Bessa, L. J., Eaton, P., Dematei, A., Placido, A., Vale, N., Gomes, P., et al. (2018). Synergistic and antibiofilm properties of ocellatin peptides against multidrug-resistant *Pseudomonas aeruginosa*. *FutureMicrobiol.* 13, 151–163. doi: 10.2217/fmb-2017-0175

Cavalli, S., Albericio, F., and Kros, A. (2010). Amphiphilic peptides and their cross-disciplinary role as building blocks for nanoscience. *Chem. Soc. Rev.* 39, 241–263. doi: 10.1039/b906701a

Chang, C.-Y. (2018). Surface sensing for biofilm formation in *Pseudomonas aeruginosa*. *Front. Microbiol.* 8:2671. doi: 10.3389/fmicb.2017.02671

Chicharro, C., Granata, C., Lozano, R., Andreu, D., and Rivas, L. (2001). N-Terminal fatty acid substitution increases the leishmanicidal activity of CA(1-7)M(2-9), a cecropin melittin hybrid peptide. *Antimicrob. Agents Chemother.* 45, 2441–2449. doi: 10.1128/AAC.45.9.2441-2449.2001

Choi, Y. L., Park, E. J., Kim, E., Na, D. H., and Shin, Y.-H. (2014). Dermal stability and in vitro skin permeation of collagen pentapeptides (KTTKS and palmitoyl-KTTKS). *Biomol. Therapeut.* 22, 321–327. doi: 10.4062/biomolther.2014.053

Chu-Kung, A. F., Bozzelli, K. N., Lockwood, N. A., Haseman, J. R., Mayo, K. H., and Tirrell, M. W. (2004). Promotion of peptide antimicrobial activity by fatty acid conjugation. *Bioconjug. Chem.* 15, 530–535. doi: 10.1021/bc0341573

CLSI (2012). *Methods for Dilution Antimicrobial Susceptibility Tests for Bacteria that Grow Aerobically – Ninth Edition: Approved Standard M7-A9*. Wayne, PA: CLSI.

Coentro, J. Q., Capella-Monsonís, H., Graceffa, V., Wu, Z., Mullen, A. M., Raghunath, M., et al. (2017). Collagen quantification in tissue specimens. *Methods Mol. Biol.* 1627, 341–350. doi: 10.1007/978-1-4939-7113-8_22

Costa, F., Teixeira, C., Gomes, P., and Martins, M. C. L. (2019). “Clinical application of AMPs,” in *Antimicrobial Peptides: Basics for Clinical Application*, ed. K. Matsuzaki (Singapore: Springer Singapore), 281–298. doi: 10.1007/978-981-13-3588-4_15

Donlan, R. M. (2002). Biofilms: microbial life on surfaces. *Emerg. Infect. Dis.* 8, 881–890. doi: 10.3201/eid0809.020063

Etzerodt, T., Henriksen, J. R., Rasmussen, P., Clausen, M. H., and Andresen, T. L. (2011). Selective acylation enhances membrane charge sensitivity of the antimicrobial peptide mastoparan-x. *Biophys. J.* 100, 399–409. doi: 10.1016/j.bpj.2010.11.040

EWMA(2014). Antimicrobials and non-healing wounds – evidence, controversies and suggestions. *J. Wound Care* 23:426. doi: 10.12968/jowc.2014.23.8.426

Fernandes, P., and Martens, E. (2017). Antibiotics in late clinical development. *Biochem. Pharmacol.* 133, 152–163. doi: 10.1016/j.bcp.2016.09.025

Gomes, A., Teixeira, C., Ferraz, R., Prudencio, C., and Gomes, P. (2017). Wound-healing peptides for treatment of chronic diabetic foot ulcers and other infected skin injuries. *Molecules* 22:E1743. doi: 10.3390/molecules22101743

Gomes, N. M., Bessa, L. J., Buttachon, S., Costa, P. M., Buaruang, J., Dethoup, T., et al. (2014). Antibacterial and antibiofilm activities of tryptoquivalines and meroditerpenes isolated from the marine-derived fungi *Neosartorya paulistensis*, *N. laciniosa*, *N. tsunodae*, and the soil fungi *N. fischeri* and *N. siamensis*. *Mar. Drugs* 12, 822–839. doi: 10.3390/md12020822

Haney, E. F., Straus, S. K., and Hancock, R. E. W. (2019). Reassessing the host defense peptide landscape. *Front. Chem.* 7:43. doi: 10.3389/fchem.2019.00043

Hollmann, A., Martinez, M., Maturana, P., Semorile, L. C., and Maffia, P. C. (2018). Antimicrobial peptides: interaction with model and biological membranes and synergism with chemical antibiotics. *Front. Chem.* 6:204. doi: 10.3389/fchem.2018.00204

Hosseini, S., Weis, M. A., Rai, J., Kim, L., Funk, S., Dahlberg, L. E., et al. (2016). Evidence for enhanced collagen type III deposition focally in the territorial matrix of osteoarthritic hip articular cartilage. *Osteoarthr. Cartil.* 24, 1029–1035. doi: 10.1016/j.joca.2016.01.001

Jones, R. R., Castelletto, V., Connon, C. J., and Hamley, I. W. (2013). Collagen stimulating effect of peptide amphiphile C-16-KTTKS on human fibroblasts. *Mol. Pharmaceut.* 10, 1063–1069. doi: 10.1021/mp300549d

Kang, S. J., Won, H. S., Choi, W. S., and Lee, B. J. (2009). De novo generation of antimicrobial LK peptides with a single tryptophan at the critical amphipathic interface. *J. Pept. Sci.* 15, 583–588. doi: 10.1002/psc.1149

Krishnamoorthy, N., Tseng, Y. T., Gajendrarao, P., Sarathchandra, P., McCormack, A., Carubelli, I., et al. (2018). A strategy to enhance secretion of extracellular matrix components by stem cells: relevance to tissue engineering. *Tissue Eng. Part A* 24, 145–156. doi: 10.1089/ten.TEA.2017.0060

Leong, H. N., Kurup, A., Tan, M. Y., Kwa, A. L. H., Liau, K. H., and Wilcox, M. H. (2018). Management of complicated skin and soft tissue infections with a special focus

on the role of newer antibiotics. *Infect. Drug Resist.* 11, 1959–1974. doi: 10.2147/IDR.S172366

Li, B., Zhao, Y., Liu, C., Chen, Z., and Zhou, D. (2014). Molecular pathogenesis of *Klebsiella pneumoniae*. *Future Microbiol.* 9, 1071–1081. doi: 10.2217/fmb.14.48

Li, C., Liu, H., Yang, Y., Xu, X., Lv, T., Zhang, H., et al. (2018). N-myristoylation of antimicrobial peptide CM4 enhances its anticancer activity by interacting with cell membrane and targeting mitochondria in breast cancer cells. *Front. Pharmacol.* 9:1297. doi: 10.3389/fphar.2018.01297

Li, W., Sun, E., Wang, Y., Pan, H., Zhang, Y., Li, Y., et al. (2019). Rapid identification and antimicrobial susceptibility testing for urinary tract pathogens by direct analysis of urine samples using a MALDI-TOF MS- based combined protocol. *Front. Microbiol.* 10:1182. doi: 10.3389/fmicb.2019.01182

Li, Y. S., Wei, S., Wu, J., Jasensky, J., Xi, C., Li, H., et al. (2015). Effects of peptide immobilization sites on the structure and activity of surface- tethered antimicrobial peptides. *J. Phys. Chem. C* 119, 7146–7155. doi: 10.1021/jp5125487

Ling, L. L., Schneider, T., Peoples, A. J., Spoering, A. L., Engels, I., Conlon, B. P., et al. (2015). A new antibiotic kills pathogens without detectable resistance. *Nature* 517, 455–459. doi: 10.1038/nature14098

Makrantonaki, E., Wlaschek, M., and Scharffetter-Kochanek, K. (2017). Pathogenesis of wound healing disorders in the elderly. *J. Dtsch. Dermatol. Ges.* 15, 255–275. doi: 10.1111/ddg.13199

Mangoni, M. L., McDermott, A. M., and Zasloff, M. (2016). Antimicrobial peptides and wound healing: biological and therapeutic considerations. *Exp. Dermatol.* 25, 167–173. doi: 10.1111/exd.12929

Mant, C. T., Jiang, Z., Gera, L., Davis, T., Nelson, K. L., Bevers, S., et al. (2019). De Novo designed amphipathic α -helical antimicrobial peptides incorporating dab and dap residues on the polar face to treat the gram-negative pathogen, *Acinetobacter baumannii*. *J. Med. Chem.* 62, 3354–3366. doi: 10.1021/acs.jmedchem.8b01785

Mottola, C., Mendes, J. J., Cristino, J. M., Cavaco-Silva, P., Tavares, L., and Oliveira, M. (2016). Polymicrobial biofilms by diabetic foot clinical isolates. *Folia Microbiol.* 61, 35–43. doi: 10.1007/s12223-015-0401-3

Nasompag, S., Dechsiri, P., Hongsing, N., Phonimdaeng, P., Daduang, S., Klaynongsruang, S., et al. (2015). Effect of acyl chain length on therapeutic activity and mode of action of the CX-KYR-NH₂ antimicrobial lipopeptide. *Biochim. Biophys. Acta* 1848(10 Pt A), 2351–2364. doi: 10.1016/j.bbamem.2015.07.004

Ogba, O. M., Nsan, E., and Eyam, E. S. (2019). Aerobic bacteria associated with diabetic foot ulcers and their susceptibility pattern. *Biomed. Dermatol.* 3:1. doi: 10.1186/s41702019-0039-x

Omar, A., Wright, J. B., Schultz, G., Burrell, R., and Nadworny, P. (2017). Microbial biofilms and chronic wounds. *Microorganisms* 5:E9. doi: 10.3390/microorganisms5010009

Otvos, L. Jr., Ostorhazi, E., Szabo, D., Zumbun, S. D., Miller, L. L., Halasohoris, S. A., et al. (2018). Synergy between proline-rich antimicrobial peptides and small molecule antibiotics against selected gram-negative pathogens in vitro and in vivo. *Front. Chem.* 6:309. doi: 10.3389/fchem.2018.00309

Park, H., An, E., and Cho Lee, A.-R. (2017). Effect of palmitoyl-pentapeptide (Pal-KTTKS) on wound contractile process in relation with connective tissue growth factor and α -smooth muscle actin expression. *Tissue Eng. Regen. Med.* 14, 73–80. doi: 10.1007/s13770-016-0017-y

Ramachandran, R., Shrivastava, M., Narayanan, N. N., Thakur, R. M., Chakrabarti, A., and Roy, U. (2017). Evaluation of antifungal efficacy of three new cyclic lipopeptides of the class bacillomycin from *Bacillus subtilis* RLID 12.1. *Antimicrob. Agents Chemother.* 62:e01457-17. doi: 10.1128/AAC.01457-17

Ramchuran, E. J., Somboro, A. M., Abdel Monaim, S. A. H., Amoako, D. G., Parboosing, R., Kumalo, H. M., et al. (2018). In vitro antibacterial activity of teixobactin derivatives on clinically relevant bacterial isolates. *Front. Microbiol.* 9:1535–1535. doi: 10.3389/fmicb.2018.01535

Reisner, A., Krogfelt, K. A., Klein, B. M., Zechner, E. L., and Molin, S. (2006). In vitro biofilm formation of commensal and pathogenic *Escherichia coli* strains: impact of environmental and genetic factors. *J. Bacteriol.* 188, 3572–3581. doi:10.1128/JB.188.10.3572-3581.2006

Remoué, N., Molinari, J., Andres, E., Lago, J. C., Barrichello, C., and Moreira, P. L. (2013). Development of an in vitro model of menopause using primary human dermal fibroblasts. *Int. J. Cosmet. Sci.* 35, 546–554. doi: 10.1111/ics.12075

Schagen, K. S. (2017). Topical peptide treatments with effective anti-aging results. *Cosmetics* 4:16. doi: 10.3390/cosmetics4020016

Schilling, N. A., Berscheid, A., Schumacher, J., Saur, J. S., Konnerth, M. C., Wirtz, S. N., et al. (2019). Synthetic lugdunin analogues reveal essential structural motifs for antimicrobial action and proton translocation capability. *Angew Chem. Int. Ed. Engl.* 58, 9234–9238. doi: 10.1002/anie.201901589

Sherman, V. R., Yang, W., and Meyers, M. A. (2015). The materials science of collagen. *J. Mech. Behav. Biomed. Mater.* 52, 22–50. doi: 10.1016/j.jmbbm.2015.05.023

Skinner, H. B. (2006). *Current Diagnosis & Treatment in Orthopedics*. New York, NY: McGraw Hill.

Stecco, C., Hammer, W., Vleeming, A., and De Caro, R. (2015). “Connective Tissues,” in *Functional Atlas of the Human Fascial System*, ed. W. Hammer (London: Churchill Livingstone Elsevier), 1–20. doi: 10.1016/b978-0-7020-4430-4.00001-4

Stepanovic, S., Vukovic, D., Hola, V., Di Bonaventura, G., Djukic, S., Cirkovic, I., et al. (2007). Quantification of biofilm in microtiter plates: overview of testing conditions and practical recommendations for assessment of biofilm production by staphylococci. *APMIS* 115, 891–899. doi: 10.1111/j.1600-0463.2007.apm_630.x

Tsai, W.-C., Hsu, C.-C., Chung, C.-Y., Lin, M.-S., Li, S.-L., and Pang, J.-H. S. (2007). The pentapeptide KTTKS promoting the expressions of type I collagen and transforming growth factor- β of tendon cells. *J. Orthop. Res.* 25, 1629–1634. doi: 10.1002/jor.20455

VanEpps, J. S., and Younger, J. G. (2016). Implantable device-related infection. *Shock* 46, 597–608. doi: 10.1097/shk.0000000000000692

Wang, J., Song, J., Yang, Z., He, S., Yang, Y., Feng, X., et al. (2019). Antimicrobial peptides with high proteolytic resistance for combating gram-negative bacteria. *J. Med. Chem.* 62, 2286–2304. doi: 10.1021/acs.jmedchem.8b01348

WHO (2014). *Antimicrobial Resistance: Global Report on Surveillance 2014*. Geneva: WHO.

WHO (2017). *WHO Publishes List of Bacteria for Which New Antibiotics are Urgently Needed*. Available at: <https://www.who.int/news-room/detail/27-02-2017-who-publishes-list-of-bacteria-for-which-new-antibiotics-are-urgently-needed> (accessed June 4, 2019).

Yamazaki, K., Fukata, H., Adachi, T., Tainaka, H., Kohda, M., Yamazaki, M., et al. (2005). Association of increased type I collagen expression and relative stromal overgrowth in mouse epididymis neonatally exposed to diethylstilbestrol. *Mol. Reprod. Dev.* 72, 291–298. doi: 10.1002/mrd.20347

Yasir, M., Willcox, M. D. P., and Dutta, D. (2018). Action of antimicrobial peptides against bacterial biofilms. *Materials* 11:E2468. doi: 10.3390/ma11122468

Zharkova, M. S., Orlov, D. S., Golubeva, O. Y., Chakchir, O. B., Eliseev, I. E., Grinchuk, T. M., et al. (2019). Application of antimicrobial peptides of the innate immune system in combination with conventional antibiotics—a novel way to combat antibiotic resistance? *Front. Cell. Infect. Microbiol.* 9:128. doi:10.3389/fcimb.2019.00128

Zheng, B., Dai, Y., Liu, Y., Shi, W., Dai, E., Han, Y., et al. (2017). Molecular epidemiology and risk factors of carbapenem-resistant *Klebsiella pneumoniae* Infections in Eastern China. *Front. Microbiol.* 8:1061. doi: 10.3389/fmicb.2017.01061

Zipperer, A., Konnerth, M. C., Laux, C., Berscheid, A., Janek, D., Weidenmaier, C., et al. (2016). Human commensals producing a novel antibiotic impair pathogen colonization. *Nature* 535, 511–516. doi: 10.1038/nature18634

2.2. Chimeric peptide stability enhancement via conjugation to an IL

“Clicking” an Ionic Liquid to a Potent Antimicrobial Peptide: On the Route towards Improved Stability

Ana Gomes, Lucinda J Bessa, Patrícia Correia, Iva Fernandes, Ricardo Ferraz, Paula Gameiro, Cátia Teixeira, Paula Gomes

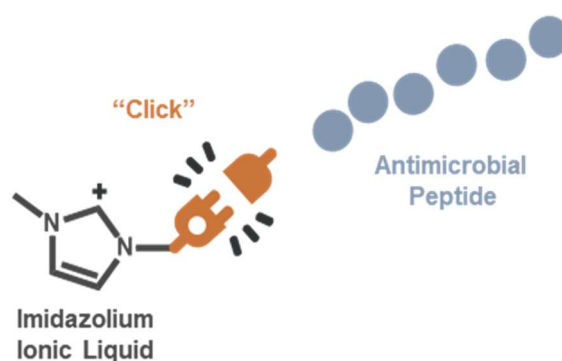
International Journal of Molecular Sciences **2020**, 21 (17), 6174

<https://doi.org/10.3390/ijms21176174>

Abstract

A covalent conjugate between an antibacterial ionic liquid and an antimicrobial peptide was produced via “click” chemistry, and found to retain the parent peptide’s activity against multidrug-resistant clinical isolates of Gram-negative bacteria, and antibiofilm action on a resistant clinical isolate of *Klebsiella pneumoniae*, while exhibiting much improved stability towards tyrosinase-mediated modifications. This unprecedented communication is a prelude for the promise held by ionic liquids -based approaches as tools to improve the action of bioactive peptides.

Keywords: antibacterial; antibiofilm; ionic liquid; multidrug resistance; peptide; skin infections; tyrosinase; wound healing



1. Introduction

Ionic Liquids (ILs), though mostly known for their potential role as “green solvents”, are becoming increasingly attractive as easily customizable and tunable organic salts for diverse specific purposes (task-specific ILs). There is an infinity of possibilities when combining organic cations with organic or inorganic anions, enabling production of ILs with diverse structural, physical and chemical properties [1] that can be adapted to the demands of areas as diverse as material sciences [2], biotechnology [3], or biomedicine [4]. Moreover, by making use of bioactive ions, ILs displaying relevant biological activities [5] can be produced, for instance, as anticancer [6], antimalarial [7], and antimicrobial agents [8].

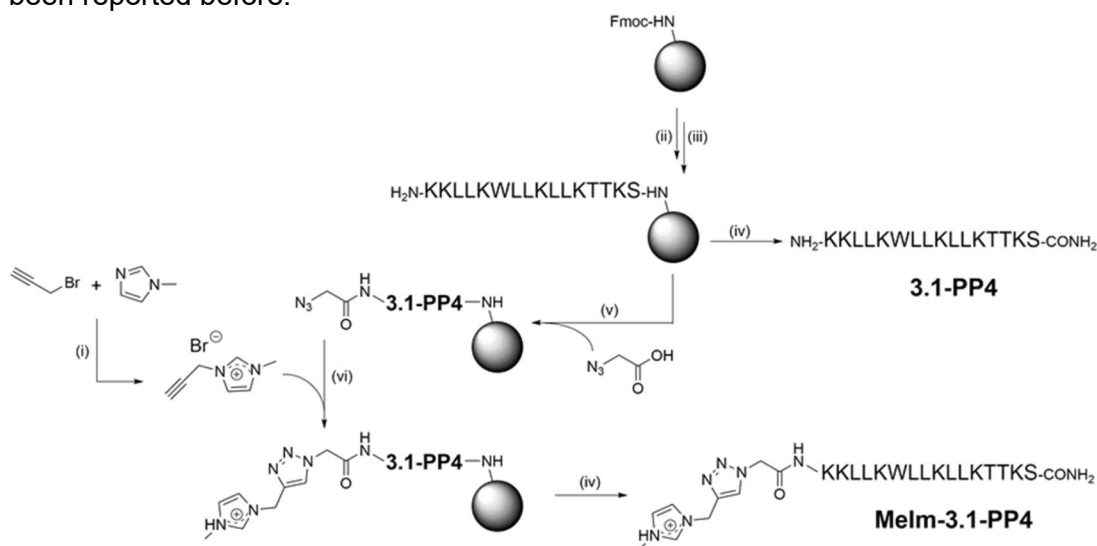
ILs showing broad-spectrum activity against both Gram-negative and Gram-positive bacteria and antibiofilm activity have been reported [9]; as such, ILs are emerging as appealing alternatives to counteract antimicrobial resistance, while the world is running out of effective antibiotics, especially against Gram-negative bacteria. Moreover, many ILs have gained attention as dermal permeation enhancers [10], making them particularly attractive for topical applications. ILs presenting both antimicrobial activity and dermal permeation enhancement can be quite helpful to treat infected skin lesions, as recently demonstrated in an *in vivo* biofilm-infected wound assay, where an IL was able to kill 95% of the bacteria [11].

In view of the above, and based on our recent disclosure of a collagenesis-inducing peptide with potent antibacterial and antibiofilm properties [12], we now investigated the effect of coupling an antimicrobial methylimidazolium IL to the *N*-terminus of that peptide on antibacterial and antibiofilm activities, as well as on stability. To this end, we opted to use the well-known copper(I)-catalyzed alkyne-azide cycloaddition (CuAAC) “click” reaction, given its chemoselectivity and mildness, and the fact that it produces a stable triazole ring [13]. Moreover, CuAAC reactions have been previously used to introduce the triazole moiety in peptides aiming at, e.g., (i) replacing unstable bonds like disulfide bridges, (ii) improving peptide stability via cyclization, (iii) attaching distinct moieties and/or functional groups to the peptide, and (iv) taking advantage of the biological properties of many triazoles to improve overall bioactivity [14].

2. Results and Discussion

2.1. Chemical Synthesis

To produce the target IL-peptide conjugate, hereafter termed Melm-3.1-PP4, the synthetic route shown in Scheme 1 was employed, starting with the synthesis of the alkyne-modified IL, by reacting 1-methylimidazole (Melm) with propargyl bromide (step i), according to Hu et al. [15]; the structure of the target propargyl-Melm (Pr-Melm) was confirmed by proton (1 H) and carbon (13 C) nuclear magnetic resonance (NMR) and electrospray ionization-ion trap mass spectrometry (ESI-IT MS), as described in detail in the Supplementary Materials (Figures S1–S3). In parallel, the amino acid sequence of 3.1-PP4 was assembled by solid-phase peptide synthesis (SPPS, steps ii and iii) as previously reported by us [12]. Cleavage of half of the peptidyl-resin (step iv) afforded the parent peptide 3.1-PP4. The other half was coupled with azidoacetic acid (step v) to produce the azide- modified peptide; this was followed by on-resin CuAAC with Pr-Melm (step vi), applying the conditions previously described by Castro et al. [16]. After cleavage and purification by reverse-phase high performance liquid chromatography (RP-HPLC), the target Melm-3.1-PP4 conjugate was obtained in high purity (Figure S4), and its structure was confirmed by ESI-IT MS analysis (Figure S5). To the best of our knowledge, on-resin “clicking” of an ionic liquid to a peptide via the CuAAC has never been reported before.



Scheme 1. Synthesis route towards Melm-3.1-PP4: (i) 1.1 molar equivalents (eq) of Melm, 1.0 eq of propargyl bromide (80% in toluene), 40 ° C, 24 h; (ii) 5 eq of Fmoc-protected amino acid, 10 eq of *N*-ethyl-*N,N*-diisopropylamine (DIEA) and 5 eq of *O*-(benzotriazol-1-yl)-*N,N,N',N'*-tetramethyluronium hexafluorophosphate (HBTU) in *N,N*-dimethylformamide (DMF), 1 h, room temperature (r.t.); (iii) 20% piperidine in DMF, 15 min, r.t.; (iv) trifluoroacetic acid (TFA)/triisopropylsilane (TIS)/distilled water (95:2.5:2.5 v/v/v), 2 h, r.t.; (v) 5 eq of azido acetic acid, 10 eq of DIEA, and 5 eq of HBTU in DMF, 1 h, r.t.; (vi) 1 eq sodium L- ascorbate, 10 eq of DIEA, 10 eq of 2,6-lutidine, 1 eq of Pr-Melm, and 1 eq of copper(I) bromide in DMF:acetonitrile (MeCN) (3:1 v/v).

2.2. Antibacterial and Antibiofilm Activity

Both the conjugate Melm-3.1-PP4 and its parent peptide 3.1-PP4 were next screened for their antibacterial activity. Minimum inhibitory concentration (MIC) values were determined following the Clinical and Laboratory Standards Institute (CLSI) protocol [17], against Gram-positive (*Staphylococcus aureus* and *Enterococcus faecalis*), and Gram-negative (*Pseudomonas aeruginosa*, *Escherichia coli* and *Klebsiella pneumoniae*) bacteria, including both reference strains (American Type Culture Collection, ATCC), and multidrug-resistant (MDR) clinical isolates. Data thus obtained are shown in Table 1, and clearly demonstrate that, with only very few exceptions, attachment of the IL to the N-terminus of 3.1-PP4 did not significantly alter the antibacterial activity of the parent peptide. Relevantly, in most cases, MIC values matched the minimum bactericidal concentration (MBC) values, highlighting a bactericidal action for both Melm-3.1-PP4 and its parent peptide.

Table 1. Minimum inhibitory concentrations (MIC) of Melm-3.1-PP4 and its parent peptide, 3.1-PP4, against reference (American Type Culture Collection, ATCC) strains and multidrug-resistant (MDR) clinical isolates of Gram-positive and Gram-negative bacteria.

| Bacterial species | Reference strain or MDR isolate | MIC in µg/mL (in µM) | |
|----------------------|---------------------------------|-------------------------|--------------------------|
| | | 3.1-PP4 | Melm-3.1-PP4 |
| <i>P. aeruginosa</i> | ATCC 27853 | 2.3 (1.2) | 1.5 (0.7) |
| | PA004 | 1.3 (0.7) | 3.1 (1.4) |
| | Pa3 | 1.3 (0.7) | 1.5 (0.7) |
| | Pa4 | 1.3 (0.7) | 0.8 (0.4) |
| <i>E. coli</i> | ATCC 25922 | 1.3 (0.7) | 0.8 (0.4) |
| | Ec2 | 1.3 (0.7) | 1.5 (0.7) |
| | EC001 | 1.3 (0.7) | 3.1 (1.4) |
| | EC002 | 1.3 (0.7) | 1.5 (0.7) |
| | EC003 | 0.6 (0.3) | 1.5 (0.7) |
| <i>K. pneumoniae</i> | KP010 | 2.3 (1.2) | 6.2 (2.9) |
| | KP004 | 2.3 (1.2) | 49.6 (23.1) |
| <i>S. aureus</i> | ATCC 25923 | 10.3 (5.3) ^a | 24.8 (11.6) ^a |
| | Sa007 | 10.3 (5.3) | 12.4 (5.8) |
| <i>E. faecalis</i> | ATCC 29212 | 41.3 (21.3) | 99.3 (46.3) |
| | Ef1 | 2.3 (1.2) ^a | 3.1 (1.4) |

^a Minimum bactericidal concentrations (MBC) were 2× the MIC; in all other cases, MBC equaled the MIC.

Since this type of IL-AMP conjugate is being developed for its potential interest to address infected skin lesions, a preliminary assessment of the toxicity of both the conjugate and the parent peptide towards HaCaT human epidermal keratinocytes was carried out by the 3-(4,5-dimethylthiazol-2-yl)-2,5-diphenyltetrazolium bromide (MTT) assay, as previously described by us [12]. Despite the IC₅₀ (24 h) obtained was somewhat lower for the conjugate (19.4 ± 0.2 µM) than for the parent peptide (34.2 ± 0.5

μM), the conjugate still exhibited selectivity indices ranging from ca. 14 to ca. 50 in most cases. In face of the excellent antibacterial properties exhibited by the Melm-3.1-PP4 conjugate, especially against Gram-negative bacteria, we next evaluated its antibiofilm activity using the *K. pneumoniae* MDR isolate, KP010, since the parent peptide, 3.1-PP4, had previously displayed a more notable effect against this isolate [12]. This activity was assessed in two different ways: (i) inhibition of biofilm formation, and (ii) effect on a preformed biofilm. For evaluation of the inhibition of biofilm formation, both conjugate and parent peptide were tested at MIC and sub-inhibitory concentrations ($\frac{1}{2}\times\text{MIC}$ and $\frac{1}{4}\times\text{MIC}$) following previously established procedures [12,18–20], and the mass of biofilm formed at these concentrations was assessed through the crystal violet assay. Figure 1 shows results obtained in absence (control) and in presence of the test compounds at the three different concentrations. Relevantly, the absorbance measured for the control (absence of test compounds) provides confirmation that the bacterial strain used is a good biofilm producer [21]. As expected, only a little amount of biofilm was formed at MIC in both cases, with a slightly higher antibiofilm effect for the parent peptide. At sub-inhibitory concentrations ($\frac{1}{2}\times\text{MIC}$ and $\frac{1}{4}\times\text{MIC}$), the biofilm biomasses formed remain lower than the control, in this case with a slightly stronger antibiofilm effect for the Melm-3.1-PP4 conjugate.

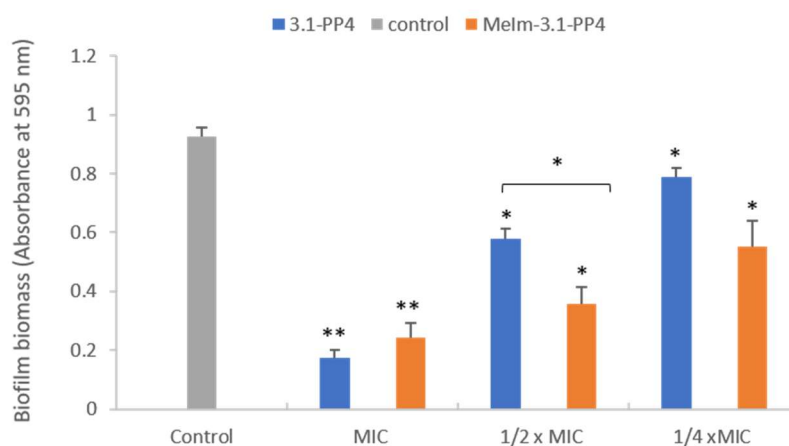


Figure 1. Effects of 3.1-PP4 and Melm-3.1-PP4 on formation of *K. pneumoniae* KP010 biofilms (biomass quantification by crystal violet absorbance at 595 nm). Three independent experiments were performed in triplicate and the bar errors represent the SD. Statistically significant differences between the biofilm formed in absence and in presence of peptide are indicated: * means ($p < 0.05$) and ** means ($p < 0.01$).

To assess the effects on preformed biofilms, much higher peptide concentrations are needed, hence biofilms of KP010 were allowed to grow for 48 h and then treated with the peptides at 20× the MIC value for 24 h. Biofilm proliferation was determined by measuring the optical density (OD) of the planktonic phase of the biofilms, both treated with the test compounds and the untreated control. Results (Table S2 in Supplementary Materials) show that Melm-3.1-PP4 and 3.1-PP4 caused a significant reduction in biofilm proliferation of 67% and 52%, respectively. Overall, these results show that the novel IL-peptide conjugate preserves not only the antibacterial but also the antibiofilm properties of the parent peptide. This improvement, afforded by the insertion of the imidazolium motif, is in line with previous reports of enhanced antibacterial activity when combining imidazolium ILs with non-peptide antibiotics, like ampicillin, including against resistant bacterial strains [22].

2.3. Enzymatic Stability

One of our main motivations to explore IL-peptide conjugates concerns improving the enzymatic stability of the peptide moiety, as poor pharmacokinetics is a major obstacle towards clinical translation of AMP and other bioactive peptides, even when topical applications are envisaged. For instance, in a non-healing infected wound, peptides are vulnerable to modification by endogenous (e.g., tyrosinase, elastase, metalloproteinases) and exogenous (produced by colonizing microbes) enzymes in the wound site [23]. Peptide 3.1-PP4 and derivatives thereof are under investigation for topical applications on infected skin lesions; thus, to evaluate how the conjugation of an IL to 3.1-PP4 could affect the enzymatic stability of this peptide, we incubated both the conjugate and the parent peptide with tyrosinase, due to its central role in melanin biosynthesis in the skin [24], and reported increased levels in the course of wound healing [25]. The choice of this particular enzyme may seem odd at a first glance, as the 3.1-PP4 sequence lacks tyrosine residues, whereas tyrosinase is best known for promoting oxidation of phenols like, e.g., the side chain of tyrosine [25].

However, recent evidence of proteolytic activity for tyrosinase, with an apparent preference for hydrophobic amino acids, e.g., isoleucine, at the cleavage site [26], stimulated our interest in investigating whether our leucine-rich peptide would be a substrate for this enzyme of undeniable relevance in skin and wound healing. Hence, both parent peptide and its ionic liquid conjugate were incubated at 37 °C and pH 6.8 in the presence of the enzyme, and in its absence as a control. The samples were collected at different time points, for 24 h, and were analyzed by HPLC. Results are presented in

Figure 2, where the complete degradation, within 6 h, of peptide 3.1-PP4 confirmed it as a substrate for tyrosinase, despite being devoid of tyrosine or any other phenol or polyphenol moieties. Additionally, about 84% of the IL-peptide conjugate Melm-3.1-PP4 remained unaltered after 24 h, demonstrating the remarkable gain in stability afforded by conjugation of the IL to the *N*-terminus of the parent peptide. Both controls remained unchanged at the end of the experiment (data not shown).

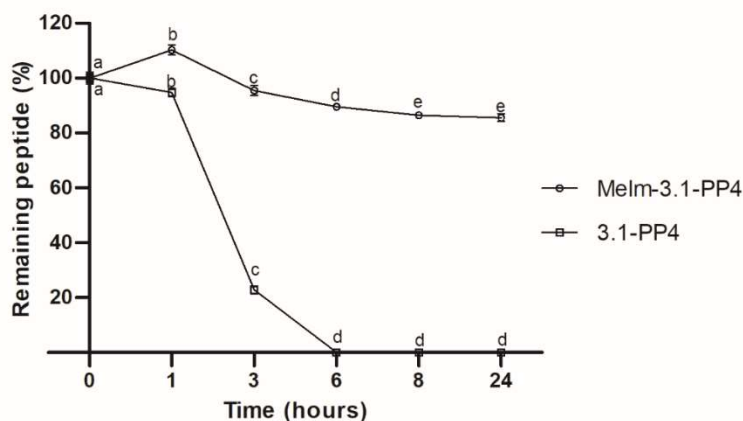


Figure 2. Compared stability of Melm-3.1-PP4 and its parent peptide, upon incubation with tyrosinase (expressed as the variation of the % of starting compound over time) of three independent experiments ($n = 3$). Values are expressed as mean \pm SD. Statistical significance, between the two test compounds for the same time point, was considered when $p < 0.0001$, and observed for all time points. Statistical significance, between time points for the same compound, was considered when $p < 0.05$ and is indicated by different letters.

The above findings are remarkable in two ways; (i) we confirm the recent observations by Biundo *et al.* in that tyrosinase can display promiscuous proteolytic activity [26], and (ii) we demonstrate that simple conjugation of an IL to the *N*-terminus of the peptide substrate prevents its degradation. Ongoing studies with these and other analogues will allow us to establish the pathway of peptide degradation by tyrosinase, and to ascertain how the peptide site at which the IL is conjugated (e.g., *C*-terminal rather than *N*-terminal conjugation) may influence enzymatic stability. Additional assays to evaluate conjugate's stability in the presence of more common enzymes and enzyme mixtures (trypsin, pronase), as well as other enzymes that are relevant in the context of chronic wounds (collagenase, elastase, metalloproteinases), will be timely carried out.

3. Concluding Remarks

In conclusion, this exploratory work holds great promise for the future, by demonstrating that “clicking” a classical imidazolium IL to the *N*-terminus of a bioactive peptide can preserve its potent antibacterial and antibiofilm action, while significantly improving its

stability towards an enzyme that is relevant in the skin wound environment. To the best of our knowledge, despite previous reports that have addressed both covalent [27] and non-covalent [28] combinations of IL with peptides, there is no precedent in using click chemistry to create IL-AMP conjugates, nor in demonstrating the substantial stabilization observed against tyrosinase-mediated modification upon conjugation of an IL to an AMP. Ongoing studies will allow us to build a wider landscape of enzymatic stability for Melm-3.1-PP4 and similar IL-peptide conjugates that are being produced, by including other analogues, and other enzymes relevant in the context of infected skin lesions and wound healing. Moreover, hemolysis assays will be carried out in order to establish whether conjugation to the IL renders the final conjugate more hemolytic than the parent peptide, at the light of previous literature reports [27,29]. Furthermore, *in vitro* wound healing and dermal permeation assays are under way that will allow us to further demonstrate the expected high value of this unprecedented approach. Finally, the potent action of the compounds herein reported against Gram-negative bacteria is noteworthy, since despite peptide-based structures with potent action against Gram-positive bacteria are being disclosed [30–33], the situation is quite different regarding MDR Gram-negative bacteria, against which real alternatives to current antibiotics remain elusive.

4. Materials and Methods

4.1. Synthesis of 1-Methyl-3-Propargyl Imidazolium Bromide

To a round-bottom flask containing 1-methylimidazole (0.78 mL; 9.89 mmol), 80% propargyl bromide in toluene (1 mL; 8.99 mmol) was slowly added, and the deep yellow oily mixture formed was kept under stirring for 24 h at 40 °C. The mixture was then cooled down to r.t., and sequentially washed with dichloromethane (DCM, 10 mL) and diethyl ether (10 mL) [15]. The resulting yellow oil was dried in a vacuum oven overnight, at 50 °C and 0.1 bar, to afford the final product in 77% yield.

¹H, ¹³C NMR and ESI-IT MS analyses allowed to confirm the product as being the desired 1-methyl-3-propargyl imidazolium bromide, according to spectral data below (spectra obtained are displayed in the Supplementary Materials—Figures S1, S2 and S3). NMR spectra were acquired on a Bruker Avance III400 spectrometer from solutions of the compound in 1,1,1-trifluoro-2,2,2-hydroxypropane (TFM) dimethyl sulfoxide (DMSO-d₆), containing tetramethylsilane (TMS) as internal reference. Multiplicity of proton NMR signals is given as: s, singlet; d, doublet; t, triplet.

δ_{H} (400 MHz, DMSO- d_6) 9.27 (s, 1H), 7.80 (t, 1H, $J = 1.8$ Hz), 7.76 (t, 1H, $J = 1.8$ Hz), 5.22 (d, 2H, $J = 2.6$ Hz), 3.88 (s, 3H), 3.84 (t, 1H, $J = 2.6$ Hz). δ_{C} (100 MHz, DMSO- d_6) 136.3, 124.1, 122.1, 79.0, 76.1, 38.5, 36.0 (ESI+) m/z calculated for $\text{C}_7\text{H}_9\text{N}_2^+$, 121.08; found, 121.20.

4.2. Peptide Synthesis

The amino acid sequence of 3.1-PP4 (KKLLKWLLKLLKTTKS, C-terminal amide) was assembled by SPPS, using the standard Fmoc/tBu orthogonal protection scheme [34]. Briefly, Fmoc-Rink-amide MBHA resin (100–200 mesh, 0.52 mmol/g) was swelled in DMF for 30 min, next treated with an excess of 20% piperidine in DMF for 15 min (r.t.); after several washing steps using DMF (3×10 mL) and DCM (3×10 mL), the Fmoc-protected C-terminal amino acid (5 eq) was coupled to the resin in the presence of the in situ coupling agent HBTU (5 eq) and the non-nucleophilic base DIEA (10 eq) in DMF, for 1 h at r.t., under stirring. After a few quick washing steps as before, the Fmoc group was removed with piperidine as above, and the coupling \rightarrow deprotection cycle was repeated until the full amino acid sequence was assembled. At this stage, the peptidyl-resin was split in two equal portions, one of which was reserved for the subsequent stage (synthesis of Melm-3.1-PP4, see Section 4.3). Peptide 3.1-PP4 was cleaved off the other portion of the peptidyl-resin via acidolytic cleavage with a cocktail containing 95% TFA, 2.5% TIS and 2.5% distilled water, for 2 h under stirring at r.t.. The crude peptide was then purified by preparative RP-HPLC, on a Hitachi-Merck LaPrep Sigma system using a C18 column (250 \times 25 mm ID, 5 μm pore size). The elution gradient of 1 to 100% of MeCN, used 0.05% aqueous TFA as solvent A and MeCN as solvent B, and was run for 60 min at 15 mL/min. Fractions containing pure peptide were pooled, and an aliquot was taken to assess final purity degree by HPLC and confirm the expected molecular weight by ESI-IT MS, as previously described [17]. The final peptide solution was freeze-dried and stored at -20 $^{\circ}\text{C}$ until further use.

4.3. Synthesis of Melm-3.1-PP4

To the reserved portion of peptidyl-resin having the 3.1-PP4 sequence fully assembled (see Section 4.2), a solution containing azidoacetic acid (18.7 mL; 5 eq), DIEA (85 mL; 10 eq), and HBTU (64 mg; 5 eq) in DMF was added, and the slurry kept under stirring for 1 h at r.t. After quick washing steps with DMF and DCM, as described in Section 4.2, a solution containing sodium L-ascorbate (10mg; 1 eq), DIEA (85 mL; 10 eq), 2,6-lutidine (58 mL; 10 eq), and 1-methyl-3-propargyl imidazolium bromide (10 mg; 1 eq) in DMF (3 mL) was added, followed by addition of a solution of copper(I) bromide (7 mg; 1 eq) in

MeCN (1 mL). The reaction was allowed to proceed at r.t. for 24 h, under stirring. Then, the resin was thoroughly washed with 1 M aqueous ethylenediaminetetraacetic acid (EDTA, 5 × 10 mL), followed by DMF and DCM as before. The crude product was cleaved from the resin via acidolysis, as in 4.2, and found (LC-MS) to be a mixture of the target conjugate (ca. 97%) and unreacted azido-peptide (ca. 2%), amongst other minor unidentified components, probably corresponding to truncated peptides (data not shown). The crude product was purified by preparative RP-HPLC, as done before for the parent 3.1-PP4 peptide (see Section 4.2). The pure conjugate was analyzed by HPLC (Figure S4) and ESI-IT MS (Figure S5), freeze-dried and stored at -20 °C until further use.

4.4. Peptide Quantitation

Peptide 3.1-PP4 and conjugate Melm-3.1-PP4 stock solutions were prepared in distilled water at ca. 10 mg/mL. Concentration was then accurately determined on a Thermo Scientific™ NanoDrop™ One microvolume UV-Vis Spectrophotometer, using method 31 that assumes an extinction coefficient ϵ_{205} of 31 mLmg⁻¹cm⁻¹ and an A280/A205 correction for the absorbance due to tryptophan (Trp) and tyrosine (Tyr) residues eventually present (only Trp was present in this case) [35].

4.5. Antibacterial Activity Assays

The MIC of the test compounds was determined according to the CLSI guidelines [17]. Briefly, the compounds were tested in the 1–1024 µg/mL concentration range, using the microdilution method in cation-adjusted Mueller-Hinton broth (MHB II) against reference strains of *P. aeruginosa* ATCC 27853, *E. coli* ATCC 25922, *S. aureus* ATCC 25923, and *Enterococcus faecalis* ATCC 29212. MIC values were also determined against MDR clinical isolates (antibiotic resistance patterns given in Supplementary Materials, Table S1) of *P. aeruginosa* (PA004, Pa3, Pa4), *E. coli* (Ec2, EC001, EC002, EC003), *K. pneumoniae* (KP004, KP010), *S. aureus* (SA007), and *Enterococcus faecalis* (Ef1). Along with the MIC values, MBC values were also determined as previously reported [12].

4.6. Toxicity to Human Keratinocytes

The cytotoxicity of peptides to HaCat cells was evaluated using the standard MTT assay. Briefly, cells were seeded at a density of 4 × 10⁴ in a 5% CO₂ cells/mL, respectively, in 96-well plates and incubated at 37°C atmosphere. Cells were allowed to grow for 24 h,

and serially diluted compound solutions (6.3–100 μM) were added to the wells. Then, cells were incubated for 24 h at 37 °C, after which wells were washed once with phosphate buffered saline (PBS, Sigma-Aldrich), followed by addition of a 0.45 mg/mL MTT solution to each well. Crystals were allowed to form for 1.5 h. Reaction was stopped by rejecting the medium followed by addition of dimethylsulfoxide (DMSO, Sigma-Aldrich). Absorbance was read at 570 nm in FlexStation® Devices, San Jose, CA, USA).

4.7. Antibiofilm Activity Assays

The ability of the test compounds to inhibit the biofilm formation by KP010 (a MDR clinical isolate of *K. pneumoniae*) was assessed at the respective MIC, $\frac{1}{2} \times \text{MIC}$ and $\frac{1}{4} \times \text{MIC}$ values in tryptic soy broth (TSB) using the crystal violet assay as previously reported [36,37]. Three independent experiments were performed in triplicate for each condition. To assess the effects of test compounds on 48 h preformed biofilms of KP010, the biofilms were first grown in TSB from a starting inoculum of 1×10^6 CFU/mL in 96-well microtiter plates. After 48 h of incubation at 37 °C, the planktonic cells were removed, and the wells were rinsed and filled with the test compound at a $20 \times \text{MIC}$ concentration. The optical density at 600 nm was measured at time 0 and after incubation for 24 h at 37 °C. The reduction in the biofilm proliferation was calculated in comparison to the respective non-treated biofilms. Three independent experiments were performed in triplicate.

4.8. Enzymatic Stability Assay

The IL-peptide conjugate and the parent peptide were both incubated at a final concentration of 10 mM in phosphate buffer (pH 6.8), with the enzyme tyrosinase (CAS:9002-10-2; T3824-250KU) at 18 U/mL, for 24 h at 37 °C. Then, 150- μL samples were collected after 0, 1, 3, 6, 8 and 24 h of incubation, and 150 μL of methanol were added to each of them to precipitate the enzyme. The mixtures were centrifuged at 1.05×10^4 RPM for 2 min with an Eppendorf miniSpin centrifuge (rotor F-45-12-11). The supernatant was then analyzed by HPLC, using a Hitachi-Merck LaChrom Elite system with a reverse-phase C18 column (125 \times 40 mm ID and 5 μm pore size). The analyses were run, in triplicates, at a flow rate of 1mL/min with a solvent gradient of 1 to 100% of B in A, using 0.05% aqueous TFA as solvent A and MeCN as solvent B, for 30 min, with a 220 nm detection wavelength.

4.9. Statistical Analysis

The results regarding the biofilm formation and preformed biofilms were expressed as mean values \pm standard deviation (mean \pm SD). The statistical significance of differences between controls and experimental groups was evaluated using the Student's t-test. P-values of < 0.05 were considered statistically significant.

Results from peptide stability were expressed as the variation of the % of starting compound over time (mean \pm SD). Data were analyzed in GraphPad Prism 8.0.1 Software using two-way analysis of variance (ANOVA) followed by Tukey's multiple comparison test. Statistical significance was considered when $p < 0.05$.

Author Contributions: Conceptualization, C.T., R.F., P.G. (Paula Gameiro), L.J.B., P.G. (Paula Gomes); Investigation, A.G., P.C., I.F., C.T., L.J.B.; Writing—Original Draft, A.G., L.J.B., I.F., P.G. (Paula Gomes); Writing—Review & Editing, C.T., R.F., P.G. (Paula Gameiro), L.J.B., I.F., P.G. (Paula Gomes); Supervision, R.F., P.G. (Paula Gameiro), C.T., P.G. (Paula Gomes). All authors have read and agreed to the published version of the manuscript.

Funding: This research was funded by FUNDAÇÃO PARA A CIÊNCIA E TECNOLOGIA (FCT, Portugal), through grants UIDB/50006/2020 (to LAQV-REQUIMTE Research Unit), PTDC/NAN-MAT/31781/2017 (ANTINFECT Project Grant), PD/BD/135073/2017 (Doctoral grant to Ana Gomes), and SFRH/BPD/86173/2012 (Research Contract to Iva Fernandes).

References

1. Egorova, K.S.; Ananikov, V.P. Fundamental importance of ionic interactions in the liquid phase: A review of recent studies of ionic liquids in biomedical and pharmaceutical applications. *J. Mol. Liq.* **2018**, *272*, 271–300, doi:10.1016/j.molliq.2018.09.025.
2. Torimoto, T.; Tsuda, T.; Okazaki, K.-I.; Kuwabata, S. New Frontiers in Materials Science Opened by Ionic Liquids. *Adv. Mater.* **2010**, *22*, 1196–1221, doi:10.1002/adma.200902184.
3. Roosen, C.; Müller, P.; Greiner, L. Ionic liquids in biotechnology: Applications and perspectives for biotransformations. *Appl. Microbiol. Biotechnol.* **2008**, *81*, 607–614, doi:10.1007/s00253-008-1730-9.

4. Egorova, K.S.; Gordeev, E.G.; Ananikov, V.P. Biological Activity of Ionic Liquids and Their Application in Pharmaceutics and Medicine. *Chem. Ver.* **2017**, *117*, 7132–7189, doi:10.1021/acs.chemrev.6b00562.
5. Ferraz, R.; Branco, L.C.; Prudêncio, C.; Noronha, J.P.; Petrovski, Z. Ionic liquids as active pharmaceutical 123enzotriazol. *ChemMedChem* **2011**, *6*, 975–985, doi:10.1002/cmdc.201100082.
6. Dias, A.R.; Costa-Rodrigues, J.; Fernandes, M.H.; Ferraz, R.; Prudêncio, C. The Anticancer Potential of Ionic Liquids. *ChemMedChem* **2017**, *12*, 11–18, doi:10.1002/cmdc.201600480.
7. Ferraz, R.; Pinheiro, M.; Gomes, A.; Teixeira, C.; Prudêncio, C.; Reis, S.; Gomes, P. Effects of novel triple- stage antimalarial ionic liquids on lipid membrane models. *Bioorg. Med. Chem. Lett.* **2017**, *27*, 4190–4193, doi:10.1016/j.bmcl.2017.07.006.
8. Pendleton, J.N.; Gilmore, B.F. The antimicrobial potential of ionic liquids: A source of chemical diversity for infection and biofilm control. *Int. J. Antimicrob. Agents* **2015**, *46*, 131–139, doi:10.1016/j.ijantimicag.2015.02.016.
9. Venkata Nancharaiah, Y.; Reddy, G.K.; Lalithamanasa, P.; Venugopalan, V.P. The ionic liquid 1-alkyl-3- methylimidazolium demonstrates comparable antimicrobial and antibiofilm behavior to a cationic surfactant. *Biofouling* **2012**, *28*, 1141–1149, doi:10.1080/08927014.2012.736966.
10. Sidat, Z.; Marimuthu, T.; Kumar, P.; du Toit, L.C.; Kondiah, P.P.D.; Choonara, Y.E.; Pillay, V. Ionic Liquids as Potential and Synergistic Permeation Enhancers for Transdermal Drug Delivery. *Pharmaceutics* **2019**, *11*, 96, doi:10.3390/pharmaceutics11020096.
11. Zakrewsky, M.; Lovejoy, K.S.; Kern, T.L.; Miller, T.E.; Le, V.; Nagy, A.; Goumas, A.M.; Iyer, R.S.; Del Sesto, R.E.; Koppisch, A.T.; et al. Ionic liquids as a class of materials for transdermal delivery and pathogen neutralization. *Proc. Natl. Acad. Sci. USA* **2014**, *111*, 13313–13318, doi:10.1073/pnas.1403995111.
12. Gomes, A.; Bessa, L.J.; Fernandes, I.; Ferraz, R.; Mateus, N.; Gameiro, P.; Teixeira, C.; Gomes, P. Turning a Collagenesis-Inducing Peptide Into a Potent Antibacterial and Antibiofilm Agent Against Multidrug- Resistant Gram-Negative Bacteria. *Front. Microbiol.* **2019**, *10*, doi:10.3389/fmicb.2019.01915.

13. Ahmad Fuaad, A.; Azmi, F.; Skwarczynski, M.; Toth, I. Peptide Conjugation via CuAAC ‘Click’ Chemistry. *Molecules* **2013**, *18*, 13148–13174, doi:10.3390/molecules181113148.
14. Li, H.; Aneja, R.; Chaiken, I. Click chemistry in peptide-based drug design. *Molecules* **2013**, *18*, 9797–9817, doi:10.3390/molecules18089797.
15. Hu, Q.; Deng, Y.; Yuan, Q.; Ling, Y.; Tang, H. Polypeptide ionic liquid: Synthesis, characterization, and application in single-walled carbon nanotube dispersion. *J. Polym. Sci. Part A: Polym. Chem.* **2014**, *52*, 149–153, doi:10.1002/pola.26991.
16. Castro, V.; Rodriguez, H.; Albericio, F. Wang Linker Free of Side Reactions. *Org. Lett.* **2013**, *15*, 246–249, doi:10.1021/ol303367s.
17. Patel J.B.; Cockerill III F.R. CLSI, *Methods for Dilution Antimicrobial Susceptibility Tests for Bacteria That Grow Aerobically—Ninth Edition: Approved Standard M7-A9*; Clinical and Laboratory Standards Institute: Wayne, PA, USA, 2012.
18. Bessa, L.J.; Manickchand, J.R.; Eaton, P.; Leite, J.R.S.A., Brand, G.D.; Gameiro, P. Intrinsic antimicrobial peptide Hs02 hampers the proliferation of single- and dual-species biofilms of *P. aeruginosa* and *S. aureus*: A promising agent for mitigation of biofilm-associated infections. *Int. J. Mol. Sci.* **2019**, *20*, 3604, doi:10.3390/ijms20143604.
19. Overhage, J.; Campisano, A.; Bains, M.; Torfs, E.C.W.; Rhem, B.H.A.; Hancock, R.E.W. Human host defense peptide LL-37 prevents bacterial biofilm formation. *Infect. Immun.* **2008**, 4176–4182, doi:10.1128/IAI.00318-08.
20. Lin, Q.; Deslouches, B.; Montelaro, R.B.; Di, Y.P. Prevention of ESKAPE pathogen biofilm formation by antimicrobial peptides WLBU2 and LL37. *Int. J. Antimicrob. Agents* **2018**, *52*, 667–672, doi:10.1016/j.ijantimicag.2018.04.019.
21. Stepanović, S.; Vuković, D.; Hola, V.; Di Bonaventura, G.; Djukić, S.; Cirković, I.; Ruzicka, F. Quantification of biofilm in microtiter plates: Overview of testing conditions and practical recommendations for assessment of biofilm production by staphylococci. *APMIS* **2007**, *115*, 891–899, doi:10.1111/j.1600-0463.2007.apm_630.x.
22. Costa, F.; Teixeira, C.; Gomes, P.; Martins, M.C.L. Clinical Application of AMPs. *Adv. Exp. Med. Biol.* **2019**, *1117*, 281–298, doi:10.1007/978-981-13-3588-4_15.

23. Grönberg, A.; Zettergren, L.; Agren, M.S. Stability of the cathelicidin peptide LL-37 in a non-healing wound environment. *Acta Derm. Venereol.* **2011**, 91, 511–515, doi:10.2340/00015555-1102.
24. Panzella, L.; Napolitano, A. Natural and Bioinspired Phenolic Compounds as Tyrosinase Inhibitors for the Treatment of Skin Hyperpigmentation: Recent Advances. *Cosmetics* **2019**, 6, 57, doi:10.3390/cosmetics6040057.
25. Süntar, I.; Akkol, E.K.; Senol, F.S.; Keles, H.; Orhan, I.E. Investigating wound healing, tyrosinase inhibitory and antioxidant activities of the ethanol extracts of *Salvia cryptantha* and *Salvia cyanescens* using in vivo and in vitro experimental models. *J. Ethnopharmacol.* **2011**, 135, 71–77, doi:10.1016/j.jep.2011.02.022.
26. Biundo, A.; Braunschmid, V.; Pretzler, M.; Kampatsikas, I.; Darnhofer, B.; Birner-Gruenberger, R.; Rompel, A.; Ribitsch, D.; Guebitz, G.M. Polyphenol oxidases exhibit promiscuous proteolytic activity. *Commun. Chem.* **2020**, 3, 62, doi:10.1038/s42004-020-0305-2.
27. Reihardt, A.; Horn, M.; Schmauck, J.P.; Bröhl, A.; Giernoth, R.; Oelkrug, C.; Neundorf, I. Novel imidazolium salt–peptide conjugates and their antimicrobial activity. *Bioconj. Chem.* **2014**, 25, 2166–2174, doi:10.1021/bc500510c
28. Saraswat, J.; Wani, F.A.; Dar, K.I.; Rizvi, M.M.A.; Patel, R. Noncovalent conjugates of ionic liquid with antibacterial peptide melittin: An eficiente combination against bacterial cells. *ACS Omega* **2020**, 5, 6376– 6388, doi:10.1021/acsomega.9b03777.
29. Frade, R.F.M.; Afonso, C.A.M. Impact of ionic liquids in environment and humans. *Hum. Exp. Toxicol.* **2010**, 29, 1038–1054, doi:10.1177/0960327110371259.
30. Tally, F.P.; DeBruin, M.F., Development of daptomycin for Gram-positive infections. *J. Antimicrob. Chemother.* **2000**, 46, 523–526, doi:10.1093/jac/46.4.523.
31. Ling, L.L.; Schneider, T.; Peoples, A.J.; Spoering, A.L.; Engels, I.; Conlon, B.P.; Mueller, A.; Schäberle, T.F.; Hughes, D.E.; Epstein, S.; et al. A new antibiotic kills pathogens without detectable resistance. *Nature* **2015**, 517, 455, doi:10.1038/nature14098.
32. Zipperer, A.; Konnerth, M.C.; Laux, C.; Berscheid, A.; Janek, D.; Weidenmaier, C.; Burian, M.; Schilling, N.A.; Slavetinsky, C.; Marschal, M.; et al. Human commensals

producing a novel antibiotic impair pathogen colonization. *Nature* **2016**, 535, 511–516, doi:10.1038/nature18634.

33. Matsui, K.; Kan, Y.; Kikuchi, J.; Matsushima, K.; Takemura, M.; Maki, H.; Kozono, I.; Ueda, T.; Minagawa, K. Stalobacin: Discovery of Novel Lipopeptide Antibiotics with Potent Antibacterial Activity against Multidrug-Resistant Bacteria. *J. Med. Chem.* **2020**, 63, 6090–6095 doi:10.1021/acs.jmedchem.0c00295.

34. Behrendt, R.; White, P.; Offer, J., Advances in Fmoc solid-phase peptide synthesis. *J. Pept. Sci.* **2016**, 22, 4–27, doi:10.1002/psc.2836.

35. Loughrey, S.; Mannion, J.; Matlock, B. Using the NanoDrop One to Quantify Protein and Peptide Preparations at 205 nm. Available online: <http://tools.thermofisher.com/content/sfs/brochures/ND-One-Protein-and-Peptide-r16-01-18.pdf> (accessed on 7 August 2020).

36. Bessa, L.J.; Eaton, P.; Dematei, A.; Plácido, A.; Vale, N.; Gomes, P.; Delerue-Matos, C.; Sa Leite, J.R.; Gameiro, P. Synergistic and antibiofilm properties of ocellatin peptides against multidrug-resistant *Pseudomonas aeruginosa*. *Future Microbiol.* **2018**, 13, 151–163, doi:10.2217/fmb-2017-0175.

37. Gomes, N.M.; Bessa, L.J.; Buttachon, S.; Costa, P.M.; Buaruang, J.; Dethoup, T.; Silva, A.M.; Kijjoa, A. Antibacterial and antibiofilm activities of tryptoquivalines and meroditerpenes isolated from the marine-derived fungi *Neosartorya paulistensis*, *N. laciniosa*, *N. tsunodae*, and the soil fungi *N. fischeri* and *N. siamensis*. *Mar. Drugs* **2014**, 12, 822–839, doi:10.3390/md12020822.

2.3. Simple structural changes to widen the antimicrobial action range

Disclosure of a promising lead to tackle complicated skin and skin structure infections: antibacterial, antibiofilm and anti-fungal action of peptide PP4-3.1

Ana Gomes, Lucinda J. Bessa, Iva Fernandes, Ricardo Ferraz, Cláudia Monteiro, Cristina Martins, Nuno Mateus, Paula Gameiro, Cátia Teixeira, Paula Gomes

Submitted to Pharmaceutics

Abstract: Efficient antibiotics are being exhausted, which compromises the treatment of infections, including complicated skin and skin structure infections (cSSTI) often associated to multidrug resistant (MDR) bacteria, being methicillin-resistant *S. aureus* (MRSA) the most prevalent. Anti-microbial peptides (AMP) are being increasingly regarded as the new hope for the post-antibiotic era. Thus, future management of cSSTI may include use of peptides that, on the one hand, behave as AMP and, on the other, are able to promote fast and correct skin rebuilding. As such, we have previously combined an AMP, 3.1, with a collagenesis-inducing peptide, the well-known cosmeceutical pentapeptide-4 (PP4). While the 3.1-PP4 conjugate thus formulated exhibited a potent and selective action against Gram-negative bacteria, including MDR clinical isolates both in planktonic and biofilm forms, its potency was lower against Gram-positive bacteria. Since MRSA and other Gram-positive MDR bacteria represent a major burden in healthcare, we have now focused on an isomeric peptide construct, PP4-3.1, where the same building blocks, 3.1 and PP4, are linked in the reverse order. Hence, herein we investigate the activity of PP4-3.1 and of its N-methyl imidazole derivative, MeIm-PP4-3.1, against Gram-negative bacteria, Gram-positive bacteria, and *Candida* spp. fungi. Additionally, the antibiofilm activity, the toxicity to human keratinocytes, and the activity against *S. aureus* in simulated wound fluid (SWF) were also assessed. Overall, data reveal that PP4-3.1 is as a promising lead for the future development of new topical treatments for severe skin infections.

Keywords: antibacterial; antibiofilm; antifungal; antimicrobial peptides; collagen; multidrug resistance; skin infections; wound-healing

Introduction

The introduction should briefly place the study in a broad context and highlight why Complicated skin and skin structure infections (cSSTI) are often caused by multidrug resistant (MDR) pathogens from the so-called ESKAPE (*Enterococcus faecium*, *Staphylococcus aureus*, *Klebsiella pneumoniae*, *Acinetobacter baumannii*, *Pseudomonas aeruginosa*, and *Enterobacter species*) group, towards which available antibiotics are on the edge of becoming ineffective [1]. For instance, it is fairly common nowadays isolate *P. aeruginosa* and *A. baumannii* that are resistant to carbapenems and third generation cephalosporins, which are last-line antibiotics to fight those bacteria. In last years, worldwide awareness has been triggered on the menace of antimicrobial resistance. It has been estimated that, by 2050, over 10 million deaths will occur due to this appalling problem [2]. Accordingly, the World Health Organization (WHO) published in 2017 a priority list of MDR bacteria for which efficient treatments are urgently needed [3]. In light of this, and within scope of the continuous search for new pathways to fight MDR bacteria, antimicrobial peptides (AMP) have emerged as an attractive alternative for conventional antibiotics [4]. AMP typically display broad-spectrum activity at very low doses, and are unlikely to induce bacterial resistance; also, they can act synergically with conventional antibiotics, reducing the required dose of the latter and therefore also decreasing their side effects and capability to induce pathogen resistance [5]. Regarding cSSTI treatment, most complicated cases may require wound debridement to remove the bacterial biofilms formed, which contribute not only to the severity and chronicity of infection, but also to the delay or even impairment of the healing process [6]. However, debridement often does not suffice to ensure complete eradication of the biofilms, and a complementary antibiotic treatment is needed. As such, after debridement, there is a “window of opportunity” where topically applied antiseptics could take a crucial action to avoid recurrence of the infection [7-9]. In parallel, timely application of adequate topical formulations could further contribute to prepare the wound bed for a fast and correct healing. Such dual – antimicrobial plus healing – action may be achieved by embedding antiseptic agents into suitable scaffolds; in this regard, recent approaches towards the treatment of cSSTI have used matrix scaffolds based on collagen, as these play an important role in several steps of the healing process [10]. For instance, during the inflammation phase, increased concentrations of matrix metalloproteinases (MMPs) in the wound bed cause collagen degradation, which is detrimental for a fast healing. Hence, when collagen is topically applied or its production is induced in the wound site,

it may act as a decoy for the MMPs, therefore shortening the inflammatory phase and accelerating skin rebuilding [11].

Having the above in mind, we have previously reported a set of hybrid constructs where a collagen boosting peptide (CBP), the well-known “pentapeptide-4” (PP4), was covalently linked to an antimicrobial peptide (AMP), 3.1, using different orientations, spacers, and *N*-terminal modifications, aiming at a dual-action peptide with therapeutic potential to tackle cSSTI [12,13]. This study revealed that the peptide 3.1-PP4 has potent and selective activity against Gram-negative bacteria, including MDR clinical isolates both in planktonic and biofilm forms [12]. Besides that, this peptide is easily modified at its *N*-terminus via the copper(I)-catalyzed alkyne-azide cycloaddition (CuAAC) reaction to introduce an imidazolium ionic liquid (IL), affording a new construct, Melm-3.1-PP4, with higher solubility and enzymatic stability towards tyrosinase [13].

Our previous focus on peptide 3.1-PP4 and its Melm-3.1-PP4 derivative was mainly driven by the higher selectivity of these constructs against MDR Gram-negative bacteria, which are the most concerning health threat due to lack of efficient alternatives to antibiotics [14]. However, the fact that methicillin-resistant *S. aureus* (MRSA), a Gram-positive bacterium, is the most prevalent pathogen in cSSTI cannot be disregarded [15]. In view of this, we have now focused our efforts on peptide PP4-3.1, which previously was found to have broader spectrum activity than its reversed order isomer, 3.1-PP4 [12]. Therefore, in this work we explored peptide PP4-3.1, its methyl imidazolium derivative Melm-PP4-3.1, and the noncovalent mixture of both peptide building blocks, PP4 and 3.1 (PP4:3.1 in equimolar proportion), regarding their *in vitro* (i) antibacterial activity against reference and MDR bacterial strains, (ii) antibiofilm activity against MDR clinical isolates of *K. pneumonia* and *S. aureus*, (iii) cytotoxicity against HaCaT cell line, and (iv) activity against *Candida* spp. The activity of the best performer of the set, peptide PP4-3.1, was further assessed against *S. aureus* in simulated wound fluid (SWF). Altogether, data obtained disclose PP4-3.1 as a valuable lead for advancing novel topical formulations to tackle cSSTI.

2. Materials and Methods

2.1. Peptide synthesis

Peptides PP4-3.1, 3.1 and PP4 were assembled by SPPS, using the Fmoc/tBu orthogonal protection scheme [16] Briefly, the solid support, Fmoc-Rink-amide MBHA resin (100-200 mesh, 0.52 mmol/g – NovaBiochem), was first swelled with *N,N*-dimethylformamide (DMF, CARLO ERBA) for 30 min at room temperature (r.t.) and next deprotected (removal of the Fmoc group) by reaction with 20% piperidine (Merck) in DMF for 20 min at r.t. After washing with DMF (3×10 mL) and dichloromethane (DCM, CARLO ERBA) (3×10mL), the C-terminal amino acid residue was incorporated through in situ activation and coupling by adding, to the resin, a mixture of 5 molar equivalents (eq) of the Fmoc-protected amino acid (Fmoc-AA-OH, Bachem), 5 eq of *O*-(130enzotriazole-1-yl)-*N,N,N',N'*-tetramethyluronium hexafluorophosphate (HBTU, NovaBiochem) and 10 eq of *N*-ethyl-*N,N*-diisopropylamine (DIEA, VWR) in DMF, and allowing to react at r.t for 1 h, under stirring. The peptide chain was grown in the $C_t \rightarrow N_t$ direction by means of this succession of deprotection, washing, and coupling steps, until the full sequence was assembled. For the modified peptide Melm-PP4-3.1, once the full sequence of PP4-3.1 was fully assembled, azido acetic acid was coupled similarly to the coupling protocol for Fmoc-AA-OH, i.e., using a mixture containing 5 eq of the azido acetic acid (Sigma-Aldrich), 5 eq of HBTU, and 10 eq of DIEA in DMF, keeping under stirring at r.t. for 1 h. After the washing cycle, the CuAAC “click” reaction was performed on-resin, by adding a solution containing propargyl-Melm (20 mg, 0.1 mmol, 1 eq) previously synthesized as earlier reported by us [13], 10 eq of 2,6-lutidine (116 μ L, Alfa Aesar), 1 eq of sodium L-ascorbate (19.8 mg, Sigma-Aldrich), and 10 eq DIEA (170 μ L) in DMF (3 mL), followed by addition of 1 eq copper(I)-bromide (14.3 mg, Fluka) in 1 mL acetonitrile (I, CARLO ERBA). The reaction was allowed to proceed for 24 h at r.t., after which the resin was washed 5 times with 10 mL of 0.1 M aqueous ethylenediaminetetraacetic acid (EDTA, PanReac AppliChem), DMF (3×10 mL), and DCM (3×10 mL). Once all peptide constructs were fully assembled on the solid support, their full deprotection and release was carried out by acidolysis using a TFA-based cocktail containing 95% TFA (VWR), 2.5% triisopropyl silane (TIS, Alfa Aesar) and 2.5% deionized water. The resulting crude products were purified by preparative RP-HPLC using a Hitachi-Merck LaPrep Sigma system equipped with an LP3104 UV detector and an LP1200 pump, employing an RP-C18 column (250×25 mm, 5 μ m pore size). The gradient elution using 0.05% aqueous TFA as a solvent A and I as solvent B, varied depending on the crude peptide, however all elutions were completed in 60min at a flow-rate of 15 mL/min. The

chromatographically pure peptide fractions were collected, pooled, and freeze-dried, to afford the final products as fluffy white solids. The purity of the final products was confirmed by RP-HPLC analysis, and their MW confirmed by ESI-IT-MS, on a Finnegan Surveyor LCQ DECA XP MAX spectrometer operating with electrospray ionization and ion trap quadrupole detection.

2.2. Solutions for *in vitro* assays

Stock solutions of the test peptide-based compounds were prepared in distilled water at approximately 10 mg/mL for testing *in vitro* antibacterial, antibiofilm and antifungal activity. After the assays, the stock solutions were accurately quantitated using a Thermo Scientific™ NanoDrop™ One microvolume UV-Vis Spectrophotometer, and the MIC values were adjusted accordingly. For the cytotoxicity and activity in SWF assays, peptide solutions were accurately quantitated prior to the assays, using the same NanoDrop™ system. In either case, the 31 quantitation method was chosen, where an extinction coefficient ϵ_{205} of $31 \text{ mL} \cdot \text{mg}^{-1} \cdot \text{cm}^{-1}$ is assumed [17].

2.3. Antibacterial activity

The MIC values of the test products were determined through the broth microdilution method against Gram-negative (*Escherichia coli*, *Pseudomonas aeruginosa*, *Klebsiella pneumoniae*) and Gram-positive (*Staphylococcus aureus*, *Enterococcus faecalis*, *Staphylococcus epidermidis*, *Streptococcus pyogenes*) bacterial reference strains (American Type Culture Collection, ATCC) and against MDR clinical isolates of *K. pneumoniae* (KP010), *S. aureus* (SA007), and *P. aeruginosa* (PA004), whose antimicrobial resistance profile is shown in Table S1 (Supplementary Materials). The medium used for these assays was the cation-adjusted Mueller-Hinton broth (MHB2, Sigma-Aldrich) medium, excepting for *S. pyogenes*, where the medium was supplemented with lysed horse blood at 2.5-5% (Sigma-Aldrich), according to the CLSI guidelines [18]. The MBC values were determined as previously de-scribed [19].

2.4. Antibiofilm activity

2.4.1 Crystal violet assay

Antibiofilm activity was assessed as the ability of the test compounds to inhibit biofilm formation by *S. aureus* (SA007) and *K. pneumoniae* (KP010) MDR clinical isolates. The peptide constructs were tested at concentrations corresponding to their MIC, $\frac{1}{2} \times \text{MIC}$, and $\frac{1}{4} \times \text{MIC}$ in TSB (Liofilchem s.r.l.), using the crystal violet assay, as previously

described [19]. The results are given as absorbance at 595 nm, and representative of two independent experiments performed in triplicate.

2.4.2 Microscopic Visualization of biofilms

Biofilms of SA007 and KP010 MDR clinical isolates were allowed to grow on 35 mm high μ -Dishes with ibidi polymer coverslips (ibidi GmbH), in tryptic soy broth (TSB; Liofilchem s.r.l., Roseto degli Abruzzi, Italy), and in TSBG (TSB + 1% Glucose), respectively. The test peptide constructs (PP4-3.1 and Melm-PP4-3.1) were previously added to each respective medium, at concentrations equal to at MIC, $\frac{1}{2}$ ×MIC and $\frac{1}{4}$ ×MIC. In the control groups, no peptides were added. After 24 h, in the case of SA007 biofilms, or after 48 h in case of KP010I biofilms, at 37°C, were stained using the Live/Dead staining mixture (LIVE/DEAD BacLight Bacterial Viability Kit, Thermo Fisher Scientific, Portugal) as described by Coelho and co-workers [20], and then visualized under a fluorescence microscope Leica DMI6000 FFW (Leica Microsystems, Carnaxide, Portugal)

2.5. Toxicity to human keratinocytes

Immortalized human keratinocytes (HaCaT cell line) were seeded at 4×10^4 cell/mL in Dulbecco's Modified Eagle Medium (DMEM, CLS) supplemented with 10% fetal bovine serum (FBS, Biowest) and 1% of antibiotic/antimycotic solution (100 units/mL of penicillin, 10 mg/mL of streptomycin, and 0.25mg/mL of amphotericin B, Sigma-Aldrich). The 96-well plates were incubated at 37 °C in a 5% CO₂ atmosphere, and the cells allowed growing until confluency was reached. At this point, the test peptides were added to the wells in the 6.3 to 100 μ M concentration range in DMEM with 2% FBS and incubated at 37 °C in a 5% CO₂ atmosphere. After 24 h, cell viability was accessed using the AlamarBlue™ Cell Viability Reagent (Resazurin sodium salt, Sigma-Aldrich). The medium was re-moved, and 20 μ L of the AlamarBlue™ reagent at 0.15 mg/mL were added to 100 μ L of Hank's Balanced Salt Solution (HBSS, Sigma-Aldrich). The plate was incubated over 2 h at 37 °C in a 5% CO₂ atmosphere, after which the fluorescence was read at 560/590 nm in a Flex Station 3 multi-mode microplate reader (Molecular Devices, USA). The IC₅₀ values, indicating the concentration of test peptides causing a 50% growth inhibition, were determined using the GraphPad Prism 9.0 software applying the equation log(inhibitor) versus response with variable slope (four parameters), whose representation is provided in the Supplementary Materials (Figure S9).

2.6. Antifungal activity

The antifungal activity was assessed against three reference strains of *Candida* spp., namely, *C. albicans* ATCC 90028, *C. glabrata* ATCC 90030, and *C. parapsilosis* ATCC 22019. The MIC values were determined through a broth microdilution method in Roswell Park Memorial Institute (RPMI) 1640 medium, supplemented with glucose (G) to a final concentration of 2% (RPMI 2% G), according to the European Committee on Antimicrobial Susceptibility Testing (EUCAST) protocol [21-24].

2.7. Activity in simulated wound fluid

The activity of PP4-3.1 against *S. aureus* (ATCC 29213) in SWF and MHB (Sigma-Aldrich) was determined. To this end, a peptide stock solution was prepared in water at 10 mg/mL, and next diluted in 0.02% aqueous acetic acid containing 0.4% of bovine serum albumin (BSA, Sigma-Aldrich) to a final concentration range from 1280 to 1.25 µg/mL. The SWF was prepared, containing 50% fetal bovine serum (FBS, Gibco) and 50% peptone water (0.9% NaCl in 0.1% aqueous peptone, Sigma-Aldrich). *S. aureus* was incubated at 10⁵ CFU/mL in either SWF or MHB, in the presence of the test peptide within the concentration range 128-0.125 µg/mL. After approximately 18 h of incubation at 37 °C, bacterial growth was monitored and MIC values determined in triplicates, as a result of 3 independent experiments. The MBC values were also accessed by incubating 10 µL of the content of the first three wells where bacterial growth was not observed, in tryptic soy agar (TSA, Sig-ma-Aldrich) at 37 °C for about 24 h [25].

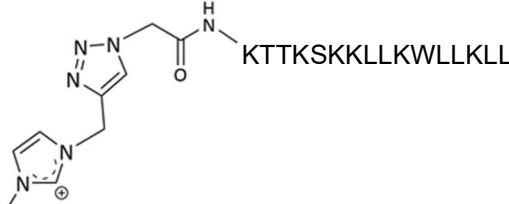
3. Results and Discussion

3.1. Peptide synthesis

Peptides PP4-3.1, PP4 and 3.1 were synthesized through solid phase peptide synthesis (SPPS) as earlier described by us [12]. For the synthesis of Melm-PP4-3.1, the amino acid sequence of peptide PP4-3.1 was first assembled by SPPS, followed by stepwise on-resin *N*-terminal modification through (i) coupling with azido acetic acid to afford the azide-modified peptide, and subsequent (ii) reaction with propargyl-methylimidazole (Pr-Melm) via CuAAC to produce the desired final construct, following the procedure previously reported for Melm-3.1-PP4.[13] After acidolytic cleavage from the resin support using a trifluoroacetic acid (TFA)-based cocktail, all crude peptide constructs were purified by preparative reverse-phase high performance liquid chromatography (RP-HPLC) and the pure fractions collected, pooled, and freeze-dried. The final peptides

(Table 1) were obtained in high purity (>95%), as confirmed by analytical RP-HPLC, and their molecular weights (MW) confirmed by electrospray ionization-ion trap mass spectrometry (ESI-IT MS). Chromatographic and spectral traces are given in the Supplementary Materials (Figures S1 to S8).

Table 1: General data on the peptide constructs synthesized

| Peptide ^a | Sequence ^b / structure | MW / Da |
|----------------------|--|---------|
| PP4-3.1 | KTTKSKKLLKWLKLL | 1940.5 |
| Melm-PP4-3.1 |  | 2144.8 |
| PP4 | KTTKS | 562.7 |
| 3.1 | KKLLKWLKLL | 1394.9 |

^a all peptides were produced as C-terminal amides; ^b amino acids are represented in single letter code as defined by the IUPAC-IUBMB guidelines on nomenclature and symbolism for amino acids and peptides.

3.2. Antibacterial activity

The minimum inhibitory concentration (MIC) values for the peptides PP4-3.1, Melm-PP4-3.1, 3.1, PP4 and noncovalent mixture of the latter two, indicated as PP4:3.1 (1:1), were assessed in cation-adjusted Mueller-Hinton broth (MHB2), following the Clinical and Laboratory Standards Institute (CLSI) protocol against Gram-negative (*Escherichia coli*, *Pseudomonas aeruginosa*, *Klebsiella pneumoniae*) and Gram-positive (*Staphylococcus aureus*, *Enterococcus faecalis*) bacterial reference strains (American Type Culture Collection, ATCC). The best performing peptides, PP4-3.1 and Melm-PP4-3.1, were additionally tested against (i) *Staphylococcus epidermidis*, since this species integrates the commensal skin flora and interferes with biofilm formation by other species like *S. aureus* [26], and (ii) *Streptococcus pyogenes*, as this is a major cause of monomicrobial necrotizing soft tissue infection [27].

Data in Table 2 show that, as expected, peptide PP4 is devoid of antibacterial activity, while 3.1 displays broad spectrum activity as previously reported [12]. The hybrid constructs, PP4-3.1 and Melm-PP4-3.1, exhibit significant activity with MIC values similar to each other against both ATCC bacterial strains and MDR clinical isolates of *P.*

aeruginosa (PA004), *S. aureus* (SA007), and *K. pneumoniae* (KP010). The minimal bactericidal concentration (MBC) values were found to match the MIC values, highlighting the bactericidal action of both peptide constructs. The noncovalent equimolar mixture of PP4 and 3.1 (PP4:3.1) was generally less active than the covalent analogue PP4-3.1, being only slightly more active against *E. faecalis* and less active against *P. aeruginosa* and *K. pneumoniae*. Therefore, the noncovalent mixture PP4:3.1 does not offer any advantage over the covalent construct PP4-3.1 regarding antimicrobial activity.

Table 2: Activity of the peptide constructs against susceptible and MDR Gram-positive and Gram-negative bacteria.

| Bacterial species | Reference strain or MDR isolate | MIC in μM (in $\mu\text{g/mL}$) ^a | | | | |
|-----------------------|---------------------------------|--|--------------|-----------------|-----------------|-----------------|
| | | PP4-3.1 | Melm-PP4.3.1 | PP4 | 3.1 | PP4:3.1 (1:1) |
| <i>E. coli</i> | ATCC 5922 | 1.4 (2.8) | 0.7 (1.5) | >60 | 3.8 | 1.9 |
| <i>P. aeruginosa</i> | ATCC 27853 | 1.4 (2.8) | 1.4 (2.9) | >60 | 3.8 | 7.5 |
| | PA004 | 1.4 (2.8) | 1.4 (2.9) | ND ^b | ND ^b | ND ^b |
| <i>K. pneumoniae</i> | ATCC 13883 | 1.4 (2.8) | 1.4 (2.9) | >60 | 3.8 | 7.5 |
| | KP010 | 2.9 (5.6) | 2.8 (5.9) | ND ^b | ND ^b | ND ^b |
| <i>S. aureus</i> | ATCC 29213 | 2.9 (5.6) | 2.8 (5.9) | >60 | 1.9 | 1.9 |
| | SA007 | 1.4 (2.8) | 1.4 (2.9) | ND ^b | ND ^b | ND ^b |
| <i>E. faecalis</i> | ATCC 29212 | 5.7 (11) | 5.5 (12) | >60 | 3.8 | 1.9 |
| <i>S. epidermidis</i> | ATCC 14990 | 0.8 (1.5) | 0.7 (1.5) | ND ^b | ND ^b | ND ^b |
| <i>S. pyogenes</i> | ATCC 19615 | 2.7 (11) | 5.5 (12) | ND ^b | ND ^b | ND ^b |

^aMBC values were found to match MIC values in all cases; ^bND, not determined.

3.3. Antibiofilm activity

3.3.1 Inhibition of biofilm formation by the crystal violet assay

The ability of the best performing peptides, PP4-3.1 and Melm-PP4-3.1, to inhibit bacterial biofilm formation was assessed against *S. aureus* (SA007) and *K. pneumoniae* (KP010) MDR clinical isolates. The noncovalent equimolar mixture PP4:3.1 was also tested in this regard, but only against the KP010 isolate. To this end, biofilms were formed in the presence of the test peptides at MIC and sub-MIC ($\frac{1}{2}\times\text{MIC}$ and $\frac{1}{4}\times\text{MIC}$) and in absence of peptide (control). Noteworthy, this type of assay is carried out in tryptic soy broth (TSB) [28], in which MIC values may differ from those obtained in the antibacterial activity assay carried out in MHB2 and listed in Table 2. Hence, MIC values referred to in this section are those displayed by the test peptides in TSB, namely, 1.3,

and 1.4 μM against *S. aureus* (SA007) and 5.7, 10.9 and 15 μM against *K. Pneumonia* (KP010) for PP4-3.1, Melm-PP4-3.1 and PP4:3.1 respectively.

The biofilm biomass formed in each case was quantified through the crystal violet assay, being expressed as absorbance at 595 nm (Figure 1). As expected, only minimal biofilm formation could be observed in the presence of the test peptides at their MIC, for both the Gram-positive and the Gram-negative MDR clinical isolates. In the specific case of the SA007 MDR isolate (Figure 1A), both PP4-3.1 and Melm-PP4-3.1 were able to inhibit biofilm formation also at sub-inhibitory concentrations without significant statistical difference between them. The same behavior was observed against KP010 MDR isolate, however the MIC of Melm-PP4-3.1 against this bacterial isolate in TSB (10.9 μM) roughly doubles that of PP4-3.1 (5.7 μM), which means that a much lower concentration of PP4-3.1 is re-quired to exert an antibiofilm action like that of Melm-PP4-3.1.

The equimolar PP4:3.1 mixture had a similar inhibitory profile to that of its covalent counterpart PP4-3.1 on biofilms of KP010 isolate. Still, once again these identical effects are observed for test peptides whose MIC values considerably differ in TSB, i.e., a much lower amount of the covalent analogue PP4-3.1 (5.7 μM), as compared to the noncovalent mixture (15 μM), is needed to inhibit biofilm formation by a similar extent.

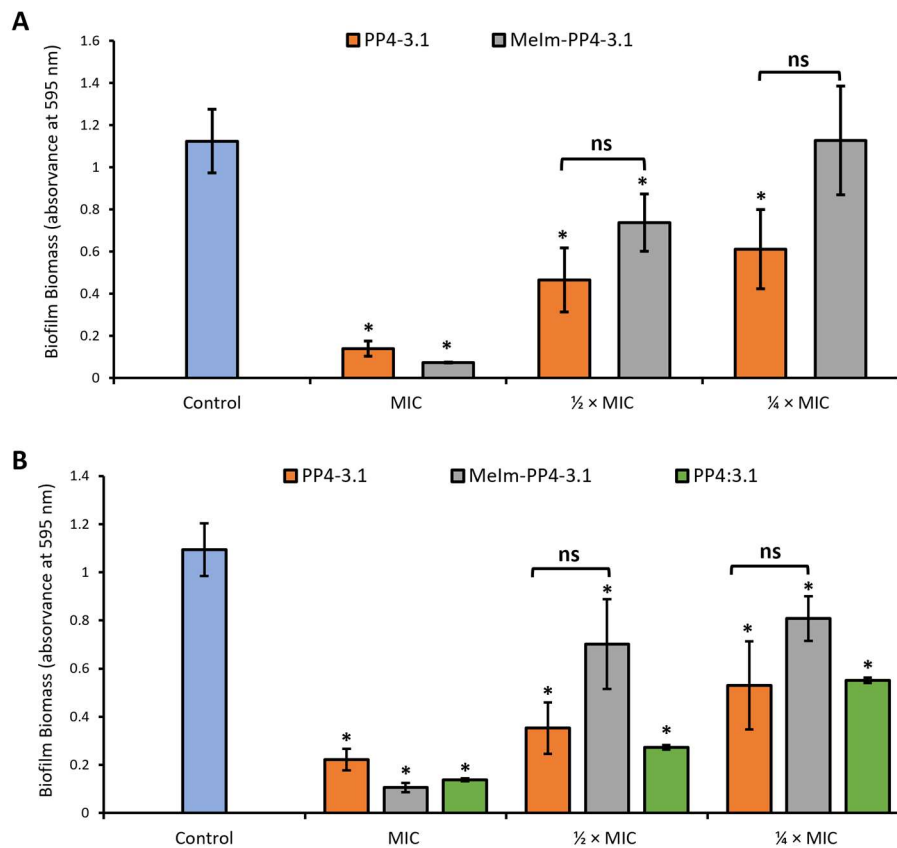


Figure 1: Biofilm biomass formed by MDR clinical isolates of (A) *S. aureus* (SA007) and (B) *K. pneumoniae* (KP010), in the presence of PP4-3.1, Melm-PP4-3.1 and the noncovalent equimolar mixture PP4:3.1. The test peptides were added to culture medium (TSB) at MIC, 1/2xMIC and 1/4xMIC (with reference to MIC values obtained in TSB, see text). Control biofilms were grown in absence of peptide. Data are representative of two independent experiments performed in triplicate; the error bars represent the standard deviation (SD); ns: not significant; Statistically significant differences between biofilms formed in the presence of the peptides and respective control biofilms without peptide ($p < 0.05$) are marked with an asterisk (*).

3.3.2. Inhibition of biofilm formation – microscopic visualization

The impact of PP4-3.1 and Melm-PP4-3.1 on bacterial biofilm development was also assessed through a Live/Dead™ BacLight™ Bacterial Viability staining assay with subsequent observation by fluorescence microscopy. The same clinical isolates, SA007 and KP010, were used, and results are depicted in Figure 2. As expected, almost no bacteria can be observed at the MIC, i.e., biofilm formation is completely impaired. At sub-inhibitory concentrations, live bacteria (green) can be spotted and biofilm formation occurs in different extents, depending on test peptide and bacterial isolate. Hence, it is quite clear that peptide PP4-3.1 (Fig. 2 – (I)A and (II)A) has a much stronger inhibitory effect on biofilm formation for both bacterial isolates, compared to the Melm-PP4-3.1 analogue (Fig. 2 – (I)B and (II)B). These observations agree with data from the crystal

violet assay, while offering string evidence of the superior performance of PP4-3.1, which becomes more obvious when comparing the images obtained at $\frac{1}{2} \times \text{MIC}$.

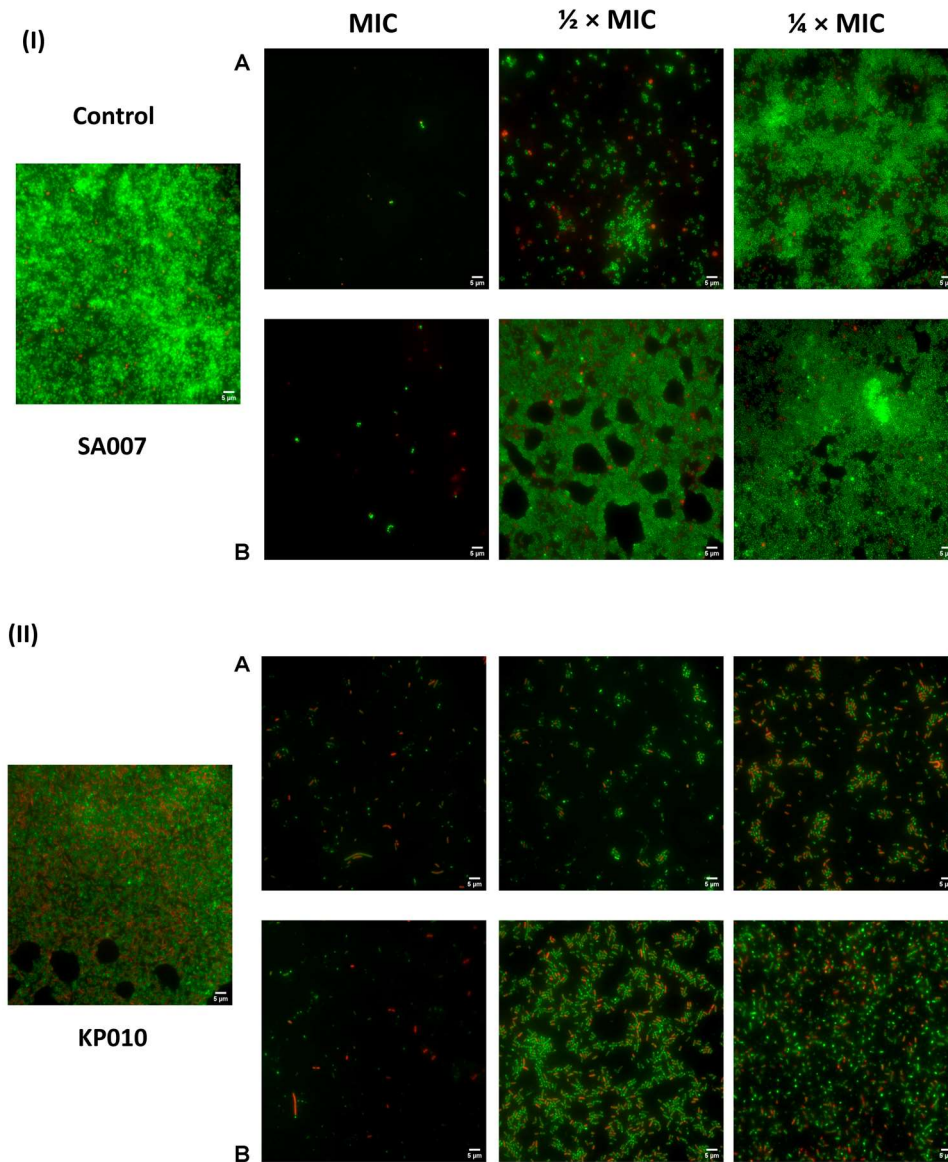


Figure 2: Fluorescence microscopy representative images of biofilms formed by MDR clinical isolates (I) *S. aureus* SA007, and (II) *K. pneumoniae* KP010, in absence (control) or in presence of the test peptides (A) PP4-3.1 and (B) Melm-PP4-3.1, at MIC, $\frac{1}{2} \times \text{MIC}$ and $\frac{1}{4} \times \text{MIC}$. The Live/Dead™ Bac-Light™ Bacterial Viability staining kit was used which stains in green (SYTO 9 fluorescence) live bacteria, and stains in red (propidium iodide) dead or dying bacteria (with a damaged membrane).

3.4. Toxicity to human keratinocytes

The cytotoxicity of the test peptide constructs was assessed using immortalized human keratinocytes (HaCaT cell line), and the AlamarBlue™ assay for quantitation of metabolically active cells. The results are expressed as concentration of peptide causing 50% growth inhibition on the cells tested (IC₅₀). As shown on Table 3, PP4-3.1 and the non-covalent equimolar mixture PP4:3.1 have similar IC₅₀ values, which means that insertion of a covalent link between both building blocks is not disadvantageous regarding cytotoxicity. On the other hand, analogue Melm-PP4-3.1 is almost twice more cytotoxic than its parent hybrid peptide PP4-3.1, hence introduction of the methyl imidazolium moiety is harmful towards the human cell line tested. Relevantly, this assay further revealed that peptide PP4-3.1 is not toxic for HaCaT cells at any of the MIC values obtained for all bacterial strains tested (see Figure S9, Supplementary Materials).

Table 3: Toxicity of test peptide constructs to HaCaT cells, after 24 h of incubation

| Peptide | IC ₅₀ (μM) ^a |
|---------------|------------------------------------|
| PP4-3.1 | 13.0 ± 1.0 |
| Melm-PP4-3.1 | 5.7 ± 1.0 |
| PP4:3.1 (1:1) | 11.7 ± 1.1 |

^a results are expressed as mean ± standard error of the mean (SEM) of two independent experiments (n=8).

3.5. Antifungal activity

It is now well established that most cSSTI have polymicrobial etiology, also involving fungal besides bacterial pathogens. Indeed, despite fungal colonization of non-healing wounds has been often overlooked [29], a high prevalence of fungal communities in chronic wounds has been previously reported, and associated with both healing time, and formation of mixed biofilms with bacteria [30]. Common fungal pathogens in cSSTI include *Cladosporidium* spp. and, mainly, *Candida* spp., with *C. albicans* and *C. parapsilosis* as the most prevalent [31]. In view of this, we have assessed the antifungal efficacy of PP4-3.1, Melm-PP4-3.1, and the noncovalent equimolar mixture of PP4 and 3.1, on *C. albicans* (ATCC 90028), *C. glabrata* (ATCC 90030), and *C. parapsilosis* (ATCC 22019). The MIC values were determined according to the European Committee on Antimicrobial Susceptibility Testing (EUCAST) protocol and are shown on Table 4.

Table 4: Activity of the peptide constructs, respective parent peptides, and reference antifungal drug fluconazole, against ATCC *Candida* spp.

| Peptide | MIC in μM ($\mu\text{g/mL}$) | | |
|---------------|---|-------------------------|-----------------------------|
| | <i>Candida albicans</i> | <i>Candida glabrata</i> | <i>Candida parapsilosis</i> |
| | ATCC 90028 | ATCC 90030 | ATCC 22019 |
| PP4-3.1 | 2.9 (5.6) | 11.5 (22.2) | 1.4 (2.8) |
| Melm-PP4-3.1 | 10.5 (23.4) | 43.7 (93.7) | 2.8 (5.9) |
| PP4 | >60 | >60 | >60 |
| 3.1 | 7.5 | 15 | 3.75 |
| PP4:3.1 (1:1) | 7.5 | 15 | 3.75 |
| Fluconazole | 1.6 (0.5) | 52 (16) | 6.5 (2) |

In line with the previous observations for antibacterial and antibiofilm activity, PP4-3.1 was once again the most potent peptide against all tested fungal strains, being even more active at lower concentrations than the reference antifungal drug, fluconazole, against *C. glabrata* and *C. parapsilosis*. The noncovalent mixture PP4:3.1 showed similar MIC values, yet still higher than those of the covalent hybrid construct. Interestingly, the imidazolium derivative Melm-PP4-3.1, though less potent than the PP4-3.1 peptide, was equally more active than fluconazole. In short, peptide PP4-3.1 further displayed a remarkable anti-fungal profile, with potent activity against all the *Candida* species tested, whose growing prevalence in nosocomial infections is a big concern [32].

3.6. Antibacterial activity in simulated wound fluid

Considering the relevant antibacterial, antibiofilm, and antifungal properties of peptide PP4-3.1, we have further assessed its activity against *S. aureus* (ATCC 29213) in simulated wound fluid (SWF), to check if it remained active in a medium that more closely reflects a real wound. The SWF was prepared as previously reported [33], and *S. aureus* bacteria were allowed to grow in this medium, in the presence of varying concentrations of peptide PP4-3.1. The MIC of PP4-3.1 in Mueller-Hinton broth (MHB) was determined in the same assay, under identical conditions, for an accurate comparison. Results shown in Table 5, indicate an improvement of the antibacterial activity of PP4-3.1 in SWF, with MIC values against *S. aureus* as low as 0.3-0.5 μM . MBC values were identical to (MHB) or only slightly higher than (SWF) MIC values, ascribing a bactericidal action for this hybrid peptide.

Table 5: MIC and MBC values in μM ($\mu\text{g}/\text{mL}$) of PP4-3.1 against *S. aureus* (ATCC 29213) in MHB and SWF^a

| Peptide | MHB | | SWF | |
|---------|---------|---------|-----------------|-------------|
| | MIC | MBC | MIC | MBC |
| PP4-3.1 | 2.1 (4) | 2.1 (4) | 0.3-0.5 (0.5-1) | 1-2.1 (2-4) |

^aresults from three independent experiments performed in triplicates.

4. Conclusion

We have previously reported hybrid peptide 3.1-PP4, encompassing an N-terminal anti-microbial peptide sequence (3.1) directly linked to a well-known collagenesis-boosting peptide (PP4) as the C-terminal segment. This hybrid peptide stood out as a very promising lead for the development of topical agents for efficient management of skin infections, since it combines collagenesis-inducing ability with a potent action against Gram-negative bacteria, including MDR clinical isolates in either planktonic form or when forming biofilm structures. Moved by the clinical relevance of Gram-negative resistant bacteria, and current lack of clinical options to fight them, we have further explored the effect of adding an N-terminal modification (insertion of a methyl imidazolium group via “click” chemistry) to this peptide, which resulted in retained antibacterial activity and improved resistance to tyrosinase-mediated modification. Yet, the 3.1-PP4 construct had an Achilles’ heel, namely, its somewhat modest activity against Gram-positive bacteria, including *S. aureus*, which has great clinical relevance. Most skin and soft tissue infections have a polymicrobial etiology, encompassing not only Gram-negative species, but also Gram-positive bacteria and fungi. Indeed, while MRSA remains as one of the major culprits for the chronicity and severity of cSSTI, involvement of fungal pathogens, especially *Candida* spp., is frequent and directly influences infection progress and wound healing. Having this in mind, and based on our previous findings, we herein explored the antibacterial, antibiofilm, and antifungal properties of the peptide construct PP4-3.1, as well as of its methyl-imidazolium derivative (MeIm-PP4-3.1) and of the noncovalent 1:1 mixture of its peptide building blocks (PP4:3.1). Altogether, results obtained are remarkable, as they allow us to both (i) advance peptide PP4-3.1 as a potent wide-spectrum antimicrobial agent, including against MDR bacterial isolates of both Gram-positive and Gram-negative bacteria, and against *Candida* spp., and (ii) highlight how a simple switch in the order through which both parent peptides, PP4 and 3.1, are linked to each other may act as a “game changer”.

Overall, peptide PP4-3.1 is disclosed as a relevant lead for topical use against cSSTI, which combines an efficient action in vitro against MDR clinical isolates of both Gram-

positive and Gram-negative bacteria, including installation of the respective biofilms, with an antifungal activity that matches or even outperforms that of fluconazole. Considering the polymicrobial nature of cSSTI and the described beneficial effect of adding fluconazole to the standard care of diabetic foot ulcers [34], our report paves the way towards future options in the post-antibiotic era.

Author Contributions: Conceptualization, C.T., R.F., P.G. (Paula Gameiro), C.M. (M. Cristina L. Martins), P.G. (Paula Gomes); Investigation, A.G., L.J.B., I.F., C.M. (Claudia Monteiro); Writing—Original Draft, A.G., L.J.B., I.F., C.M. (Claudia Monteiro); Writing—Review & Editing, C.T., R.F., P.G. (Paula Gameiro), N.M., C.M. (M. Cristina L. Martins), P.G. (Paula Gomes); Supervision, R.F., P.G. (Paula Gameiro), C.T., N.M., C.M. (M. Cristina L. Martins), P.G. (Paula Gomes). All authors have read and agreed to the published version of the manuscript.

Funding: This work received financial support from PT national funds (FCT/MCTES, Fundação para a Ciência e Tecnologia and Ministério da Ciência, Tecnologia e Ensino Superior) through project UIDB/50006/2020.

Acknowledgments: A.G. thanks FCT and the European Social Fund (ESF) for her PhD grant ref. PD/BD/135073/2017, through Programa Operacional Capital Humano (POCH). I.F. would like to thank FCT for her research contract (SFRH/BPD/86173/2012).

References

1. Boucher, H.W.; Talbot, G.H.; Bradley, J.S.; Edwards, J.E.; Gilbert, D.; Rice, L.B.; Scheld, M.; Spellberg, B.; Bartlett, J. Bad bugs, no drugs: No escape! An update from the infectious diseases society of America. *Clin Infect Dis* **2009**, *48*, doi: 10.1086/595011.
2. O'Neill, J.; Resistance, R.o.A.; Trust, W. Tackling drug-resistant infections globally: Final report and recommendations; Review on Antimicrobial Resistance: **2016**; Available online: <https://amr-review.org/Publications.html> (accessed on 21 August 2021)
3. Who publishes list of bacteria for which new antibiotics are urgently needed. Available online: <https://www.who.int/news-room/detail/27-02-2017-who-publishes-list-of-bacteria-for-which-new-antibiotics-are-urgently-needed> (accessed on 10 August 2021)

4. Wang, J.; Dou, X.; Song, J.; Lyu, Y.; Zhu, X.; Xu, L.; Li, W.; Shan, A. Antimicrobial peptides: Promising alternatives in the post feeding antibiotic era. *Med. Res. Rev.* **2019**, *39*, 831-859, doi: <https://doi.org/10.1002/med.21542>.
5. Pfalzgraff, A.; Brandenburg, K.; Weindl, G. Antimicrobial peptides and their therapeutic potential for bacterial skin infections and wounds. *Front. pharmacol.* **2018**, *9*, 281, doi:10.3389/fphar.2018.00281.
6. Omar, A.; Wright, J.B.; Schultz, G.; Burrell, R.; Nadworny, P. Microbial biofilms and chronic wounds. *Microorganisms* **2017**, *5*, doi:10.3390/microorganisms5010009.
7. Alves, P.J.; Barreto, R.T.; Barrois, B.M.; Gryson, L.G.; Meaume, S.; Monstrey, S.J. Update on the role of antiseptics in the management of chronic wounds with critical colonisation and/or biofilm. *Int. Wound J.* **2021**, *18*, 342-358, doi:<https://doi.org/10.1111/iwj.13537>.
8. Wolcott, R.D.; Rumbaugh, K.P.; James, G.; Schultz, G.; Phillips, P.; Yang, Q.; Watters, C.; Stewart, P.S.; Dowd, S.E. Biofilm maturity studies indicate sharp debridement opens a time-dependent therapeutic window. *J. Wound Care* **2010**, *19*, 320-328, doi:10.12968/jowc.2010.19.8.77709.
9. Schultz, G.; Bjarnsholt, T.; James, G.A.; Leaper, D.J.; McBain, A.J.; Malone, M.; Stoodley, P.; Swanson, T.; Tachi, M.; Wolcott, R.D., et al. Consensus guidelines for the identification and treatment of biofilms in chronic nonhealing wounds. *Wound Repair Regen* **2017**, *25*, 744-757, doi:<https://doi.org/10.1111/wrr.12590>.
10. Holmes, C.; Wrobel, J.S.; Maceachern, M.P.; Boles, B.R. Collagen-based wound dressings for the treatment of diabetes-related foot ulcers: A systematic review. *Diabetes Metab. Syndr. Obes.: Targets Ther.* **2013**, *6*, 17-29, doi:10.2147/dms0.s36024.
11. Mathew-Steiner, S.S.; Roy, S.; Sen, C.K. Collagen in wound healing. *Bioeng.* **2021**, *8*, doi:10.3390/bioengineering8050063.
12. Gomes, A.; Bessa, L.J.; Fernandes, I.; Ferraz, R.; Mateus, N.; Gameiro, P.; Teixeira, C.; Gomes, P. Turning a collagenesis-inducing peptide into a potent antibacterial and antibiofilm agent against multidrug-resistant gram-negative bacteria. *Front Microbiol* **2019**, *10*, doi:10.3389/fmicb.2019.01915.
13. Gomes, A.; Bessa, L.J.; Correia, P.; Fernandes, I.; Ferraz, R.; Gameiro, P.; Teixeira, C.; Gomes, P. "Clicking" an ionic liquid to a potent antimicrobial peptide: On the route towards improved stability. *Int. J. Mol. Sci.* **2020**, *21*, doi:<https://doi.org/10.3390/ijms21176174>.
14. Exner, M.; Bhattacharya, S.; Christiansen, B.; Gebel, J.; Goroncy-Bermes, P.; Hartemann, P.; Heeg, P.; Ilschner, C.; Kramer, A.; Larson, E., et al. Antibiotic

- resistance: What is so special about multidrug-resistant gram-negative bacteria? *GMS Hyg Infect Control* **2017**, 12, 1-24, doi:10.3205/dgkh000290.
15. Leong, H.N.; Kurup, A.; Tan, M.Y.; Kwa, A.L.H.; Liao, K.H.; Wilcox, M.H. Management of complicated skin and soft tissue infections with a special focus on the role of newer antibiotics. *Infect Drug Resist* **2018**, 11, 1959-1974, doi:10.2147/IDR.S172366.
 16. Behrendt, R.; White, P.; Offer, J. Advances in fmoc solid-phase peptide synthesis. *J. Pept. Sci.* **2016**, 22, 4-27, doi:10.1002/psc.2836
 17. Loughrey, S.; Mannion, J.; Matlock, B. Using the NanoDrop One to Quantify Protein and Peptide Preparations at 205 nm. Available online: <http://tools.thermofisher.com/content/sfs/brochures/ND-One-Protein-and-Peptide-r16-01-18.pdf> (accessed on 20 August 2021).
 18. Patel J.B.; Cockerill III F.R. CLSI, Methods for Dilution Antimicrobial Susceptibility Tests for Bacteria That Grow Aerobically—Ninth Edition: Approved Standard M7-A9; Clinical and Laboratory Standards Institute: Wayne, PA, USA, 2012.
 19. Bessa, L.J.; Eaton, P.; Dematei, A.; Placido, A.; Vale, N.; Gomes, P.; Delerue-Matos, C.; Sa Leite, J.R.; Gameiro, P. Synergistic and antibiofilm properties of ocellatin peptides against multidrug-resistant pseudomonas aeruginosa. *Future Microbiol.* **2018**, 13, 151-163, doi:10.2217/fmb-2017-0175.
 20. Coelho, P.; Oliveira, J.; Fernandes, I.; Araújo, P.; Pereira, A.R.; Gameiro, P.; Bessa, L.J. Pyranoanthocyanins interfering with the quorum sensing of pseudomonas aeruginosa and staphylococcus aureus. *Int J Mol Sci* **2021**, 22, doi:https://doi.org/10.3390/ijms22168559.
 21. EUCAST. The European committee on antimicrobial susceptibility testing. In Method for susceptibility testing of yeasts, version 7.3.2 2020. Available online: https://www.eucast.org/astoffungi/methodsinantifungalsusceptibilitytesting/susceptibility_testing_of_yeasts/
 22. EUCAST. The European committee on antimicrobial susceptibility testing. Method for the determination of broth dilution minimum inhibitory concentrations of antifungal agents for yeasts version 7.3.2, 2020. Available online: https://www.eucast.org/fileadmin/src/media/PDFs/EUCAST_files/AFST/Files/EUCAST_E_Def_7.3.2_Yeast_testing_definitive_revised_2020.pdf
 23. EUCAST. The european committee on antimicrobial susceptibility testing. In Antifungal MIC method for yeasts, version 10.0, 2020. Available online: <https://www.eucast.org/astoffungi/clinicalbreakpointsforantifungals/>

24. EUCAST. The European committee on antimicrobial susceptibility testing. Breakpoint tables for interpretation of MICs for antifungal agents, version 10.0, 2020, Available online: https://www.eucast.org/fileadmin/src/media/PDFs/EUCAST_files/AFST/Clinical_breakpoints/AFST_BP_v10.0_200204_updated_links_200924.pdf
25. Wiegand, I.; Hilpert, K.; Hancock, R.E.W. Agar and broth dilution methods to determine the minimal inhibitory concentration (mic) of antimicrobial substances. *Nat. Protoc.* **2008**, 3, 163-175, doi:10.1038/nprot.2007.521.
26. Büttner, H.; Mack, D.; Rohde, H. Structural basis of staphylococcus epidermidis biofilm formation: Mechanisms and molecular interactions. *Front Cell Infect Microbiol* **2015**, 5, doi:10.3389/fcimb.2015.00014.
27. Bruun, T.; Kittang, B.R.; de Hoog, B.J.; Aardal, S.; Flaatten, H.K.; Langeland, N.; Mylvaganam, H.; Vindenes, H.A.; Skrede, S. Necrotizing soft tissue infections caused by streptococcus pyogenes and streptococcus dysgalactiae subsp. Equisimilis of groups c and g in western norway *Clin. Microbiol. Infect* **2013**, 19, E545-E550, doi:10.1111/1469-0691.12276.
28. Gomes, N.M.; Bessa, L.J.; Buttachon, S.; Costa, P.M.; Buaruang, J.; Dethoup, T.; Silva, A.M.; Kijjoa, A. Antibacterial and antibiofilm activities of tryptoquivalines and meroditerpenes isolated from the marine-derived fungi neosartorya paulistensis, n. Laciniosa, n. Tsunodae, and the soil fungi n. Fischeri and n. Siamensis. *Mar. Drugs* **2014**, 12, 822-839, doi:10.3390/md12020822.
29. Gunaydin, S.D.; Arikan-Akdagli, S.; Akova, M. Fungal infections of the skin and soft tissue. *Curr. Opin. Infect. Dis.* **2020**, 33, 130-136, doi:10.1097/qco.0000000000000630.
30. Kalan, L.; Loesche, M.; Hodgkinson, B.P.; Heilmann, K.; Ruthel, G.; Gardner, S.E.; Grice, E.A. Redefining the chronic-wound microbiome: Fungal communities are prevalent, dynamic, and associated with delayed healing. *mBio* **2016**, 7, doi:10.1128/mBio.01058-16.
31. Kalan, L.; Grice, E.A. Fungi in the wound microbiome. *Adv. Wound Care* **2018**, 7, 247-255, doi:10.1089/wound.2017.0756.
32. Taei, M.; Chadeganipour, M.; Mohammadi, R. An alarming rise of non-albicans candida species and uncommon yeasts in the clinical samples; a combination of various molecular techniques for identification of etiologic agents. *BMC Res Notes* **2019**, 12, doi:10.1186/s13104-019-4811-1.
33. Price, B.L.; Lovering, A.M.; Bowling, F.L.; Dobson, C.B. Development of a novel collagen wound model to simulate the activity and distribution of antimicrobials in

soft tissue during diabetic foot infection. *Antimicrob Agents Chemother* **2016**, 60, 6880-6889, doi:10.1128/AAC.01064-16 .

34. Chellan, G.; Neethu, K.; Varma, A.K.; Mangalanandan, T.S.; Shashikala, S.; Dinesh, K.R.; Sundaram, K.R.; Varma, N.; Jayakumar, R.V.; Bal, A., et al. Targeted treatment of invasive fungal infections accelerates healing of foot wounds in patients with type 2 diabetes. *Diabet. Med.* **2012**, 29, e255-262, doi:10.1111/j.1464-5491.2012.03574.x.

2.4. Conjugation to IL to confer antimicrobial action on to pentapeptide-4

Boosting cosmeceutical peptides: coupling imidazolium-based ionic liquids to pentapeptide-4 originates new leads with antimicrobial and collagenesis-inducing activities

Ana Gomes, Lucinda J. Bessa, Iva Fernandes, Luísa Aguiar, Ricardo Ferraz, Cláudia Monteiro, M. Cristina L. Martins, Nuno Mateus, Paula Gameiro, Cátia Teixeira, Paula Gomes

Submitted to International Journal of Antimicrobial Agents

ABSTRACT

Following our previous reports on dual-action antibacterial and collagenesis-inducing hybrid peptide constructs based on “pentapeptide-4” (KTTKS), whose N-palmitoyl derivative is the well-known cosmeceutical ingredient Matrixyl®, herein we disclose novel ionic liquid/pentapeptide-4 conjugates (IL-KTTKS). These conjugates present equally potent activity against either antibiotic-susceptible strains or multidrug resistant clinical isolates of both Gram-positive and Gram-negative bacterial species belonging to the so-called “ESKAPE” group of pathogens. Noteworthy, their antibacterial activity is preserved in simulated wound fluid, which anticipate an effective action in the setting of a real wound bed. Moreover, their collagenesis-inducing effects in vitro are comparable or higher to those of Matrixyl®. Altogether, IL-KTTKS were able to exert a triple antibacterial, antifungal, and collagenesis-inducing action in vitro. These findings provide solid grounds for us to advance IL-KTTKS conjugates as promising leads towards future development of topical formulations for complicated skin and soft tissue infections (cSSTI).

Keywords: antibacterial, antifungal, collagenesis-induction, cosmeceutical peptides, ionic liquid, Matrixyl.

INTRODUCTION

The treatment of complicated skin and soft tissue infections (cSSTI) requires debridement or incision and drainage, complemented with antibiotic therapy. The guidelines for cSSTI treatment recommend the administration of systemic antibiotics that are effective against methicillin-resistant *Staphylococcus aureus* (MRSA) strains, which are amongst the multidrug-resistant (MDR) pathogens that prevail in healthcare facilities, followed by an antibiotic therapy program based on the culture assessments for a definitive treatment [1]. However, resistance to the available antibiotics is rapidly increasing and currently widespread to many different species of Gram-positive and Gram-negative bacteria. Equally, fungal infections are also more and more difficult to treat due to the development and spread of antifungal resistance among fungi species.

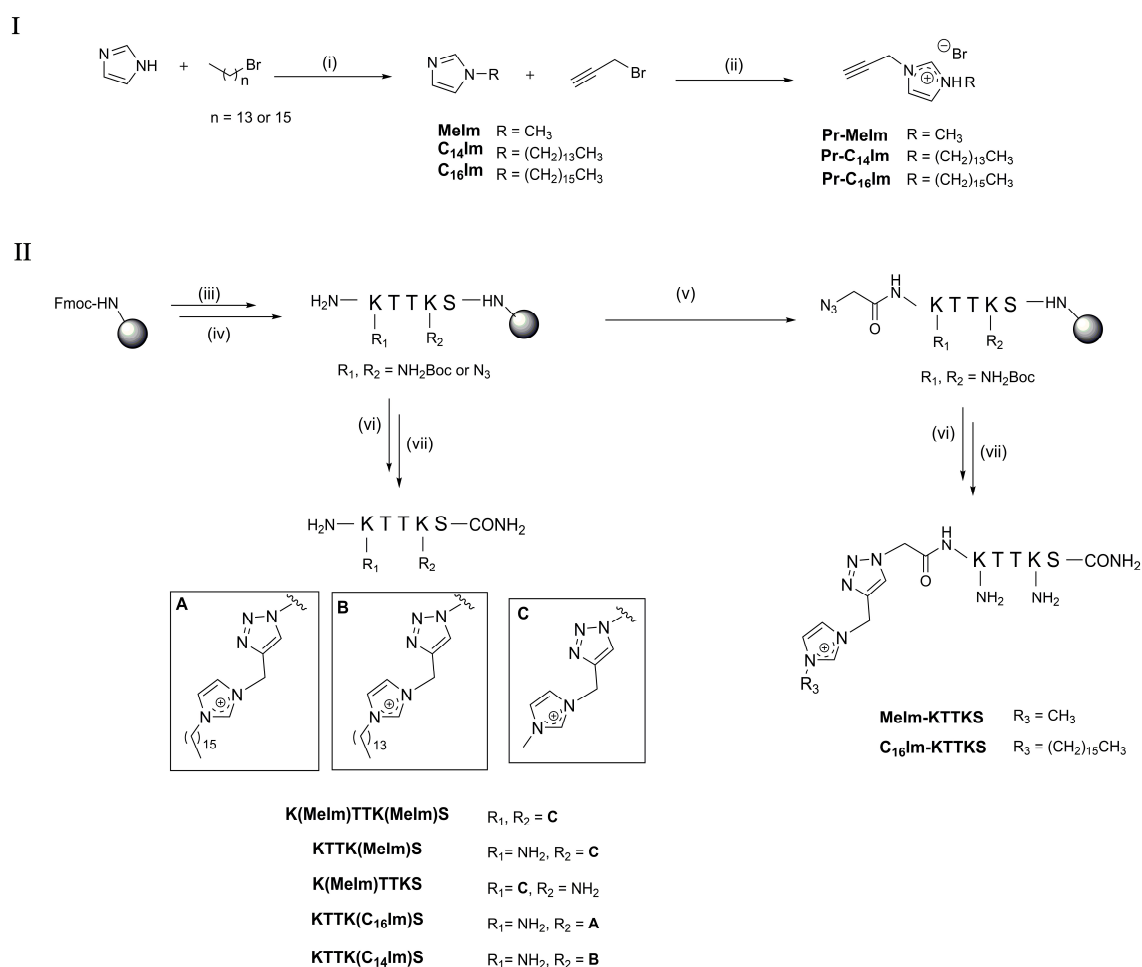
Peptide-based antimicrobials, like the cyclic lipopeptide daptomycin, offer clinicians an alternative to tackle MDR bacteria in hospital settings, however daptomycin is exclusively active against Gram-positive species, including as MRSA [2]. However, most cSSTI are of polymicrobial nature, also involving Gram-negative bacteria and fungi, meaning that new options are urgently needed for the post-antibiotic era [3]. Fungal colonization of non-healing wounds has been traditionally neglected [4], but Kalan *et al.* have highlighted the importance of identifying not only bacterial, but also fungal species involved in cSSTI: these authors analyzed samples from 100 subjects with non-healing DFU by high-throughput sequencing, and found that 80% of them contained fungi. Moreover, they reported that: (i) fungal communities in chronic wounds are predictive of the healing time, and (ii) fungi were prevalent over the bacteria within polymicrobial biofilms [4]. Fungi commonly associated to cSSTI are *Cladosporidium* spp. and *Candida* spp., including *C. albicans* and *C. parapsilosis* [5].

The healing process in cSSTI is often delayed or even impaired not only by the microbial infection itself, including biofilm formation in the wound bed, but also by other comorbidities such as diabetes, renal failure, vascular, neuropathic, and genetic disorders, or even aging [6]. In such cases, effective treatment of cSSTI must both quell infection and promote a fast and correct healing. In this regard, collagen, as a structural protein from the extracellular matrix (ECM), plays an important role in key steps of wound healing and closure, namely, migration, proliferation, remodeling phase, and wound contraction [7]. Since collagen is an endogenous protein, it is regarded as a desirable component for the development of biocompatible and biodegradable wound dressings/biomaterials [8]. Along with collagen itself, collagen-derived/inspired peptides

have been also considered potential promoters of cell migration and proliferation, capable of inducing fibroblasts to produce new collagen, and consequently promoting faster wound healing [9]. For instance, cryptic collagen peptides from the bovine Achilles' tendon were reported to promote faster wound contraction *in vivo*. The biochemical analysis of the wound tissue showed increasing levels of collagen and amino sugar synthesis, reflecting a faster ECM formation, hence corroborating the accelerated healing observed, as well as the higher tensile strength of the healed wound tissue [10]. This and other similar findings motivated the development of the so-called matrikine peptides and derivatives thereof for topical application in the treatment of cSSTI, acting by promoting faster wound closure. Matrikine peptides are small peptide fragments that result from proteolysis of ECM macromolecules like collagen or elastin, with diverse potential biomedical applications, including Cosmetics [11, 12]. For instance, "pentapeptide-4" (with the sequence KTTKS) is a widely studied matrikine that derives from human collagen type I, and is the smallest peptide sequence known to retain a potent ability to stimulate ECM (collagen and fibronectin) production [13, 14]. The *N*-palmitoylated form of KTTKS, known as "palmitoyl pentapeptide-4" or Matrixyl®, is used in the cosmetics industry, due to its ability to cause a skin-rejuvenation/anti-wrinkle effect, probably due to its collagenesis-inducing action [15, 16].

The potential of pentapeptide-4 to promote wound healing in the context of cSSTI has recently attracted our attention. Thus, given that this matrikine peptide is devoid of antimicrobial action, we have developed a chimeric peptide where the KTTKS sequence was conjugated to an antimicrobial peptide (AMP), and which displayed potent (i) antibacterial activity against reference and MDR bacteria from clinical isolates; (ii) antibiofilm action; and (iii) a collagenesis-inducing effect comparable to that of Matrixyl® [17]. Further *N*-terminal modification of the aforementioned chimeric peptide with an imidazolium-based ionic liquid (IL) through a "click" copper(I)-catalyzed alkyne-azide cycloaddition (CuAAC) afforded an equally potent antimicrobial construct [18]. Indeed, IL are becoming quite attractive for biomedical applications given their unique physico-chemical characteristics, low cost, and high structural diversity, enabling the synthesis of a wide panoply of different IL that can be easily tuned to meet specific requirements, including broad spectrum activity against bacteria [19] and fungi [20]. Recently, alkyimidazolium-based IL have been proposed as an alternative antibacterial treatment for cSSTI focusing on Gram-positive pathogens [21]. Several IL or alkyimidazolium derived IL have been found to improve the skin permeation of drugs [22, 23], including Ceftazidime, an antibiotic possessing poor water solubility and low skin permeation [24].

In view of the above, we have now investigated if the coupling of alkyylimidazolium-based IL to the non-antimicrobial KTTKS sequence would afford a new type of peptide-based construct displaying collagenesis-inducing and antimicrobial action, despite not harboring an AMP motif. To this end, three different alkyl imidazole IL were chemically modified to introduce the alkyne moiety required for subsequent coupling, *via* CuAAC, to different azide derivatives of KTTKS (Scheme 1). Seven different IL-KTTKS conjugates were produced, and their antibacterial, antifungal, and collagenesis-inducing properties studied, as herein reported.



Scheme 1. Route to the target IL-KTTKS conjugates. **(I)** Synthesis of the alkyne derivatives of the IL: (i) 1 molar equivalent (eq) of imidazole, 1.5 eq of potassium hydroxide, 1-bromotetradecane or 1-bromohexadecane in dimethyl sulfoxide (DMSO), 70 °C, 5 h; (ii) 1.1 eq of C₁₆Im, C₁₄Im or Melm and 1.0 eq of propargyl bromide (80% in toluene), 40 °C, 24 h. **(II)** Synthesis of the azide derivatives of KTTKS and their coupling to the alkynyl-IL *via* CuAAC: (iii) 5 eq of Fmoc-protected amino acid, 10 eq of *N*-ethyl-*N,N*-diisopropylamine (DIEA) and 5 eq of *O*-(benzotriazol-1-yl)-*N,N,N',N'*-tetramethyluronium hexafluorophosphate (HBTU) in *N,N*-dimethylformamide (DMF), 1 h, room temperature (r.t.); (iv) 20% piperidine in DMF, 15 min, r.t.; (v) 5 eq of azido acetic, 10 eq of DIEA, 5 eq of HBTU, 1 h, r.t.; (vi) 10 eq of DIEA, 10 eq of 2,6-lutidine, 1 eq of copper(I) bromide, 1 eq of sodium *L*-ascorbate and 1 eq of either Pr-Melm, Pr-C₁₆Im, or Pr-C₁₄Im, in DMF:acetonitrile (ACN) (3:1 v/v), 24 h, r.t.; (vii) trifluoroacetic acid (TFA) / triisopropylsilane (TIS) / distilled water (95:25:2.5 v/v/v).

MATERIAL AND METHODS

Chemical Synthesis

1-tetradecylimidazole (C₁₄-Im) and 1-hexadecylimidazole (C₁₆-Im)

Imidazole (0.5 g; 7.3 mmol; 1 eq; Sigma-Aldrich) and potassium hydroxide (0.62 g, 11.0 mmol, 1.5 eq) were added to a round-bottom flask and dissolved in DMSO (12 mL; MERCK). The reaction mixture was left at 70 °C under magnetic stirring for 30 min, after which either 1-bromotetradecane (2.18 mL; 7.3 mmol; 1.0 eq; Sigma-Aldrich) or 1-bromohexadecane (2.26 mL, 7.3 mmol, 1.0 eq; Sigma-Aldrich) was slowly added. The reaction was allowed to proceed under magnetic stirring at 70 °C for 5 h, then the mixture was cooled down to room temperature (r.t.), and water (30 mL) was added. After placing this mixture in an ice bath, a white solid was formed and next filtered, washed with water (3 × 250 mL), and dried under vacuum overnight to afford the final 1-alkylimidazoles in 88% (C₁₄-Im) and 84% (C₁₆-Im) yield. The structures of these final compounds were confirmed by ¹H-NMR and ¹³C-NMR, according with the spectral data below (spectral traces provided in the Supplementary material). The multiplicity of ¹H-NMR signals is given as: s, singlet; d, doublet; t, triplet; m, unresolved multiplet; q, quintuplet.

1-tetradecyl-imidazole Yellow oil (1.71 g, 88%); δ_{H} /ppm (400 MHz, CDCl₃) 7.46 (s, 1H), 7.02 (s, 1H), 6.90 (s, 1H), 3.89 (t, 2H, $J=7.6$ Hz), 1.73 (q, 2H, $J=7.0$ Hz), 1.27-1.22 (m, 22H), 0.85 (t, 3H, $J=6.9$ Hz); δ_{C} /ppm (100 MHz, CDCl₃) 137.1, 129.2, 118.8, 47.2, 32.0, 31.1, 29.7-29.4, 26.6, 22.7, 14.2;

1-hexadecylimidazole White solid (1.81 g, 84%); δ_{H} /ppm (400 MHz, CDCl₃) 7.57 (s, 1H), 7.06 (s, 1H), 6.90 (s, 1H), 3.93 (t, 2H, $J=7.1$ Hz), 3.53 (q, 2H, $J=7.1$ Hz), 1.29-1.24 (m, 26H), 0.87 (t, 3H, $J=6.9$ Hz); δ_{C} /ppm (100 MHz, CDCl₃) 137.0; 128.8; 119.0; 47.4; 32.0; 31.1; 29.8-29.1; 26.6; 22.8; 14.2;

1-methyl-3-(prop-2-enyl)imidazolium bromide (Pr-Melm), 1-tetradecyl-3-(prop-2-enyl)imidazolium bromide (Pr-C₁₄Im) and 1-hexadecyl-3-(prop-2-enyl)imidazolium bromide (Pr-C₁₆Im)

An 80% solution of propargyl bromide in toluene (250 μ L; 2.24 mmol, 1.0 eq; Fluorochem) was slowly added to a round-bottom flask containing 1-methyl-imidazole (Alfa Aesar; 195 μ L, 2.5 mmol, 1.1 eq), 1-tetradecyl-imidazole (0.664 g, 2.5 mmol, 1.1 eq) or 1-hexadecylimidazole (0.723 g, 2.5 mmol, 1.1 eq), and the mixture kept under magnetic stirring at 40 °C for 24 h. After cooling down the yellow oily mixture formed to r.t., dichloromethane (DCM, 4 mL; CARLO ERBA) was added, followed by addition of cold diethyl ether (10 mL; Fisher chemical). The suspension was placed in an ice bath, occurring precipitation of a white solid that was filtered and washed with diethyl ether (10 mL). This solid was re-dissolved and re-precipitated three times upon alternate addition of 5-mL portions of DCM and 10-mL portions of diethyl ether, to afford the final products in 77% (Pr-Melm), 45% (Pr-C₁₄Im) and 97% (Pr-C₁₆Im) yields. The structures of the final alkyimidazolium ILs were confirmed by ¹H-NMR, ¹³C-NMR, and ESI-IT MS, according with the spectral data below (spectral traces provided in the Supplementary material; spectral data (not shown) for Pr-Melm agreed with those previously reported [18]). The multiplicity of ¹H-NMR signals is given as before.

1-tetradecyl-3-(prop-2-enyl)imidazolium bromide White solid (0.3887g, 45.2%); δ_{H} /ppm (400 MHz, CDCl₃) 10.45 (s, 1H), 7.63 (t, 1H, $J=1.6$ Hz), 7.40 (t, 1H, $J=1.6$ Hz), 5.44 (d, 2H, $J=2.6$ Hz), 4.31 (t, 2H, $J=7.5$ Hz), 2.72 (t, 1H, $J=2.6$ Hz), 1.91(q, 2H, $J= 7.4$ Hz), 1.33-1.23 (m, 22H), 0.86 (t, 3H, $J=6.9$ Hz); δ_{C} /ppm (100 MHz, CDCl₃) 137.1; 122.0; 121.9; 77.9; 74.3; 50.6; 40.1; 32.0; 30.3; 29.7-29.4; 26.4; 22.8; 14.2; (EI⁺) m/z calculated for C₂₀H₃₅N₂⁺: 303.28; found: 303.87 [M]⁺; 687.47 [2M+Br]⁺.

1-hexadecyl-3-(prop-2-enyl)imidazolium bromide White solid (0.634 g, 97%); δ_{H} /ppm (400 MHz, CDCl₃) 10.5 (s, 1H), 7.65 (s, 1H), 7.43 (s, 1H), 5.45 (d, 2H, $J=3.0$ Hz), 4.31 (t, 2H, $J=7.5$ Hz), 2.72 (t, 1H, $J=2.4$ Hz), 1.90 (q, 2H, $J=7.1$ Hz), 1.33-1.23 (m, 26H), 0.85 (t, 3H, $J=6.9$ Hz); δ_{C} /ppm (100 MHz, CDCl₃) 137.1, 122.1, 122.0; 77.9, 74.3, 50.6, 40.1, 32.0, 30.3, 29.8-29.4, 29.1, 26.4, 22.8, 14.2; (EI⁺) m/z calculated for C₂₂H₃₉N₂⁺: 331.31, found 331.50 [M]⁺; 743.24 [2M+Br]⁺.

On-resin peptide sequence assembly

All peptide derivatives based on the amino acid sequence of the parent “pentapeptide-4” (KTTKS), and this reference peptide itself, were assembled by standard SPPS procedures using the Fmoc/^tBu orthogonal protection scheme [25]. The Fmoc-Rink-amide MBHA resin (100-200 mesh, 0.52 mmol/g; NovaBiochem) was used as solid support for the assembly of all peptides except for peptide C₁₆-KTTKS-OH that was assembled on a preloaded Fmoc-Ser(^tBu)-Wang resin (100-200 mesh, 0.69 mmol/g; NovaBiochem). In all cases, the commercial Fmoc-protected resin was first swelled in *N,N*-dimethylformamide (DMF; CARLO ERBA) for 30 min and next treated with piperidine (20%; MERCK) in DMF for 20 minutes at r.t., for removal of the Fmoc protecting group. After washing steps using DMF and DCM (3 × 10 mL), coupling of the desired amino acid residue was performed using a mixture of the Fmoc-protected amino acid (5 eq; Bachem), *O*-(benzotriazol-1-yl)-*N,N,N',N'*-tetramethyluronium hexafluorophosphate (HBTU, 5 eq; NovaBiochem), and *N*-ethyl-*N,N*-diisopropylamine (DIEA, 10 eq; VWR) in DMF, which was added to the resin and kept at r.t for 1 h, under stirring. The deprotection and coupling cycles were repeated in the same conditions until the full amino acid sequence was assembled and, whenever desired, the Fmoc-Lys(Boc)-OH (NovaBiochem) standard building block was replaced by its ϵ -azide analogue, Fmoc-Lys(N₃)-OH. For the synthesis of the *N*-terminally modified peptides, namely, 2-azidoethanoyl-KTTKS (N₃-KTTKS) and the reference palmitoyl peptides C₁₆-KTTKS-NH₂ and C₁₆-KTTKS-OH, the same general procedure was adopted, with an additional sequence elongation step using, respectively, 2-azidoacetic (37.5 μ L, 0.5 mmol, 5 eq; Sigma-Aldrich) or palmitic (0.128 mg, 0.5 mmol, 5 eq; Sigma-Aldrich) acids instead of a Fmoc-protected amino acid.

On-resin “click” reaction (CuAAC)

While still anchored to the resin, azide-modified peptides were further reacted with the relevant propargyl-ILs *via* CuAAC. To this end, a solution containing the relevant propargyl-IL [Pr-Melm (20 mg, 0.1 mmol, 1 eq), Pr-C₁₆Im (53 mg, 0.12 mmol, 1.2 eq) or Pr-C₁₄Im (38.3 mg, 0.1 mmol, 1eq)], 2,6 lutidine (116 μ L, 1 mmol, 10 eq; Alfa Aesar), sodium L-ascorbate (19.8 mg, 0.1 mmol, 1 eq; Sigma-Aldrich), and DIEA (170 μ L, 1 mmol, 10 eq; VWR) in DMF (3 mL) was added to the desired azido-peptidyl resin, followed by addition of copper(I)-bromide (14.3 mg, 0.1 mmol, 1 eq; Fluka) in ACN (1 mL; CARLO ERBA). The “click” reaction was allowed to proceed at r.t. under stirring for 24 h. After draining the resin, this was thoroughly washed with 0.1 M aqueous

ethylenediaminetetraacetic acid (EDTA, 5 × 10 mL; PanReac AppliChem) to ensure full removal of copper, followed by DMF (3 × 10 mL) and DCM (3 × 10 mL), to wash out all other unreacted materials and side products.

Cleavage and purification of final peptides and their IL conjugates

Once fully assembled, the peptides were fully deprotected and released from the solid support through a 2h acidolysis using a cleavage cocktail containing 95% of TFA (VWR), 2.5% of triisopropylsilane (TIS; Alfa Aesar), and 2.5% of deionized water. The crude peptide material thus obtained was next purified by RP-HPLC on a Hitachi-Merck LaPrep Sigma system equipped with an LP3104 UV detector and an LP1200 pump, using an RP-C₁₈ column (250 × 25 mm, 5 μm pore size) and an elution gradient using 0.05% aqueous TFA as solvent A and acetonitrile (ACN) as solvent B. The pure peptide fractions were collected, pooled, and freeze-dried to afford the final peptide as a fluffy white solid.

Quantitation of final peptides and their IL conjugates

Peptide stock solutions were prepared at approximately 10 mg/mL in distilled water except for C₁₆-KTTKS-OH that was solubilized in DMSO. Accurate quantitation of the peptide solutions were quantitated by microvolume spectrophotometry at 205 nm, using a Thermo Scientific™ NanoDrop™ One system and quantitation method 31 that assumes an extinction coefficient ϵ_{205} of 31 mL·mg⁻¹·cm⁻¹[26]. Exception was made for the reference peptide C₁₆-KTTKS-OH, which was quantified through amino acid analysis (AAA) due to its poor solubility in water, making it inadequate for NanoDrop™. To this end, the peptide was hydrolyzed using 6 M aqueous hydrochloric acid containing phenol (10% v/v), for 24 h at 110 °C. The hydrolysate was next evaporated to dryness and the residue dissolved in HPLC-grade water (500 μL) containing β-aminobutyric acid as internal standard. The mixture thus obtained was then derivatized by the AccQ-Tag protocol from Waters using 6-aminoquinoyl-*N*-hydroxysuccinimidyl carbamate [27], and the resulting solution analyzed by HPLC (WATERS 600) with the UV-detector (WATERS 2487) set at 254 nm.

***In vitro* assays**

Antibacterial activity in standard conditions

The test conjugates and reference compounds were evaluated for their activity against three reference strains of Gram-negative bacteria, namely, *Escherichia coli* (ATCC 25922), *Pseudomonas aeruginosa* (ATCC 27853), and *Klebsiella pneumoniae* (ATCC 13883), and the four following reference strains of Gram-positive bacteria, *Staphylococcus aureus* (ATCC 29213), *Staphylococcus Epidermidis* (ATCC 14990), *Enterococcus faecalis* (ATCC 29212), and *Streptococcus pyogenes* (ATCC 19615). MIC values were assessed using the broth microdilution method in cation adjusted Muller-Hinton broth (MHB2 - Sigma-Aldrich), except for *S. pyogenes* (a group A β -hemolytic *Streptococcus*), where the medium was previously supplemented with lysed horse blood (Sigma-Aldrich) at 2.5 % according to the CLSI guidelines [28]. MBC values were also determined as previously reported [29]. The two conjugates displaying higher antibacterial activity were further evaluated by determining their MIC against MDR clinical isolates of *K. pneumoniae* (KP010), *P. aeruginosa* (PA004), and *S. aureus* (SA007), whose antibiotic resistance patterns are provided in the Supplementary Table S1.

Antibacterial activity in simulated wound fluid

MIC values of the most active conjugates, C₁₆Im-KTTKS and KTTK(C₁₆Im)S, were also determined in SWF against *S. aureus* (ATCC 29213). Briefly, the conjugates were dissolved in water and diluted in 0.02% aqueous acetic acid containing 0.4% of bovine serum albumin (BSA; Sigma-Aldrich) to final concentrations ranging from 1280 to 1.25 μ g/mL. In parallel, SWF was prepared to a final composition of 50% fetal bovine serum (FBS; Sigma-Aldrich) and 50% peptone water (0.9% NaCl in 0.1% aqueous peptone; Sigma-Aldrich) [30]. *S. aureus* was incubated (10^5 CFU/mL) in either MHB or SWF in the presence of the test conjugates at concentrations between 128 and 0.125 μ g/mL, and bacterial growth assessed after 18 h of incubation at 37 °C. MIC values were determined in triplicates and are a result of three independent experiments. MBC values were also determined by plating 10 μ L of the content of the first three wells where bacterial growth was not observed, followed by incubation in Tryptic Soy Agar (TSA; Sigma-Aldrich) for 24h at 37 °C.

Antifungal activity

The two conjugates with stronger antibacterial action, and relevant parent compounds and their mixture, were also tested for antifungal activity, using three reference strains of *Candida* spp., namely, *C. albicans* ATCC 90028, *C. glabrata* ATCC 90030, and *C. parapsilosis* ATCC 22019. MIC values were determined using a broth microdilution method in RPMI 1640, supplemented with glucose to a final concentration of 2% (RPMI 2% G), according to the EUCAST protocol [31-33].

Toxicity to human cells

Human Immortalized keratinocytes (HaCaT) and human foreskin fibroblasts (HFF-1) were seeded at 4×10^4 cell/mL in 96-well plate using in Dulbecco's Modified Eagle Medium (DMEM; CLS) supplemented with 2% FBS (Biowest) and 1% of antibiotic/antimycotic solution (100 units/mL of penicillin, 10 mg/mL of streptomycin, and 0.25 mg/mL of amphotericin B, Sigma-Aldrich). The plate was incubated at 37 °C in a 5% CO₂ atmosphere, and the cells allowed to grow until confluence was reached. Then, solutions of the test compounds in DMEM supplemented with 2% FBS, in a concentration range between 6.3 and 100 µM, were added to the wells. After 24h of incubation at 37 °C in a 5% CO₂ atmosphere the cell viability was assessed through the resazurin reduction assay. Briefly, the medium was removed and then 20 µL of the AlamarBlue™ Cell Viability Reagent (Resazurin sodium salt, Sigma-Aldrich) at 0.15 mg/mL in 100 µL of Hank's Balanced Salt Solution (HBSS; Sigma-Aldrich) were added to each well; the plate was next incubated for 2 h at 37 °C in a 5% CO₂ atmosphere, after which fluorescence was read at 560/590 nm on a Flex Station 3 multi-mode microplate reader (Molecular Devices) [34]. The IC₅₀ values were thus determined using the GraphPad Prism 9.0 software, by applying the equation *log(inhibitor) versus response* with variable slope (four parameters).

Collagen production in human dermal fibroblasts

The amount of collagen produced by Human Dermal Fibroblasts (HDF) was determined using the SIRCOL™ Kit Assay (Biocolor) according to the manufacturers' instructions [35]. Briefly, the cells were seeded in 6-well plates, using Dulbecco's Modified Eagle Medium (DMEM) supplemented with 10% FBS and 1% antibiotic/antimycotic solution. When confluence was achieved, DMEM supplemented with 2% of FBS and containing the test conjugates at 5 µM was added to the cell cultures, which were then incubated over 48 h at 37 °C in a 5% CO₂ atmosphere. Medium was then removed, and quantitation of the newly formed collagen proceeded as follows:

collagen was solubilized in cold 0.5 M aqueous acetic acid (Fisher chemical) and concentrated overnight with deposition of a transparent pellet; after centrifugation, the supernatant was discarded and the pellet was labeled with the SIRCOL™ dye reagent; after removing the unbound dye with the acid-salt wash reagent, the collagen-bound dye was dissolved with the alkali reagent and absorbance was measured at 555 nm on Flex Station 3 multi-mode microplate reader. The collagen concentration was then determined by interpolation in a standard curve built by using the same quantitation method on standard solutions of rat collagen in 0.5 aqueous acetic acid (Figure S31 in the Supplementary material). Results were expressed as mean \pm standard error of mean (SEM) values for collagen amount (% of control) and the statistical analysis was performed in GraphPad Prism 9.0.0 Software using T student, paired test, P values two-tailed with confidence interval of 95%.

RESULTS AND DISCUSSION

Chemical synthesis

The route towards the target IL-KTTKS conjugates started by the synthesis of the alkyne-modified imidazolium IL (Scheme 1 - I). Briefly, 1-bromohexadecane and 1-bromotetradecane were first reacted with imidazole, following a procedure previously described by Colonna *et al.* (step i, Scheme 1 - II) [36], to afford 1-tetradecyl-imidazole (C₁₄Im) and 1-hexadecylimidazole (C₁₆Im), respectively. After confirming the structures of both C₁₄Im and C₁₆Im by Nuclear Magnetic Resonance (¹H- and ¹³C-NMR) these were reacted with propargyl bromide according to Hu *et al.* (step ii, Scheme 1 - I) [37]. The structures of the three target ILs, propargyl-Melm (Pr-Melm), propargyl-C₁₄Im (Pr-C₁₄Im) and propargyl-C₁₆Im (Pr-C₁₆Im), were confirmed by ¹H-NMR, ¹³C-NMR, and ESI-IT MS (spectral data for Pr-C₁₆Im and Pr-C₁₄Im are supplied in the Supplementary material; spectral data for Pr-Melm agreed with those previously reported [18]).

In parallel, conveniently modified derivatives of the “pentapeptide-4” sequence (KTTKS) were produced by Solid Phase Peptide Synthesis (SPPS), to produce diverse final IL-KTTKS conjugates (Figure 1) that differed in the: (a) propargyl-imidazolium building blocks used, (b) insertion site of the latter (*N*-terminus, side chain of either or of both lysine residues), and (c) length of the spacer between the imidazolium moiety and the peptide’s *N*-terminus. To this end, the pentapeptide-4 sequence was first assembled, according to steps iii and iv in Scheme 1 - II, and conveniently protected lysine (Fmoc-Lys(Boc)-OH) or azido-lysine (Fmoc-Lys(N₃)-OH) building blocks were inserted in the

respective positions of the sequence, according to the desired site for the subsequent introduction of the imidazolium moiety *via* CuAAC. To produce the peptides modified at the *N*-terminus, the sequence bearing two natural Lys residues was assembled and further elongated through coupling of azido acetic (step v, Scheme 1 - II) to afford a 2-carbon (ethyl) spacer between the *N*-terminal lysine and the imidazolium moiety to be incorporated *via* CuAAC. This click reaction was next performed on-resin on all precursor azido-peptides, using the desired propargyl-imidazolium IL (step vi, Scheme 1 - II) and CuAAC conditions previously reported by us [18]. After acidolytic cleavage (step vii, Scheme 1 - II) and purification of the crude conjugates thus obtained by reverse-phase preparative high performance liquid chromatography (RP-HPLC), all the resulting IL-KTTKS conjugates were isolated in high purity (>95%), and their expected molecular weights confirmed by ESI-IT-MS (*c.f.* Supplementary material).

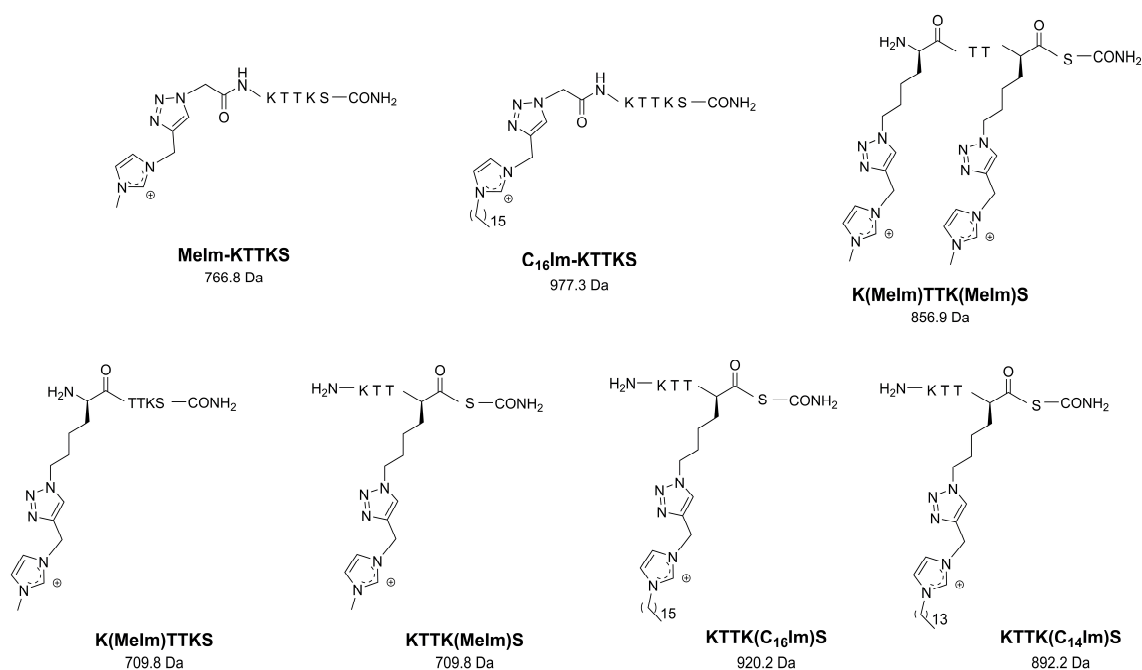


Figure 1: Structure of IL-KTTKS conjugates and corresponding molecular weight (in Da). The amino acids are represented in single letter code as defined by the IUPAC-IUBMB guidelines on nomenclature and symbolism for amino acids and peptides; exception is made to the amino acid residues whose side chain was coupled to ionic liquids *via* click chemistry, in which case the full modified structure is shown.

In addition to the target conjugates, the reference cosmeceutical peptide Matrixyl® (C_{16} -KTTKS-*OH*), its C-terminal carboxamide analogue (C_{16} -KTTKS-*NH*₂), and the native “pentapeptide-4” (KTTKS) were also assembled by SPPS, following procedures recently reported by us [17]. For the palmitoylated peptides, after the full amino acid sequence (KTTKS) was assembled, palmitic acid (C_{16}) was coupled. Then, acidolytic cleavage from the solid support delivered the crude peptides that were purified by RP-HPLC. The final peptides were obtained in high purity and their molecular weights confirmed by ESI-IT MS (*c.f.* Supplementary material).

Antibacterial activity *in vitro*

Against antibiotic-susceptible bacteria

The antimicrobial activity of the IL-KTTKS conjugates was assessed *in vitro* against reference bacterial strains (American Type Culture Collection, ATCC). The minimal inhibitory concentration (MIC) was determined according to the Clinical and Laboratory Standards Institute (CLSI) guidelines [28] against Gram-positive (*S. aureus*, *E. faecalis*) and Gram-negative (*E. coli*, *P. aeruginosa*) bacteria. The MIC values obtained are shown in Table 1. Notably, the reference peptides C_{16} -KTTKS-*NH*₂ and C_{16} -KTTKS-*OH* were respectively soluble in water and dimethyl sulfoxide (DMSO), but both precipitated when diluted in cation-adjusted Mueller-Hinton broth (MHB2), the culture medium recommended by the CLSI guidelines, thus hampering the determination of the MIC values for these reference peptides. Interestingly, all conjugates bearing methyl imidazolium (Melm) units were inactive against the tested bacterial species, even at the highest concentrations used, regardless the number or position of the Melm moieties in the overall structure. In turn, replacing the methyl substituent in the imidazolium ring by either a tetradecyl (C_{14}) or a hexadecyl (C_{16}) group, led to a great improvement in the antibacterial activity, delivering MIC values from 6.45 to 52.6 $\mu\text{g/mL}$, hence adding antimicrobial activity to the parent KTTKS peptide. This observation is in line with previous findings on improving the antimicrobial activity of imidazolium-based ILs by increasing the length of the alkyl substituent on the imidazole ring [38]. Another couple of simple structure-activity relationships (SAR) can be drawn: (i) the peptides KTTK($C_{16}\text{Im}$)S and KTTK($C_{14}\text{Im}$)S are significantly active, but the former is slightly more active than the latter against the tested bacterial species; (ii) when moving the modification from the side chain of a lysine to the peptide’s N-terminus, *i.e.*,

KTTK(C₁₆Im)S *versus* C₁₆Im-KTTKS, MIC values are not significantly altered. Given that this latter couple of peptides showed the strongest antibacterial activities, and reflect two different conjugation positions, both peptides were further investigated by determining their MIC against *S. epidermidis*, *S. pyogenes* (both Gram-positive) and *K. pneumoniae* (Gram-negative), chosen due to their abundance in the skin (*S. epidermidis*) [39], relevance to cSSTI (*S. pyogenes*) [40-42], and relation to the so-called “ESKAPE” pathogens (*K. pneumoniae*) [43]. Moreover, for comparison, MIC values were also determined for the parent building blocks KTTKS and [C₁₆ M1Im][Br], as well as for their noncovalent equimolar mixture, indicated as KTTKS:[C₁₆ M1Im][Br] (1:1), so that the importance of covalent conjugation could be assessed. The results presented in Table 1 show, as expected, that the peptide KTTKS alone is devoid of significant antibacterial activity, and that MIC values for the [C₁₆ M1Im][Br] IL are in agreement with the previously reported [44]. The noncovalent mixture KTTKS:[C₁₆ M1Im][Br] (1:1) presented MIC values similar to those of [C₁₆ M1Im][Br] alone, confirming that the IL building block is the main responsible for the activity observed for the mixture. Interestingly, when comparing the MIC values of the noncovalent mixture KTTKS:[C₁₆ M1Im][Br] (1:1) with those of the covalent conjugates KTTK(C₁₆Im)S and C₁₆Im-KTTKS, it is apparent that covalent conjugation is clearly beneficial for activity against Gram-negative bacteria, but not so much against Gram-positive bacteria. Still, whereas the noncovalent mixture is bacteriostatic for Gram-positive species at MIC values, the covalent conjugates are bactericidal at these concentrations. These results indicate that the antibacterial activity of the covalent conjugates KTTK(C₁₆Im)S and C₁₆Im-KTTKS is not only modulated by the IL building block, but also by its conjugation to the peptide, eventually due to the CuAAC-mediated insertion of the 1,2,3-triazole ring that has been proven as an important antimicrobial pharmacophore [45].

Table 1: MIC values in μM (in $\mu\text{g/mL}$) of the IL-KTTKS conjugates against Gram-negative and Gram-positive bacteria (ATCC reference strains).

| Peptide | MIC in μM (in $\mu\text{g/mL}$) | | | | | | |
|--|---|------------------------------------|--------------------------------|----------------------------------|------------------------------------|-------------------------------------|----------------------------------|
| | <i>E. coli</i> ATCC 25922 | <i>P. aeruginosa</i> ATCC 27853 | <i>S. aureus</i> ATCC 29213 | <i>E. faecalis</i> ATCC 29212 | <i>K. pneumonia</i> ATCC 138830 | <i>S. epidermidis</i> ATCC 14990 | <i>S. pyogenes</i> ATCC 19615 |
| K(Melm)TTKS | | > 1030.1 (731.2) | | | | ND ^a | |
| KTTK(Melm)S | | > 954.2 (677.3) | | | | ND ^a | |
| K(Melm)TTK(Melm)S | | > 1245.5 (1067.4) | | | | ND ^a | |
| KTTK(C ₁₄ Im)S | 29.5 (26.3) | 58.9 (52.6) ^b | 29.5 (26.3) | 58.9 (52.6) ^b | | ND ^a | |
| KTTK(C ₁₆ Im)S | 7.0 (6.45) | 32.5 (29.9) | 14.0 (12.9) | 32.5 (29.9) | 53.8 (49.5) | 5.4 (5.0) | 10.9 (10.0) |
| Melm-KTTKS | | > 825.9 (633.4) | | | | ND ^a | |
| C ₁₆ Im-KTTKS | 14.3 (14.0) | 28.7 (28.0) | 14.3 (14.0) | 28.7 (28.0) | 27.4 (26.8) | 9.5 (9.3) | 18.9 (18.5) |
| KTTKS | | >1820 ^e | | | | ND ^a | |
| [C ₁₆ M1Im][Br] | 60 | >240 | 0.94 ^d | 0.94 ^c | 60 | | ND ^a |
| KTTKS:[C ₁₆ M1Im][Br] (1:1) | 60 | >240 | 0.94 ^d | 0.18 ^c | 60 | | ND ^a |

^a Not Determined; ^b the MBC was 2× the MIC; ^c MBC = 15 μM ; ^d MBC = 30 μM ; in all other cases, the MBC was equal to the MIC; ^e value from ref [17]

Against MDR bacterial clinical isolates

Antibacterial activity of the best couple of conjugates, i.e., C₁₆Im-KTTKS and KTTK(C₁₆Im)S, was further assessed against MDR clinical isolates of *K. pneumoniae* (KP010), *S. aureus* (SA007), and *P. aeruginosa* (PA004). MIC values thus obtained are displayed in Table 2 and show that both conjugates preserve their antibacterial activity close to that observed against susceptible ATCC bacterial strains. This is a relevant finding, considering that the three clinical isolates tested refer to bacterial species belonging to the “ESKAPE” group, which encompasses life-threatening nosocomial pathogens, namely, *Enterococcus faecium*, *Staphylococcus aureus*, *Klebsiella pneumoniae*, *Acinetobacter baumannii*, *Pseudomonas aeruginosa*, and *Enterobacter* spp. The ability of “ESKAPE” pathogens to escape the action of currently available antibiotics is one of the major healthcare threats of our times, especially for Gram-negative bacteria, against which the world is running out of effective options [46].

Table 2: MIC values in μM (in $\mu\text{g}/\text{mL}$) for C₁₆Im-KTTKS and KTTK(C₁₆Im)S against MDR clinical isolates of Gram-positive and Gram-negative bacteria

| MDR | Peptide | |
|-------|--------------------------|---------------------------|
| | C ₁₆ Im-KTTKS | KTTK(C ₁₆ Im)S |
| KP010 | 37.9 (37.0) | |
| PA004 | 18.9 (18.5) | 21.7 (20.0) |
| SA007 | 18.9 (18.5) ^a | |

^a The MBC was 2× the MIC; In all other cases the MBC was equal to the MIC

In simulated wound fluid

The antibacterial activity of the best performing conjugates was also assessed against *S. aureus* (ATCC 29213) in simulated wound fluid (SWF) [30], to check if activity was preserved in this medium. MIC values were obtained in both SWF and MHB media in three independent experiments run in triplicates (Table 3), and indicated that the antibacterial activity in SWF was similar to that in MHB for C₁₆Im-KTTKS, whereas slightly decreased for KTTK(C₁₆Im)S. The real wound fluids contain proteins, growth factors, proteases, among other constituents, depending on if it is a healing or a non-healing wound. In fact, the fluid formed in the open wound generally has wound-healing properties and is beneficial for a fast wound recovery, however in a high amount of certain constituents or in presence of microorganisms, it can delay the healing process [47]. Moreover, the presence of metalloproteinases and other enzymes may rapidly inactivate any peptide-based wound treatments. Therefore, these preliminary observations using SWF, which mimics the wound exudate, are quite relevant as they are indicative that the IL-peptide conjugates, especially C₁₆Im-KTTKS, can be more stable in the

wound environment as compared to analogues where the peptide fragment is not protected at the *N*-terminus [18].

Table 3: MIC [MBC] values in $\mu\text{g/mL}$ for $\text{C}_{16}\text{Im-KTTKS}$ and $\text{KTTK}(\text{C}_{16}\text{Im})\text{S}$ against *S. aureus* (ATCC 29213) in MHB and SWF.

| Peptide | MIC in $\mu\text{g/mL}$ [MBC] | |
|---|-------------------------------|---------------------|
| | MHB | SWF |
| $\text{C}_{16}\text{Im-KTTKS}$ | 16-32 [32-64] | 16-32 [32 - >64] |
| $\text{KTTK}(\text{C}_{16}\text{Im})\text{S}$ | 32 [64-128] | 64-128 [128 - >128] |

Antifungal activity *in vitro*

The antifungal activity of the best couple of IL-KTTKS conjugates, their parent building blocks, and respective noncovalent 1:1 mixture, were all assessed against three species of *Candida*, namely, *Candida albicans* (ATCC 90028), *Candida glabrata* (ATCC 90030), and *Candida parapsilosis* (ATCC 22019). The MIC values were determined according to the European Committee on Antimicrobial Susceptibility Testing (EUCAST) protocol [31-33] and are shown on Table 4. Both conjugates, $\text{KTTK}(\text{C}_{16}\text{Im})\text{S}$ and $\text{C}_{16}\text{Im-KTTKS}$, were equally active against all *Candida* spp., with MIC values ranging from 2.4 to 5.4 μM . Both peptides were slightly more active against *C. parapsilosis* than the other two *Candida* spp.. This is an interesting finding given that *C. parapsilosis* is one of the most common non-*C. albicans* species of *Candida*, which are regarded as important nosocomial pathogens of concern as they were reported to be involved in cases of sepsis [48] and cSSTI [5]. Relevantly, the noncovalent mixture $\text{KTTKS}:[\text{C}_{16}\text{M1Im}][\text{Br}]$ (1:1) showed a potent activity against all *Candida* spp., being equipotent to the parent IL alone, and both more active than the reference antifungal drug fluconazole. Our results reinforce recent findings by Reddy *et al.*, showing that imidazolium ILs with long alkyl chains, e.g. dodecyl and hexadecyl, present a potent activity against *C. albicans* [20].

Table 4. MIC values in μM (in $\mu\text{g/mL}$) for the best performing conjugates, their parent building blocks, and respective 1:1 noncovalent mixture on ATCC *Candida* spp.

| Peptide | MIC in μM (in $\mu\text{g/mL}$) | | |
|--|---|--------------------|------------------------|
| | <i>C. albicans</i> | <i>C. glabrata</i> | <i>C. parapsilosis</i> |
| | ATCC 90028 | ATCC 90030 | ATCC 22019 |
| KTTK(C ₁₆ m)S | 5.4 (5.0) | 5.4 (5.0) | 2.7 (2.5) |
| C ₁₆ Im-KTTKS | 4.7 (4.6) | 4.7 (4.6) | 2.4 (2.3) |
| KTTKS | >60 | >60 | >60 |
| [C ₁₆ M1Im][Br] | 0.93 | 0.93 | 0.93 |
| KTTKS:[C ₁₆ M1Im][Br] (1:1) | 0.93 | 0.93 | 0.93 |
| Fluconazole | 1.6 (0.5) | 26 (8) | 6.5 (2) |

Toxicity to HFF-1 and HaCaT cells

The cytotoxicity of the best IL-KTTKS conjugates, KTTK(C₁₆Im)S and C₁₆Im-KTTKS, was assessed on human foreskin fibroblasts (HFF-1) and human immortalized keratinocytes (HaCaT). The results shown in Table 5, are expressed as the conjugate concentration causing a 50% cell growth inhibition (IC₅₀). The evaluation of the cytotoxicity of the IL-KTTKS conjugates is important on its own, to check for selectivity, but also due to the toxicity effects often associated to IL, depending on, e.g., cation alkyl chain length [49] or specific ions used [50]. As expected from previous reports [51], both the parent “pentapeptide-4” KTTKS and the reference cosmeceutical Matrixyl® (C₁₆-KTTKS-OH) did not show relevant toxicity against the cell lines tested, at up to 100 μM . In turn, the parent IL [C₁₆ M1Im][Br] and its covalent equimolar mixture with the peptide, KTTKS:[C₁₆ M1Im][Br] (1:1), were significantly toxic, in line with previous reports on ILs [19]. Interestingly, covalent conjugation of the peptide to the IL resulted in an intermediate situation, as conjugates were more toxic than the peptide alone, but clearly less toxic than the IL alone or its noncovalent mixture with the peptide. Therefore, covalent conjugation of the IL to the peptide confers on the one hand, antimicrobial activity to an otherwise peptide building block devoid of such activity and, on the other, reduced cytotoxicity to the IL moiety.

Table 5: IC₅₀ values, in μM , obtained for the best performing conjugates, their parent building blocks, and respective noncovalent 1:1 mixture, against HFF-1 and HaCaT cells (after 24 h incubation)

| Peptide | IC ₅₀ \pm SEM (μM) ^a | |
|--|---|------------------|
| | HaCaT | HFF-1 |
| KTTK(C ₁₆ Im)S | 23.05 \pm 1.10 | 12.71 \pm 1.06 |
| C ₁₆ Im-KTTKS | 36.60 \pm 1.09 | 22.46 \pm 1.08 |
| C ₁₆ -KTTKS-OH | >100 | 79.74 \pm 2.82 |
| KTTKS | >100 | ND |
| [C ₁₆ M1Im][Br] | 6.27 \pm 1.02 | ND |
| KTTKS:[C ₁₆ M1Im][Br] (1:1) | 6.46 \pm 1.01 | 8.47 \pm 1.03 |

^a data expressed as mean \pm SEM of 2 independent experiments (n= 8)

Collagen production *in vitro*

The point of conjugating antimicrobial ILs to a collagenesis-inducing peptide was to afford a simple construct able to exert a dual antimicrobial and skin rebuilding action. Therefore, the two best IL-KTTKS conjugates were further tested for their ability to promote collagen production by human dermal fibroblasts (HDF) *in vitro*. This was assessed using the Sircol™ kit assay, whereby the amount of newly formed collagen in the ECM that is deposited in the microwell plated cell cultures is solubilized in an acidic medium and next quantified through a collagen standard curve according with the Sircol™ kit assay procedure [35]. Assays were conducted in different conditions for comparison, namely, in the presence of the reference cosmeceutical Matrixyl® (positive control – C₁₆-KTTKS-OH), of the KTTK(C₁₆Im)S and C₁₆Im-KTTKS conjugates, and in the absence of any peptide (negative control). Data presented in Figure 2 show that both conjugates induce HDF cells to produce more collagen, as compared to the negative control. No significant difference was observed between both conjugates or between KTTK(C₁₆Im)S conjugate and reference Matrixyl, demonstrating that the ability of Matrixyl® to induce collagenesis is not affected by the introduction of the imidazolium IL at the Lys side chain of the peptide sequence. The mechanism behind the collagen inducing effect of Matrixyl® is not well explored, although Jones *et al.* have suggested that the self-assembling properties of the Matrixyl® amphiphilic structure favors recognition of pro-collagen residues, *via* formation of nanotapes that expose relevant peptide epitopes [52]. Irrespective of that, our finding is remarkable, as it clearly demonstrates that the designed conjugates do enclose the potential to be regarded as lead structures for the future development of dual-action formulations to tackle skin disorders where skin rebuilding and antimicrobial action are both required, such as cSSTI.

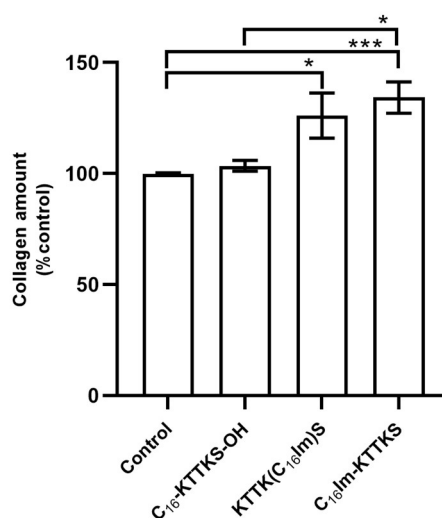


Figure 2: Collagen synthesis by HDF, in presence of C₁₆-KTTKS-OH (Matrixyl®), KTTK(C₁₆Im)S and C₁₆Im-KTTKS at 5 μM, using the Sircol™ Kit. Data are presented as mean±SEM (3 independent experiments in triplicates) expressed in collagen amount (% of control).

CONCLUDING REMARKS

Recently, we have demonstrated that it is possible to produce a dual-action antimicrobial and collagenesis-inducing chimeric peptide [17], by (i) combining the amino acid sequence of an AMP to that of the non-antimicrobial well-known cosmeceutical peptide KTTKS, and (ii) coupling an imidazolium IL to its *N*-terminus *via* the CuAAC “click” approach [18]. Based on these findings, and on the widely reported antimicrobial properties of imidazolium (and other) ILs [21, 53, 54], we hypothesized that it might be possible to preserve the dual antimicrobial and collagenesis-inducing activity by leaving the AMP sequence out and coupling the IL directly to the KTTKS cosmeceutical peptide. The work herein reported provides confirmation for this hypothesis, by advancing a couple of IL-peptide conjugates, C₁₆Im-KTTKS and KTTK(C₁₆Im)S, that possess antibacterial, antifungal, and collagenesis-inducing activity *in vitro*, the latter being actually comparable to that of the cosmeceutical ingredient Matrixyl® based on the KTTKS peptide. Notably, these two conjugates were equally potent against either reference (antibiotic-susceptible ATCC strains) or MDR (clinical isolates) strains of Gram-positive and Gram-negative bacterial species included in the so-called “ESKAPE” group of pathogens that are currently one of the major health treats worldwide [46]. Moreover, the antibacterial activity of the conjugates was preserved in simulated wound fluid, offering a promising indicator on their stability and efficacy in the real wound bed.

The set of IL-peptide conjugates produced further allowed us to advance a couple of SAR on the (i) IL insertion site, as the covalent graft was at either the *N*-terminus or the Lys1/Lys4 side chains of the KTTKS sequence, and (ii) length of the alkyl substituent in the imidazole ring, which was varied between one (methyl or Me spacer), fourteen (tetradecyl or C₁₄ spacer), and sixteen (hexadecyl or C₁₆ spacer) carbons. Hence, it was possible to establish that the antimicrobial activity of the conjugates increases with the length of these alkyl substituents [KTTK(C₁₄Im)S *versus* KTTK(C₁₆Im)S] and is depleted in all conjugates bearing the methyl substituent, regardless of their other structural features. This alkyl chain length effect is in agreement with previous studies on antimicrobial ILs [55]. Further, the site of insertion of the IL does not significantly affect the overall *in vitro* properties of the conjugates [C₁₆Im-KTTKS *versus* KTTK(C₁₆Im)S], although *N*-terminal conjugation seems to better preserve the conjugates' antibacterial action in simulated wound fluid and improves the collagen synthesis by human dermal fibroblasts.

In summary, this is an unprecedented disclosure of IL-cosmeceutical peptide conjugates as a promising start for future development of topical formulations for the treatment of skin disorders like cSSTI.

Acknowledgements / Funding

This work received financial support from PT national funds (Fundação para a Ciência e Tecnologia/Ministério da Ciência, Tecnologia e Ensino Superior - FCT/MCTES) through project UIDB/50006/2020. A.G. thanks FCT and the European Social Fund (ESF) for her PhD grant ref. PD/BD/135073/2017, through Programa Operacional Capital Humano (POCH). Thanks are also due to the Portuguese NMR network (RNRMN), for support to the Laboratory for Structural Elucidation (LAE) of the Materials Centre of the University of Porto (CEMUP). I.F. would like to thank FCT for her research contract (SFRH/BPD/86173/2012).

Author contributions

Conceptualization, C.T., R.F., P.G. (Paula Gameiro), C.M. (M. Cristina L. Martins), P.G. (Paula Gomes); Investigation, A.G., L.J.B., I.F., L.A., C.M. (Cláudia Monteiro); Writing—Original Draft, A.G., L.J.B., I.F., C.M. (Cláudia Monteiro); Writing—Review & Editing, C.T., R.F., P.G. (Paula Gameiro), N.M. (Nuno Mateus), C.M. (M. Cristina L. Martins), P.G. (Paula Gomes); Supervision, R.F., P.G. (Paula Gameiro), C.T., N.M., C.M. (M.

Cristina L. Martins), P.G. (Paula Gomes). All authors have read and agreed to the published version of the manuscript.

References

- [1] Leong HN, Kurup A, Tan MY, Kwa ALH, Liau KH, Wilcox MH. Management of complicated skin and soft tissue infections with a special focus on the role of newer antibiotics. *Infect Drug Resist.* 2018;11:1959-74.
- [2] Golan Y. Current Treatment Options for Acute Skin and Skin-structure Infections. *Clin Infect Dis.* 2019;68:S206-S12.
- [3] Esposito S, Ascione T, Pagliano P. Management of bacterial skin and skin structure infections with polymicrobial etiology. *Expert Rev Anti Infect Ther.* 2019;17:17-25.
- [4] Kalan L, Loesche M, Hodkinson BP, Heilmann K, Ruthel G, Gardner SE, et al. Redefining the Chronic-Wound Microbiome: Fungal Communities Are Prevalent, Dynamic, and Associated with Delayed Healing. *mBio.* 2016;7:1-12.
- [5] Kalan L, Grice EA. Fungi in the Wound Microbiome. *Adv Wound Care.* 2018;7:247-55.
- [6] Beyene RT, Derryberry SL, Jr., Barbul A. The Effect of Comorbidities on Wound Healing. *Surg Clin North Am.* 2020;100:695-705.
- [7] Gonzalez ACdO, Costa TF, Andrade ZdA, Medrado ARAP. Wound healing - A literature review. *An Bras Dermatol.* 2016;91:614-20.
- [8] Chattopadhyay S, Raines RT. Review collagen-based biomaterials for wound healing. *Biopolymers.* 2014;101:821-33.
- [9] Sato K, Asai TT, Jimi S. Collagen-Derived Di-Peptide, Prolylhydroxyproline (Pro-Hyp): A New Low Molecular Weight Growth-Initiating Factor for Specific Fibroblasts Associated With Wound Healing. *Front Cell Dev Biol.* 2020;8.
- [10] Banerjee P, Suguna L, Shanthi C. Wound healing activity of a collagen-derived cryptic peptide. *Amino Acids.* 2015;47:317-28.
- [11] Sivaraman K, Shanthi C. Matrikines for therapeutic and biomedical applications. *Life Sci.* 2018;214:22-33.
- [12] Maquart FX, Bellon G, Pasco S, Monboisse JC. Matrikines in the regulation of extracellular matrix degradation. *Biochimie.* 2005;87:353-60.
- [13] ABU SAMAH NH, HEARD CM. Topically applied KTTKS: a review. *Int J Cosmet Sci.* 2011;33:483-90.
- [14] Katayama K, Armendariz-Borunda J, Raghov R, Kang AH, Seyer JM. A pentapeptide from type I procollagen promotes extracellular matrix production. *J Biol Chem.* 1993;268:9941-4.

- [15] Aldag C, Nogueira Teixeira D, Leventhal PS. Skin rejuvenation using cosmetic products containing growth factors, cytokines, and matrikines: a review of the literature. *Clin Cosmet Investig Dermatol*. 2016;9:411-9.
- [16] Robinson LR, Fitzgerald NC, Doughty DG, Dawes NC, Berge CA, Bissett DL. Topical palmitoyl pentapeptide provides improvement in photoaged human facial skin. *Int J Cosmet Sci*. 2005;27:155-60.
- [17] Gomes A, Bessa LJ, Fernandes I, Ferraz R, Mateus N, Gameiro P, et al. Turning a Collagenesis-Inducing Peptide Into a Potent Antibacterial and Antibiofilm Agent Against Multidrug-Resistant Gram-Negative Bacteria. *Front Microbiol*. 2019;10:1-11.
- [18] Gomes A, Bessa LJ, Correia P, Fernandes I, Ferraz R, Gameiro P, et al. "Clicking" an Ionic Liquid to a Potent Antimicrobial Peptide: On the Route towards Improved Stability. *Int J Mol Sci*. 2020;21:1-11.
- [19] Egorova KS, Gordeev EG, Ananikov VP. Biological Activity of Ionic Liquids and Their Application in Pharmaceuticals and Medicine. *Chem Rev*. 2017;117:7132-89.
- [20] Reddy GKK, Nancharaiah YV. Alkylimidazolium Ionic Liquids as Antifungal Alternatives: Antibiofilm Activity Against *Candida albicans* and Underlying Mechanism of Action. *Front Microbiol*. 2020;11:730-.
- [21] Forero Doria O, Castro R, Gutierrez M, Gonzalez Valenzuela D, Santos L, Ramirez D, et al. Novel Alkylimidazolium Ionic Liquids as an Antibacterial Alternative to Pathogens of the Skin and Soft Tissue Infections. *Molecules*. 2018;23:2354.
- [22] Sidat Z, Marimuthu T, Kumar P, du Toit LC, Kondiah PPD, Choonara YE, et al. Ionic Liquids as Potential and Synergistic Permeation Enhancers for Transdermal Drug Delivery. *Pharmaceutics*. 2019;11:96.
- [23] Zhang D, Wang H-J, Cui X-M, Wang C-X. Evaluations of imidazolium ionic liquids as novel skin permeation enhancers for drug transdermal delivery. *Pharm Dev Technol*. 2016;22:1-10.
- [24] Zakrewsky M, Lovejoy KS, Kern TL, Miller TE, Le V, Nagy A, et al. Ionic liquids as a class of materials for transdermal delivery and pathogen neutralization. *Proc Natl Acad Sci USA*. 2014;111:13313-8.
- [25] Behrendt R, White P, Offer J. Advances in Fmoc solid-phase peptide synthesis. *J Pept Sci*. 2016;22:4-27.
- [26] Loughrey S, Mannion J, Matlock B. Using the NanoDrop One to Quantify Protein and Peptide Preparations at 205 nm. <http://tools.thermofisher.com/content/sfs/brochures/ND-One-Protein-and-Peptide-r16-01-18.pdf>: Thermo Fisher Scientific, Wilmington, DE.

- [27] Corporation W. AccQ-Tag Ultra derivatization Kit <https://www.waters.com/webassets/cms/support/docs/715001331.pdf> 2014.
- [28] CLSI. Methods for dilution antimicrobial susceptibility tests for bacteria that grow aerobically; Approved Standard—Ninth Edition. CLSI document M07-A9. Wayne, PA: Clinical and Laboratory Standards Institute 2012.
- [29] Gomes NM, Bessa LJ, Buttachon S, Costa PM, Buaruang J, Dethoup T, et al. Antibacterial and antibiofilm activities of tryptoquivalines and meroditerpenes isolated from the marine-derived fungi *Neosartorya paulistensis*, *N. laciniosa*, *N. tsunodae*, and the soil fungi *N. fischeri* and *N. siamensis*. *Mar Drugs*. 2014;12:822-39.
- [30] Price BL, Lovering AM, Bowling FL, Dobson CB. Development of a Novel Collagen Wound Model To Simulate the Activity and Distribution of Antimicrobials in Soft Tissue during Diabetic Foot Infection. *Antimicrob Agents Chemother*. 2016;60:6880-9.
- [31] EUCAST. The European Committee on Antimicrobial Susceptibility Testing. Method for susceptibility testing of yeasts, version 732 2020.
- [32] EUCAST. The European Committee on Antimicrobial Susceptibility Testing. Clinical breakpoints for fungi (*Candida* and *Aspergillus* species), version 1002020.
- [33] EUCAST. The European Committee on Antimicrobial Susceptibility Testing. Breakpoint tables for interpretation of MICs for antifungal agents, version 1002020.
- [34] Riss TL, Moravec RA, Niles AL, Duellman S, Benink HA, Worzella TJ, et al. Cell Viability Assays. In: Markossian S, Sittampalam GS, Grossman A, Brimacombe K, Arkin M, Auld D, et al., editors. *Assay Guidance Manual*. Bethesda (MD): Eli Lilly & Company and the National Center for Advancing Translational Sciences; 2004.
- [35] Sircol Collagen Assay Kit. <https://www.biocolor.co.uk/product/sircol-soluble-collagen-assay/>.
- [36] Colonna M, Berti C, Binassi E, Fiorini M, Sullalti S, Acquasanta F, et al. Synthesis and characterization of imidazolium telechelic poly(butylene terephthalate) for antimicrobial applications. *React Funct Polym*. 2012;72:133-41.
- [37] Hu Q, Deng Y, Yuan Q, Ling Y, Tang H. Polypeptide ionic liquid: Synthesis, characterization, and application in single-walled carbon nanotube dispersion. *J Polym Sci Part A: Polym Chem*. 2014;52:149-53.
- [38] Carson L, Chau PKW, Earle MJ, Gilea MA, Gilmore BF, Gorman SP, et al. Antibiofilm activities of 1-alkyl-3-methylimidazolium chloride ionic liquids. *Green Chem*. 2009;11:492-7.
- [39] Büttner H, Mack D, Rohde H. Structural basis of *Staphylococcus epidermidis* biofilm formation: mechanisms and molecular interactions. *Front Cell Infect Microbiol*. 2015;5:1-14.

- [40] Sadeghpour Heravi F, Zakrzewski M, Vickery K, G Armstrong D, Hu H. Bacterial Diversity of Diabetic Foot Ulcers: Current Status and Future Prospectives. *J Clin Med*. 2019;8:1935.
- [41] Walker Mark J, Barnett Timothy C, McArthur Jason D, Cole Jason N, Gillen Christine M, Henningham A, et al. Disease Manifestations and Pathogenic Mechanisms of Group A Streptococcus. *Clin Microbiol Rev*. 2014;27:264-301.
- [42] Pato C, Melo-Cristino J, Ramirez M, Friães A, TPGftSoSI, Vaz T, et al. Streptococcus pyogenes Causing Skin and Soft Tissue Infections Are Enriched in the Recently Emerged emm89 Clade 3 and Are Not Associated With Abrogation of CovRS. *Front Microbiol*. 2018;9.
- [43] Mulani MS, Kamble EE, Kumkar SN, Tawre MS, Pardesi KR. Emerging Strategies to Combat ESKAPE Pathogens in the Era of Antimicrobial Resistance: A Review. *Front Microbiol*. 2019;10:539-.
- [44] Postleb F, Stefanik D, Seifert H, Giernoth R. BIONic Liquids: Imidazolium-based Ionic Liquids with Antimicrobial Activity. *Z Naturforsch B*. 2013;68:1123-8.
- [45] Agalave SG, Maujan SR, Pore VS. Click Chemistry: 1,2,3-Triazoles as Pharmacophores. *Chem Asian J*. 2011;6:2696-718.
- [46] Breijyeh Z, Jubeh B, Karaman R. Resistance of Gram-Negative Bacteria to Current Antibacterial Agents and Approaches to Resolve It. *Molecules*. 2020;25:1340.
- [47] Harding K, Carville k, Chadwick P, Moore Z, Nicodème M, Percival S, et al. WUWHS Consensus Document: Wound Exudate, effective assessment and management. 2019.
- [48] Delaloye J, Calandra T. Invasive candidiasis as a cause of sepsis in the critically ill patient. *Virulence*. 2014;5:161-9.
- [49] Fatemi MH, Izadiyan P. Cytotoxicity estimation of ionic liquids based on their effective structural features. *Chemosphere*. 2011;84:553-63.
- [50] Egorova KS, Seitkalieva MM, Posvyatenko AV, Ananikov VP. An unexpected increase of toxicity of amino acid-containing ionic liquids. *Toxicol Res*. 2015;4:152-9.
- [51] Tałałaj U, Uścińowicz P, Bruzgo I, Surażyński A, Zaręba I, Markowska A. The Effects of a Novel Series of KTTKS Analogues on Cytotoxicity and Proteolytic Activity. *Molecules*. 2019;24:3698.
- [52] Jones RR, Castelletto V, Connon CJ, Hamley IW. Collagen Stimulating Effect of Peptide Amphiphile C-16-KTTKS on Human Fibroblasts. *Mol Pharmaceut*. 2013;10:1063-9.
- [53] Iwai N, Nakayama K, Kitazume T. Antibacterial activities of imidazolium, pyrrolidinium and piperidinium salts. *Bioorg Med Chem Lett*. 2011;21:1728-30.

[54] Pendleton JN, Gilmore BF. The antimicrobial potential of ionic liquids: A source of chemical diversity for infection and biofilm control. *Int J Antimicrob Agents*. 2015;46:131-9.

[55] Postleb F, Stefanik D, Seifert H, Giernoth R. BIONic Liquids: Imidazolium-based Ionic Liquids with Antimicrobial Activity. *Zeitschrift für Naturforschung B*. 2013;68:1123 - 8.

2.5. Conjugation of cosmeceutical tripeptides to IL

Conjugation with imidazole-based ionic liquids as an innovative tool to confer antimicrobial activity to cosmeceutical tripeptides

Ana Gomes, Lucinda J. Bessa, Natália Tassi, Ricardo Ferraz, Paula Gameiro, Cátia Teixeira, Paula Gomes

Manuscript in preparation

ABSTRACT

Our group has been looking for new peptide-based strategies to tackle skin infections by conjugating an antimicrobial with a collagenesis-inducing building block. This approach aims at providing control of bacterial infection in the wound bed, while promoting a fast regeneration via the enhancement of collagen production. Recently, we have shown that the combination of an imidazole-based ionic liquid to a cosmeceutical peptide (KTTKS), widely used in the cosmetics industry in anti-ageing products, yielded a new peptide-based ionic liquid (IL-KTTKS) exhibiting antimicrobial activity with improved collagen production by human dermal fibroblasts. Herein, as a proof-of-concept, we show that the replacement of a palmitoyl group, usually linked to the *N*-terminus of short cosmeceutical peptides (KVK or GHK) devoid of intrinsic antimicrobial activity, by a palmityl-imidazolium ionic liquid originates new peptide constructs with antimicrobial activity against antibiotic-susceptible as well as multidrug-resistant bacteria.

Keywords: antibacterial; cosmeceutical; GHK; ionic liquid; KVK; Matrixyl

INTRODUCTION

Extracellular matrix (ECM) macromolecules are produced intracellularly and play an important role in cells support, migration, and differentiation. The major components of the ECM are structural proteins like collagen, elastin, fibronectin, and laminin. ECM proteins can be degraded through cleavage induced by matrix metalloproteinases (MMP), affording small peptide fragments with significant bioactivity.[1] These bioactive peptides, generally termed matrikines,[2] have been employed in the fabrication of biomaterials and in tissue engineering,[3] and have also caught the attention of the cosmetics industry.[4] In this regard, matrikines have been used in anti-ageing cosmeceutical products, to decrease the wrinkles expression by increasing tensile strength and firmness in the skin, often associated to a collagenesis-boosting action.[5,6] Due the small molecular weight of matrikines, as compared to other products that can also induce collagen production, e.g. human growth factors, cytokines, and soluble ECM proteins, matrikines have an enhanced ability to penetrate the skin. Moreover, a recurrent strategy to improve skin permeation of small peptides is their modification through *N*-terminal palmitoylation, where palmitic acid acts as chemical permeation enhancer.[7]

The first cosmeceutical peptide introduced in cosmetics was the tripeptide GHK, whose complex with copper(II), GHK-Cu has shown ability to: (i) enhance wound healing; (ii) increase collagen synthesis in fibroblasts; (iii) improve overall skin appearance; (iv) protect the skin from UV radiation-induced effects; (v) reduce fine lines and the depth of wrinkles, and therefore improve the structure of aged skin, among other effects.[8] The palmitoylated form of GKH (Pal-GHK) also named as Palmitoyl Tripeptide-1, is broadly used in cosmeceutical products, often mixed with other matrikines.[6] Another relevant cosmeceutical oligopeptide is KVK, also known as Palmitoyl Tripeptide-5. This peptide is commercialized under the brand Syn®-Coll by DMS, and has shown a high anti-wrinkle efficacy likely due to stimulating TGF- β , a growth factor that induces collagen production in fibroblasts.[9] In the dawn of the 21st century, a new successful collagenesis-inducing cosmeceutical peptide, the *N*-palmitoylated derivative of the matrikine pentapeptide 4 (PP4), or Pal-KTTKS, named Matrixyl, was advanced by the team led by Prof. Dr. Karl Lintner, in Sederma.[10] The success of Matrixyl as an anti-ageing cosmeceutical prompted Sederma to produce other peptide-based cosmeceutical products, namely, Matrixyl® 3000, in 2003, and Matrixyl® synthe'6®, in 2012. In other words, currently, the brand name Matrixyl comprises several matrikine-like peptides as active pharmaceutical ingredients (API).[11]

Interestingly, many antimicrobial peptides (AMP) like, e.g., LL-37, display both antimicrobial action and skin regeneration (including wound-healing) ability, which makes them appealing for the development of new treatments for skin and soft tissue infections, by providing both antimicrobial protection to the open wound and regeneration of the skin tissue.[12] Yet, many such peptides are too long to be considered as a cost-effective way to afford dual-action (i.e., antimicrobial and skin rebuilding) peptide-based ingredients for cosmeceutical and biomedical applications. In turn, matrikines and other cosmeceutical short peptides do enclose the potential to act as wound healing/skin rebuilding agents but are devoid of intrinsic antimicrobial activity. In view of this, we have previously tested whether it was possible to confer antimicrobial activity to the matrikine peptide KTTKS, through its conjugation to the synthetic antimicrobial peptide (AMP) 3.1.[13] The excellent results obtained, along with the fact that the whole chimeric peptide construct was longer than desirable for the intended applications, motivated us to further test if the AMP could be replaced by an imidazole-based ionic liquid (IL), as this type of low-cost building block has been reported to possess antimicrobial activity *per se*. [14] This led to recent disclosure of conjugates C₁₆Im-KTTKS and KTTK(C₁₆Im)S (Figure 1) as potent antimicrobial and antifungal agents that further showed an improvement in collagen production by human dermal fibroblasts, as compared to the reference cosmeceutical peptide Matrixyl.[15] Encouraged by these latest findings, we have now tested if the same approach would equally bestow antimicrobial activity upon other well-known short cosmeceutical peptides, namely, GHK and KVK, hence affording proof-of-concept on our innovative approach. The results herein reported for the synthetic IL-peptide conjugate analogues of C₁₆-GHK and C₁₆-KVK (Figure 1) confirm that replacing the palmitoyl group usually linked to the *N*-terminus of short cosmeceutical peptides by a palmityl-imidazolium IL confers otherwise inexistent antimicrobial activity to those peptides [16]. To the best of our knowledge, this is an unprecedented finding that paves the way towards future IL-based strategies to formulate dual-action cosmeceutical peptides able to simultaneously display antimicrobial and skin rebuilding/wound-healing action.

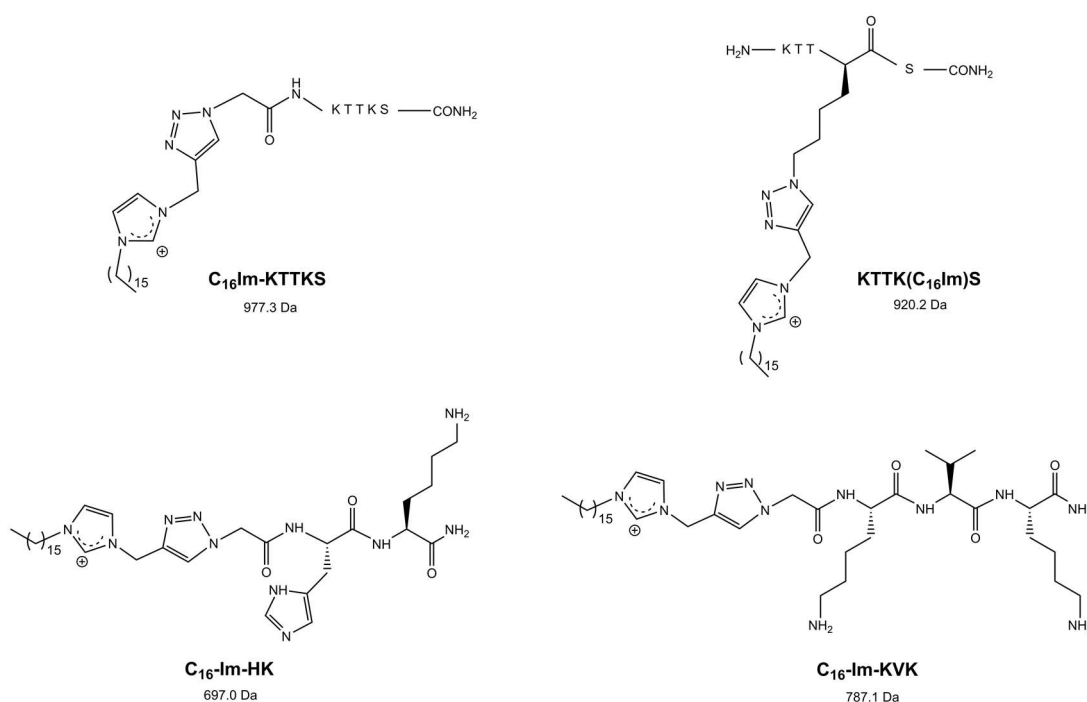


Figure 1: Structures of ionic liquid-peptide (top row) conjugates derived from the cosmeceutical “pentapeptide-4”, as previously communicated, [15] and (bottom row) analogues of tripeptides GHK and KVK, herein reported.

MATERIALS AND METHODS

Peptide synthesis

The peptides were synthesized using the Fmoc/^tBu orthogonal protection scheme.[17] The solid support Fmoc-Rink-amide MBHA resin (100-200 mesh, 0.52 mmol/g - NovaBiochem) was first swell in *N,N*-dimethylformamide (DMF, CARLO ERBA) for 30 min at room temperature (r.t.) followed by the deprotection step using a solution of 20% of piperidine (Merck) in DMF for 20 minutes at r.t.. After the three washing steps using 10mL of DMF and DCM, the amino acid was incorporated through *in situ* activation and coupling by adding, to the resin, a solution containing 5 molar equivalents (eq) of the Fmoc-protected amino acid (Fmoc-AA-OH, Bachem), 5 eq of *O*-(benzotriazol-1-yl)-*N,N,N',N'*-tetramethyluronium hexafluorophosphate (HBTU, NovaBiochem) and 10 eq of *N*-ethyl-*N,N*-diisopropylamine (DIEA, - VWR) in DMF. The reaction was performed for 1h at r.t. under stirring. The peptide chain was grown as a succession of deprotection, washing, and coupling steps until the full sequence are assembled to the resin. After the peptide full sequence are assembled, the peptides were then modified, by the coupling of the azido acetic acid, using a mixture containing 5 eq of the acid, 5 eq of HBTU, and 10 eq of DIEA in DMF, that was kept for 1h at r.t. under stirring. After the washing steps

with DMF (3x10mL) and DCM (3x 10mL), was performed, on-resin, copper(I)-catalyzed azide-alkyne cycloaddition (CuAAC) “click” reaction by adding a solution of propargyl- C_{16} -Im (95.6 mg, 0.2 mmol, 1 eq) previously synthesized as earlier reported by us,[15] 10 eq of 2,6-lutidine (232 μ L, Alfa Aesar), 1 eq of sodium L-ascorbate (39.6 mg, Sigma-Aldrich), and 10 eq DIEA (340 μ L) in DMF (3 mL), followed by addition of 1 eq copper(I)-bromide (28.6 mg, Fluka) in 1 mL acetonitrile (ACN, CARLO ERBA). The reaction was kept under stirring for 24h at r.t. and at the end of the reaction, the solid support was washed with (3 x10 mL) of 0.1 M aqueous ethylenediaminetetraacetic acid (EDTA, PanReac AppliChem), DMF (3 x10mL) and DCM (3X10mL). The new peptide construct was then deprotected and released from the solid support by acidolysis using a cocktail containing 95% trifluoro acetic acid (TFA - PanReac AppliChem), 2.5% triisopropyl silane (TIS, Alfa Aesar) and 2.5% deionized water. The peptide crudes were purified by preparative Reverse Phase High Performance Liquid Chromatography (RP-HPLC) using a Hitachi-Merck LaPrep Sigma system equipped with an LP3104 UV detector and an LP1200 pump and employing an RP-C18 column (250x25 mm, 5 μ m pore size). The pure fractions were then collected, pooled, and freeze-dried, to afford the final peptide white solid. The purity of the final peptides was confirmed by RP-HPLC analysis using a Hitachi-Merck LaChrom Elite system equipped with an L-2130 quaternary pump, an L220 thermostatted automated sampler and an L-2455 diode-array detector (DAD). The samples were injected in a reverse-phase C18 column (125x4.0 mm ID and 5 μ m pore size) with the elution gradient of 1 to 100% of B in A, using 0.05% aqueous TFA as solvent A and ACN as solvent B. The final analysis of both peptides was run for 30 min at the flow rate of 1mL/min and the detection was performed at 220 nm. The molecular weight of the peptides was confirmed by an electrospray ionization – ion trap mass spectrometry (ESI-IT MS) analysis of the final and pure peptides, using an Thermo Finnigan LCQ Deca XP Max LC/MS instrument operating with electrospray ionization and ion-trap (ESI-IT) quadrupole detection.

Peptide quantification

The peptide stock solutions were prepared in distilled water and quantified using a Thermo Scientific™ NanoDrop™ One microvolume UV-Vis Spectrophotometer. The 31 quantitation method chosen, assumed an extinction coefficient ϵ_{205} of 31 mL.mg⁻¹.cm⁻¹ [18].

Antibacterial activity

The minimal inhibitory concentrations (MIC) were assessed against Gram-negative (*Escherichia coli*, *Pseudomonas aeruginosa*, *Klebsiella pneumoniae*) and Gram-positive (*Staphylococcus aureus*, *Enterococcus faecalis*, *Staphylococcus epidermidis*, *Streptococcus pyogenes*) reference strains (American Type Culture Collection, ATCC). Moreover, the MIC of the peptides was also accessed against multi drug resistant (MDR) clinical isolates of *K. pneumonia* (KP010), *S. aureus* (SA007), and *P. aeruginosa* (PA004). The medium used was Mueller-Hinton Broth (MHB2) with the exception for *S. pyogenes* where the medium was supplemented with lysed horse blood at 2.5-5% (Sigma-Aldrich). The procedure following the Clinical and Laboratory Standards Institute (CLSI) protocol [19]. The minimal bactericidal concentration (MBC) was determined as previously reported [20].

Results and discussion

The peptides were synthesized manually using standard protocols in solid peptide phase synthesis (SPPS) through the Fmoc/tBu orthogonal protection scheme [17]. Hence, as previously described by us,[21] after on-resin assembly of the full peptide sequences, these were further modified by stepwise (i) coupling with azido acetic acid to afford the azide-modified peptide, and (ii) coupling with the propargyl-modified IL previously prepared (see Experimental Section), *via* CuAAC. Noteworthy, in the case of the GHK analogue, azido acetic acid was directly coupled to the *N*-terminus of the HK dipeptide (Figure 1), since azido acetic acid can be regarded as the azide analogue of the amino acid glycine. After cleavage from the resin support using a TFA-based cocktail, the crude products were purified by preparative reverse-phase high performance liquid chromatography (RP-HPLC) to a high purity degree (>95%), as checked by analytical RP-HPLC. The molecular weights (MW) of the target constructs, C₁₆-Im-HK and C₁₆-Im-KVK, were confirmed by electrospray ionization-ion trap mass spectrometry (ESI-IT MS). Chromatographic and spectral traces are given in the Supplementary Materials (Figures S1 to S4).

The MIC values of both the IL-peptide conjugates, C₁₆-Im-HK and C₁₆-Im-KVK, were determined *in vitro* against *E. coli* ATCC 25922, *P. aeruginosa* ATCC 27853, *S. aureus* ATCC 25923, *E. faecalis* ATCC 29212, *S. epidermidis* ATCC 14990, *S. pyogenes* ATCC 19615, according to the recommendations of the Clinical and Laboratory Standards Institute (CLSI). MIC values were further obtained for both peptide constructs against

multidrug resistant (MDR) clinical isolates of *K. pneumonia* (KP010), *P. aeruginosa* (PA004), and *S. aureus* (SA007).

The obtained results are shown in table 1, and outline the remarkable broad-spectrum antimicrobial activity that both conjugates possess against all bacterial species tested, including MDR clinical isolates of relevant Gram-negative (*P. aeruginosa*, *K. pneumoniae*) and Gram-positive (*S. aureus*) species that belong to the well-known ESKAPE group of most concerning bacterial pathogens [22].

Table 1: MIC values in µg/mL (µM) obtained for C₁₆-Im-KVK and C₁₆-Im-HK against ATCC reference strains and MDR clinical isolates of Gram-negative and Gram-positive bacteria.

| Bacterial species | Reference strain or MDR isolate | MIC in µg/mL (µM) | |
|-----------------------|---------------------------------|-------------------------|------------------------|
| | | C ₁₆ -Im-KVK | C ₁₆ -Im-HK |
| <i>E. coli</i> | ATCC 25922 | 4 (5.1) | 16 (22.9) |
| <i>P. aeruginosa</i> | ATCC 27853 | 16 ^a (20.3) | 32 (45.8) |
| | PA004 | 16 (20.3) | 32 (45.8) |
| <i>K. pneumoniae</i> | KP010 | 16 (20.3) | 32 (45.8) |
| <i>S. aureus</i> | ATCC 29213 | 8 ^a (10.2) | 16 ^a (22.9) |
| | SA007 | 8 (10.2) | 16 (22.9) |
| <i>E. faecalis</i> | ATCC 29212 | 16 (20.3) | 32 (45.8) |
| <i>S. epidermidis</i> | ATCC 14990 | 2 ^a (2.5) | 8 ^a (11.5) |
| <i>S. pyogenes</i> | ATCC 19615 | 8(10.2) | 16 (22.9) |

^a The MBC was 2x the MIC value; in all other cases the MBC was found to match the MIC value

Moreover, MBC values matched MIC values in most cases, highlighting the bactericidal action of the IL-peptide conjugates. Furthermore, the fact that MIC values remain unchanged between antibiotic-sensitive and MDR strains of a same bacterial species (e.g., *P. aeruginosa* ATCC 27853 vs. PA004 or *S. aureus* ATCC 2921 vs. SA007) show that the conjugates can elude any of the resistance mechanisms developed by the MDR bacteria tested. All these findings gain even higher relevance when considering that, to the best of our knowledge, antimicrobial activity has never been reported for KVK and derivatives, whereas MIC values reported for the native GHK peptide against *S. aureus* (approx. 800 µg/mL, i.e., 2.35mM) and *E. coli* (approx. 100 µg/mL, i.e., 294 µM) are too high to have clinical interest.[16] Globally, C₁₆-Im-KVK was the most potent conjugate showing high potential to exert strong antibacterial action against *E. coli*, *S. aureus*, *S. epidermidis*, and *S. pyogenes*, all of which are frequently involved in skin and soft tissue diseases, particularly *S. aureus* (e.g., atopic dermatitis; chronically infected

wounds)[23,24] and *S. pyogenes* (e.g., impetigo; erysipelas; or rare, but life-threatening necrotizing fasciitis)[25,26], but also *S. epidermidis* that, despite being normally a harmless member of the skin flora, can become pathogenic by, for instance, the disruption of skin barrier [27].

CONCLUDING REMARKS

The results herein presented, together with those already reported for the IL-KTTKS conjugates,[15] establish excellent grounds towards the development of novel peptide-based ionic liquid strategies to tackle complicated skin and soft tissue infections. Further complementary studies are now ongoing, such as: (i) *in vitro* cytotoxicity assays against HaCat and Human dermal fibroblasts, and (ii) assessment of the collagen inducing effect of well know cosmeceutical peptides, C₁₆-GHK and C₁₆-KVK and their new analogues herein reported, in human dermal fibroblasts.

Based on the data collected so far, the approach of conjugating imidazolium-based ILs to cosmeceutical peptides seems to hold great promise as a way to enhance the antimicrobial activity of peptides otherwise devoid of such intrinsic activity, aiming at their topical application in cases of skin infections or as prophylaxis to keep a healthy skin.

ACKNOWLEDGEMENTS / FUNDING

This work received financial support from PT national funds (FCT/MCTES, Fundação para a Ciência e Tecnologia and Ministério da Ciência, Tecnologia e Ensino Superior) through project UIDB/50006/2020. A.G. thanks FCT and the European Social Fund (ESF) for her PhD grant ref. PD/BD/135073/2017, through Programa Operacional Capital Humano (POCH).

CONFLICT OF INTEREST: The authors declare no conflict of interest.

AUTHOR CONTRIBUTIONS

Conceptualization, C.T., R.F., P.G. (Paula Gameiro), P.G. (Paula Gomes); Investigation, A.G., L.J.B., L. A., N. T.; Writing—Original Draft, A.G., L.J.B., L.A.; Writing—Review & Editing, C.T., R.F., P.G. (Paula Gameiro), P.G. (Paula Gomes); Supervision, R.F., P.G. (Paula Gameiro), C.T., P.G. (Paula Gomes). All authors have read and agreed to the published version of the manuscript.

REFERENCES

1. Wells, J.M.; Gaggar, A.; Blalock, J.E. MMP generated matrikines. *Matrix Biol* **2015**, *44-46*, 122-129, doi:10.1016/j.matbio.2015.01.016.
2. Maquart, F.X.; Bellon, G.; Pasco, S.; Monboisse, J.C. Matrikines in the regulation of extracellular matrix degradation. *Biochimie* **2005**, *87*, 353-360, doi:<https://doi.org/10.1016/j.biochi.2004.10.006>.
3. Sivaraman, K.; Shanthi, C. Matrikines for therapeutic and biomedical applications. *Life Sci.* **2018**, *214*, 22-33, doi:<https://doi.org/10.1016/j.lfs.2018.10.056>.
4. Aguilar-Toalá, J.E.; Hernández-Mendoza, A.; González-Córdova, A.F.; Vallejo-Cordoba, B.; Liceaga, A.M. Potential role of natural bioactive peptides for development of cosmeceutical skin products. *Peptides* **2019**, *122*, 170170, doi:<https://doi.org/10.1016/j.peptides.2019.170170>.
5. Aldag, C.; Nogueira Teixeira, D.; Leventhal, P.S. Skin rejuvenation using cosmetic products containing growth factors, cytokines, and matrikines: a review of the literature. *Clin Cosmet Investig Dermatol* **2016**, *9*, 411-419, doi:10.2147/CCID.S116158.
6. Ferreira, M.S.; Magalhães, M.C.; Sousa-Lobo, J.M.; Almeida, I.F. Trending Anti-Aging Peptides. *Cosmetics* **2020**, *7*, doi:10.3390/cosmetics7040091.
7. Ledwoń, P.; Errante, F.; Papini, A.M.; Rovero, P.; Latajka, R. Peptides as Active Ingredients: A Challenge for Cosmeceutical Industry. *Chem. Biodivers.* **2021**, *18*, e2000833, doi:<https://doi.org/10.1002/cbdv.202000833>.
8. Pickart, L.; Margolina, A. Regenerative and Protective Actions of the GHK-Cu Peptide in the Light of the New Gene Data. *Int. J. Mol. Sci.* **2018**, *19*, 1987, doi:10.3390/ijms19071987.
9. Errante, F.; Ledwon, P.; Latajka, R.; Rovero, P.; Papini, A.M. Cosmeceutical Peptides in the Framework of Sustainable Wellness Economy. *Front Chem* **2020**, *8*, doi:ARTN 57292310.3389/fchem.2020.572923.
10. The 25 Years of Innovation Award goes to Matrixyl. Available online: <https://www.cossma.com/ingredients/article/the-25-years-of-innovation-award-goes-to-matrixyl-33065.html?&searchword=peptide&ref=search> (accessed on 15 September 2021).
11. Matrixyl Inside by Sederma Available online: <https://www.matrixylinside.com/en-gb/default> (accessed on 16 Set 2021).

12. Gomes, A.; Teixeira, C.; Ferraz, R.; Prudencio, C.; Gomes, P. Wound-Healing Peptides for Treatment of Chronic Diabetic Foot Ulcers and Other Infected Skin Injuries. *Molecules* **2017**, *22*, doi:10.3390/molecules22101743.
13. Gomes, A.; Bessa, L.J.; Fernandes, I.; Ferraz, R.; Mateus, N.; Gameiro, P.; Teixeira, C.; Gomes, P. Turning a Collagenesis-Inducing Peptide Into a Potent Antibacterial and Antibiofilm Agent Against Multidrug-Resistant Gram-Negative Bacteria. *Front Microbiol* **2019**, *10*, 1-11, doi:10.3389/fmicb.2019.01915.
14. Forero Doria, O.; Castro, R.; Gutierrez, M.; Gonzalez Valenzuela, D.; Santos, L.; Ramirez, D.; Guzman, L. Novel Alkylimidazolium Ionic Liquids as an Antibacterial Alternative to Pathogens of the Skin and Soft Tissue Infections. *Molecules* **2018**, *23*, 2354, doi:10.3390/molecules23092354.
15. Gomes, A.; Bessa, L.; Fernandes, I.; Aguiar, L.; Ferraz, R.; Monteiro, C.; Martins, C.; Mateus, N.; Gameiro, P.; Teixeira, C.; et al. Boosting cosmeceutical peptides: coupling imidazolium-based ionic liquids to pentapeptide-4 originates new leads with antimicrobial and collagenesis-inducing activities. *Int. J. Antimicrob. Agents* **2021**, *submitted*
16. Kukowska, M.; Kukowska-Kaszuba, M.; Dzierzbicka, K. In vitro studies of antimicrobial activity of Gly-His-Lys conjugates as potential and promising candidates for therapeutics in skin and tissue infections. *Bioorg Med Chem Lett* **2015**, *25*, 542-546, doi:<https://doi.org/10.1016/j.bmcl.2014.12.029>.
17. Behrendt, R.; White, P.; Offer, J. Advances in Fmoc solid-phase peptide synthesis. *J. Pept. Sci.* **2016**, *22*, 4-27, doi:<https://doi.org/10.1002/psc.2836>.
18. Loughrey, S.; Mannion, J.; Matlock, B. Using the NanoDrop One to Quantify Protein and Peptide Preparations at 205 nm. Available online: <http://tools.thermofisher.com/content/sfs/brochures/ND-One-Protein-and-Peptide-r16-01-18.pdf> (accessed on 20 August 2021).
19. CLSI. *Methods for dilution antimicrobial susceptibility tests for bacteria that grow aerobically; Approved Standard—Ninth Edition*; CLSI document M07-A9. Wayne, PA: Clinical and Laboratory Standards Institute, 2012.
20. Gomes, N.M.; Bessa, L.J.; Buttachon, S.; Costa, P.M.; Buaruang, J.; Dethoup, T.; Silva, A.M.; Kijjoa, A. Antibacterial and antibiofilm activities of tryptoquivalines and meroditerpenes isolated from the marine-derived fungi *Neosartorya paulistensis*, *N. laciniosa*, *N. tsunodae*, and the soil fungi *N. fischeri* and *N. siamensis*. *Mar. Drugs* **2014**, *12*, 822-839, doi:10.3390/md12020822.
21. Gomes, A.; Bessa, L.J.; Correia, P.; Fernandes, I.; Ferraz, R.; Gameiro, P.; Teixeira, C.; Gomes, P. "Clicking" an Ionic Liquid to a Potent Antimicrobial

- Peptide: On the Route towards Improved Stability. *Int. J. Mol. Sci.* **2020**, *21*, 1-11, doi:<https://doi.org/10.3390/ijms21176174>.
22. Mulani, M.S.; Kamble, E.E.; Kumkar, S.N.; Tawre, M.S.; Pardesi, K.R. Emerging Strategies to Combat ESKAPE Pathogens in the Era of Antimicrobial Resistance: A Review. *Front Microbiol* **2019**, *10*, 539-539, doi:10.3389/fmicb.2019.00539.
 23. Blicharz, L.; Rudnicka, L.; Samochocki, Z. Staphylococcus aureus: an underestimated factor in the pathogenesis of atopic dermatitis? *Postepy Dermatol Alergol* **2019**, *36*, 11-17, doi:10.5114/ada.2019.82821.
 24. Serra, R.; Grande, R.; Butrico, L.; Rossi, A.; Settimio, U.F.; Caroleo, B.; Amato, B.; Gallelli, L.; de Franciscis, S. Chronic wound infections: the role of Pseudomonas aeruginosa and Staphylococcus aureus. *Expert Review of Anti-infective Therapy* **2015**, *13*, 605-613, doi:10.1586/14787210.2015.1023291.
 25. Stevens, D.L.; Bryant, A.E. Impetigo, Erysipelas and Cellulitis. In *Streptococcus pyogenes : Basic Biology to Clinical Manifestations*, Ferretti, J.J., Stevens, D.L., Fischetti, V.A., Eds.; Oklahoma City (OK), 2016.
 26. Bruun, T.; Kittang, B.R.; de Hoog, B.J.; Aardal, S.; Flaatten, H.K.; Langeland, N.; Mylvaganam, H.; Vindenes, H.A.; Skrede, S. Necrotizing soft tissue infections caused by Streptococcus pyogenes and Streptococcus dysgalactiae subsp. equisimilis of groups C and G in western Norway *Clin. Microbiol. Infect* **2013**, *19*, E545-E550, doi:10.1111/1469-0691.12276.
 27. Brown, M.M.; Horswill, A.R. Staphylococcus epidermidis—Skin friend or foe? *Plos Pathog* **2020**, *16*, e1009026, doi:10.1371/journal.ppat.1009026.

Chapter 3. Conclusion and future perspectives

Conclusion and Future Perspectives

Overall, results presented in Chapter 2 provide a confirmation of the working hypothesis associated to this Doctoral Thesis, as it was possible to advance ionic liquid/peptide-based constructs that could exhibit potent and wide-spectrum antimicrobial activity, along with collagenesis-boosting properties. Specifically, it was possible to provide enlightening answers to the scientific questions initially posed, since:

- dual-action peptide chimeras able to retain the antimicrobial and collagenesis-boosting properties of the two parent peptides, 3.1 and PP4, were produced;
- resistance to enzyme-mediated modification of a chimeric peptide could be increased, with no loss in activity, through *N*-terminal modification with an imidazolium ionic liquid *via* copper(I)-catalyzed azide-alkyne cycloaddition;
- the order through which both the 3.1 and PP4 building blocks are linked to each other was found to be relevant, since peptide PP4-3.1 presented wider scope antimicrobial action than its isomer 3.1-PP4;
- it is possible to retain antimicrobial and collagenesis-inducing activity by replacing the AMP sequence (3.1) in the chimeric 3.1-PP4 peptide by an antimicrobial imidazolium-based ionic liquid;
- the *N*-terminal coupling of an imidazolium-based ionic liquid to a non-antimicrobial peptide bestows antimicrobial activity to cosmeceutical peptides other than PP4, e.g., GHK and KVK.

In conclusion, this Doctoral Thesis conveys an advance in the frontiers of knowledge regarding development of innovative strategies to tackle skin and soft tissue infections.

Subsequent work in this line of research should start by making a full proof of concept on the value of ionic liquid-cosmeceutical peptide conjugates as dual-action leads for development of novel active pharmaceutical ingredients to integrate topical formulations for cSSTI. Namely, *ex vivo* and *in vivo* studies should be undertaken soon, enabling future lead-to-candidate optimization, and ensuing preclinical to clinical development.

Annexes

Supplementary Figures and Tables for section 2.1

Frontiers in Microbiology 2019, 10 (1915); doi:10.3390/fmicb.2019.01915

1.1 Supplementary Table S1

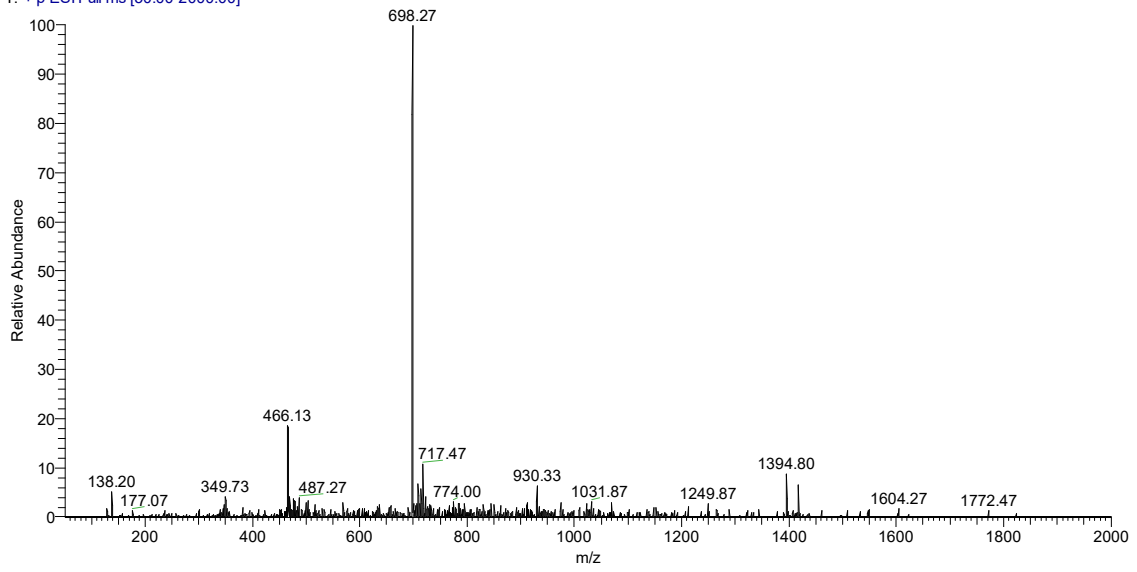
Supplementary Table S1. Antimicrobial resistance pattern of MDR isolates used in this work

| Isolate | Antimicrobial resistance pattern |
|----------------|--|
| PA002 | AMK, CIP, COL, GEN, TOB |
| PA004 | CIP, GEN, IPM, TOB, TZP |
| Pa3 | ATM, CIP, FEP, GEN |
| Pa4 | ATM, CAZ, CIP, FEP, IPM |
| Ec1 | AMP, ATM, CAZ, CIP, CTX, SXT, TET |
| Ec2 | AMP, ATM, CAZ, CIP, CTX, TET |
| EC001 | AMP, CIP, CXM, SXT, LEV |
| EC002 | AMC, AMP, CIP, CXT, CXM, GEN, LEV, SXT, TOB, TZP |
| EC003 | CIP, CXM, LEV |
| KP004 | AMC, AMP, CAZ, CTX, CXM, ERT, MER, SXT, TZP |
| KP007 | AMC, AMP, CAZ, CIP, CTX, CXM, ERT, IPM, LEV, MER, NIT, SXT, TOB, TZP |
| KP010 | AMC, AMP, CAZ, CIP, CTX, CXM, ERT, IPM, LEV, NIT, TZP |

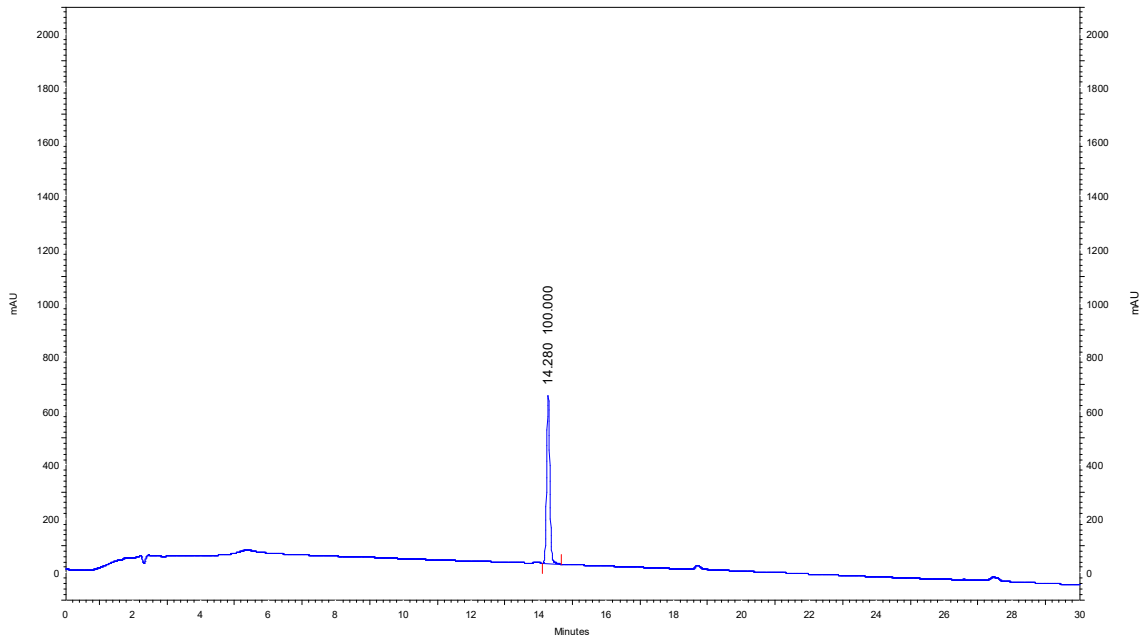
AMC: amoxicillin/clavulanic acid; AMK: amikacin; AMP: ampicillin; ATM: aztreonam; CAZ: ceftazidime; CIP: ciprofloxacin; COL: colistin; CTX: cefotaxime; CXM: cefuroxime sodium; ERT: ertapenem; FEP: cefepime; GEN: gentamicin; IPM: imipenem; LEV: levofloxacin; MER: meropenem; NIT: nitrofurantoin; SXT: Trimethoprim/Sulfamethoxazole; TET: tetracycline; TOB: tobramycin; TZP: piperacillin/Tazobactam

1.2 Supplementary Figures S1 to S18

3_1A_final#46 RT: 1.26 AV: 1 NL: 7.74E6
 T: +p ESI Full ms [50.00-2000.00]

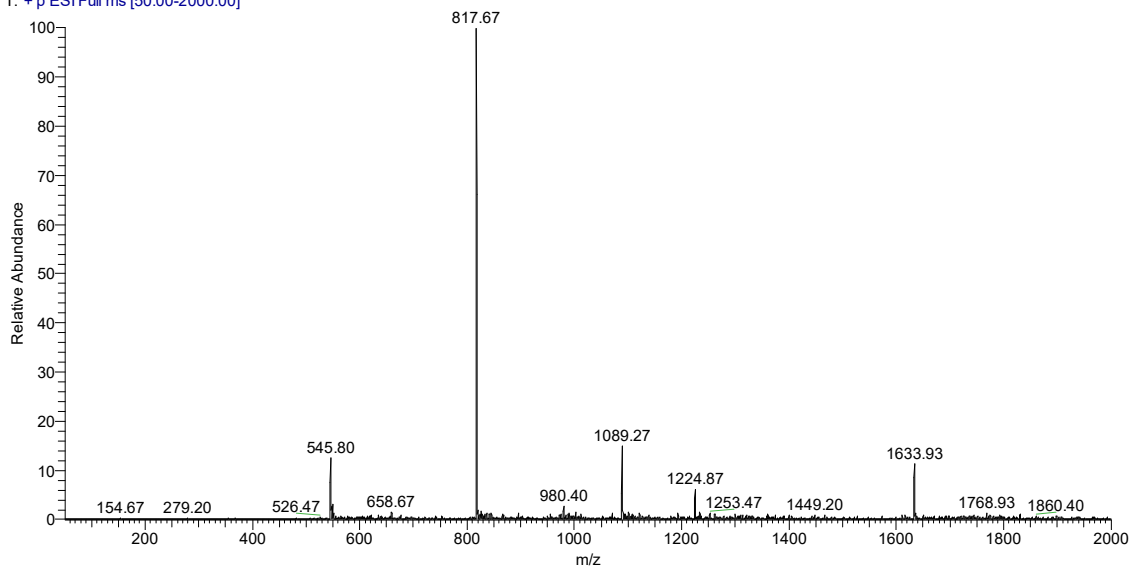


Supplementary Figure S1. ESI-IT mass spectrum (positive mode) of peptide 3.1

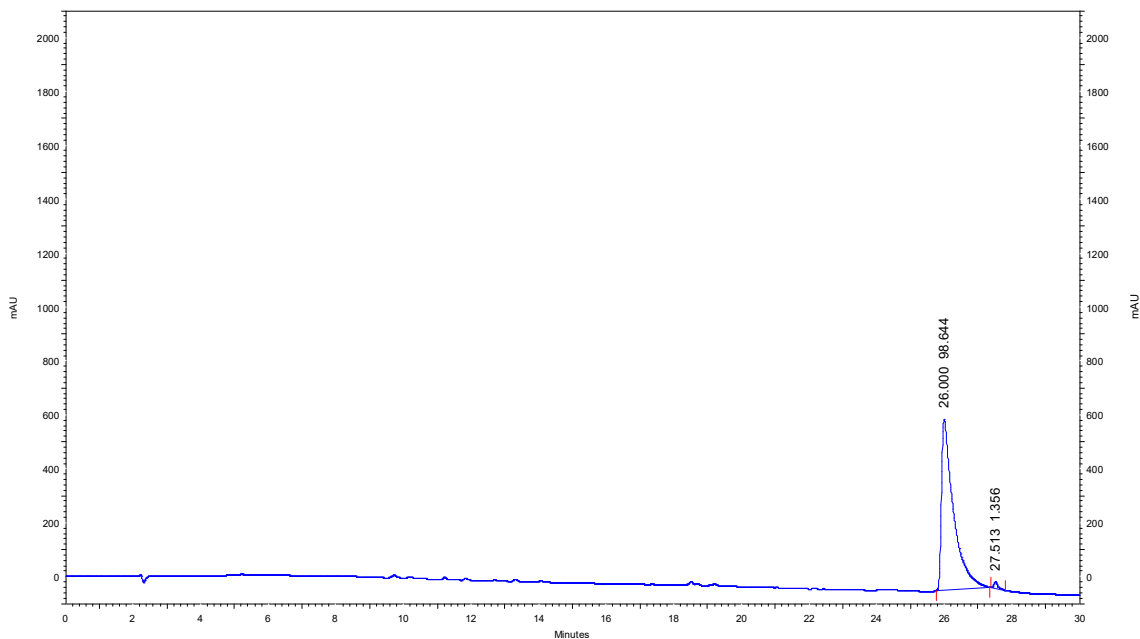


Supplementary Figure S2. HPLC chromatogram of peptide 3.1

PG-3_1B-1of #53 RT: 1.43 AV: 1 NL: 8.43E8
 T: +p ESI Full ms [50.00-2000.00]

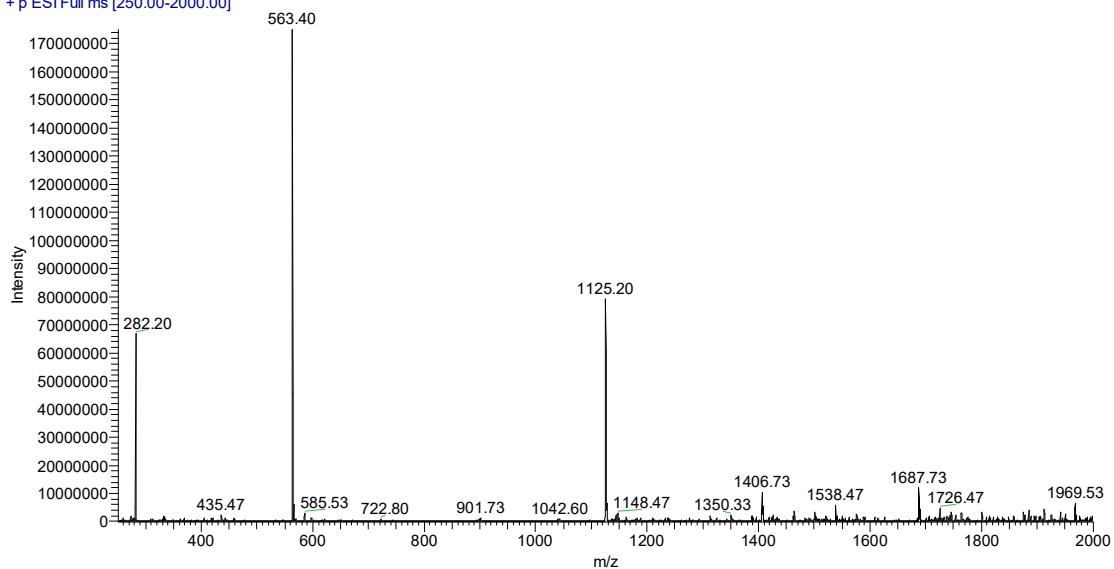


Supplementary Figure S3. ESI-IT mass spectrum (positive mode) of peptide C₁₆-3.1

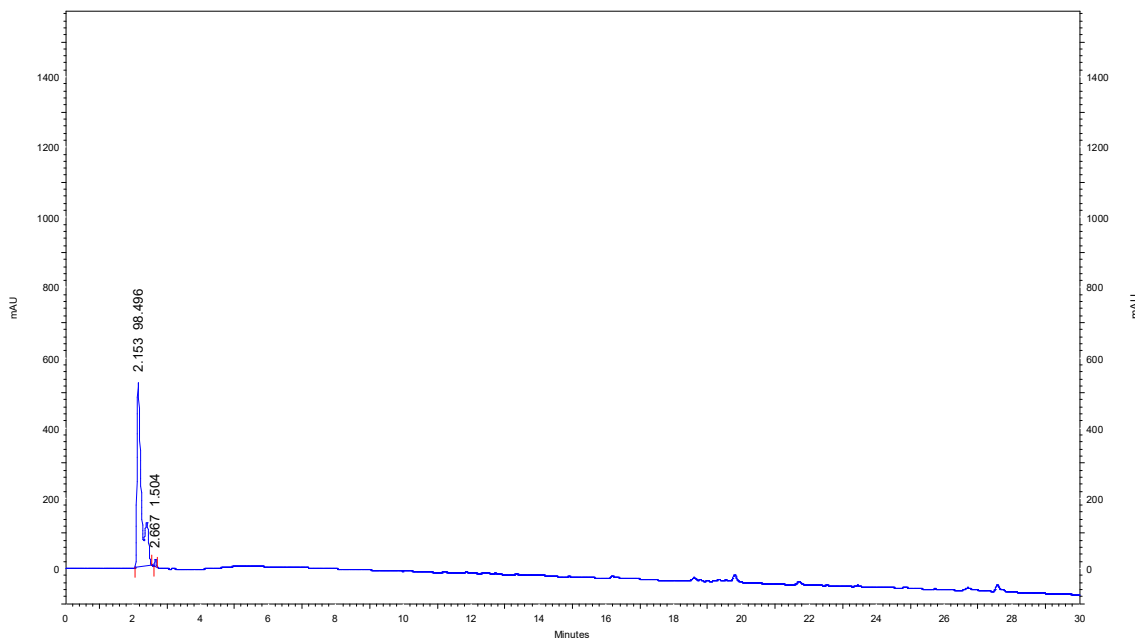


Supplementary Figure S4. HPLC chromatogram of peptide C₁₆-3.1

PG-PP4-A-Final-Liof #136 RT: 3.41 AV: 1 NL: 1.75E8
 T: + p ESI Full ms [250.00-2000.00]

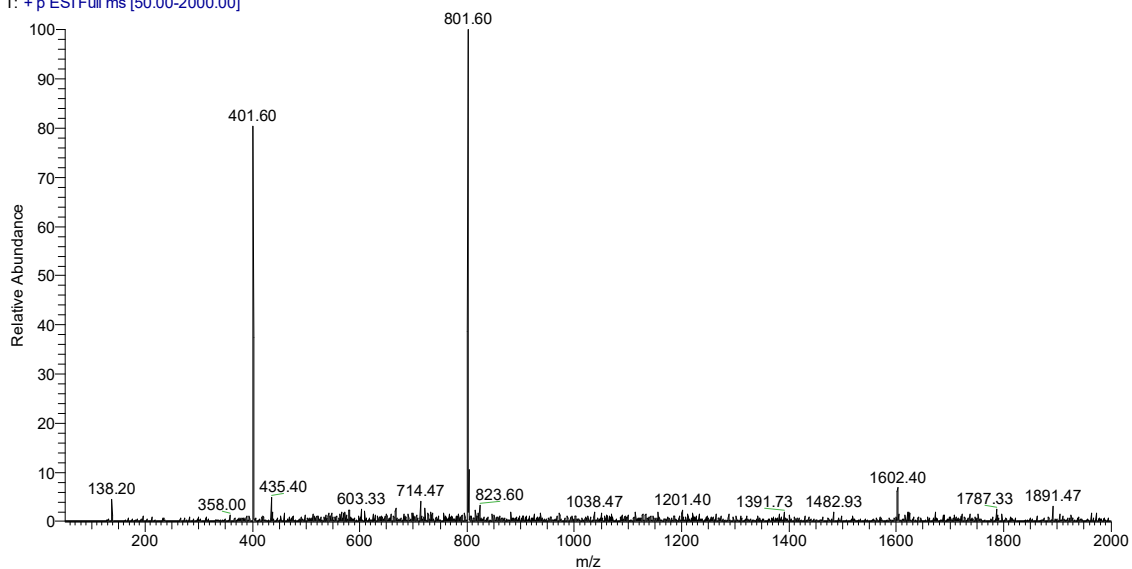


Supplementary Figure S5. ESI-IT mass spectrum (positive mode) of peptide PP4

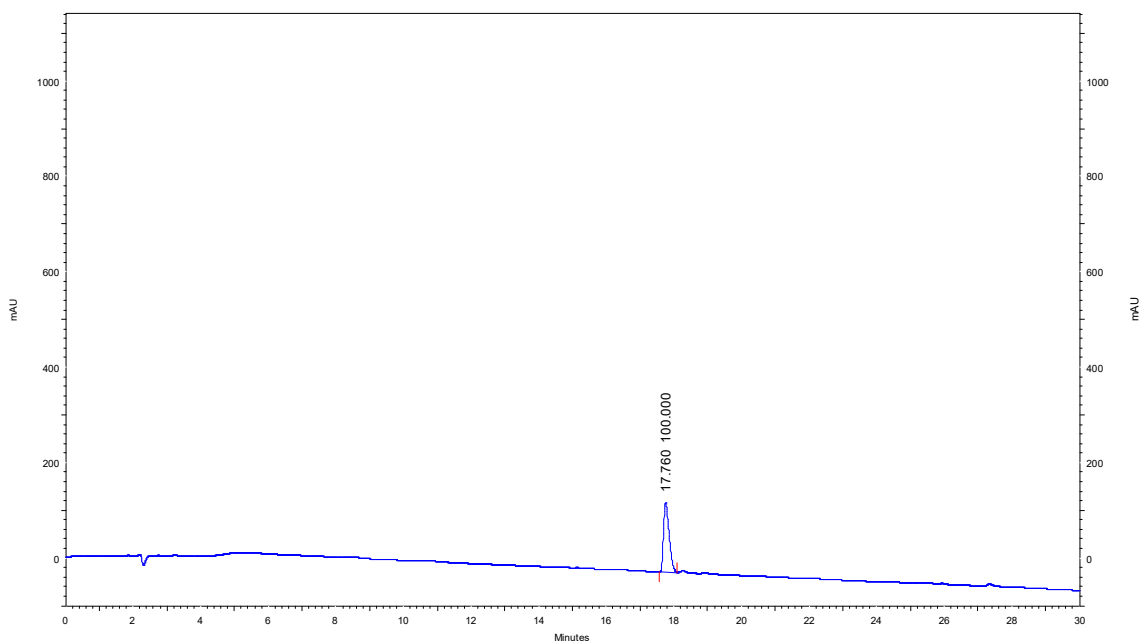


Supplementary Figure S6. HPLC chromatogram of peptide PP4

CT-PP4B-pvf_170928132825 #32 RT: 0.65 AV: 1 NL: 5.86E7
 T: + p ESI Full ms [50.00-2000.00]

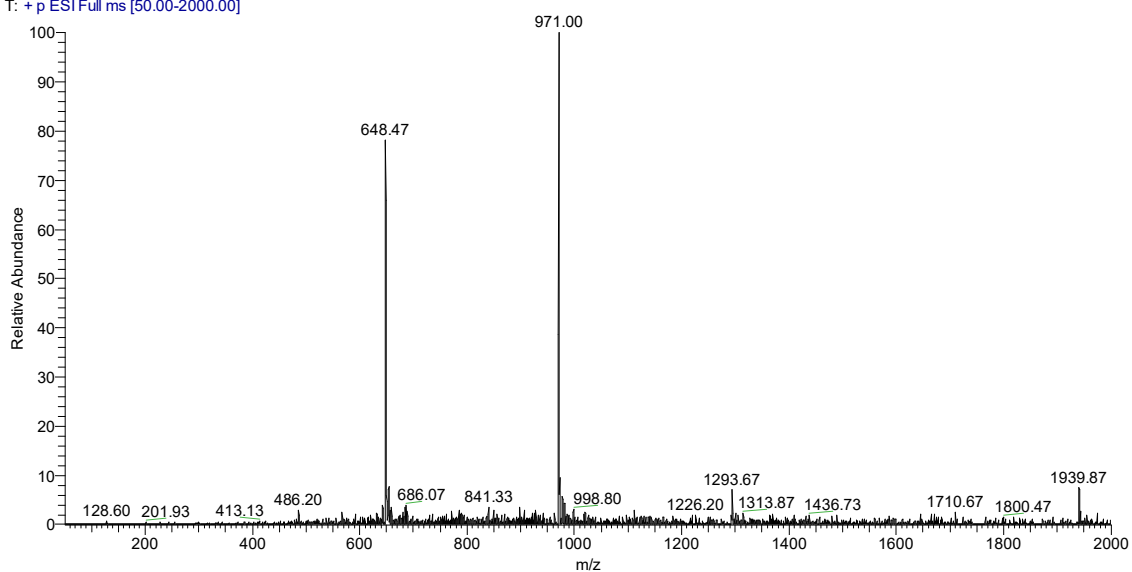


Supplementary Figure S7. ESI-IT mass spectrum (positive mode) of peptide C₁₆-PP4

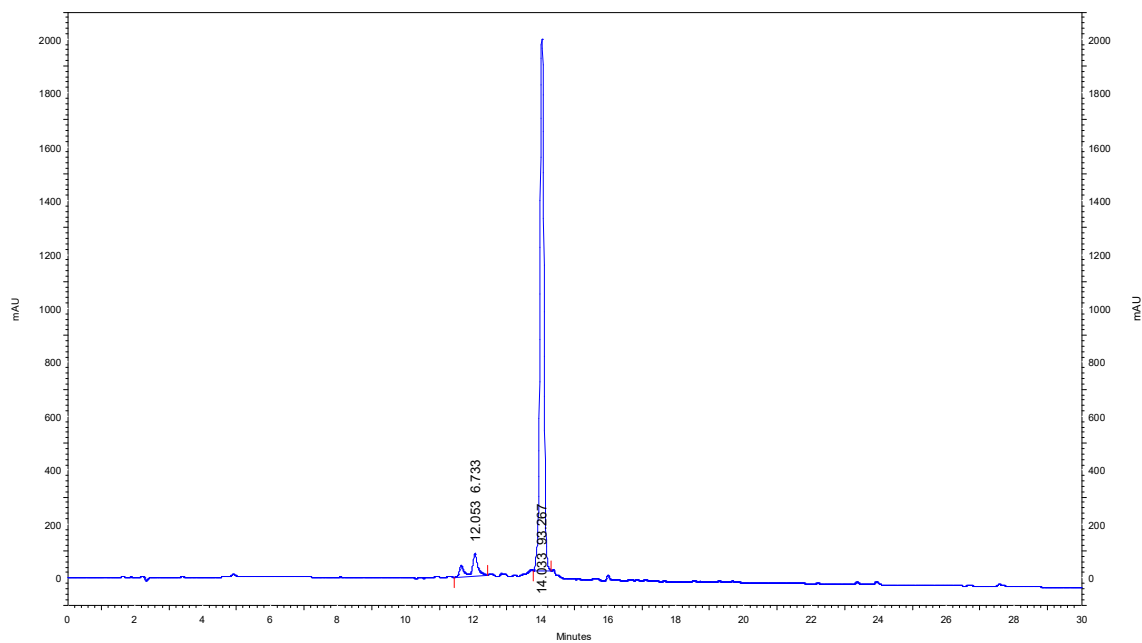


Supplementary Figure S8. HPLC chromatogram of peptide C₁₆-PP4

AG-PP4-3_180327162213 #2 RT: 0.04 AV: 1 NL: 1.94E8
 T: + p ESI Full ms [50.00-2000.00]

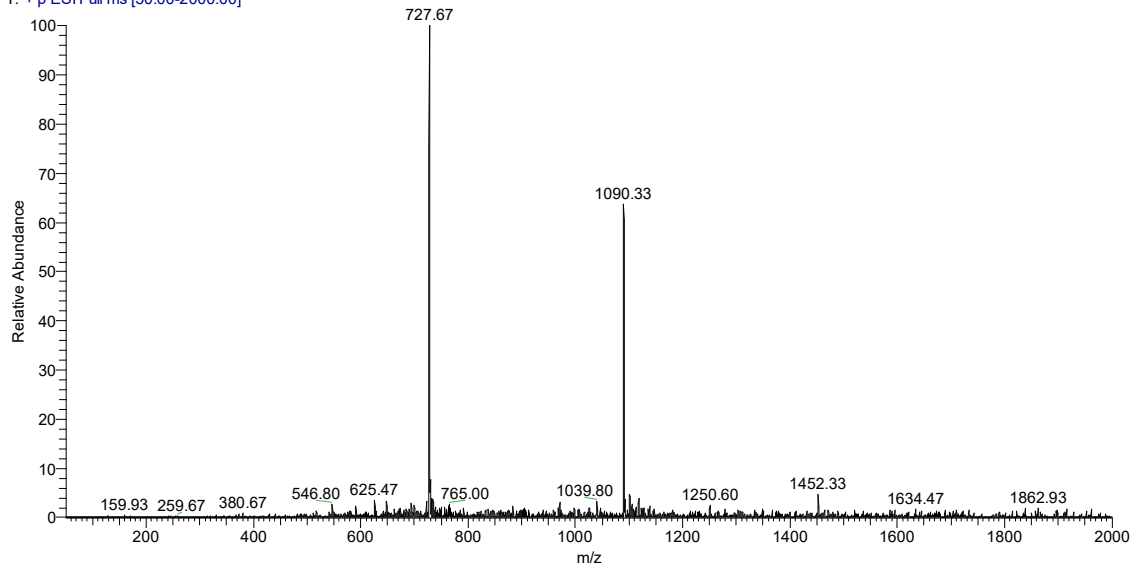


Supplementary Figure S9. ESI-IT mass spectrum (positive mode) of peptide PP4-3.1

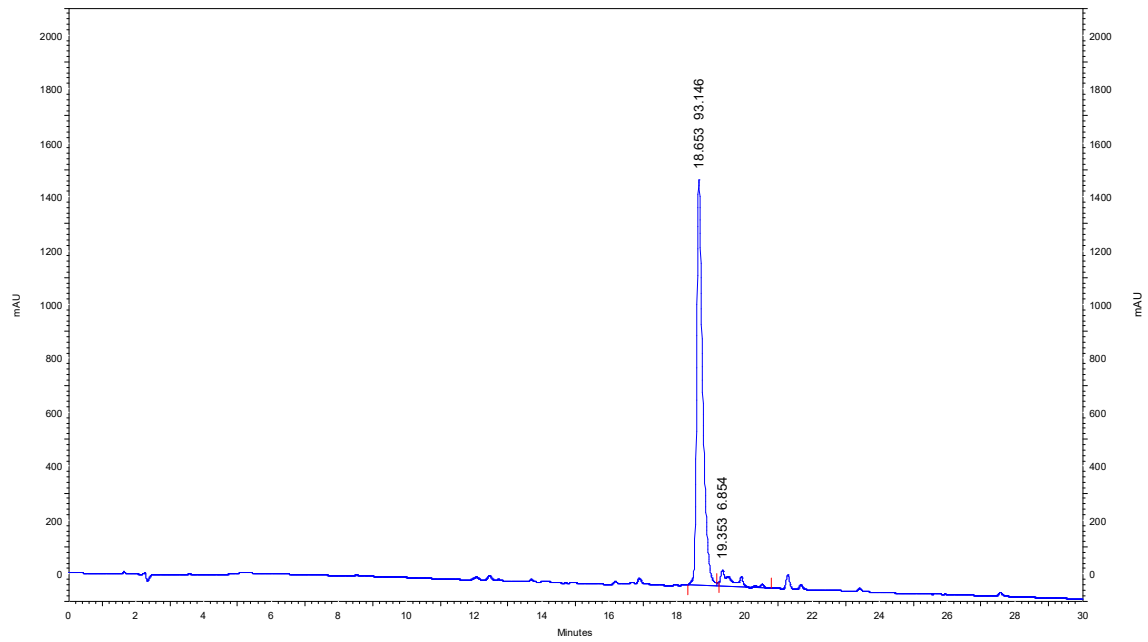


Supplementary Figure S10. HPLC chromatogram of peptide PP4-3.1

AG-C16-PP4-3_180327163727 #7 RT: 0.17 AV: 1 NL: 2.99E8
 T: +p ESI Full ms [50.00-2000.00]

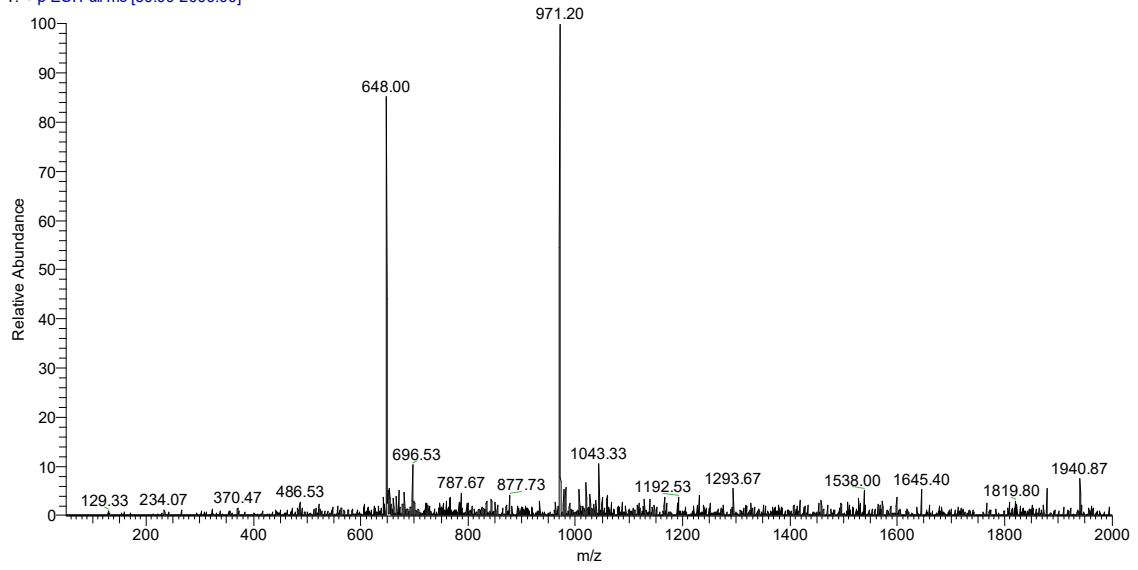


Supplementary Figure S11. ESI-IT mass spectrum (positive mode) of peptide C₁₆-PP4-3.1

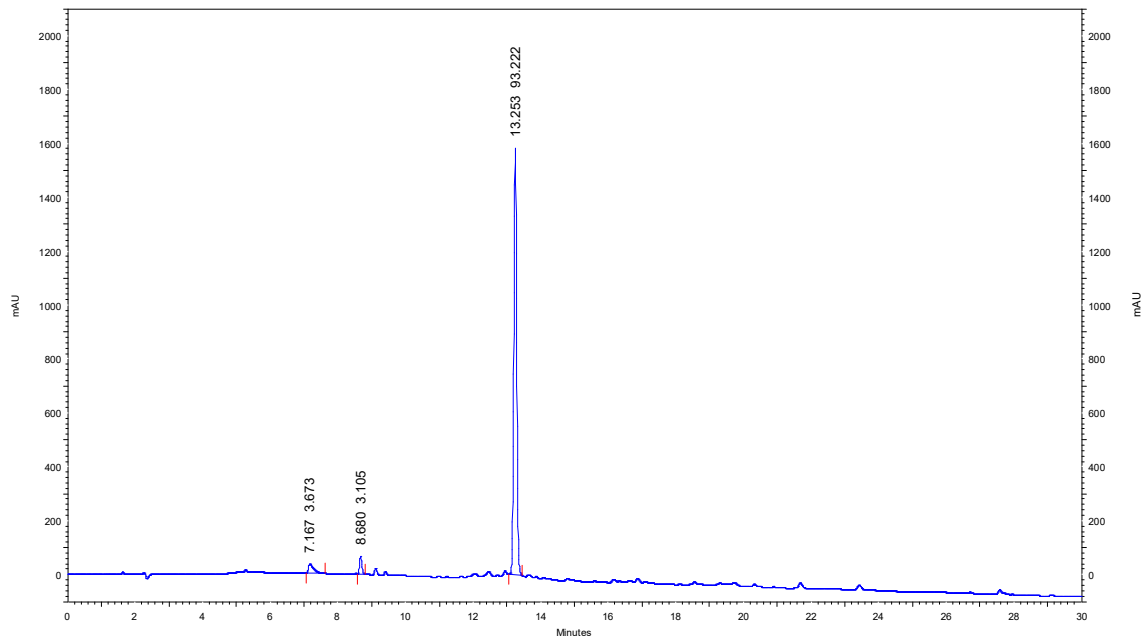


Supplementary Figure S12. HPLC chromatogram of peptide C₁₆-PP4-3.1

AG-3_1_PP4-180327163226 #4 RT: 0.08 AV: 1 NL: 5.57E7
 T: +p ESI Full ms [50.00-2000.00]

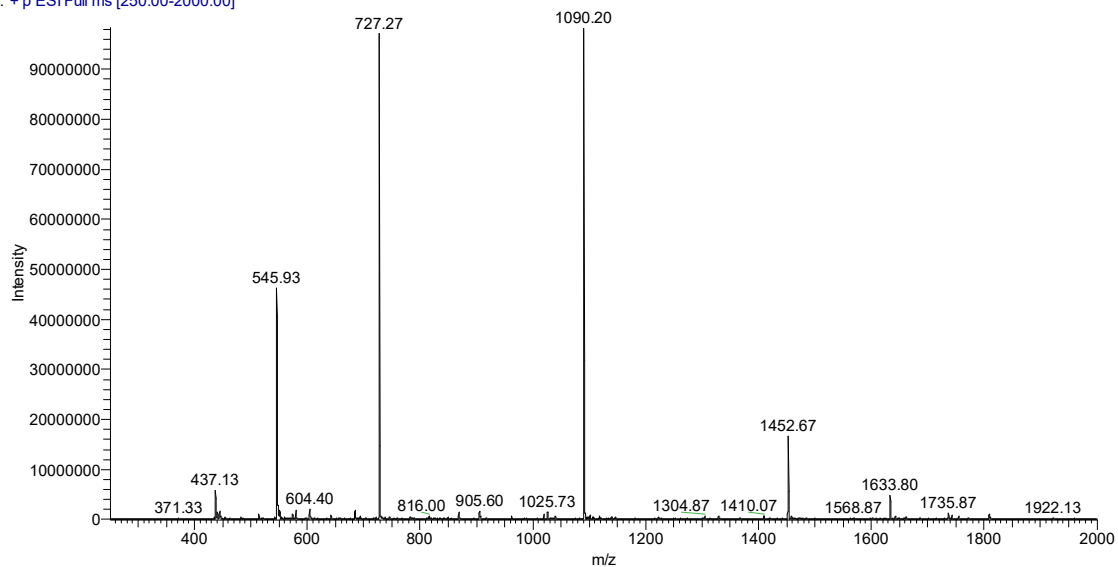


Supplementary Figure S13. ESI-IT mass spectrum (positive mode) of peptide 3.1-PP4

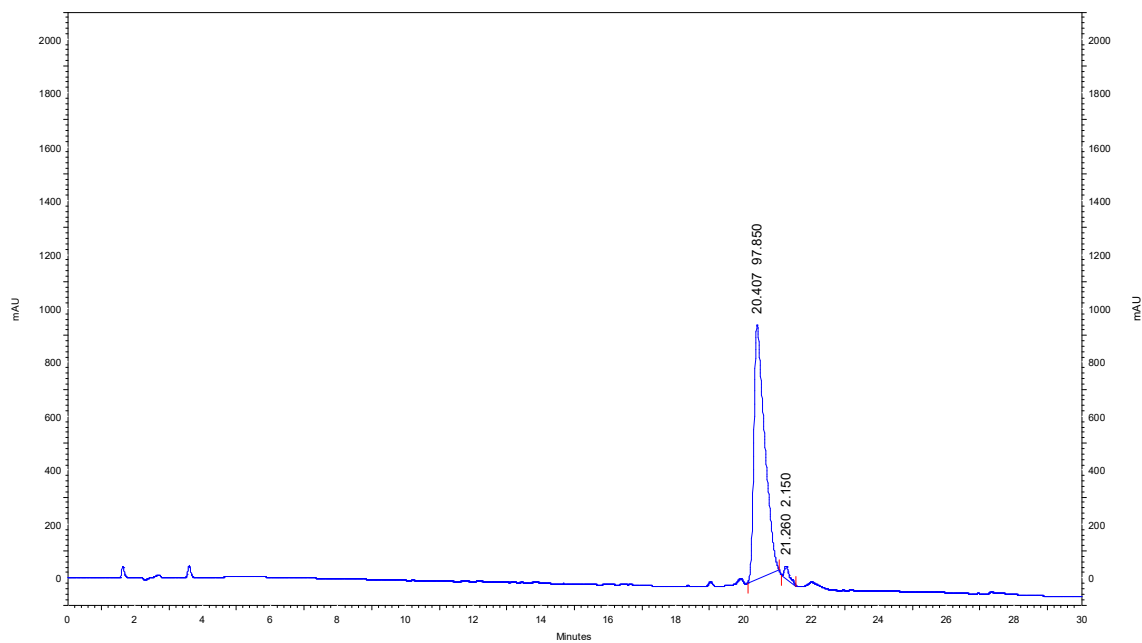


Supplementary Figure S14. HPLC chromatogram of peptide 3.1-PP4

PG-AGD-33-finalLof #821-856 RT: 21.09-21.94 AV: 36 NL: 9.83E7
 T: +p ESI Full ms [250.00-2000.00]

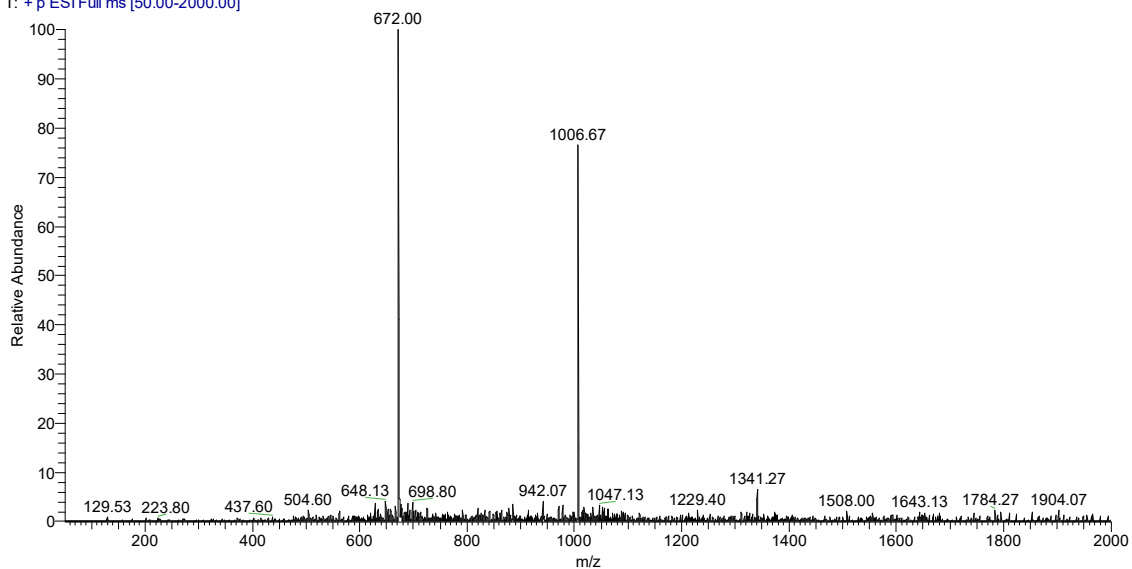


Supplementary Figure S15. ESI-IT mass spectrum (positive mode) of peptide C₁₆-3.1-PP4

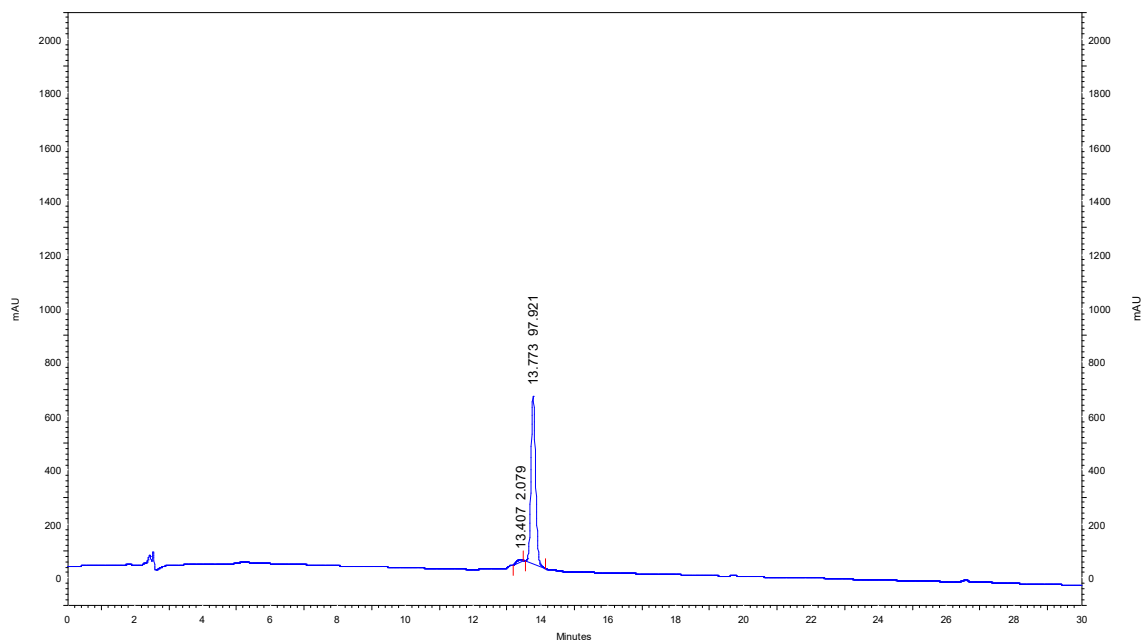


Supplementary Figure S16. HPLC chromatogram of peptide C₁₆-3.1-PP4

AG-PP4-B-Ala-3_180327162732#21 RT: 0.56 AV: 1 NL: 2.18E8
 T: + p ESI Full ms [50.00-2000.00]



Supplementary Figure S17. ESI-IT mass spectrum (positive mode) of peptide PP4-βAla-3.1



Supplementary Figure S18. HPLC chromatogram of peptide PP4-βAla-3.1

Supplementary Materials for section 2.2

International Journal of Molecular Sciences **2020**, *21* (17), 6174;
<https://doi.org/10.3390/ijms21176174>

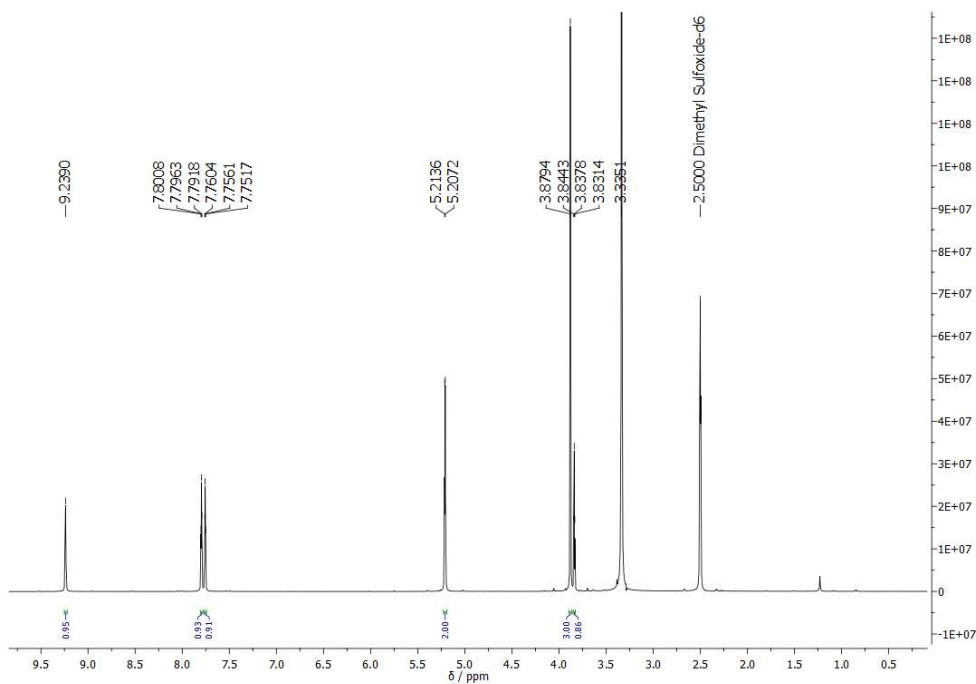


Figure S1. ¹H-NMR spectrum of 1-methyl-3-propargyl imidazolium bromide (400 MHz, DMSO-d₆).

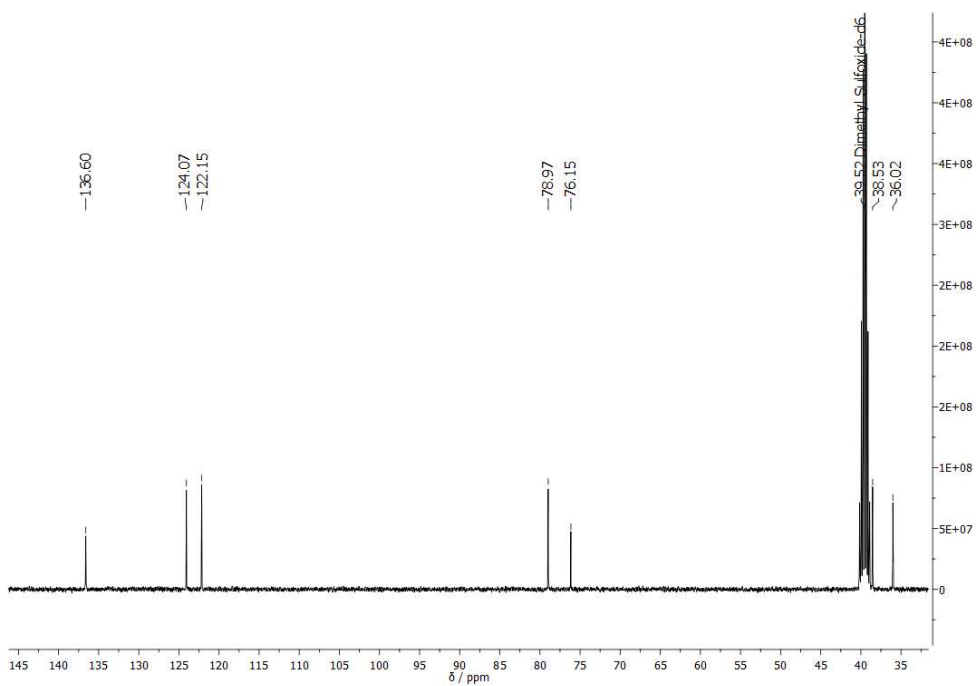


Figure S2. ¹³C-NMR spectrum of 1-methyl-3-propargyl imidazolium bromide (100 MHz, DMSO-d₆).

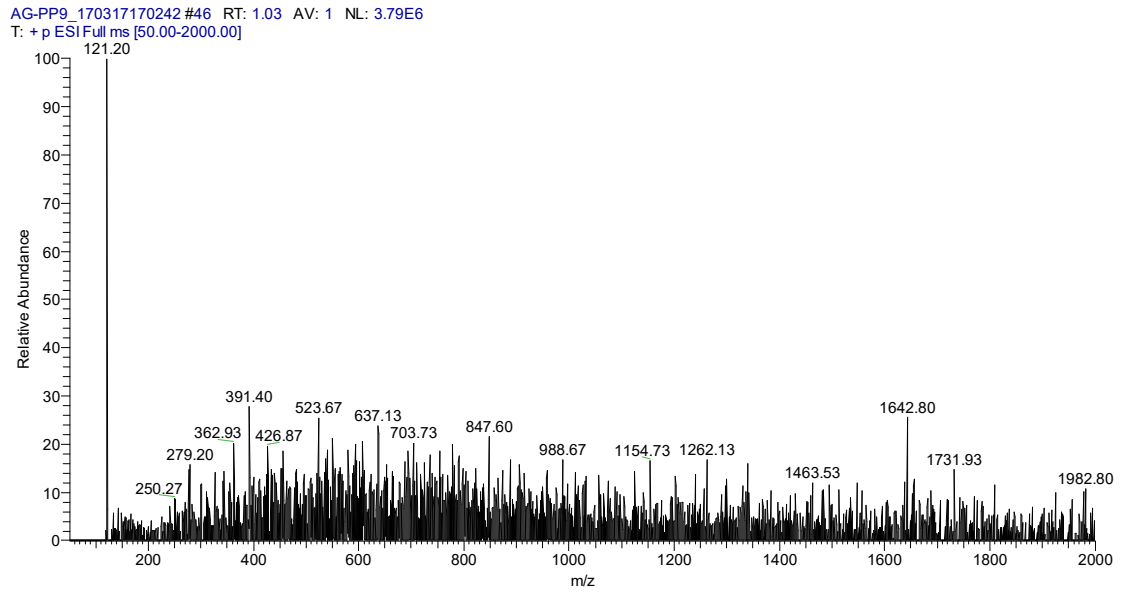


Figure S3. ESI-IT(+) mass spectrum of 1-methyl-3-propargyl imidazolium bromide.

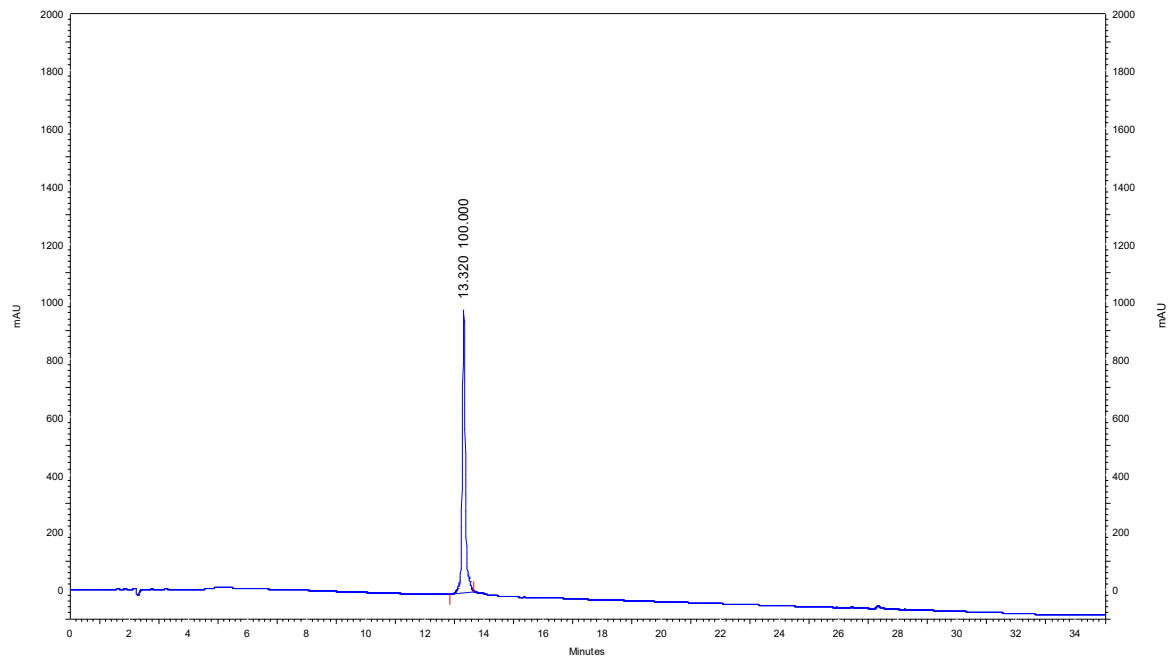


Figure S4. RP-HPLC chromatogram of Melm-3.1-PP4.

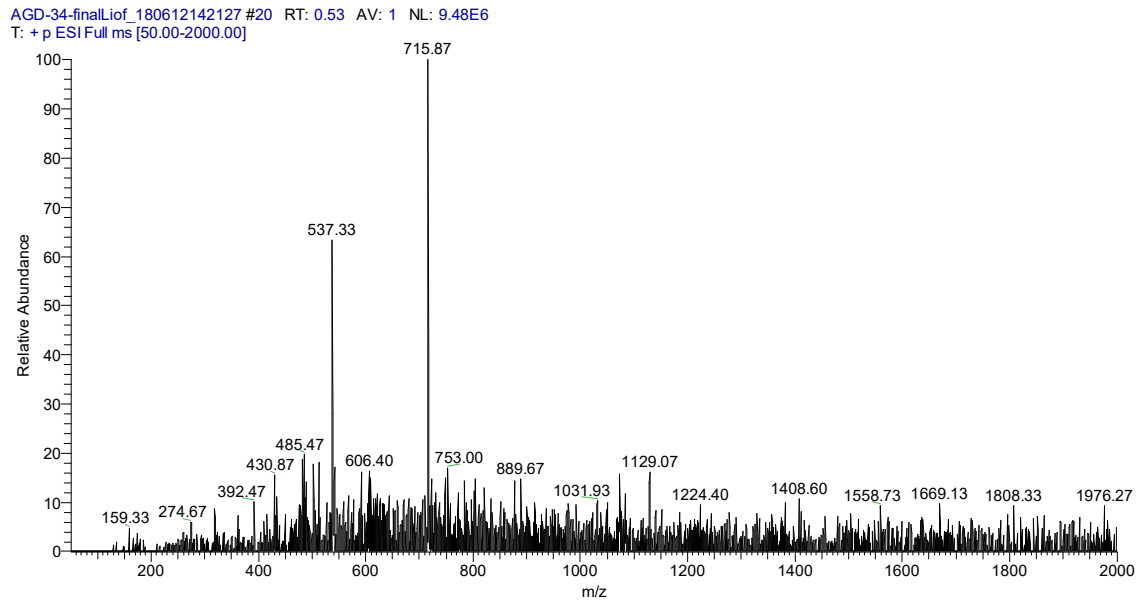


Figure S5. ESI-IT(+) mass spectrum of Melm-3.1-PP4, where both the tri- and tetra-protonated adducts are observed at m/z 715.87 and 537.33, respectively.

Table 1. Antimicrobial resistance pattern of MDR isolates used in this work.

| Isolate | Antimicrobial resistance pattern |
|---------|---|
| PA004 | CIP, GEN, IPM, TOB, TZP |
| Pa3 | ATM, CIP, FEP, GEN |
| Pa4 | ATM, CAZ, CIP, FEP, IPM |
| Ec2 | AMP, ATM, CAZ, CIP, CTX, TET |
| EC001 | AMP, CIP, CXM, SXT, LEV |
| EC002 | AMC, AMP, CIP, CXT, CXM, GEN, LEV, SXT, TOB, TZP |
| EC003 | CIP, CXM, LEV |
| KP004 | AMC, AMP, CAZ, CTX, CXM, ERT, MER, SXT, TZP |
| KP010 | AMC, AMP, CAZ, CIP, CTX, CXM, ERT, IPM, LEV, NIT, TZP |
| Sa007 | CIP, CLI, ERI, FOX, GEN, LEV, MOX, OXA |
| Ef1 | AMP, CIP, VAN |

AMC: amoxicillin/clavulanic acid; AMK: amikacin; AMP: ampicillin; ATM: ztreonam; CAZ: ceftazidime; CIP: ciprofloxacin; CLI: clindamycin; COL: colistin; CTX: cefotaxime; CXM: cefuroxime sodium; ERI: erythromycin; ERT: ertapenem; FEP: cefepime; FOX: ceftoxitin; GEN: gentamicin; IPM: imipenem; LEV: levofloxacin; MER: meropenem; MOX: moxifloxacin; NIT: nitrofurantoin; OXA: oxacillin; SXT: Trimethoprim/Sulfamethoxazole; TET: tetracycline; TOB: tobramycin; TZP: piperacillin/Tazobactam; VAN: vancomycin

Table S2. Effect of Melm-3.1-PP4 and 3.1-PP4 at 20×MIC on 24 h preformed biofilms of KP010 (a MDR clinical isolate of *K. pneumoniae*).

| Peptide | OD ₆₀₀ of planktonic phase in untreated biofilms | OD ₆₀₀ of planktonic phase of peptide-treated biofilms | % of Reduction in biofilm proliferation ^a |
|---------------------|---|---|--|
| 3.1-PP4 | 0.740 ± 0.047 | 0.384 ± 0.049 | 51.8 |
| Melm-3.1-PP4 | | 0.497 ± 0.050 | 67.1 |

^a Results are the mean of three independent experiments performed in triplicate.

Supplementary Materials for section 2.3

Submitted to Pharmaceutics

INSTRUMENTAL ANALYSIS

All RP-HPLC analyses were performed in a Hitachi-Merck LaChrom Elite system equipped with an L-2130 quaternary pump, an L220 thermostatted automated sampler, and an L-2455 diode-array detector (DAD). The samples were injected in a reverse-phase C18 column (125×4.0 mm ID and 5 µm pore size) with the elution gradient of 1 to 100% of B in A, using 0.05% aqueous trifluoro acetic acid (TFA) as solvent A and acetonitrile (ACN) as solvent B, and was run for 30 min at the flow rate of 1mL/min. The detection was performed at 220 nm.

All ESI-IT-MS analyses were performed in a Finnigan Surveyor LCQ DECA XP MAX spectrometer operating with electrospray ionization and ion trap quadrupole detection, at the department of Chemistry and Biochemistry University of Porto.

Chromatographic and spectral traces thus obtained are given below.

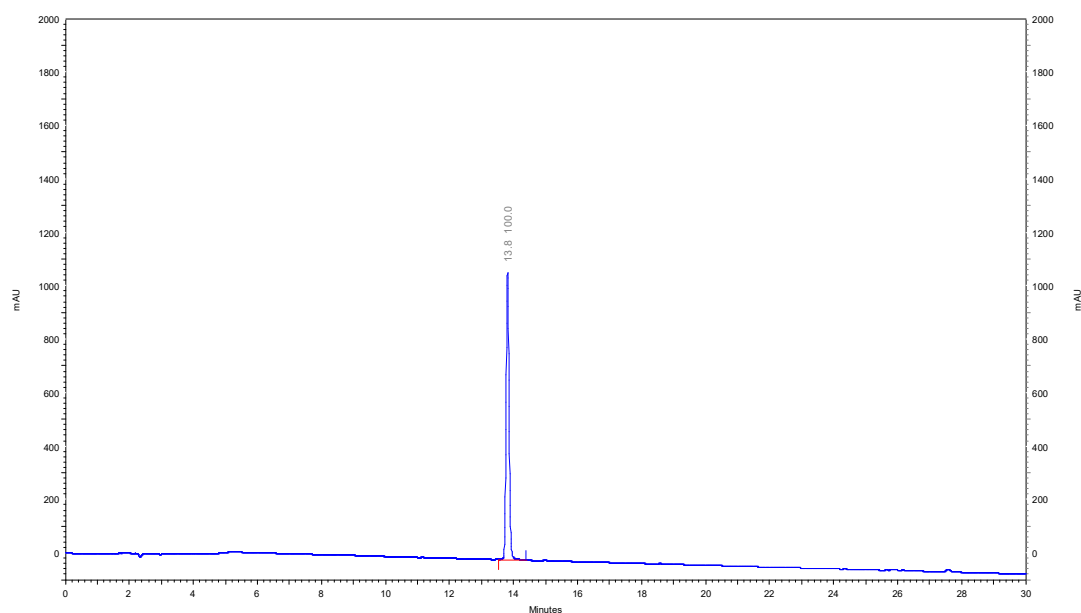


Figure S1: RP-HPLC chromatogram obtained for PP4-3.1.

PG-AGD-PP4-3_1-Maio2021 #6 RT: 0.16 AV: 1 NL: 4.87E6
 T: + p ESI Full ms [50.00-2000.00]

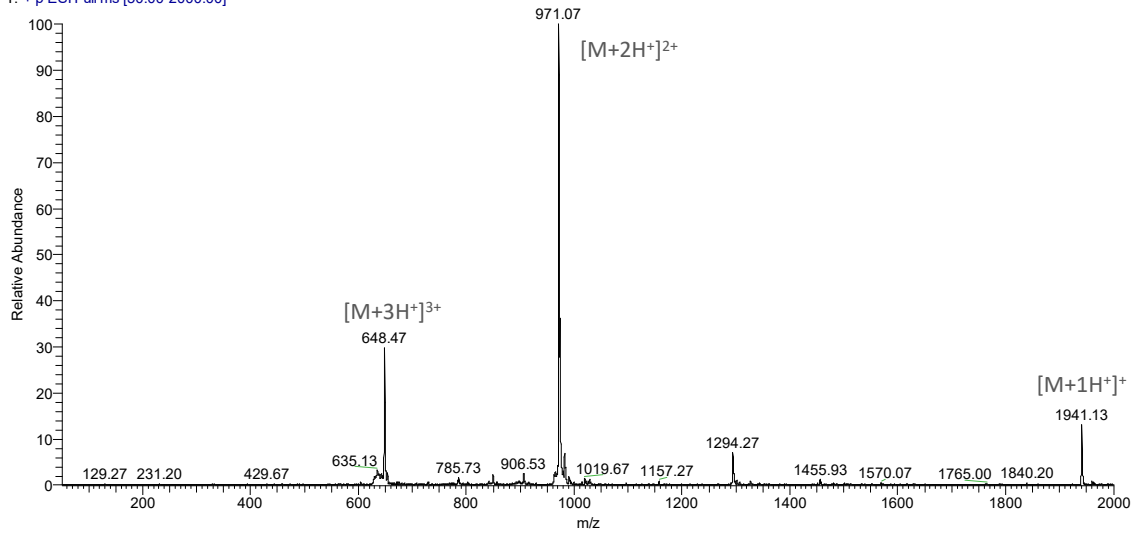


Figure S2: Full ESI-IT MS (positive mode) obtained for PP4-3.1.

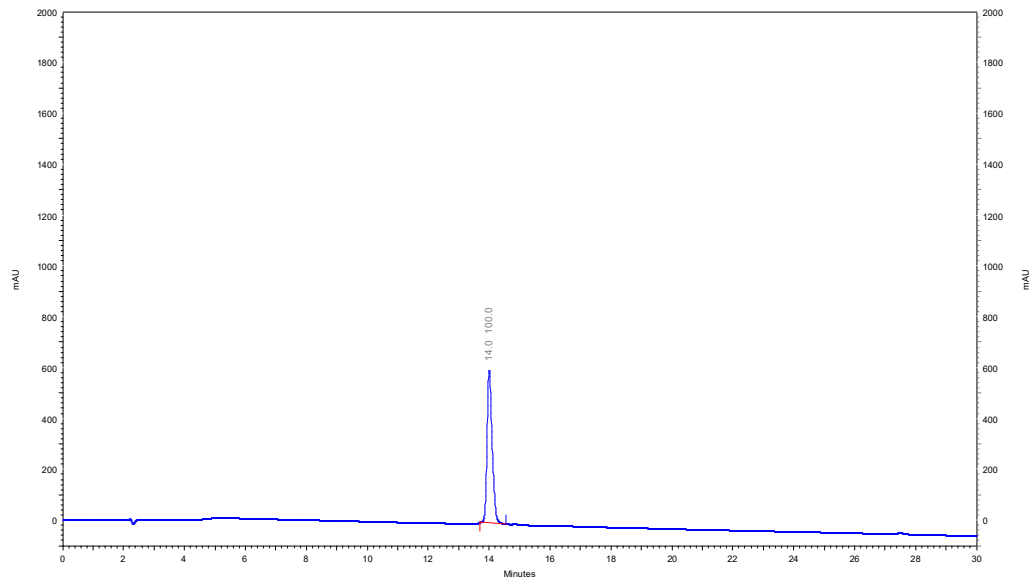


Figure S3: RP-HPLC chromatogram obtained for Melm-PP4-3.1.

PG-AGD-75Junho2021 #1 RT: 0.01 AV: 1 NL: 4.39E7
 T: + p ESI Full ms [50.00-2000.00]

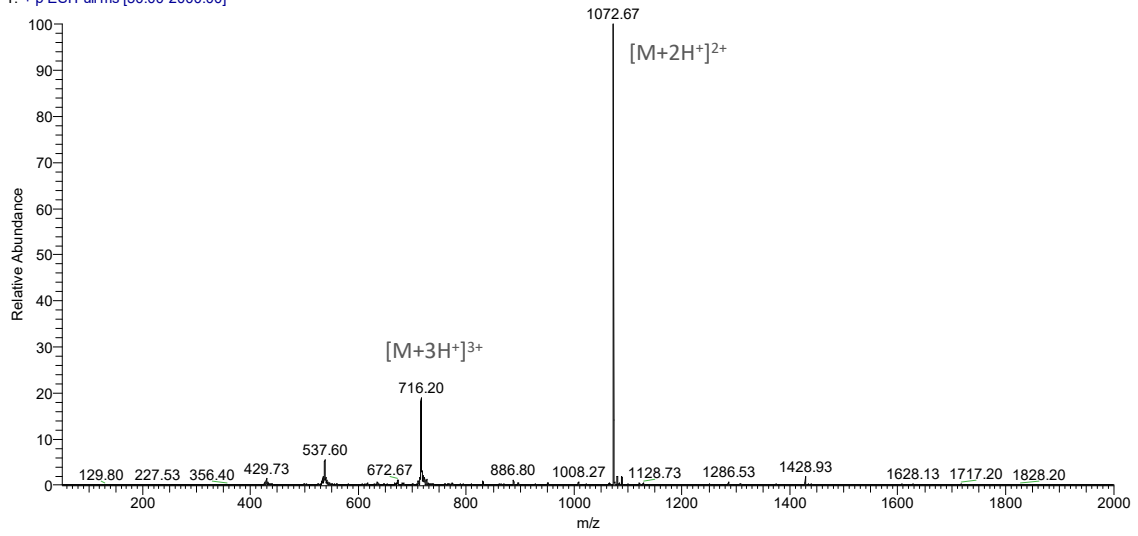


Figure S4: Full ESI-IT MS (positive mode) obtained for Melm-PP4-3.1.

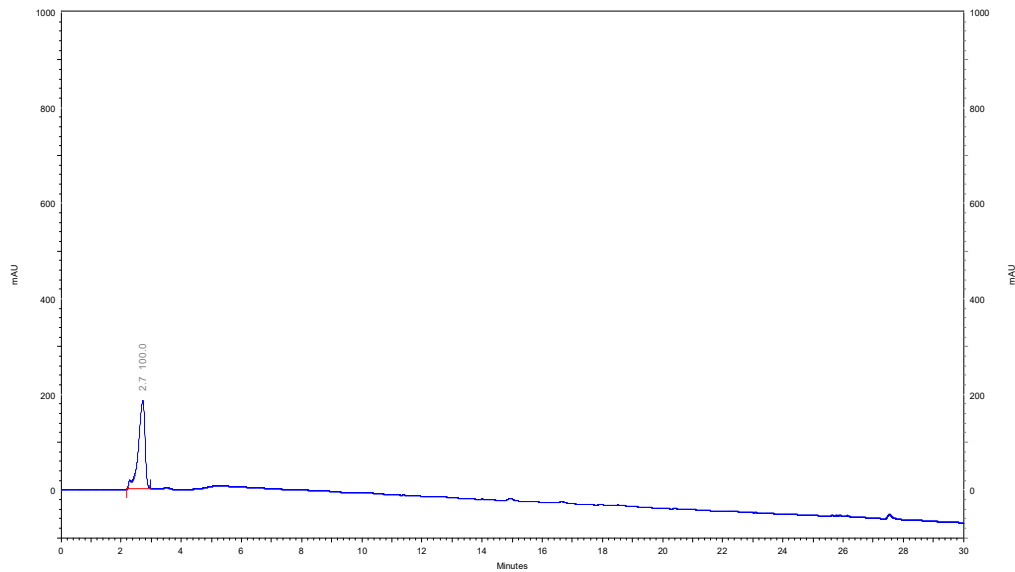


Figure S5: RP-HPLC chromatogram obtained for PP4.

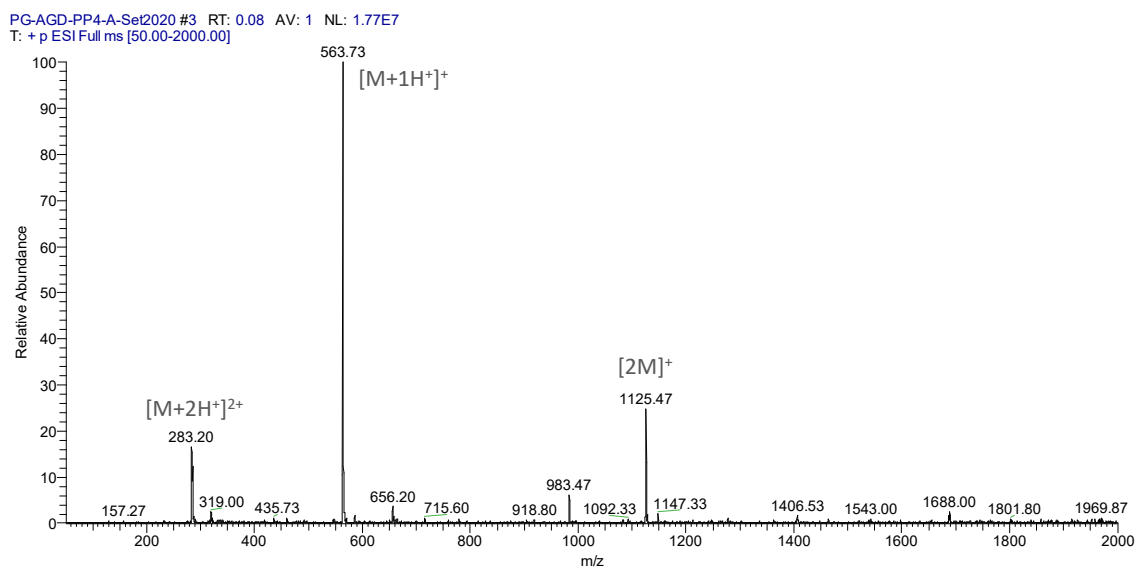


Figure S6: Full ESI-IT MS (positive mode) obtained for PP4.

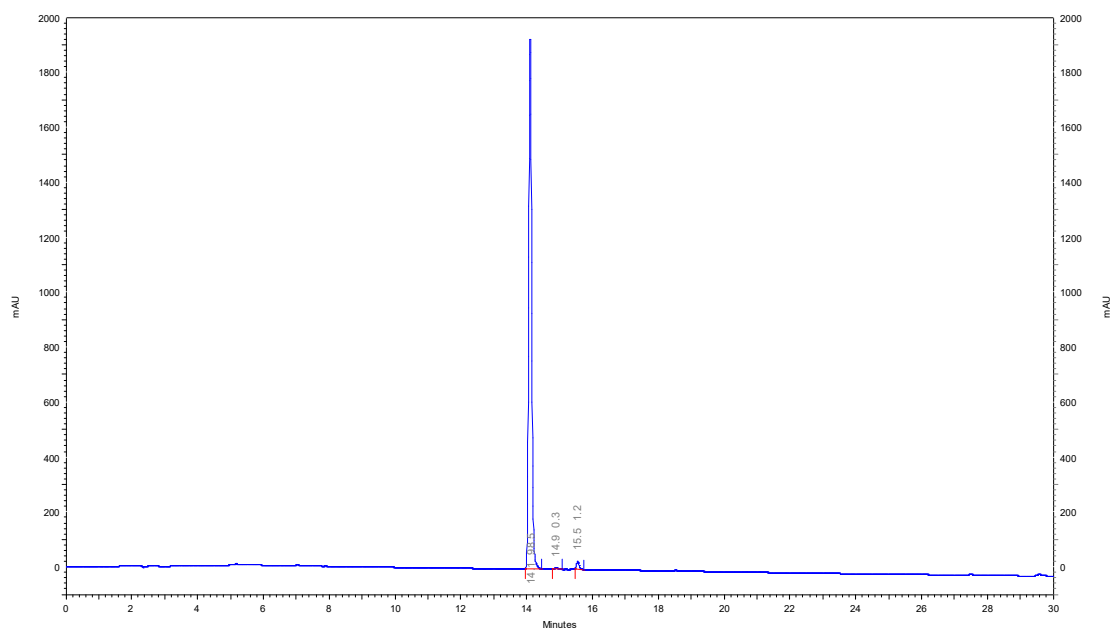


Figure S7: RP-HPLC chromatogram obtained for 3.1.

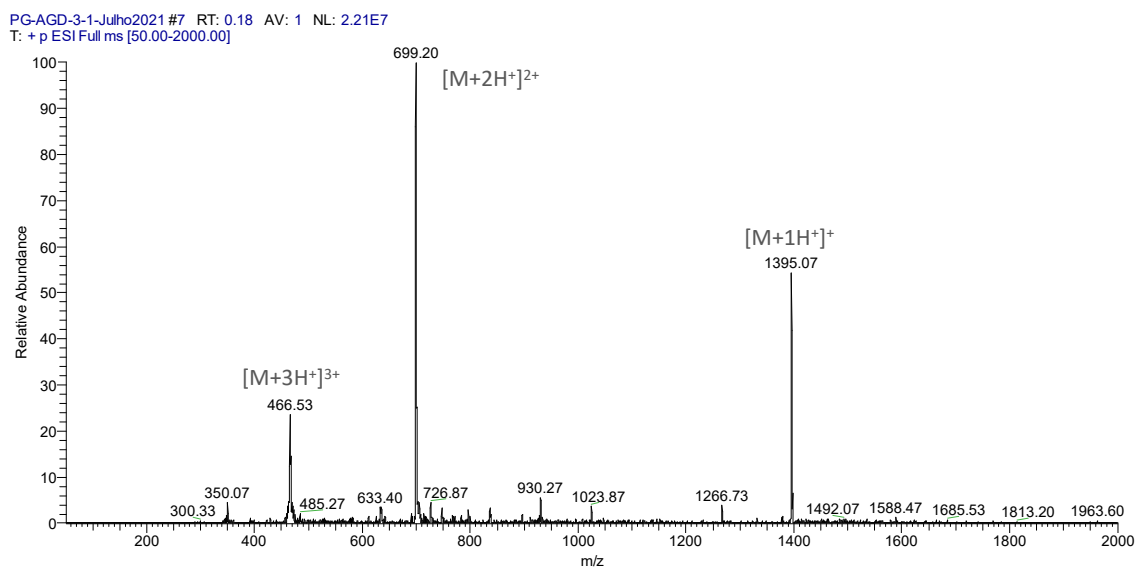


Figure S8: Full ESI-IT MS (positive mode) obtained for 3.1.

Table S1: Antibiotic resistance pattern of MDR clinical isolates PA004, KP010 and SA007

| Isolate | Antibiotic resistance pattern |
|---------|---|
| PA004 | CIP, GEN, IPM, TOB, TZP |
| KP010 | AMC, AMP, CAZ, CIP, CTX, CXM, ERT, IPM, LEV, NIT, TZP |
| SA007* | CIP, CLI, ERI, FOX, GEN, LEV, MOX, OXA |

AMC: amoxicillin/clavulanic acid; AMP: ampicillin; CAZ: ceftazidime; CIP: ciprofloxacin; CLI: clindamycin; CTX: cefotaxime; CXM: cefuroxime sodium; ERI: erythromycin; ERT: ertapenem; FOX: ceftoxitin; GEN: gentamicin; IPM: imipenem; LEV: levofloxacin; MOX: moxifloxacin; NIT: nitrofurantoin; OXA: oxacillin; TOB: tobramycin; TZP: piperacillin/tazobactam; * Methicillin-resistant *S. aureus* (MRSA)

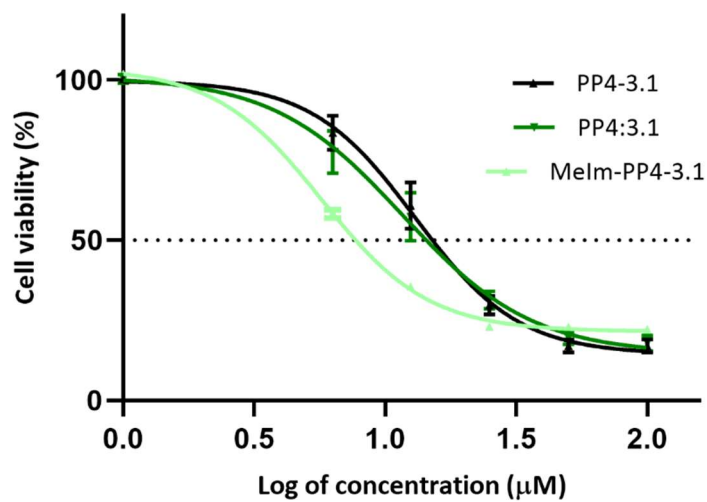


Figure S9: Cell viability (%) versus the logarithm of test peptide concentration (µM).

Supplementary Materials for section 2.4

Submitted to International Journal of Antimicrobial Agents

INSTRUMENTAL ANALYSIS

The ESI-IT-MS analysis were run in a Thermo Finnigan LCQ Deca XP Max LC/MSn instrument operating with electrospray ionization and ion-trap (ESI-IT) quadrupole detection and the NMR analysis were run using a Bruker Avance III400 spectrometer from solutions of the compounds in Deuterated chloroform (CDCl_3 - Eurisotop), containing tetramethylsilane (TMS) as internal reference.

The RP-HPLC analyses were performed in a Hitachi-Merck LaChrom Elite system equipped with an L-2130 quaternary pump, an L-2455 diode-array detector (DAD) and an L220 thermostatted automated sampler. The samples were injected in a reverse-phase C18 column (125×4.0 mm ID and 5 μm pore size) with the elution gradient of 1 to 100% of B in A, using 0.05% aqueous trifluoro acetic acid (TFA) as solvent A and acetonitrile (ACN) as solvent B, and was run for 30 min at the flow rate of 1mL/min. The detection was performed at 220 nm.

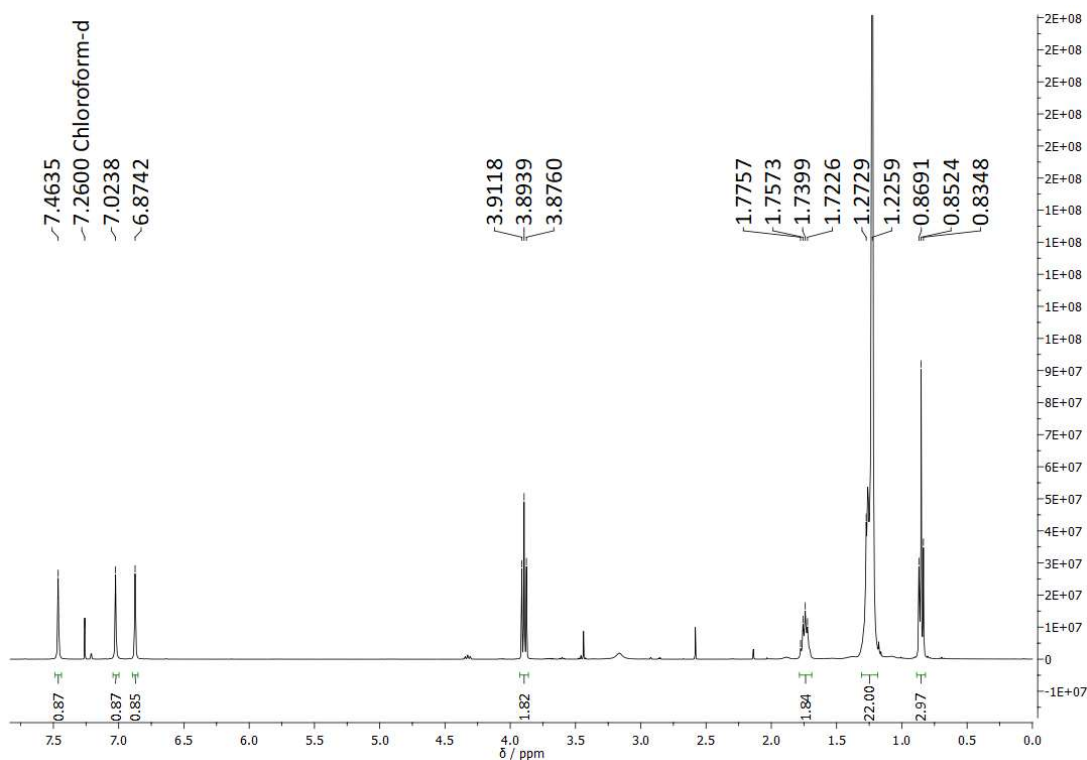


Figure S1. ¹H-NMR spectrum of 1-tetradecylimidazole (C₁₄-Im) (400 MHz, CDCl₃).

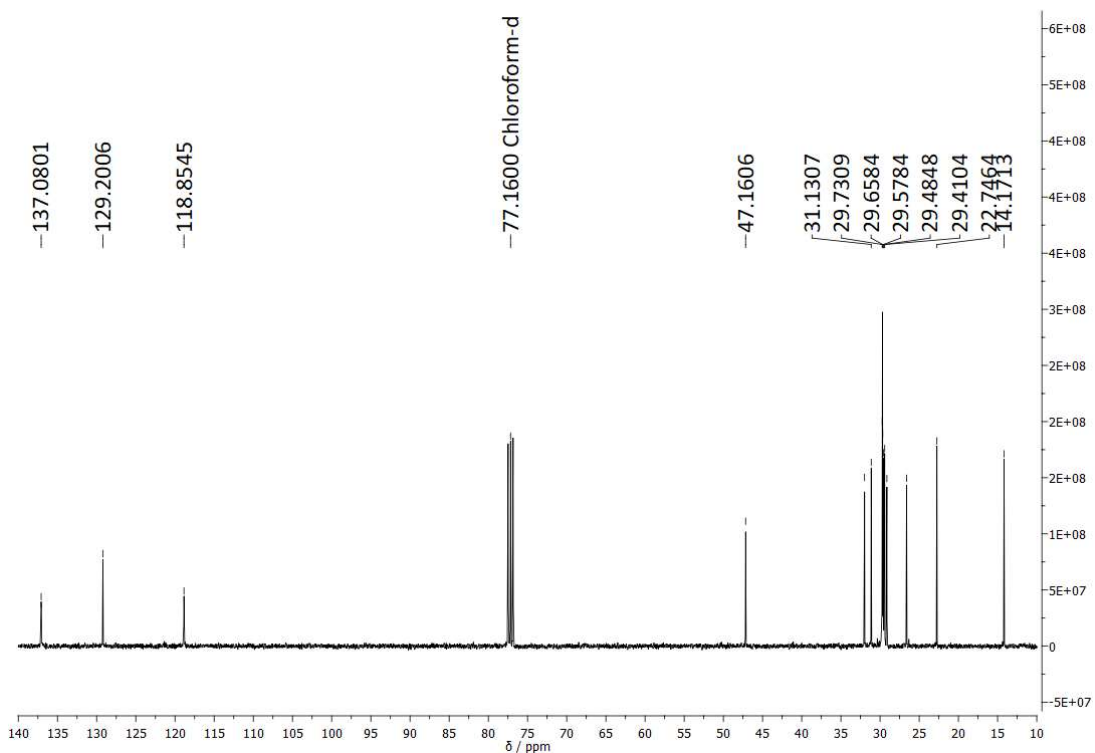


Figure S2. ¹³C-NMR spectrum of 1-tetradecylimidazole (C₁₄-Im) (100 MHz, CDCl₃).

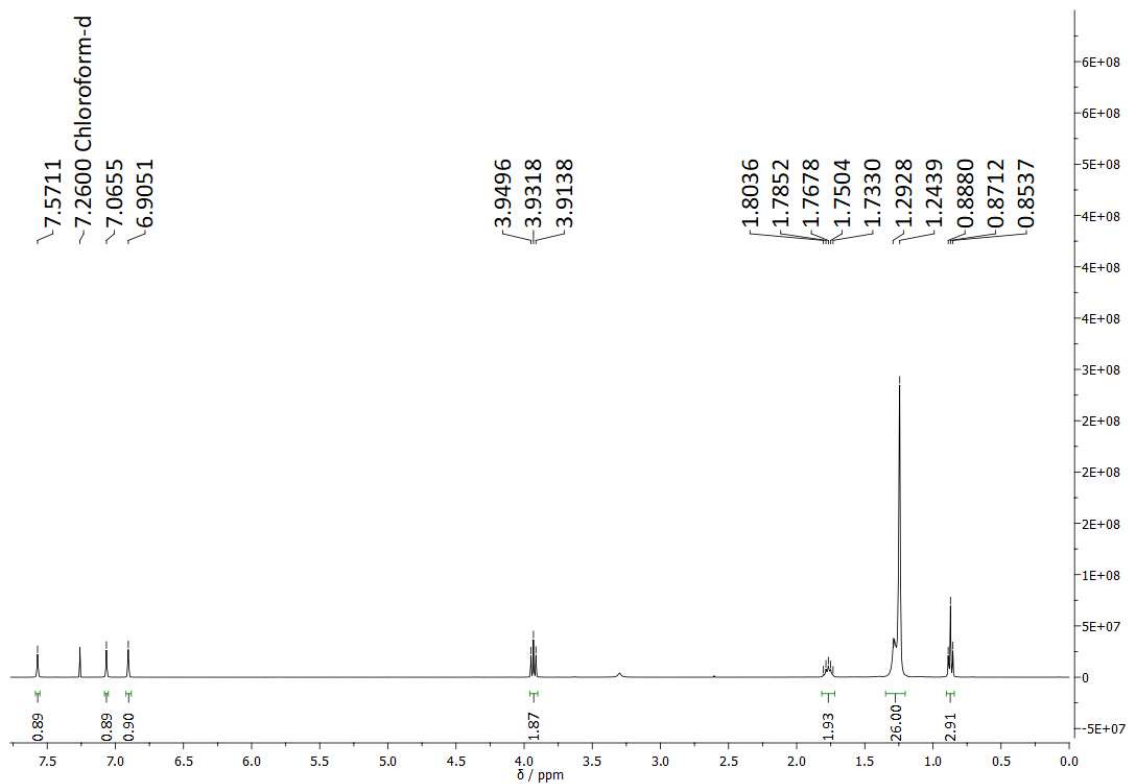


Figure S3. $^1\text{H-NMR}$ spectrum of 1-hexadecylimidazole ($\text{C}_{16}\text{-Im}$) (400 MHz, CDCl_3).

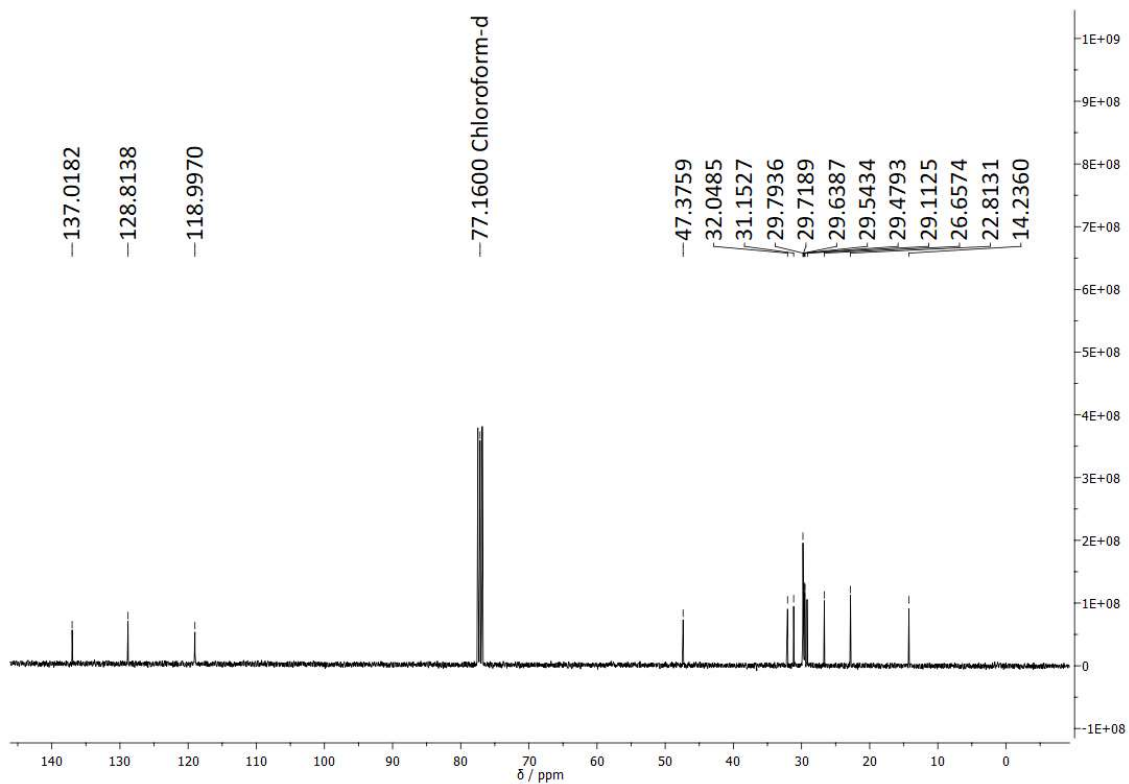


Figure S4. $^{13}\text{C-NMR}$ spectrum of 1-hexadecylimidazole ($\text{C}_{16}\text{-Im}$) (100 MHz, CDCl_3).

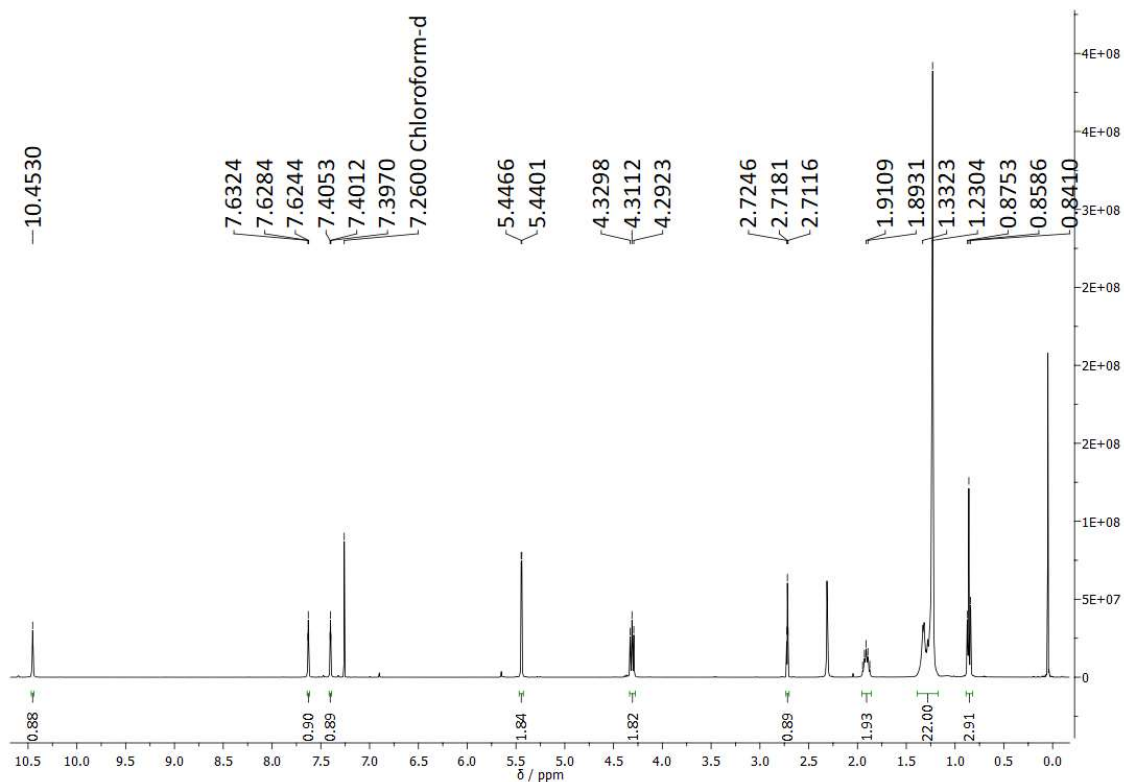


Figure S5. $^1\text{H-NMR}$ spectrum of 1-tetradecyl-3-(prop-2-enyl)imidazolium bromide (Pr- C_{14}Im) (400 MHz, CDCl_3).

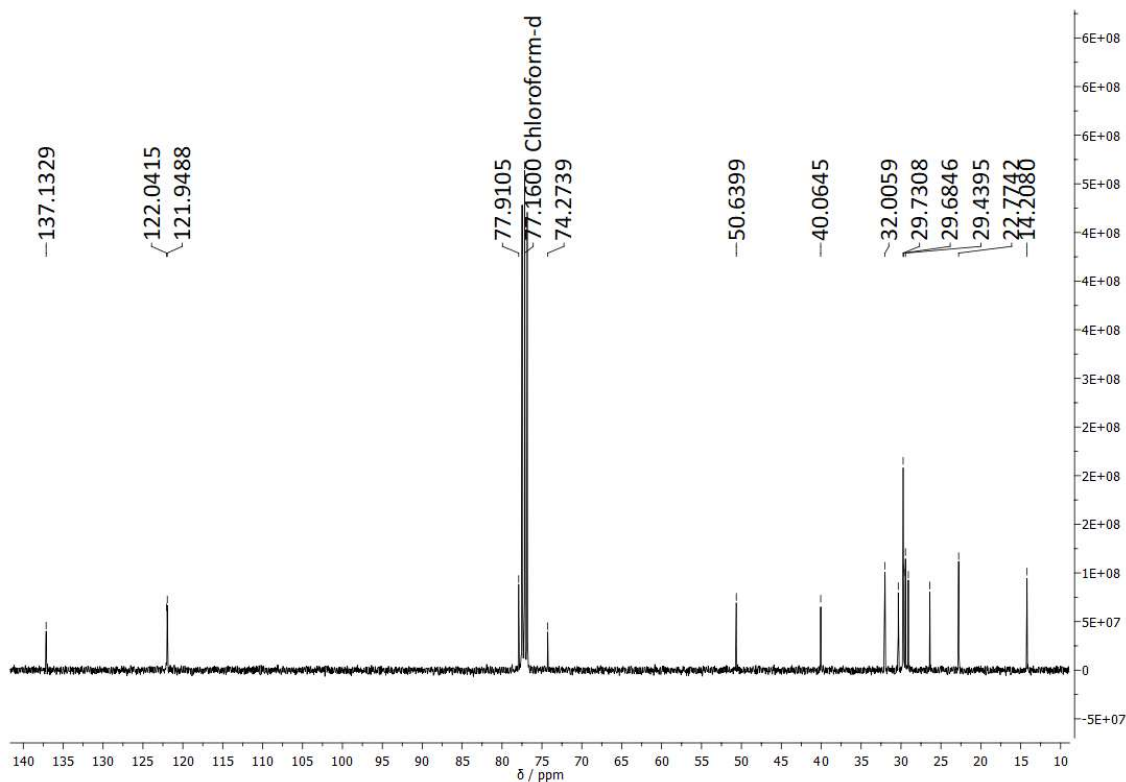


Figure S6. $^{13}\text{C-NMR}$ spectrum of 1-tetradecyl-3-(prop-2-enyl)imidazolium bromide (Pr- C_{14}Im) (100 MHz, CDCl_3).

PG-AGD-38 #27 RT: 0.78 AV: 1 NL: 1.09E8
T: + p ESI Full ms [50.00-2000.00]

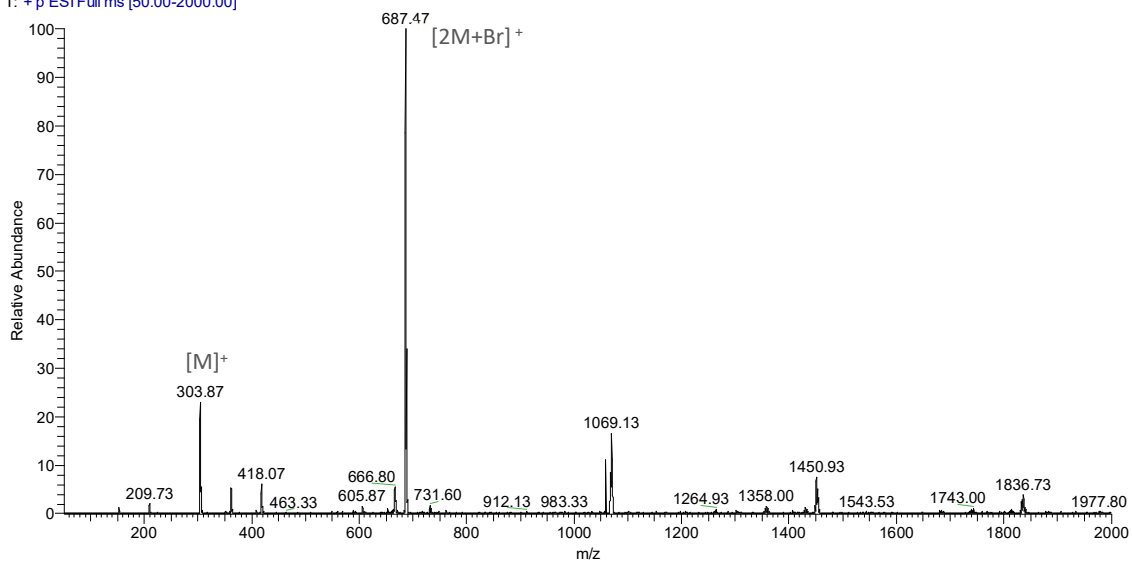


Figure S7. ESI-IT(+) mass spectrum 1-tetradecyl-3-(prop-2-enyl)imidazolium bromide (Pr-C₁₄Im).

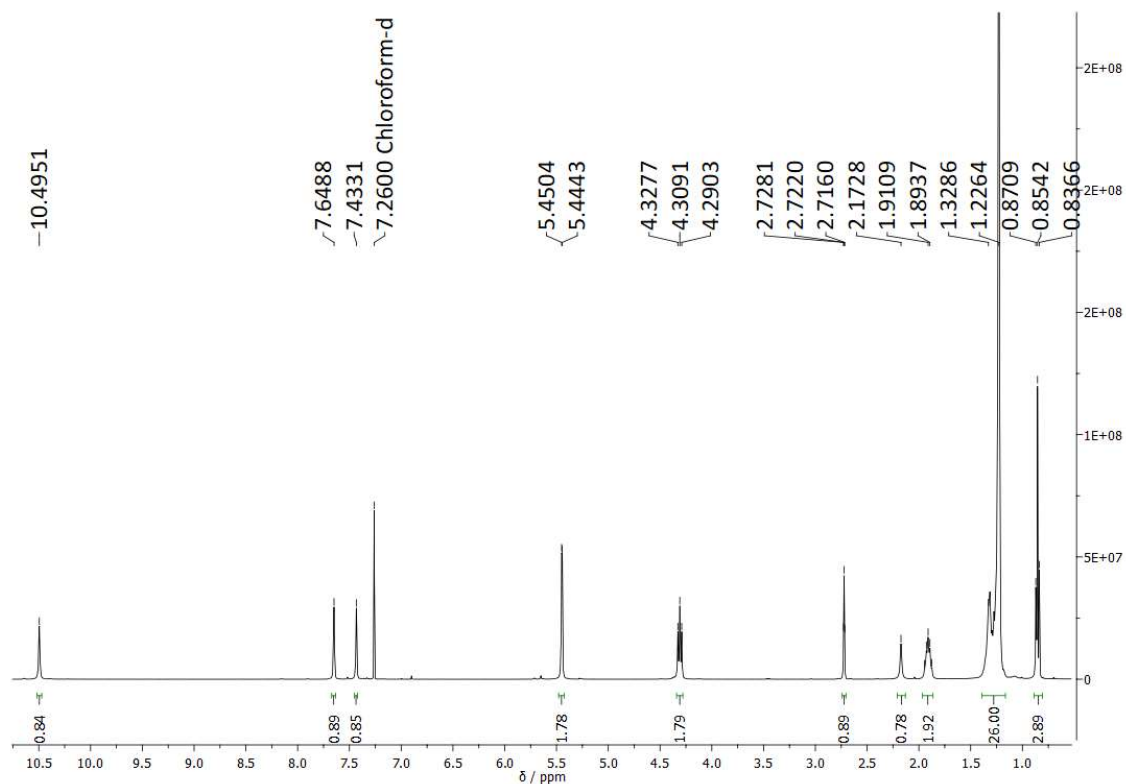


Figure S8. ¹H-NMR spectrum of 1-hexadecyl-3-(prop-2-enyl)imidazolium bromide (Pr-C₁₆Im) (400 MHz, CDCl₃).

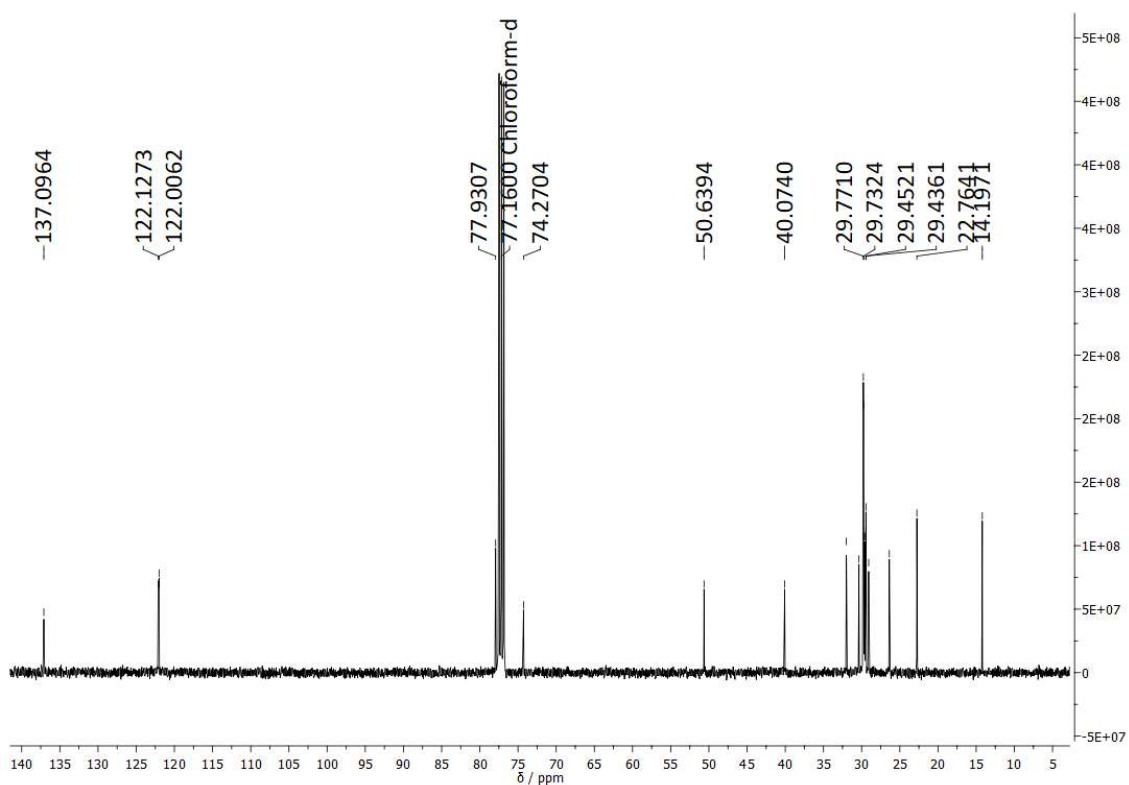


Figure S9. ^{13}C -NMR spectrum of 1-hexadecyl-3-(prop-2-enyl)imidazolium bromide (Pr-C₁₆Im) (100 MHz, CDCl₃).

AGD-25_180323093146 #88 RT: 1.52 AV: 1 NL: 3.44E6
T: +p ESI Full ms [90.00-2000.00]

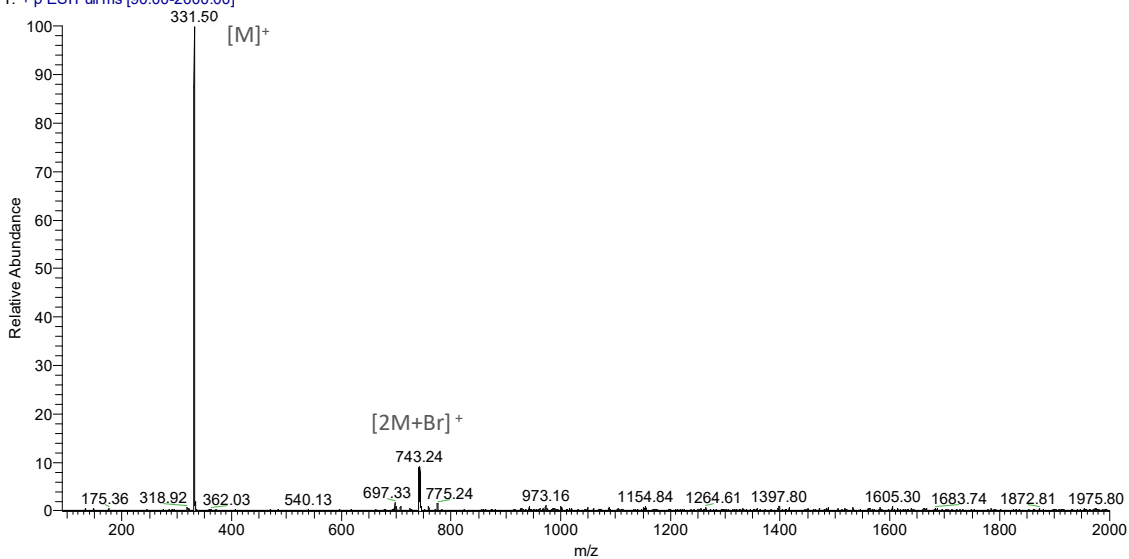


Figure S10. ESI-IT(+) mass spectrum 1-hexadecyl-3-(prop-2-enyl)imidazolium bromide (Pr-C₁₆Im).

PG-AGD-9-Junho2020_200618084315 #11 RT: 0.30 AV: 1 NL: 1.27E7
 T: +p ESI Full ms [50.00-2000.00]

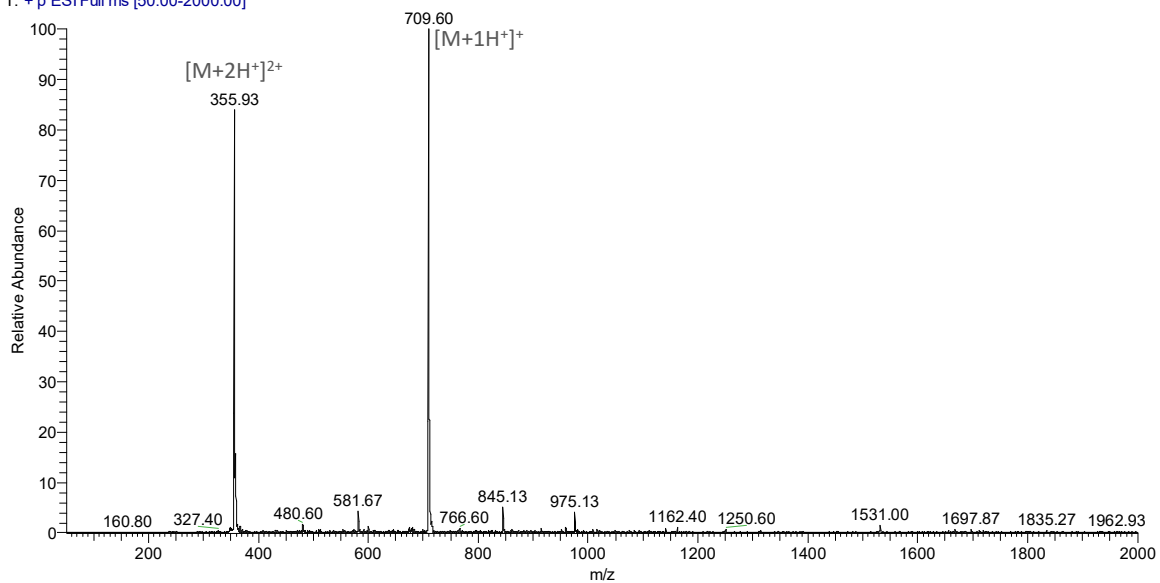


Figure S11. ESI-IT(+) mass spectrum of the KTTK(Melm)S conjugate

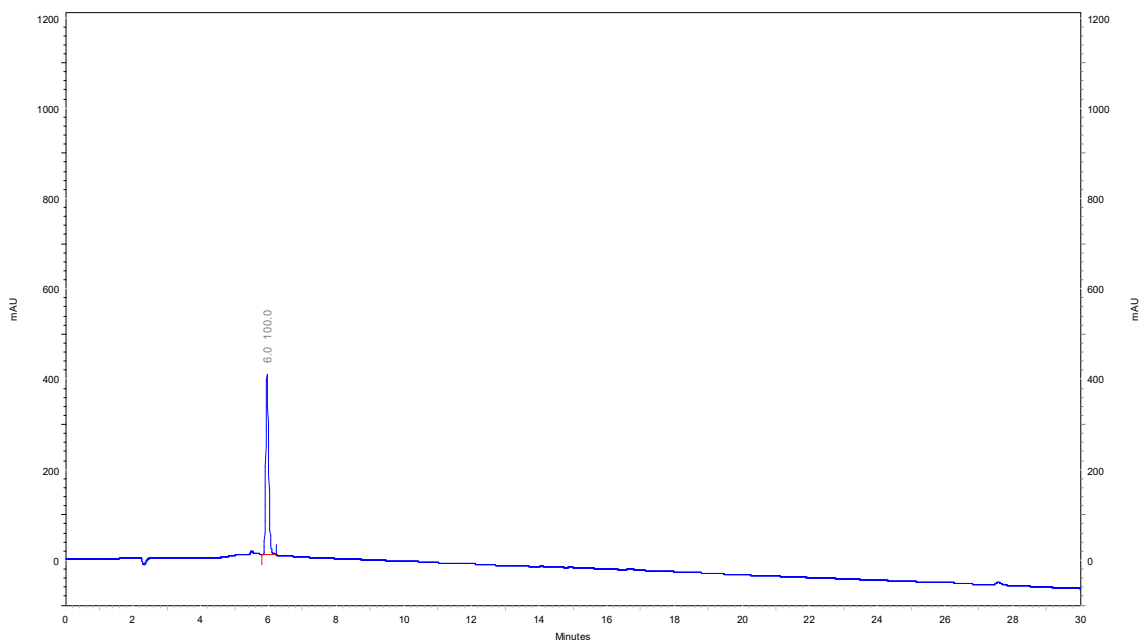


Figure S12. RP-HPLC chromatogram of the KTTK(Melm)S conjugate

PG-AGD-11-Junho2020_200623102258 #2 RT: 0.05 AV: 1 NL: 5.30E7
 T: +p ESI Full ms [50.00-2000.00]

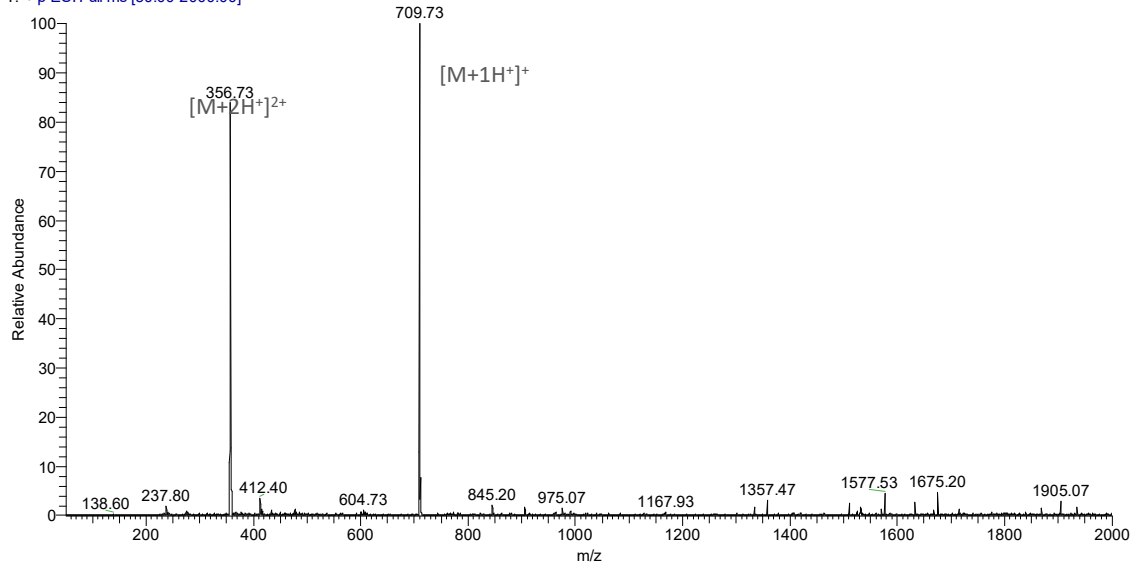


Figure S13. ESI-IT(+) mass spectrum of the K(Melm)TTKS conjugate

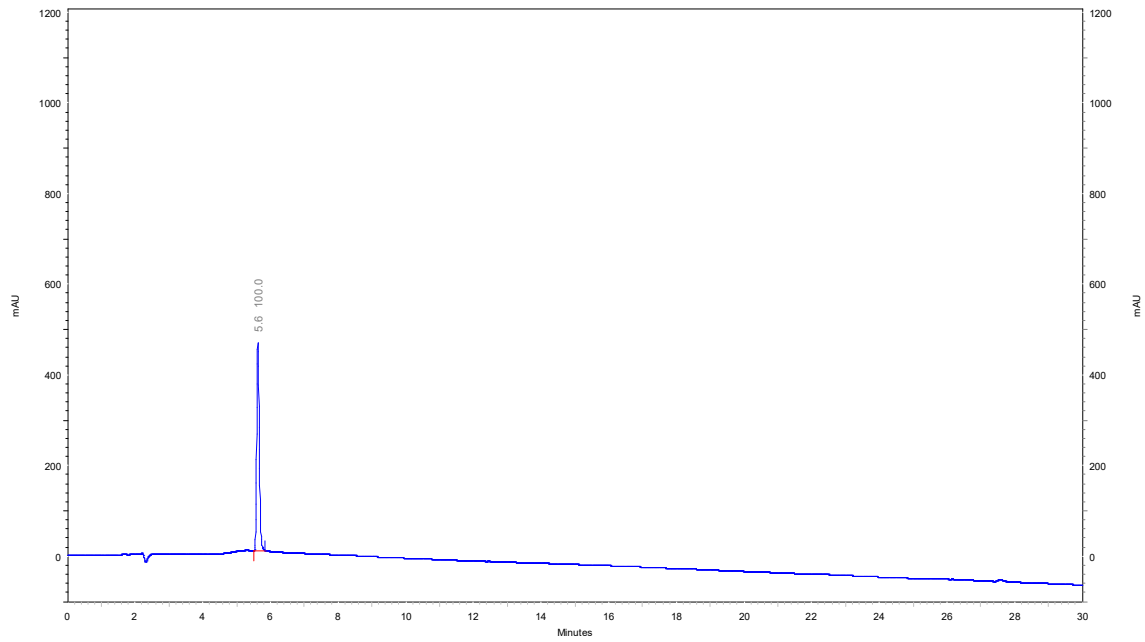


Figure S14. RP-HPLC chromatogram of the K(Melm)TTKS conjugate

AGD-13-FinalLiof_180327083635 #12 RT: 0.33 AV: 1 NL: 2.83E7
 T: + p ESI Full ms [50.00-2000.00]

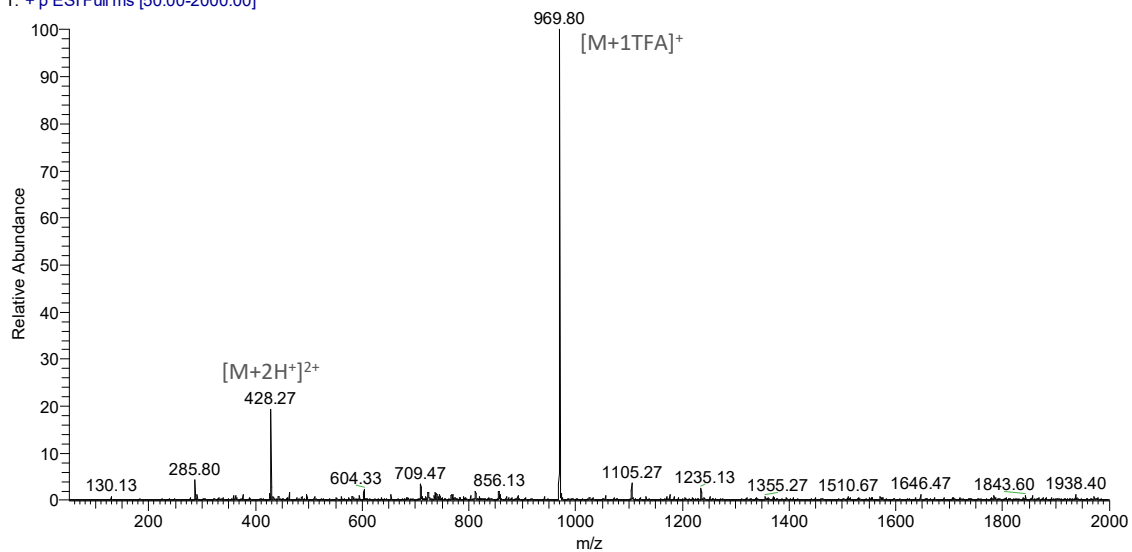


Figure S15. ESI-IT(+) mass spectrum of the K(Melm)TTK(Melm)S conjugate

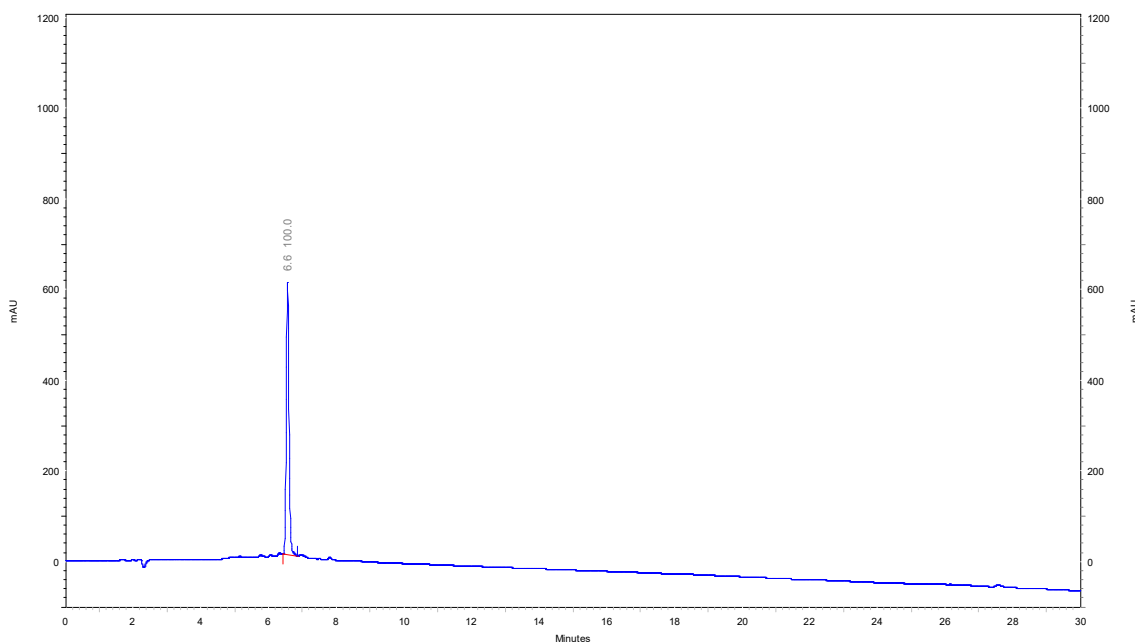


Figure S16. RP-HPLC chromatogram of the K(Melm)TTK(Melm)S conjugate

PG-AGD-28-Junho2020_200623103201 #5 RT: 0.12 AV: 1 NL: 5.03E7
 T: +p ESI Full ms [50.00-2000.00]

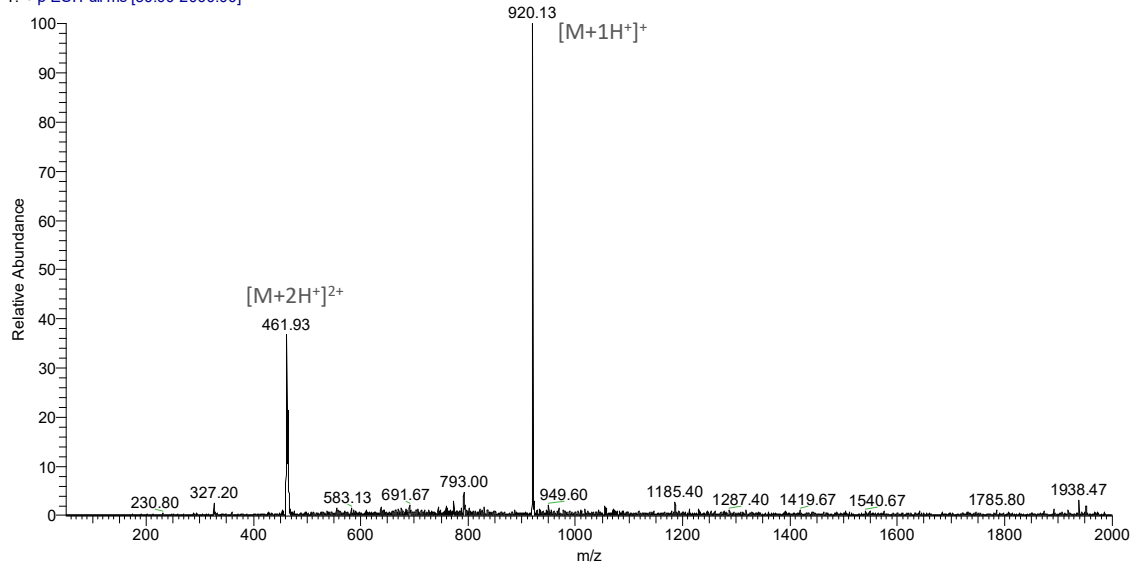


Figure S17. ESI-IT(+) mass spectrum of the KTTK(C₁₆Im)S conjugate

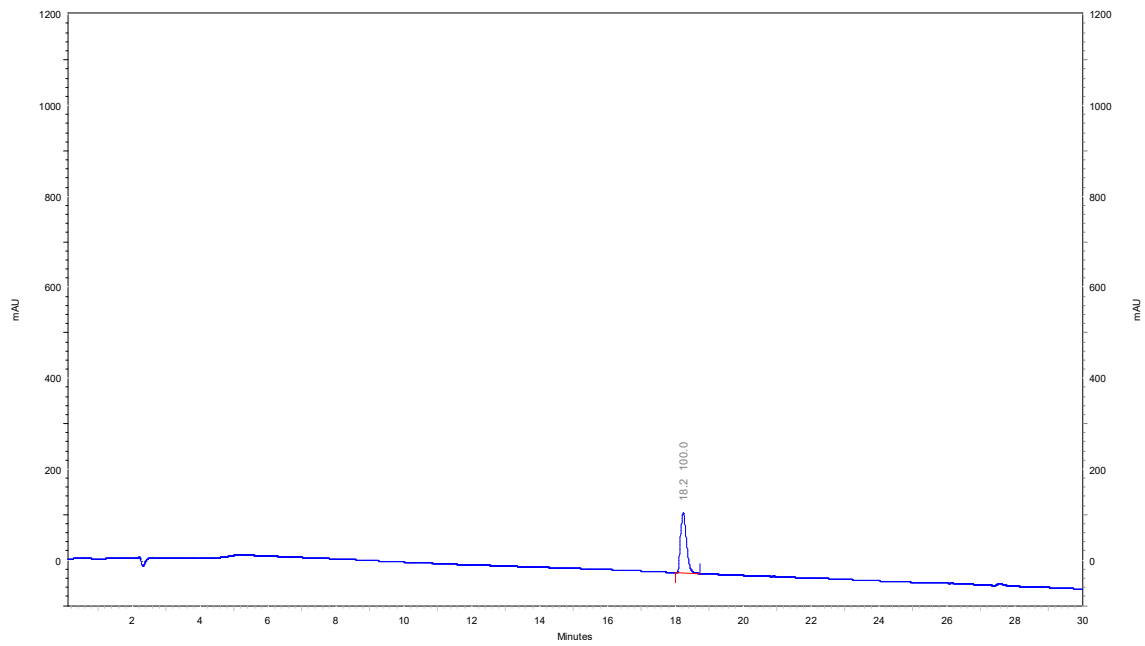


Figure S18. RP-HPLC chromatogram of the KTTK(C₁₆Im)S conjugate

PG-AGD-65-Junho2020_200623103615 #1 RT: 0.00 AV: 1 NL: 4.30E7
 T: +p ESI Full ms [50.00-2000.00]

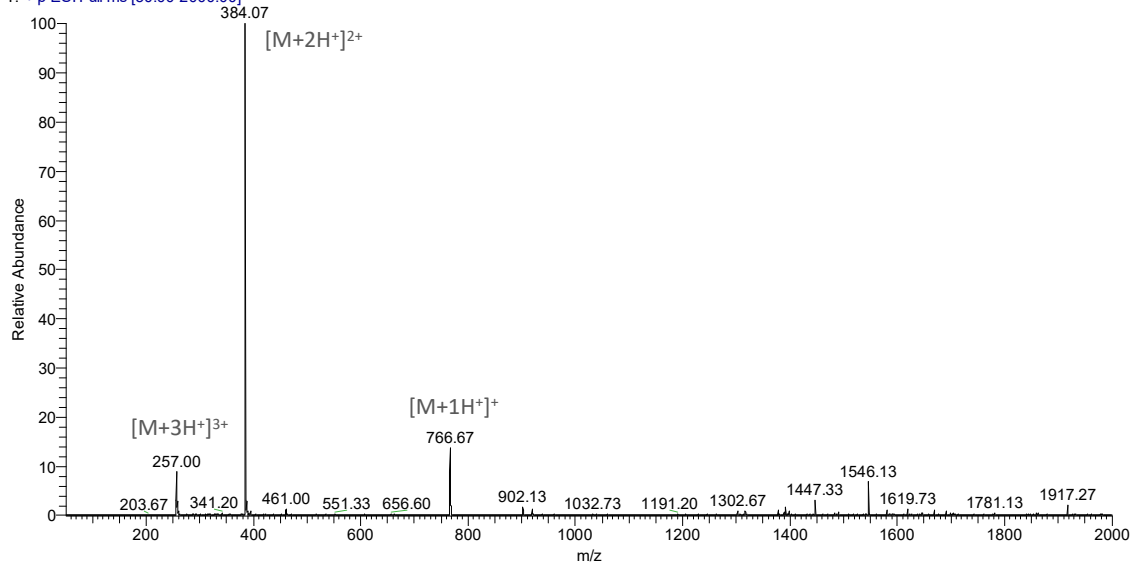


Figure S19. ESI-IT(+) mass spectrum of the Melm-KTTKS conjugate

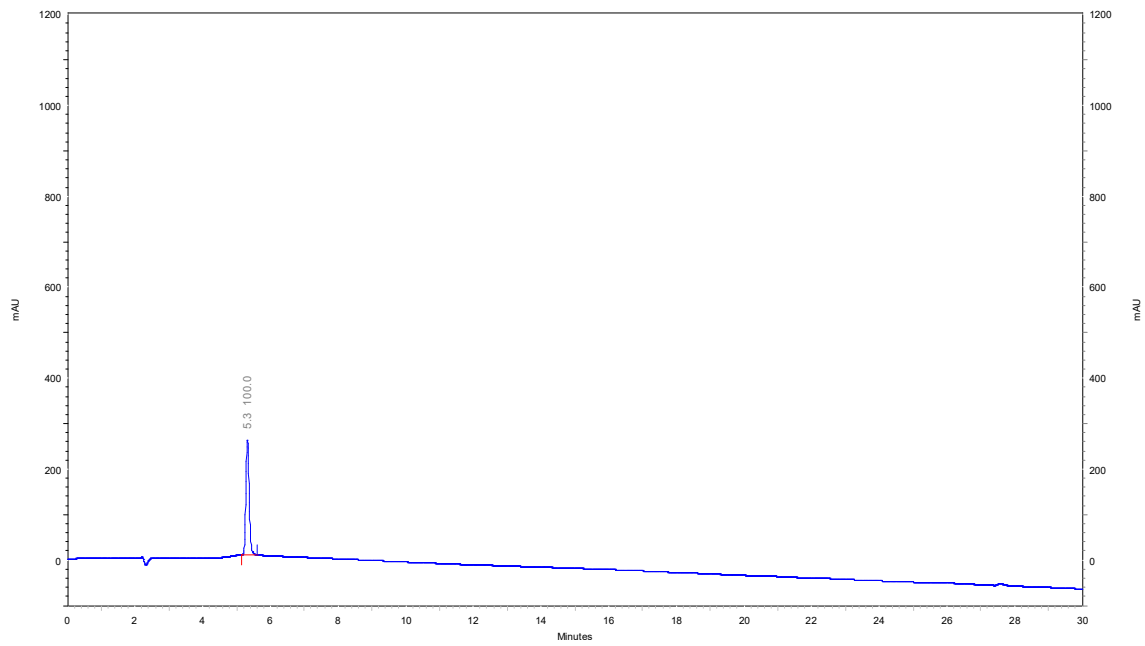


Figure S20. RP-HPLC chromatogram of the Melm-KTTKS conjugate

PG-AGD-66-Junho2020_200623103906 #5 RT: 0.12 AV: 1 NL: 7.56E7
 T: +p ESI Full ms [50.00-2000.00]

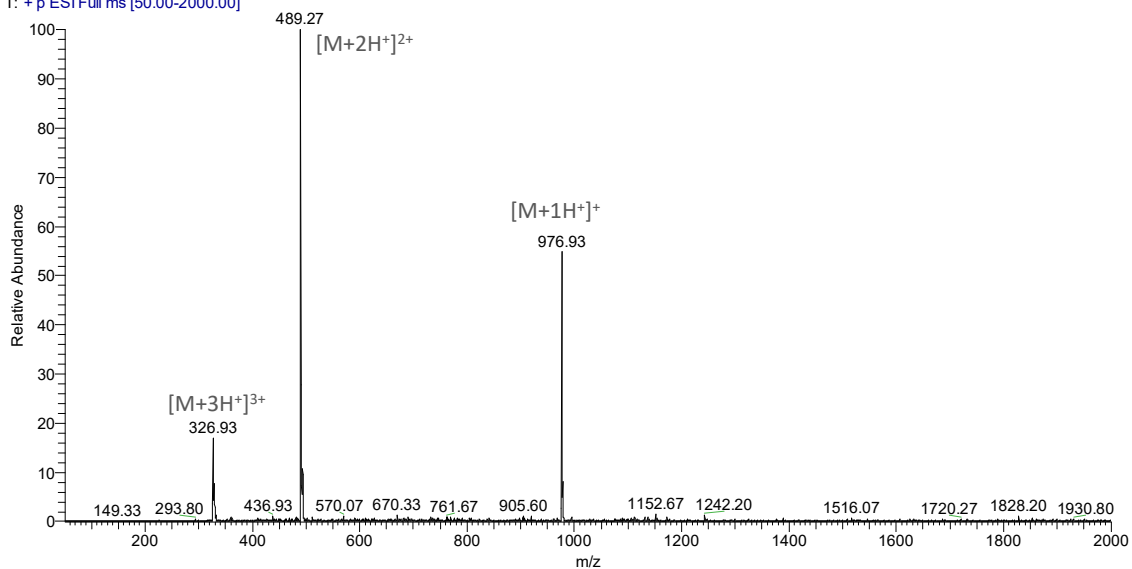


Figure S21. ESI-IT(+) mass spectrum of the C₁₆Im-KTTKS conjugate

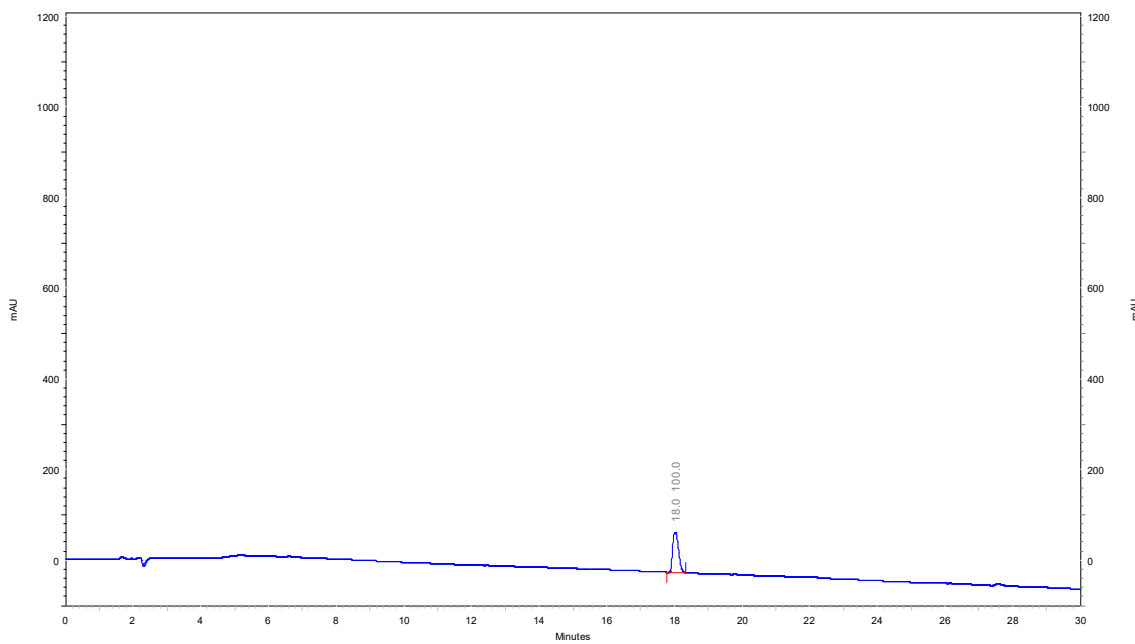


Figure S22. RP-HPLC chromatogram of the C₁₆Im-KTTKS conjugate

AGD-41-Final_Liof_181126141348 #16 RT: 0.42 AV: 1 NL: 3.52E7
 T: +p ESI Full ms [50.00-2000.00]

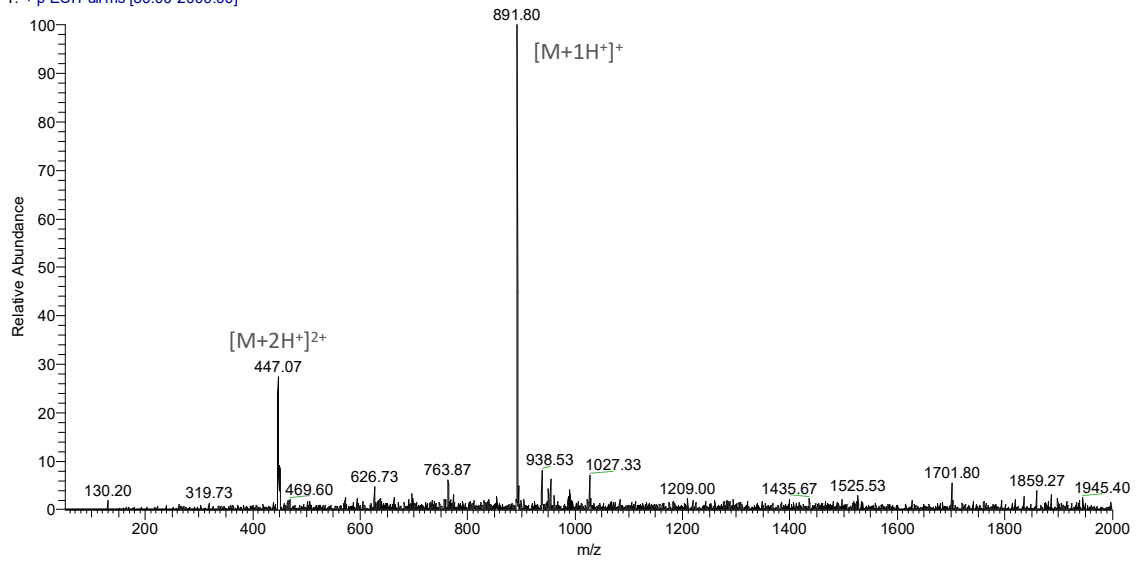


Figure S23. ESI-IT(+) mass spectrum of the KTTK(C₁₄Im)S conjugate

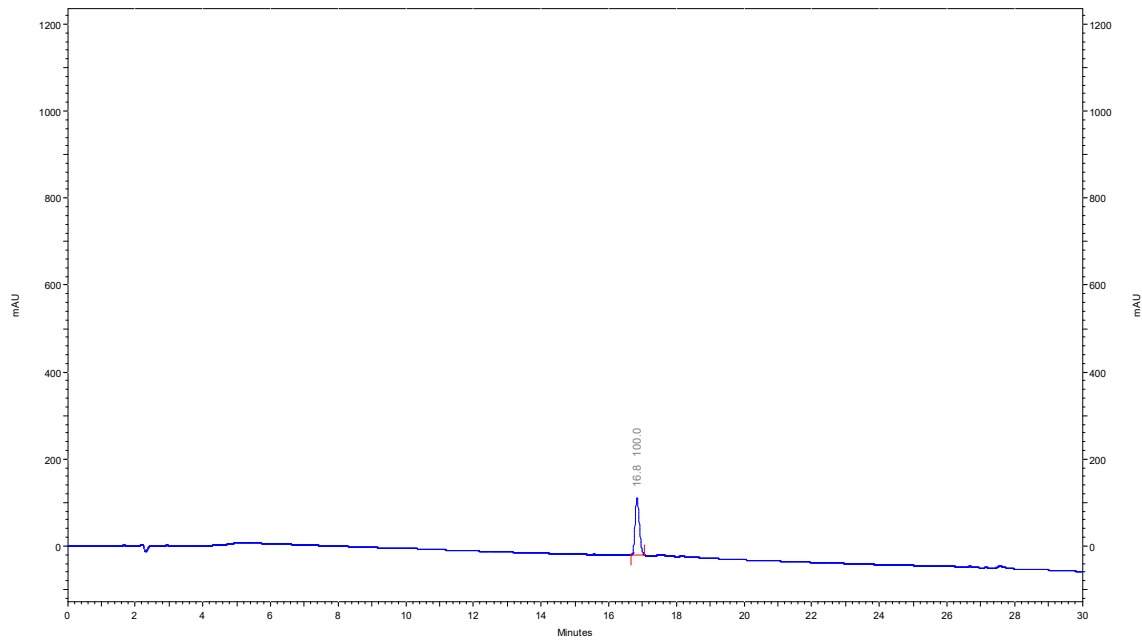


Figure S24. RP-HPLC chromatogram of the KTTK(C₁₄Im)S conjugate

PP4B_final_170928132825 #33 RT: 0.68 AV: 1 NL: 3.79E7
 T: +p ESI Full ms [50.00-2000.00]

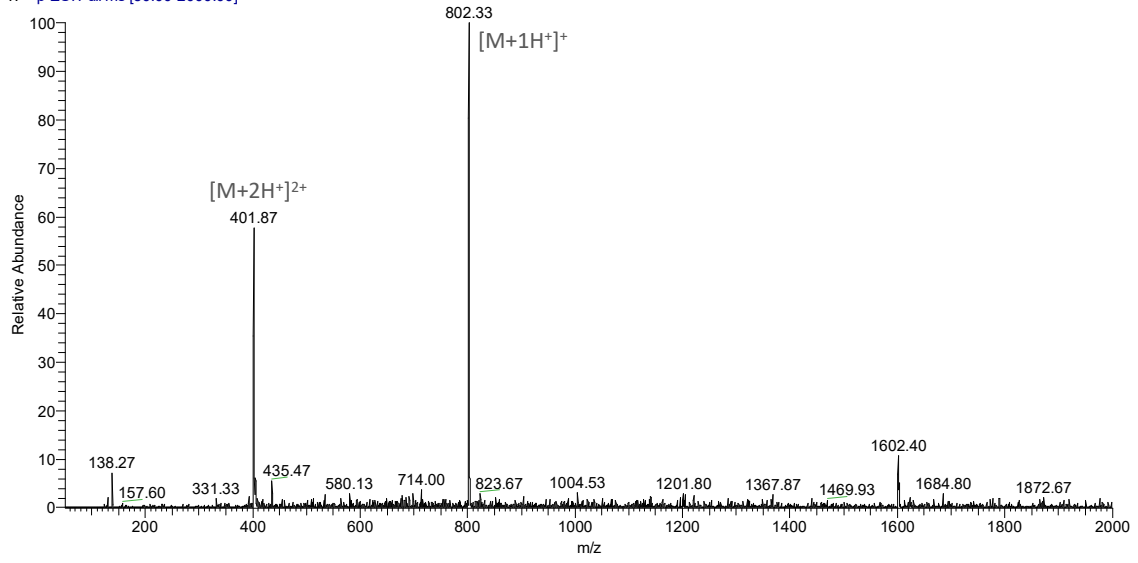


Figure S25. ESI-IT(+) mass spectrum of the reference lipopeptide C_{16} -KTTKS- NH_2

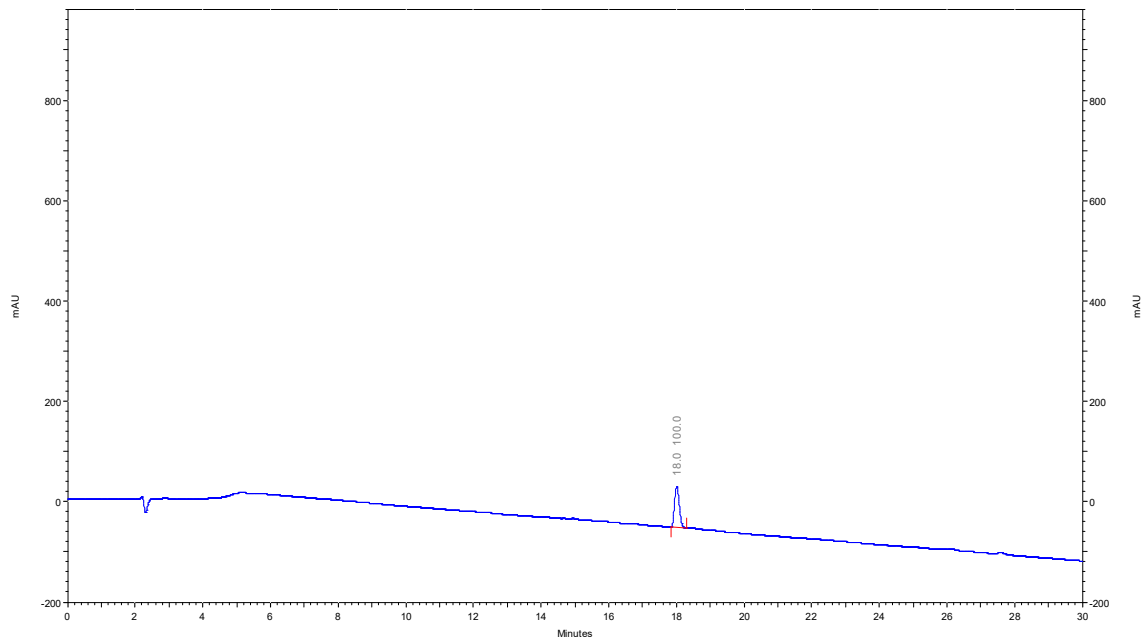


Figure S26. RP-HPLC chromatogram of the reference lipopeptide C_{16} -KTTKS- NH_2

PG-AGD-81-crudeLiof_200623104616 #3 RT: 0.07 AV: 1 NL: 1.33E8
 T: +p ESI Full ms [50.00-2000.00]

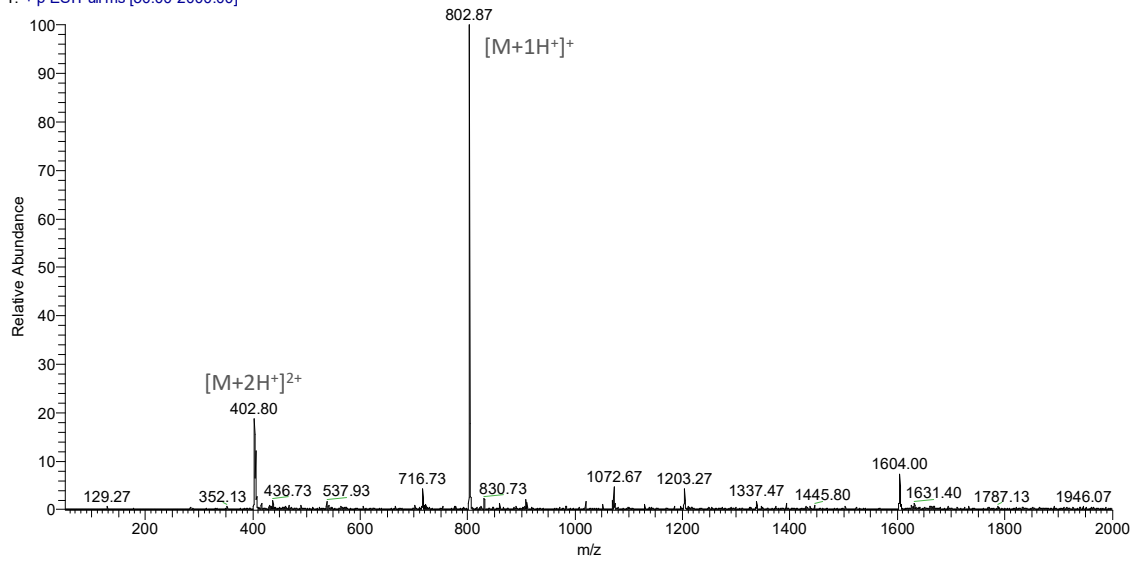


Figure S27. ESI-IT(+) mass spectrum of the reference lipopeptide C₁₆-KTTKS-OH

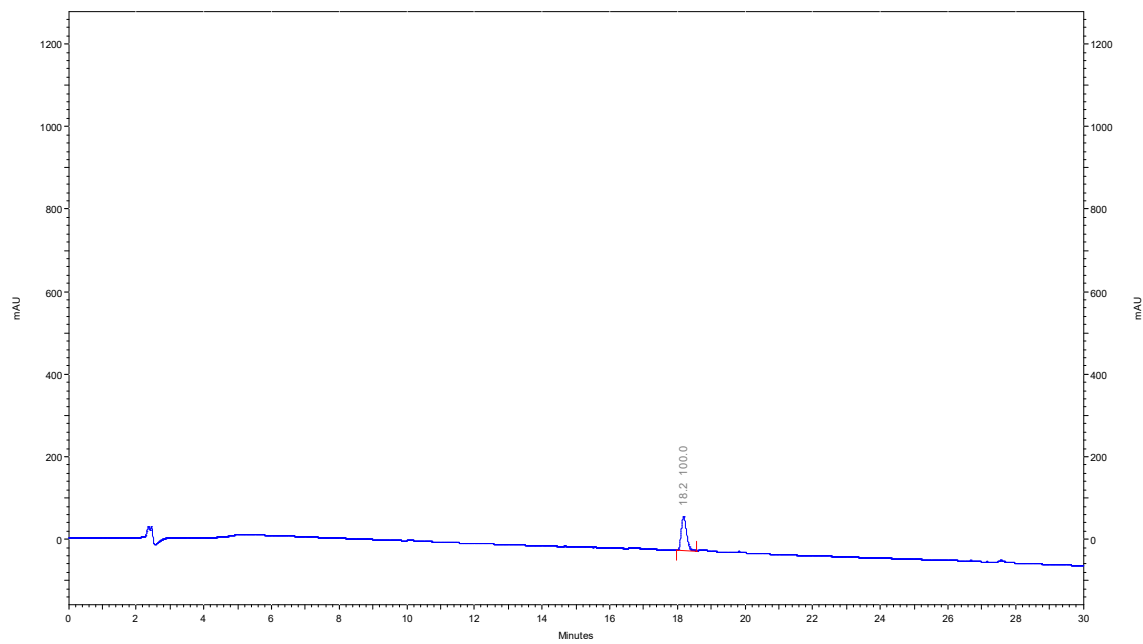


Figure S28. RP-HPLC chromatogram of the reference lipopeptide C₁₆-KTTKS-OH

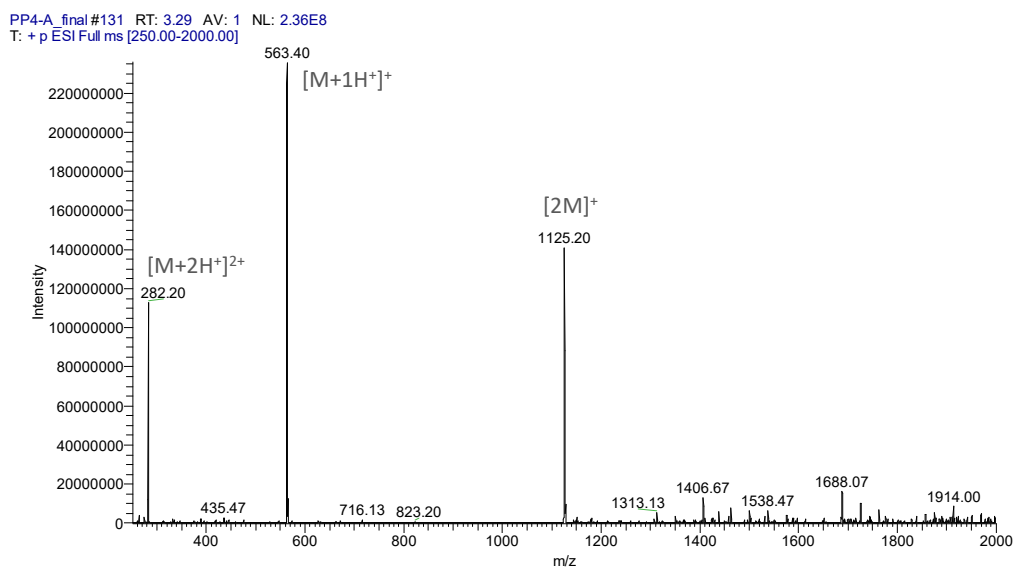


Figure S29. ESI-IT(+) mass spectrum of the parent "pentapeptide-4", KTTKS

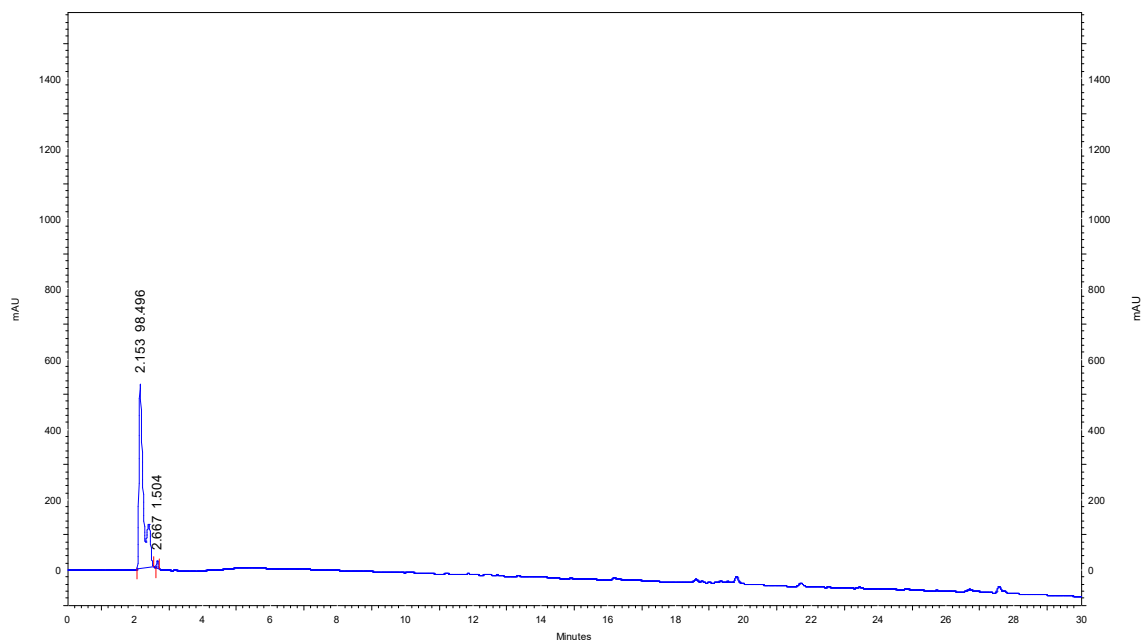


Figure S30. RP-HPLC chromatogram of the parent "pentapeptide-4", KTTKS

Table S1. Antibiotic resistance pattern of MDR clinical isolates of PA004, KP010 and SA007.

| Isolate | Antibiotic resistance pattern |
|---------|---|
| PA004 | CIP, GEN, IPM, TOB, TZP |
| KP010 | AMC, AMP, CAZ, CIP, CTX, CXM, ERT, IPM, LEV, NIT, TZP |
| SA007* | CIP, CLI, ERI, FOX, GEN, LEV, MOX, OXA |

AMC: amoxicillin/clavulanic acid; AMP: ampicillin; CAZ: ceftazidime; CIP: ciprofloxacin; CLI: clindamycin; CTX: cefotaxime; CXM: cefuroxime sodium; ERI: erythromycin; ERT: ertapenem; FOX: cefoxitin; GEN: gentamicin; IPM: imipenem; LEV: levofloxacin; MOX: moxifloxacin; NIT: nitrofurantoin; OXA: oxacillin; TOB: tobramycin; TZP: piperacillin/Tazobactam; * Methicillin-resistant *S. aureus* (MRSA)

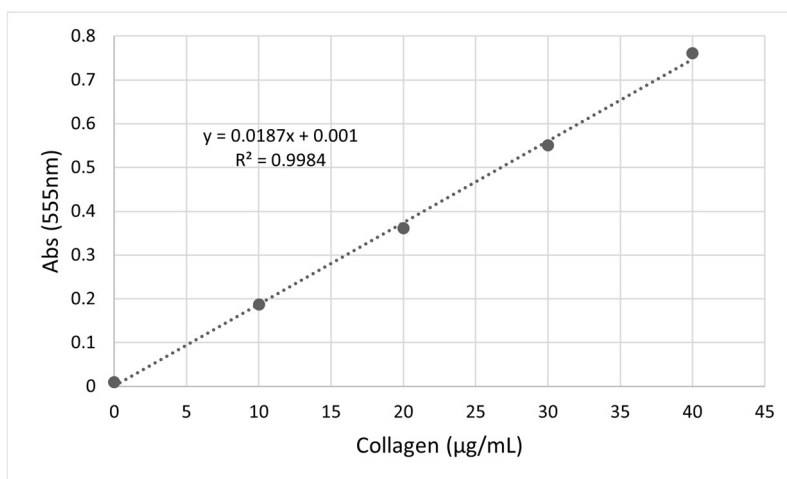


Figure S31. Collagen reference standard curve using rat collagen standard solutions.

Supplementary Materials for section 2.5

Manuscript in preparation

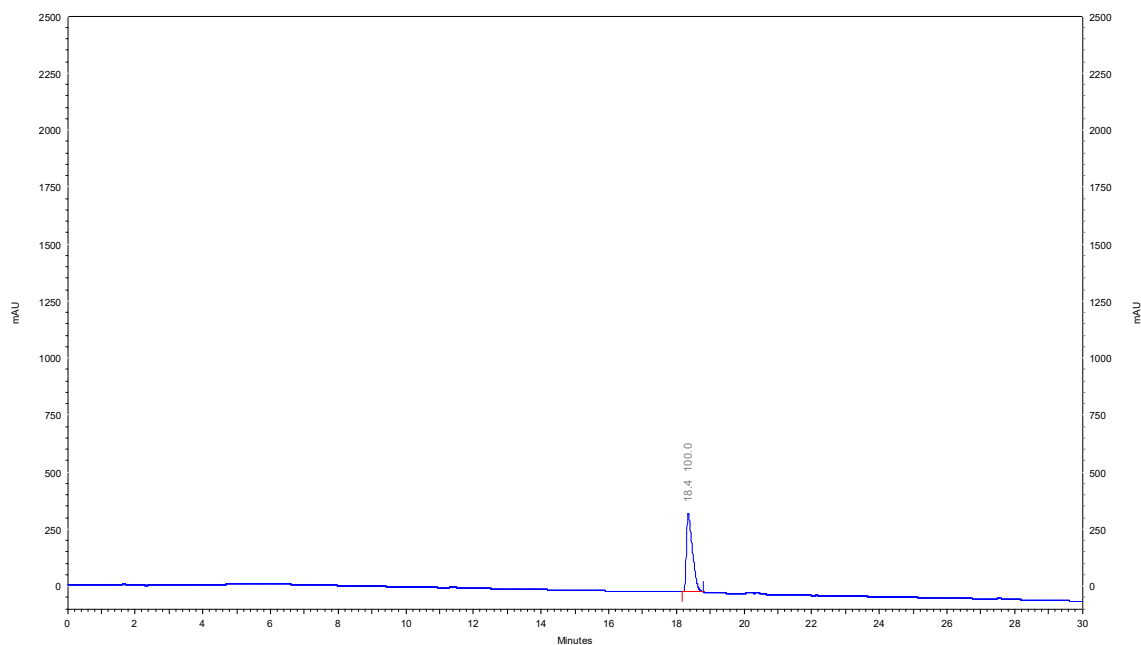


Figure S1. RP-HPLC chromatogram of the C₁₆-Im-KVK conjugate

PG-NT-AGD-56 #7 RT: 0.19 AV: 1 NL: 1.19E6
T: +p ESI Full ms [50.00-2000.00]

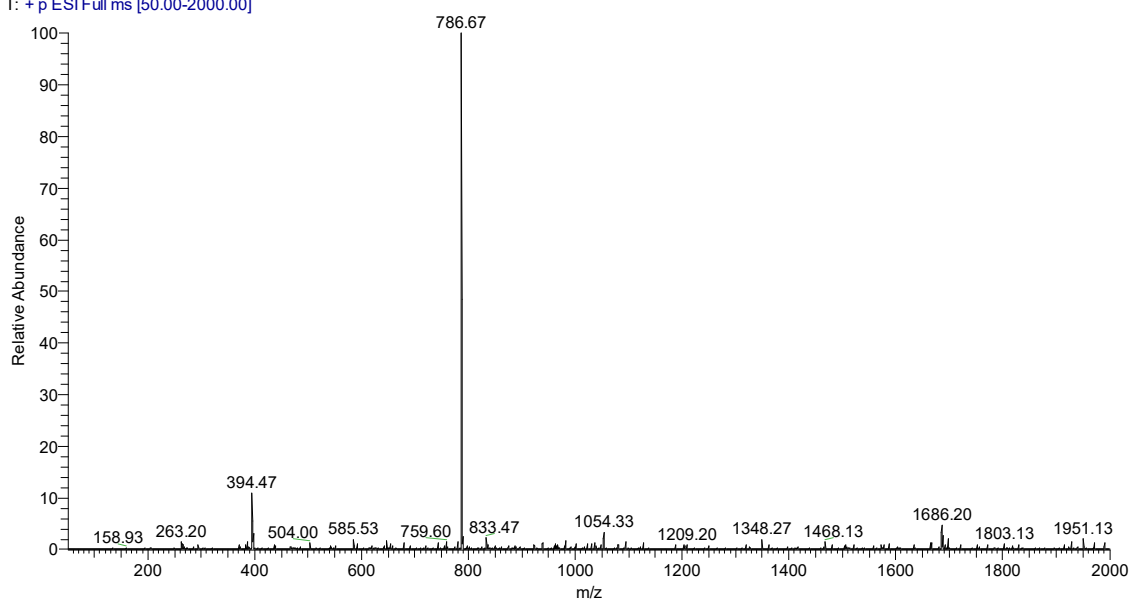


Figure S2. ESI-IT(+) mass spectrum of the C₁₆-Im-KVK conjugate

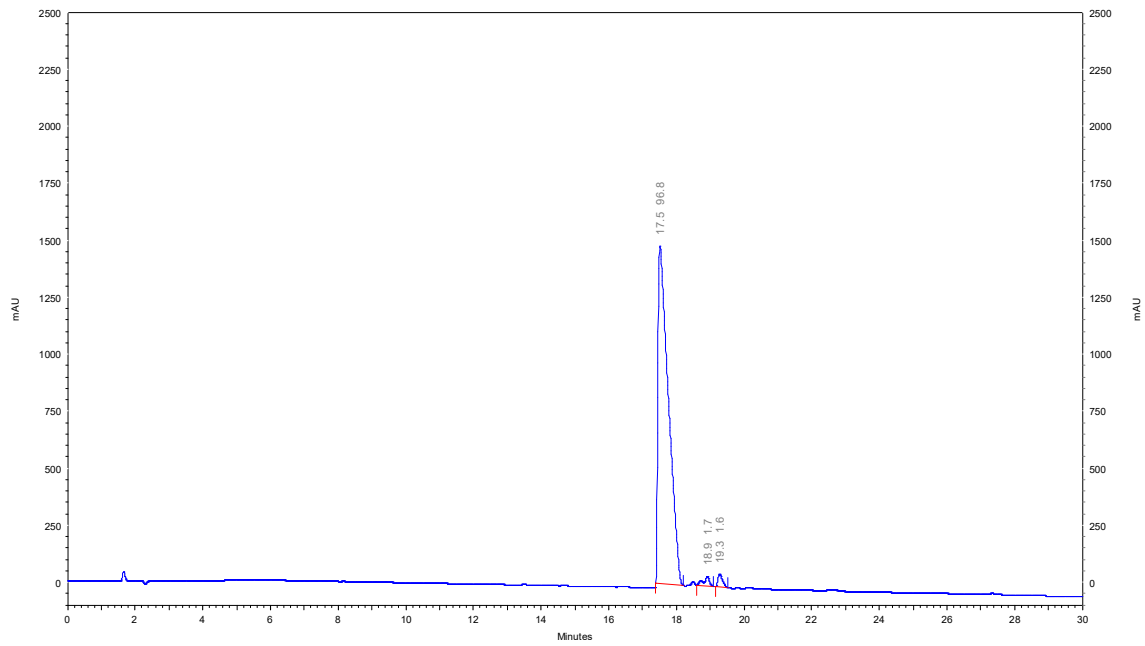


Figure S3. RP-HPLC chromatogram of the C₁₆-Im-HK conjugate

PG-NT-AGD-57-puro #5 RT: 0.13 AV: 1 NL: 3.65E7
 T: + p ESI Full ms [50.00-2000.00]

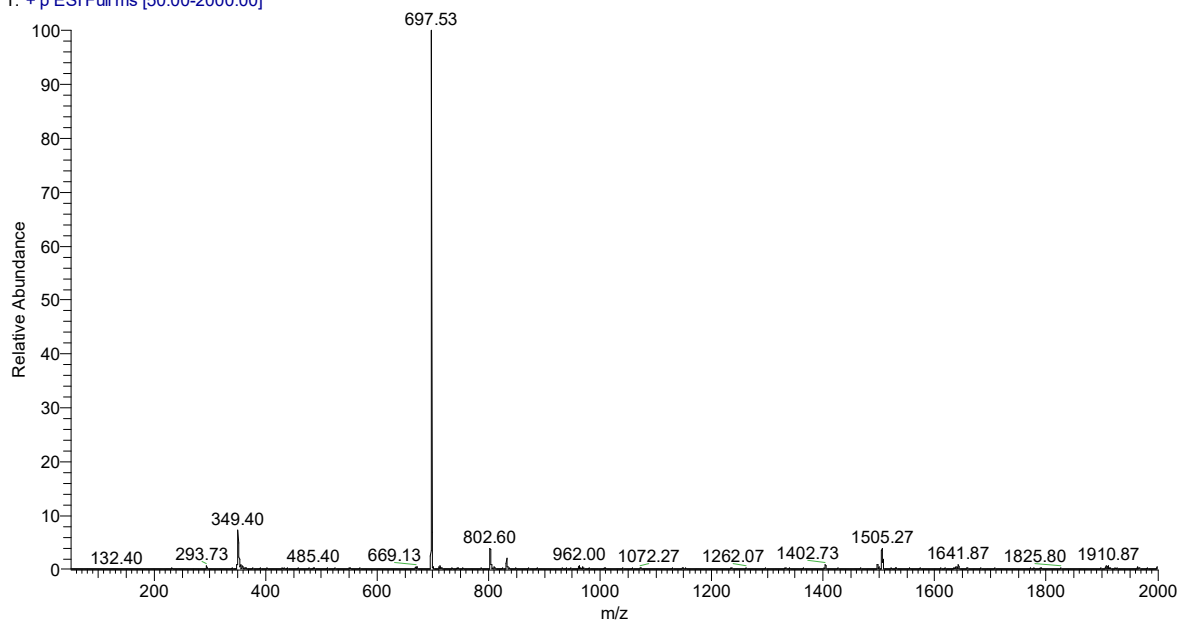


Figure S4. ESI-IT(+) mass spectrum of the C₁₆-Im-HK conjugate

